# LIGAND DESIGN, COORDINATION AND ELECTROCHEMISTRY OF NONBENZENOID ARYL ISOCYANIDES

BY

Stephan Francis Deplazes

Submitted to the Department of Chemistry
and the Faculty of the Graduate School of the University of Kansas
In partial fulfillment of the requirements for the degree of
Doctor of Philosophy

_____
Dr. Mikhail V. Barybin – Chairperson

_____

_____

_____

_____

Date Defended _____

The Dissertation Committee for Stephan Deplazes certifies
That this is the approved Version of the following dissertation:

LIGAND DESIGN, COORDINATION AND ELECTROCHEMISTRY
OF NONBENZENOID ARYL ISOCYANIDES

_____
Dr. Mikhail V. Barybin – Chairperson

_____

_____

_____

_____

Date approved: _____

## Abstract

In this work, the strategy for accessing planar chiral isocyanides has been developed and the first member of this family has been isolated in the optically pure form and fully characterized. 2-Methyl-substituted isocyanoferrocene can be synthesized from commercial ferrocenylcarboxylic acid and S- or R-forms of valinol. Both $_{p}$S and $_{p}$R forms of this new organometallic isocyanide were isolated in excellent percent enantiomeric excess. The unambiguous assignment of the absolute configuration was obtained through the X-ray chrystallographic study of the $PdI_2$ adduct with ($_{p}$S)-1-isocyano-2-methylferrocene that contains two planar chiral isocyanoferrocene ligands bound to the $Pd^{II}$ center in the *trans* fashion. Electrochemical analysis of the $[Cr(CNR)_6]^{0,1+,2+}$ (R = ferrocenyl and cymantrenyl) series indicated that the electronic influence of the ferrocenyl moiety within a ligand is similar to that of a hydrocarbon aryl substituent, rather than an alkyl group (e.g., methyl). In addition, this work has demonstrated that electronic (especially, the π-acidity) tuning of the isocyanocyclopentadienide ligand can be accomplished within a substantial range by changing the nature of the transition metal fragment bound to its ring.

A systematic electrochemical investigation of the first isocyanoazulene ligands and their electron-rich complexes has been accomplished. The electronic properties of azulene and its isocyanide derivatives have been investigated by electronic spectroscopy, cyclic voltammetry, and theoretical calculations. Through this work, the properties of the Frontier molecular orbitals of isocyanoazulenes were

determined quantitatively. The previous qualitative theory predicting the effect of substituents on the magnitude of azulene's HOMO-LUMO gap (and, hence, its optical properties) popularized by Liu *et al.*[81] does not hold in the case of the isocyanide substituent. The unexpected directions of the shifts of the $S_0 \rightarrow S_1$ transition for 1- and 2-isocyanoazulenes have been fully rationalized by considering together the electronic spectra, electrochemical properties, and the time-dependant density functional theory structures of these species. Furthermore, the first comprehensive quantitative electrochemical assessment of electronic inhomogeneity of the azulenic scaffold has been perfomed by analyzing the redox properties of the complexes $Cr(CN^{x}Az)_6$ (Az = azulenyl' x = 1, 2, 4, 5, 6). The quantitative series of the donor/acceptor ratios of the isocyanoazulene ligands has been obtained.

The first large gold macrocycle incorporating the redox-active ferrocene unit has been isolated and fully characterized. The 1,1'-diisocyanoferrocene ligand employed in this study undergoes $\mu_2$ coordination to a pair of $Au^{I}$ ions under thermodynamic control, i.e., no oligomeric structures are produced at all. Formation of the cyclic product is facilitated by the near perfect match between the interplanar distance involving the five-membered rings of the diisocyanoferrocene ligand and the Au·· Au separation within the di-gold precursor that features an aurophilic interaction. Overall, the "parent" motifs to be incorporated in the potential novel mesogenic materials containing both ferrocene and azulene units have been established and the reasons for challenges in isolating gold(I) complexes with mixed isocyanide ligands have been uncovered.

## Acknowledgements

I would first like to thank my advisor Misha Barybin, without whose patient, understanding, great teaching ability and his contagious drive to succeed none of this would be possible today. Throughout my graduate career Misha has instilled these traits in me through his careful mentoring. I will miss the conversations we have had both in terms of chemistry and outside of chemistry as they have allowed me to grow unfettered as a chemist and as a human being. I would like to also thank the faculty of the Chemistry department, especially the Inorganic faculty, for the time they have spent with me over the course of my class work, teaching me the basic nature of chemistry and driving me to increase my knowledge and to become a better chemist while at the University of Kansas. I would like to also thank my Committee members, Dr. Dave Benson, Dr. Daryl Busch, Dr. Kyle Camarda, Dr. Julian Limburg, and. Dr. Cindy Berrie for the time they have spent in the various capacities in my learning process here at KU.

A very warm thank you is also in line for Dr. Randall Robinson, whose groundbreaking work on isocyanoazulenes in the Barybin group allowed for much of the research I was able to perform. Not only that, but his patience in the lab and teaching methods have helped to develop my synthetic techniques over the course of the years. It was a sad day when Randy and Janet moved to Arizona.

I would also like to thank the collaborators that have influenced my work through the course of the years at KU, Dr. Gerald Lushington and Dr. Ward Thompson, whose theoretical work has given me a greater insight in the inner

workings of the systems that I have worked on. Dr. Victor Day and Dr. Douglas Powell, whose expertise in X-ray crystallography has provided me the fine details of the molecules that I have been able to construct. To Dr. David VanderVelde and Sarah Neuenswander, again I would like to thank you for the time that you have spent helping me with my NMR experiments. I would also like to thank Dr. Masaharu Toriyama for the time he spent in the lab and for his synthetic skills. Early in my career he made some ligand systems that I was able to unfortunately polymerize.

To the friends that I have made during my stay at KU, I am also very appreciative. To start, my classmate and labmate, Dr. Tom Holovics, I can honestly say it has been a fun ride. We did a lot with the chemistry and had fun along the way. I would also like to thank Tiffany Maher, Alexandre Vorouchilov, Yumiko Tomotsugu and David McGinnis for helping to make the Barybin group what it is today.

Finally, I need to thank my family, starting with my wife Svetlana, whose love and support have helped me through any trial or tribulation that has been thrown at me. Without your support I would not be who or where I am today, I love you very much. To my parents, I thank you for encouraging me throughout this process, as well as when I was young. Letting me play with mixing different things and seeing what it would do, and always encouraging me to learn and to be the best I can be. To my extended family and all my other mothers that have looked out for me and helped me learn, again, I am very thankful, without you, I would be a shell of a man. And last but not least, to anyone that I have not had the time to mention that has supported

me on this road, I would like to thank you as well. There have been too many names and faces that have passed through my life and all of you have benefited me and helped me grow as a person and, also, as a chemist.

Table of Contents

## List of Tables

## List of Figures

### Chapter One



### Chapter Two

**Chapter Three**

## List of Schemes

### Chapter One



### Chapter Three

## Publication List

- Barybin, M. V.; Holovics, T. C.; Deplazes, S. F.; Lushington, G. H.; Powell, D. R.; Toriyama, M. "First Homoleptic Complexes of Isocyanoferrocene," *J. Am. Chem. Soc.* **2002**, *124*, 13668-13669.

- Robinson, R.E.; Holovics, T. C.; Deplazes, S. F.; Lushington, G. H.; Powell, D. R.; Barybin, M. V. "First Isocyanoazulene and Its Homoleptic Complexes," *J. Am. Chem. Soc.* **2003**, *125,* 4432-4433.

- Holovics, T.C.; Deplazes, S.F.; Lushington, G.H.; Toriyama, M.; Powell, D.R.; Lushington, G.H.; Barybin, M.V. "Organometallic Isocyanocyclopentadienides: A Combined Synthetic, Spectroscopic, Structural, electrochemical and Theoretical Investigation," *Organometallics*, **2004**, *23*, 2927-2938.

- Robinson, R. E.; Holovics, T. C.; Deplazes, S. F.; Lushington, G. H.; Powell, D. R.; Thompson, W. H. Barybin, M. V. "Five Possible Isocyanoazulenes and Electron-Rich Complexes Thereof: A Quantitative Organometallic Approach For Probing Electronic Inhomogeneity of the Azulenic Framework," *Organometallics,* **2005,** *24*, 2386-2397.

- Deplazes, S. F.; Holovics, T. C.; Barybin, M. V. "Planar-Chiral Derivatization of $\eta^5$-Isocyanocyclopentadienides," in preparation for submission to *Organometallics.*

# Chapter One

Chemistry of the First Planar Chiral Organometallic Isocyanocyclopentadienide Ligand and Related Complexes

## 1.1. Introduction

Isonitriles, also known as isocyanides and carbylamines, (:C≡N–R), are among the few relatively stable molecules containing a lone pair of electrons on a terminal carbon atom. These highly reactive substances have an important role in organic and organometallic synthesis, catalysis, materials science, drug discovery, and diagnostic medicine.[1-15] To this day, however, the extensive use of isocyanides has relied on a fundamentally very limited pool of molecules.

Organic isocyanides are widely used in multi-component reactions (MCR) (**Scheme 1.1**). Since 1995, MCR of isocyanides involving mainly commercially available $CN^tBu$, $CNC_6H_{11}$, and $CNCH_2Ph$ have become a powerful method for developing new drug candidates for the pharmaceutical industry.[1-5] The example in **Scheme 1.1** is a one pot, four component reaction, which has led to a major improvement in the synthesis of Crixivan® (**Figure 1.1**), an HIV protease inhibitor produced by Merk & Co.[6] There have been very few reports on the use of aryl isocyanides in MCR, which include the synthesis of the anti-cancer agent Ecteinascidin 743.[7-10] The reasoning behind this limited number of aryl isocyanides employed may be associated with their restricted accessibility and/or the difficulty in handling and storage.

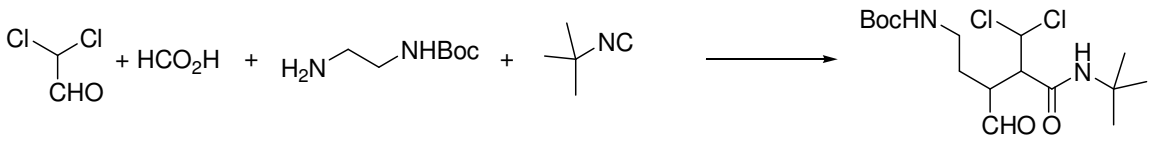


**Scheme 1.1**. The key four-component step in the synthesis of Crixivan®.

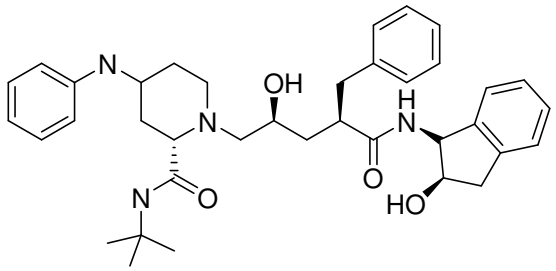


**Figure 1.1**. Structure of Crixivan®

Another use of isocyanides in the medical field involves isocyanide complexes of 99m-technetium, which function as radiotracers for diverse diagnostic purposes.[11] The most widely investigated and used compound of this type is $[^{99m}Tc(2\text{-methoxyisobutylisocyanide})_6]^+$ also known as Tc-99m-MIBI and Cardiolite®. This complex was originally used as a radiopharmaceutical for myocardial perfusion imaging.[12,13] Later, it was found to show promise as a non-invasive marker for the diagnosis of P-glycoprotein (Pgp) and related multi-drug resistant protein overexpressions in tumors associated with multiple myeloma, thyroid carcinoma, and breast and lung cancers.[14-19] Furthermore, aryl isocyanide complexes of $Tc^I$, in particular $[^{99m}Tc(3,4,5\text{-trimethoxyphenylisocyanide}]^+$, appear to be direct inhibitors of Pgp transport and may be used as a basis for the development of non-radioactive, specifically $Re^I$-based, inhibitors of multi-drug resistance suitable for drug manufacturing.[20,21]

The list of applications of isocyanides in organic/organometallic syntheses is quite extensive. Low-valent transition metal - isocyanide complexes can function as catalysts or precursors in certain catalytic polymerization processes.[22-24] A very good example of these processes is the polymerization of butadiene by $M(CNAr)_6$ (M = Cr, Mo, W), which produces either isotactic or syndiotactic polybutadienes. The nature of

the polybutadiene is determined by the nature of the metal center and the aryl groups of the isocyanide.[24] Also, nickel isocyanides have been shown to effect efficient dimerization of butadiene to form cyclooctadiene, as well as trimerization of substituted acetylenes to give highly functionalized benzenes.[24] In addition, these nickel-isocyanide complexes have been employed as catalysts in the selective hydrogenation of acetylenes, isocyanides and nitriles.[24] Finally, Lippard *et al.* have demonstrated that high coordinate, early transition metal-isocyanide complexes have the ability to facilitate C-C reductive coupling of isocyanides to give functionalized diaminoacetylenes.[25] The low valent transition metal is a prerequisite for this type of linkage to occur.

Organic isocyanide substrates have been subject to transition metal-catalyzed polymerizations, which produced poly(isocyanide)s, $\{\text{-C(=NR)-}\}_n$, also called poly(iminomethylenes).[26,27] The most notable feature of these polymers is that every carbon atom in the main chain has a substituent. These polymers can often assume a helical conformation if the isocyanide monomers possess sterically bulky substituents (**Figure1.2**). Such supramolecular chiral poly(isocyanide)s have been subject to rigorous spectroscopic and theoretical investigations[26-30] and have found a variety of practical applications such as the design of nonlinear optical materials[31,32] and molecular recognition devices (e.g., chiral stationary phases for liquid chromatography).[33]

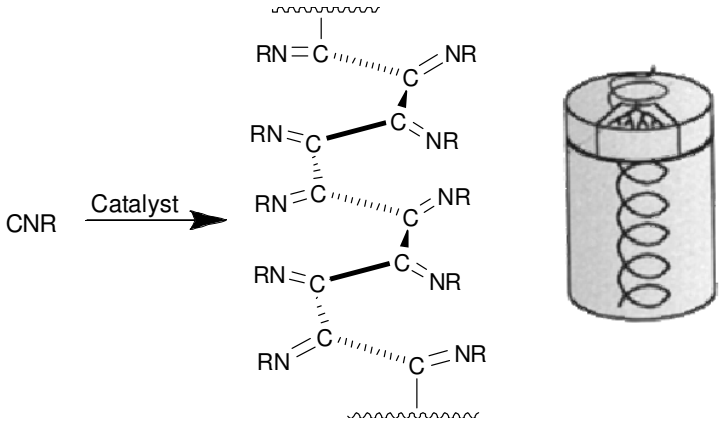


**Figure 1.2.** Example of a chiral optical polymer

Until recently, essentially all known aryl isocyanides (ArNC) incorporated benzenoid substituents, Ar. These species are typically more air-sensitive and less thermally stable than their alkyl congeners.[34] For example, phenyl isocyanide (PhNC) and a number of its substituted variants decompose rapidly once exposed to air. They undergo facile isomerization into the more thermodynamically favored organic cyanides upon heating to 40-50 ºC.[35] One fundamental advantage of the aryl isocyanides over their alkyl counterparts is electronic coupling between the π systems of the –NC functionality and the organic substituent. [22-25,36-41]

Prior to the recent work of Barybin and co-workers , [42-45] the only examples of nonbenzenoid aromatic isocyanides had been isocyanoferrocene[46-48] (FcNC) and 1,1'-diisocyanoferrocene.[49] Both of these species can be regarded as organometallic derivatives of the isocyanocyclopentadienide anion. Even though isocyanoferrocene has, in principle, been accessible since the late 1980's,[46-48] its chemistry has remained essentially unexplored. This can be attributed to a tedious reaction sequence involved in the original synthesis of FcNC. Indeed, only an 8-12% overall yield of aminoferrocene, a precursor to FcNC, could be isolated when starting from ferrocene.

The problem of efficiency in the synthesis of aminoferrocene ($FcNH_2$) has only recently been overcome.[49-52] Moreover, conversion of $FcNH_2$ to the corresponding formamide was difficult to reproduce resulting in yields of this step as low as 20%.[46] Dehydration of ferrocenyl formamide ultimately affords FcNC and the previously reported yields of this step were as low as 25%.[46] A highly efficient formylation and subsequent dehydration of $FcNH_2$ has been recently reported Barybin *et al*.[43,45]

Until recent publications by the Barybin group,[43,45] isolated complexes of the FcNC ligand had been limited to $(OC)_5Cr(FcNC)$,[47,48] and $(OC)_4Fe(FcNC)$.[46] Based on electrochemical studies of $(OC)_5Cr(CNR)$ (R = Fc, Me) and relying on the long-held knowledge[53] that ferrocenyl is only a slightly better electron-donating substituent than methyl, it was suggested that FcNC was quite similar to MeNC in its electronic properties as a ligand.[47,48] In both of these zero-valent Cr complexes, however, the isocyanide ligands function essentially as σ-donors due to the presence of five highly π-acidic carbonyl ligands. In addition, because of ferrocene's five-membered rings each possessing an effective negative charge of ca. 0.35,[53] its π system has not been explored experimentally as a potential electron acceptor. This is despite the fact that there are many parallels between the chemistries of ferrocene and benzenoid aromatics.

For many years, tuning properties of aryl isocyanides has been focused on installing and/or modifying the substituents on the benzene ring attached to the isocyanide functionality. (e.g., *cf.* phenyl isocyanide with the more electron-rich 2,6-xylyl isocyanide). The metallocene framework would provide a fundamentally

different way of adjusting both sterics and electronics of the aromatic substituent within CNAr by altering the transition metal fragment that is coordinated to the isocyanocyclopentadienyl unit in the $\eta^5$-mode.

In addition, the metallocene scaffold can, in principle, provide another important avenue for altering properties of the isocyanocyclopentadienide ligand through C-H substitution at the isocyanide-functionalized ring. Indeed, substitution at the α-position with respect to the –NC group would result in the phenomenon referred to as planar chirality (**Figure 1.3**). A potential synthetic strategy to access this class of ligands is described in **Figure 1.4**. In this sequence, the oxazoline moiety is used to ensure enantioselective substitution at the α position of the functionalized Cp ring. This is then followed by nucleophilic substitution of the bromine to install a nitrogen-based group to be converted to the primary amine. The amine can then be transformed into the isocyanide moiety.

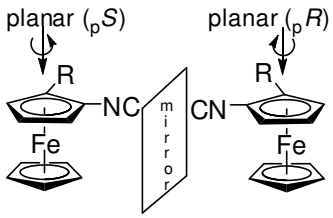


**Figure 1.3.** Two enantiomers of the functionalized FcNC molecule illustrating the phenomenon of planar chirality

As illustrated in Figure 1.3, $\eta^5$-coordinated cyclopentadienides featuring multiple non-identical substituents on one ring are not superimposable with their mirror images. This results in *planar* chirality of the molecule (*cf.* central chirality).

Assignment of the planar chirality configuration is based on the Cahn-Ingold-Prelog rules by viewing the molecule from the side of the ring to be assigned.[54]

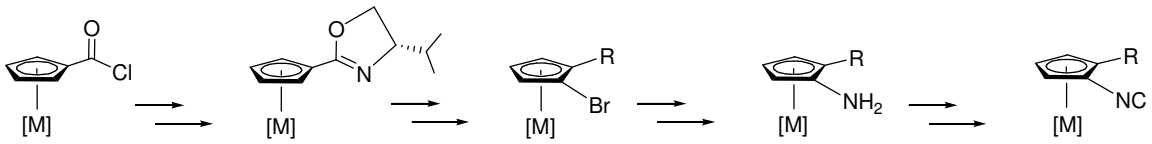


**Figure 1.4.** Strategy for the synthesis of planar-chiral isocyanides described in this Chapter

In the last decade, there has been a surge in efforts to design novel planar-chiral organometallics as evidenced by a large number of articles, reviews, and books on the subject.[55-67] One potential use for a chiral ferrocene derivative is in the synthesis of analogues of prostaglandin. The synthesis uses the ability to add side chains to the cyclopentadienyl moiety and to cleave the iron off at a later step in the synthesis. Unfortunately, due to the stability of the ferrocene moiety, the only decomplexation method that does not destroy the product involves palladium in an acidic medium, typically triflouroacetic acid.[55] This cleaves the ferrocene as the double bounds of the cyclopentadiene are reduced to the saturated cyclopentane derivative. Regrettably, racemic products are produced in this last step.[55] Nevertheless, there is some optimism that the organometallic precursors would be useful in medicines, if *in vivo* decomplexation can be accomplished.[55]

A chiral ferrocene unit can also be used as a chiral auxiliary, if it is incorporated into a larger molecule where the chiral information on the ferrocene is transmitted to the new chiral unit to be formed. The ferrocenyl moiety is then cleaved from the target compound later in the synthesis and potentially could be recycled.

The typical compounds used in such syntheses are chiral, ferrocenyl-containing primary amines as the auxiliary.[55] The classic types of reaction sequences that follow this format are four component condensations and the synthesis of alanine.[55]

Chiral ferrocenes can be used as chiral catalysts. The most common of such catalysts are phosphine derivatives, though there is some progress in employing sulfides, selenides and amino-alcohols.[55] The common outcomes of these catalytic reactions involve C-C coupling, hydrogenation, and hydrosilation.[55] Furthermore, there have been examples of the use of chiral ferrocenylphosphines in allylations and aldol type reactions.[55]

While the most prevalent type of the planar-chiral ligands is ferrocene based, non-metallocene-based systems that exhibit planar chirality,[57] e.g., those based on on the $(\eta^5\text{-}C_5H_5)Mn(CO)_3$ (cymantrene)[68-71] and $(\eta^6\text{-}C_6H_6)Cr(CO)_3$[72,73] scaffolds, have been steadily emerging.

## 1.2. Work Described in Chapter One

The synthesis and characterization of the first planar chiral isocyanide is described in the following sections of Chapter 1. Both $_{p}$S and $_{p}$R enantiomers, as well as the racemic mixture, were synthesized for the purpose of establishing the enantiomeric excess (% ee) of the procedure. The $_{p}$S form was accessed via a ferrocenyloxazoline intermediate originally described by Richards and coworkers.[74-76] In addition, systematic electrochemical and DFT analyses of isocyanoferrocene, isocyanocymantrene, and electron-rich complexes thereof are presented in this Chapter.

## 1.3. Experimental Section

### 1.3.1. General Procedures and Starting Materials

Unless specified otherwise, all procedures were performed under an Ar atmosphere (99.5% purified by passage through columns of activated BASF catalyst and molecular sieves). All connections involving the gas purification system were made of glass, metal or other materials impermeable to air. Standard schlenk techniques were employed using a double-manifold vacuum line. Solvents, including deuterated solvents were freed of impurities by standard procedures and stored under Ar. Synthesis of ($_p$S)-1-bromo-2-methylferrocene followed literature methods.[74,77,78] Bis($\eta^6$-naphthalene)chromium(0) was prepared according to a literature procedure.[79] FTIR spectra were collected on a Thermo Nicolet Avatar 360 FTIR spectrometer with samples sealed in a 0.1 mm gastight NaCl cell. NMR samples were analyzed on Bruker DRX-400 and Bruker Avance 500 Spectrometers. $^1$H and $^{13}$C chemical shifts are given with reference to residual solvent resonances relative to $SiMe_4$. Melting points are uncorrected and were determined for samples in sealed capillary tubes. Chiral HPLC was performed using a Chiralpak OD column (0.46 cm x 25 cm,Dancel Chemical Ind., LTD) installed on a Shimadzu LC-10AD HPLC with a Shimadzu SPD-10 VP UV-Vis Detector. Elemental analyses were carried out by Desert Analytics, Tucson, AZ. Synthesis of the $_p$R form of the methyl-substituted FcNC was performed following the procedure established for the preparation of the $_p$S form of the compound but changing the chirality of the valinol precursor.

### 1.3.2. Synthesis of ($_p$S)-1-pthalimide(Pth)-2-methylferrocene

To a stirring pink slurry/solution of copper(I) oxide (0.836 g, 5.80 mmol) and pthalimide (2.79 g, 190 mmol) in 15 mL pyridine, ($_p$S)-1-bromo-2-methylferrocene (3.26 g, 11.6 mmol) dissolved in 10 mL pyridine was added via cannula. This solution was then refluxed for 48 hours, during which time its color changed from pink to orange, and finally to a dark brown color. The pyridine was removed under reduced pressure leaving a dark brown residue. The solid was triturated with hexanes and then ether to provide an orange solution/slurry. Column chromatography was performed on the resulting solution using silica gel with gradient elution starting with hexanes and changing the solvent system to diethyl ether. The solvent was removed at reduced pressure to provide a 68% yield (2.23 g, 6.50 mmol) of the product. MP = 96-98 $^{o}$C. FTIR ($CH_2Cl_2$) $\nu_{CO}$ 1730 cm$^{-1}$. $^1$H NMR (400 MHz, $CDCl_3$, 25 $^{o}$C): $\delta$ 2.0 (s, 3H), 4.15 (t, 1H, $^3J_{HH}$= 2.4 Hz), 4.21 (broad s, 1H), 4.27 (s, 5H), 4.32 (t, 1H, $^3J_{HH}$=0.8 Hz), 7.76 (dd, 2H, $^3J_{HH}$=3.0 Hz, $^3J_{HH}$=5.4 Hz), 7.91 (dd, 1H, $^3J_{HH}$=3.0 Hz, $^3J_{HH}$=5.4 Hz) ppm. $^{13}$C{$^1$H} NMR(100.6 MHz, $CDCl_3$, 25 ºC): $\delta$ 13.99, 64.86, 65.11, 68.04, 70.53, 80.22, 87.01, 123.47, 132.27, 134.30, 167.50 ppm.

### 1.3.3. Synthesis of ($_p$S)-1-amino-2-methylferrocene

To a stirring orange solution of ($_p$S)-1-Pth-2-methylferrocene (0.40 g, 1.15 mmol) in 10 mL of deoxygenated absolute MeOH, 2.2 mL (44 mmol) of hydrazine was added via syringe. The resulting solution was refluxed for 2 hours. Then 20 mL of $H_2O$ was added resulting in precipitation of a light orange solid. This was placed

into a separatory funnel, together with 50 mL $H_2O$ and 30 mL of $Et_2O$. All of the residue in the funnel was dissolved. The ether layer was then collected and the aqueous layer was extracted four times using two 20 mL portions of ether. The organic layer was dried over $Na_2SO_4$ for two hours, after which time the drying agent was removed via filtration and the solvent was evaporated under vacuum giving an essentially 100% yield (247 mg, 1.15 mmol) of the yellow product. MP = 101 – 103 °C $^1$H NMR (400 MHz, $CDCl_3$, 25 $^o$C): δ 1.91 (s, 3H), 2.41 (s, 2H), 3.77 (s, 1H), 3.90 (s, 1H), 4.00 (s, 1H), 4.03 (s, 5H) ppm. $^{13}C\{^1H\}$ NMR(100.6 MHz, $CDCl_3$, 25 °C): δ 12.57, 58.26, 60.96, 65.72, 69.74, 72.48 ppm.

### 1.3.4. Synthesis of ($_p$S)-1-formamido-2-methylferrocene

To a stirring orange solution of ($_p$S)-1-amino-2-methylferrocene (0.700 g, 3.25 mmol), 1.16 g (11.4 mmol) of acetic-formic anhydride in 10 mL $CH_2Cl_2$ was added dropwise via syringe. The solution was stirred for 1 hour. Then the solvent was removed under vacuum and the residue was dried resulting in an orange oil. The residue was chromatographed using $Et_2O$ and silica gel, which afforded the orange oil that solidified upon standing overninght at -15 °C giving a 90% yield (0.815 g, 2.92 mmol) of the product. MP = 133 – 136 °C. FTIR ($CH_2Cl_2$) $\nu_{CO}$ = 1693 cm$^{-1}$.

### 1.3.5. Synthesis of ($_p$S)-1-isocyano-2-methylferrocene

To a stirring solution of ($_p$S)-1-formamido-2-methylferrocene (0.350 g, 1.43 mmol) and diisopropyl amine (0.61 mL, 4.3 mmol) in 30 mL of $CH_2Cl_2$, $POCl_3$ (0.135 mL, 1.45 mmol) was added dropwise via syringe over a 5 minute period. The

resulting solution was allowed to stir for a period of four hours, over the course of which the solution color changed from orange to orange-brown. The reaction mixture was then quenched using 100 mL aqueous $K_2CO_3$ (10 % by weight). The organic layer was separated and washed with water (2 × 50 mL). The organic layer was then dried over $MgSO_4$ for two hours. The drying agent was removed by filtration and the solvent was removed from the filtrate under vacuum. Column chromatography was then performed on the resulting orange residue using 1:1 $Et_2O$/hexanes and silica gel. The first fraction was collected and the solvent was removed under reduced pressure. The resulting solid was dried in vacuo yielding a 90% yield (0.273 g, 1.27 mmol) of the yellow-orange product. MP = 44 – 46 °C. FTIR ($CH_2Cl_2$) $\nu_{CN}$ = 2127 $cm^{-1}$. $^1H$ NMR (400 MHz, $CDCl_3$, 25 °C): δ 2.14 (s, 3H), 3.99 (t, 1H, $^3J_{HH}$=2.4 Hz), 4.10 (t, 1H), 4.21 (s, 5H), 4.48 (dd, 1H, $^3J_{HH}$=1.57 Hz and 2.20 Hz) ppm. $^{13}C\{^1H\}$ NMR(100.6 MHz, $CDCl_3$, 25 °C): δ 12.44, 64.93, 65.65, 67.83, 71.27, 81.81, 164.3 ppm.

### 1.3.6. Synthesis of $PdI_2(({}_pS)$-1-isocyano-2-methylferrocene$)_2$ (1)

To a stirring grey slurry of $PdI_2$ (0.076 g, 0.21 mmol) in 10 mL $CH_2Cl_2$, 0.100 g (0.440 mmol) of ($_p$S)-1-isocyano-2-methylferrocene dissolved in 10 mL of $CH_2Cl_2$ was added via cannula. The resulting orange solution was allowed to stir for 2.5 hours, during which time the solution color changed to a deep red. The solution was then filtered through celite and the solvent removed in vacuo from the filtrate. The red solid product was collected in a 59% yield (0.101 g, 0.123 mmol) after drying at

reduced pressure. MP = decomposes at 155-169 °C. Anal. Calcd. For $C_{24}H_{22}N_2I_2Fe_2Pd$: C 35.57, H 2.74, N 3.46. Found: C 35.61, H 2.51, N 3.51. FTIR($CH_2Cl_2$): $\nu_{CN}$ = 2203 $cm^{-1}$. $^1H$ NMR (400 MHz, $CDCl_3$, 25 °C): δ 2.27 (s, 3H), 4.12 (t, 1H, $^3J$=2.54 Hz), 4.22 (s, 1H), 4.35 (s, 5H), 4.64 (s, 1H) ppm. $^{13}C\{^1H\}$ NMR(100.6 MHz, $CDCl_3$, 25 °C): δ 12.72, 65.95, 66.19, 68.90, 71.29, 71.77, 83.46, 124.5 ppm.

### 1.3.7. Synthesis of Cr(($_p$S)-1-isocyano-2-methylferrocene)$_6$ (2)

To a dark brown stirring solution of bis($\eta^6$-naphthalene)chromium(0) (0.047 g, 0.154 mmol) in 10 mL of THF cooled to 0 °C, ($_p$S)-1-isocyano-2-methylferrocene (0.225 g, 1.00 mmol) dissolved in in 10 mL of THF was added via cannula. The reaction was allowed to stir overnight. During this time, a red solution formed. Most solvent was removed under vacuum and heptane was added to precipitate a red/pink product. The solid was collected on a glass frit giving a 74.4 % yield (0.160 g, 0.114 mmol) of **2**. MP = decomposes above 230 °C without melting. FTIR (THF): $\nu_{CN}$ = 1937 and 1947 $cm^{-1}$. $^1H$ NMR (400 MHz, $CDCl_3$, 25 °C): δ 2.56 (s, 3H), 3.74 (s, 1H), 4.13 (s, 6H), 4.36 (s, 1H).

### 1.3.8. Synthesis of (rac)-1-Pth-2-methylferrocene

To a stirring pink slurry/solution of copper(I) oxide (0.12 g, 0.86 mmol) and pthalimide (0.416 g, 2.83 mmol) in 3 mL pyridine, (rac)-1-bromo-2-methylferrocene (0.567 g, 1.73 mmol) dissolved in 2 mL pyridine was added via cannula. The solution was refluxed for 48 hours, during which time it turned from pink to orange to

dark brown color. The pyridine was removed under vacuum until dryness, leaving a dark brown residue. The solid was triturated, starting with hexanes and changing to ether to provide an orange solution. This solution was subject to column chromatography using silica gel and ether. The solvent was removed under vacuum to provide a 34% yield (0.204 g, 0.588 mmol) of the product. MP = 96-98 °C. FTIR ($CH_2Cl_2$): $\nu_{CO}$ 1730 $cm^{-1}$ $^1H$ NMR (400 MHz, $CDCl_3$, 25 °C): δ 2.0 (s, 3H), 4.15 (t, 1H, $^3J_{HH}$= 2.4 Hz), 4.21 (broad s, 1H), 4.27 (s, 5H), 4.32 (t, 1H, $^3J_{HH}$=0.8 Hz), 7.76 (dd, 2H, $^3J_{HH}$=3.0 Hz, $^3J_{HH}$=5.4 Hz), 7.91 (dd, 1H, $^3J_{HH}$=3.0 Hz, $^3J_{HH}$=5.4 Hz) ppm. $^{13}C\{^1H\}$ NMR(100.6 MHz, $CDCl_3$, 25 °C): δ 13.99, 64.86, 65.11, 68.04, 70.53, 80.22, 87.01, 123.47, 132.27, 134.30, 167.50 ppm.

### 1.3.9. Synthesis of (rac)-1-amino-2-methyl ferrocene

To a stirring orange solution of (rac)-1-Pth-2-methylferrocene (0.143 g, 0.414 mmol) in 3 mL of deoxygenated absolute MeOH under argon, 0.80 mL (16 mmol) of hydrazine was syringed in dropwise. The resulting mixture was then refluxed for 2 hours. After the solution cooled to room temperature, 5 mL of $H_2O$ was added causing a white/orange solid to form. This was placed into a separatory funnel, with 20 mL $H_2O$ and 20 mL of $Et_2O$. All of the solid dissolved. The organic layer was then collected. The aqueous layer was extracted four times using 5 mL portions of $Et_2O$. The combined organic fractions were dried over $Na_2SO_4$ for two hours. The drying agent was filtered off and the solvent removed from the filtrate under vacuum giving an 88% yield (79.2 mg, 0.364 mmol) of the pure yellow product. MP = 101 –

103 °C. $^{1}$H NMR (400 MHz, $CDCl_3$, 25 °C): δ 1.91 (s, 3H), 2.41 (s, 2H), 3.77 (s, 1H), 3.90 (s, 1H), 4.00 (s, 1H), 4.03 (s, 5H) ppm. $^{13}C\{^{1}H\}$ NMR(100.6 MHz, $CDCl_3$, 25 °C): δ 12.57, 58.26, 60.96, 65.72, 69.74, 72.48 ppm.

### 1.3.10. Electrochemical Measurements

Cyclic voltammetric (CV) experiments on $2\times10^{-3}$ M solutions of $Cr(FcNC)_6$, $Cr(CmNC)_6$, **1**, and **2** in $CH_2Cl_2$ were conducted at room temperature using an EPSILON (Bioanalytical Systems INC., West Lafayette, IN) electrochemical workstation. The electrochemical cell was placed in an argon-filled Vacuum Atmospheres dry-box. Tetrabutylammonium hexafluorophosphate (0.1 M solution in $CH_2Cl_2$) was used as a supporting electrolyte. Cyclic voltammograms were recorded at 22 ± 2 °C using a three component system consisting of a platinum working electrode, a platinum wire auxiliary electrode, and a glass encased non-aqueous silver/silver chloride reference electrode. The reference $Ag/Ag^+$ electrode was monitored with the ferrocene/ferrocenium couple. Under the experimental conditions employed, $\Delta E_{pa,pc}$ of the $Fc^+/Fc$ couple was 89 mV at the scan rate of 100 mV/s. This peak-to-peak separation is identical to that previously observed for the $Fc^+/Fc$ couple at 100 mV/s in a very similar electrochemical setup, which employed a 0.2 M solution of $[^{n}Bu_4N][PF_6]$ in $CH_2Cl_2$ as a supporting electrolyte.[80] The systems internal resistance (IR) compensation was achieved before each CV run by measuring the uncompensated solution resistance followed by incremental compensation and circuit stability testing. Background cyclic voltammograms of the electrolyte solution

were recorded before adding the analytes. The half-wave potentials ($E_{1/2}$) were determined as averages of the cathodic and anodic peak potentials of reversible couples and are referenced to the $Fc^+/Fc$ couple.[81] No significant difference (< 0.01 V) between external and internal referencing with $Fc^+/Fc$ was documented.

### 1.3.11. Computational Work

All computational work was performed by Dr. Gerald Lushington from the Molecular Modeling Lab at the Univeristy of Kansas. Electronic structure calculations were conducted on FcNC and CmNC at the all-electron density functional theory level using the Gaussian 98 program. The computations were performed using Becke's three parameter hybrid exchange functional[82] with the LYP correlation functional.[83,84] The standard 6-31G split valence basis set[85] was employed in both cases, including a single d polarization function on all heavy atoms and a single p function on all hydrogen atoms.[86] The initial molecular geometries were obtained by extracting the coordinates of single FcNC and CmNC moieties from the crystal structures of $Cr(FcNC)_6 \cdot CH_2Cl_2$ and $Cr(CmNC)_6$. The geometries of the C-N-C fragments were refined through quantum chemical optimization at the theory level described above. The ferrocenyl portion of FcNC was frozen during the calculations, but in a subsequent validation step, the unsubstituted ring was twisted by 36º relative to the substituted ring in order to confirm that ring rotations play a negligible role in the structure and energetics of the frontier orbitals. All computational parameters not explicitly specified above were set to their default values.

### 1.3.12. Single Crystal X-ray Analysis of 1

X-ray quality crystals of **1** were grown by dissolving the red solid in a minimum amount of $CH_2Cl_2$ and then carefully layering the resulting solution with pentane. The two-solvent mixture was allowed to slowly diffuse at 4 °C. After two weeks, X-ray quality crystals of **1** formed. The experimental portion of the X-ray analysis of **1** was conducted by Dr. Douglas R. Powell at the Univeristy of Kansas.

From these crystals a yellow plate-shaped crystal of dimensions 0.31×0.29×0.03 mm was selected for structural analysis. Intensity data for this compound were collected using a Bruker APEX ccd area detector using graphite-monochromated Mo Kα radiation (λ = 0.71073 Å). The sample was cooled to 100(2) K. The intensity data were measured as a series of ω oscillation frames each of 0.3 ° for 10 sec / frame. Coverage of unique data was 99.9 % complete to 26.00 degrees in θ. Cell parameters were determined from a non-linear least squares fit of 7766 peaks in the range $2.62 < \theta < 26.00°$. A total of 21789 data were measured in the range $1.97 < \theta < 26.00°$. The data were corrected for absorption by the semi-empirical method giving minimum and maximum transmission factors of 0.3453 and 0.8804. The data were merged to form a set of 9762 independent data with R(int) = 0.0272.

The monoclinic space group $P2_1$ was determined by systematic absences and statistical tests and verified by subsequent refinement. The structure was solved by direct methods and refined by full-matrix least-squares methods on $F^2$. Hydrogen atom positions were initially determined by geometry and refined by a riding model. Non-hydrogen atoms were refined with anisotropic displacement parameters.

Hydrogen atom displacement parameters were set to 1.2 (1.5 for methyl) times the displacement parameters of the bonded atoms. A total of 559 parameters were refined against 1 space group restraint and 9762 data to give wR($F^2$) = 0.0637 and S = 1.006 for weights of w = 1/[$\sigma^2$ ($F^2$) + (0.0370 P)$^2$ + 1.0000 P], where P = [$F_o^2$ + 2$F_c^2$] / 3. The final R($F$) was 0.0256 for the 9520 observed, [$F > 4\sigma(F)$], data. The largest shift/s.u. was 0.003 in the final refinement cycle. The final difference map had maxima and minima of 1.827 and -0.449 e/Å$^3$, respectively. The absolute structure was determined by refinement of the Flack parameter.[87] The polar axis restraints were taken from Flack and Schwarzenbach.[88] The crystal data and structural refinements for **1** are summarized in **Table A.1** in Apendix 1.A. Complete crystallographic data for **1** are provided in Appendix A.

## 1.4 Results and Discussion

### 1.4.1. Synthesis and Characterization of 1

The synthesis of the first planar chiral metallocene isocyanide generated the product in reasonable yields. The preparation of both the $_pR$ and $_pS$ forms of isocyanoferrocene following the same reaction pathway was easily achieved by changing the chirality of the oxazoline fragment. The preparation of the racemic isocyanide proved more of a challenge than the synthesis of the two chiral forms, though the amine and formamide were synthesized successfully.

The method of synthesis for the isocyanoferrocene was based upon the method introduced by Richards and coworkers[74,75,77,78,89,90] which uses a chiral oxazoline[91] moiety to direct lithiation of the ferrocene, giving a selective deprotonation. Oxazoline functions as a director through the coordination of the nitrogen atom of the oxazoline and the lithium of the lithiating agent. There are two possible structures that can be envisioned when looking at this reaction (**Figure 1.5**), one in which the isopropyl group is aligned away from the coordinated base(exo). The other possible form, has the group aligned toward the base(endo).:

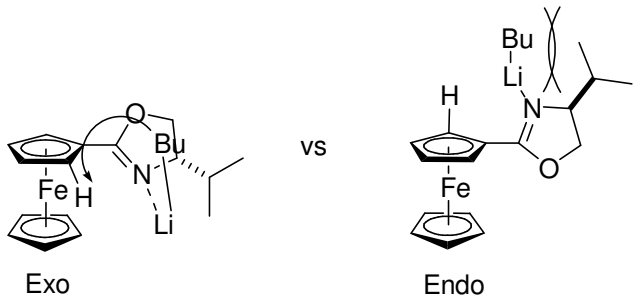


**Figure 1.5.** Alignment of Oxazoline-BuLi

The endo alignment, as seen will have an unfavorable steric interaction between the base (n-butyl lithium (n-BuLi) in this instance) and the isopropyl group, thus the deprotonation is preferred via the exo conformation. "Even though the isopropyl group then lies endo to the iron, the distance between them is too great for any repulsive interaction to disfavour this rotamer. A model of this kind has previously been used to account for the stereoselective addition of organolithium reagents to tricarbonyl(2-phenyloxazoline)chromium(0) complexes".[78]

The degree of selectivity was investigated by Latham and coworkers examining the effects of the solvent, lithiating agent and additives to the reaction mixture. What they found was that the reaction conditions employed in this synthesis should have approximately a 100:1 diastereotopic ratio. This could be improved to a 500:1 by replacing the n-BuLi with sec-BuLi.[92]

This methodology had previously been used in synthesis of planar chiral phosphene compounds, where not only the isopropyl moiety on the oxazoline ring was tested but numerous other substituents as well.[77,78,90,93-98] For the installment of the isocyano moiety into the molecule once the bromine was placed on the Cp ring, the method perfected in the Barybin group was followed (**Scheme 1.2**),[45] where the halogen was displaced by a pthalamide in the presence of $Cu_2O$. The pthalamide fragment was then reduced to the amine via hydrazine in near quantitative yields. Finally formylation and dehydration were done under standard conditions to produce the optically active (pS)-1-isocyano-2-methyl ferrocene. The final product is robust and can be stored for extended periods at low temperatures.

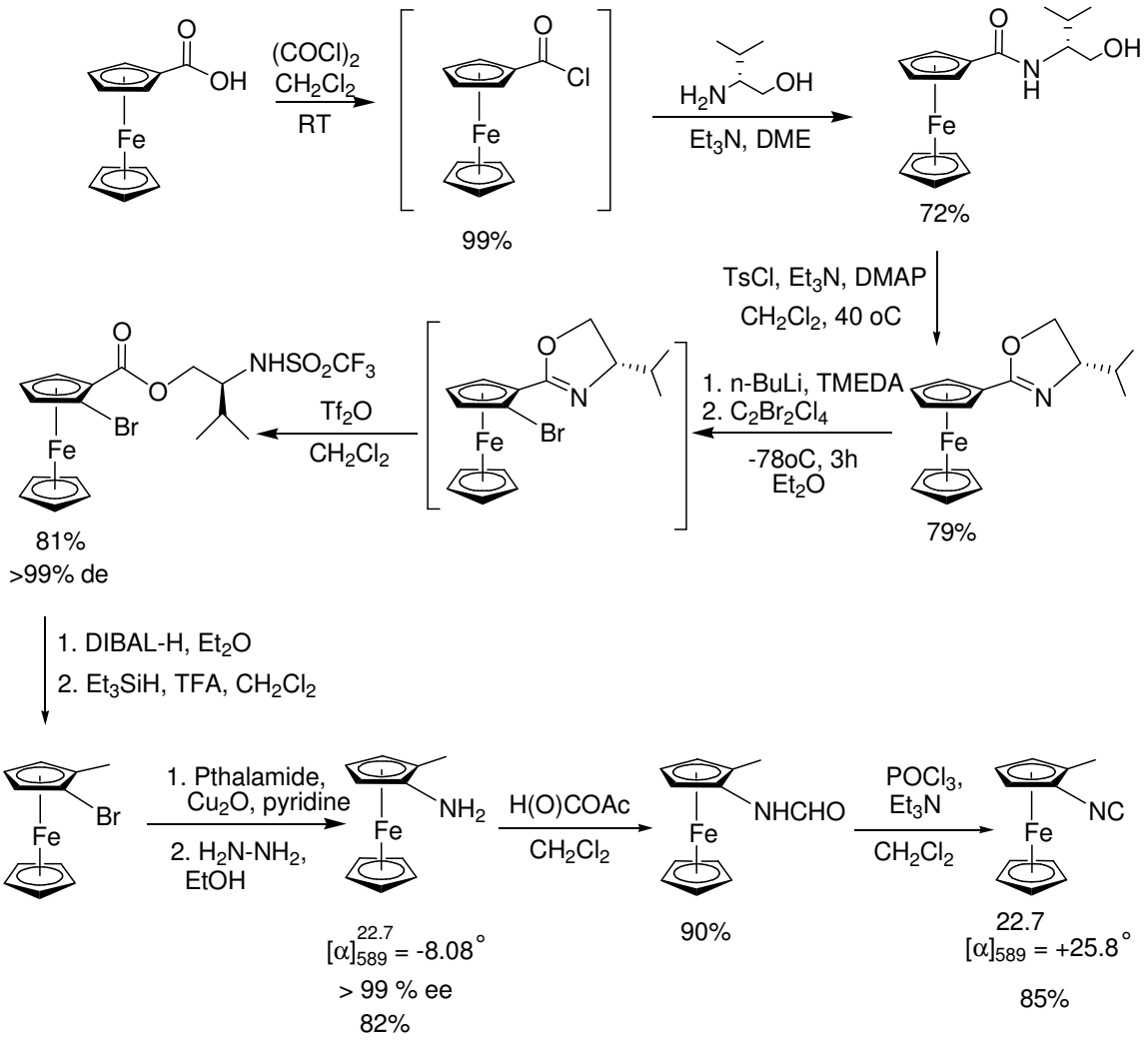


**Scheme 1.2.** Synthesis of Optically Active Methyl-isocyanoferrocene

To verify the %ee of the desired chiral ferrocenyl isocyanide, the racemic congener was needed. The synthesis of the (rac)-1-iodo-2-methyl ferrocene was based upon the reaction sequence described by Patti and coworkers,[99] where lithiation occurs at either position α to the di-methyl-amino methyl substituent on the ferrocene ring. This is then quenched using iodine, and the dimethyl amine was reduced to the methyl group to form (rac)-1-iodo-2-methyl ferrocene. The preparation of the (rac)-1-amino-2-methyl ferrocene then proceeded through the preparation of the racemic

pthalamide as previously described for its chiral cousin with the resulting compound having an identical mp, $^{1}H$ and $^{13}C$ NMR spectra to the chiral amine, with its racemic nature being verified by a chiral high pressure liquid chromatography (HPLC).

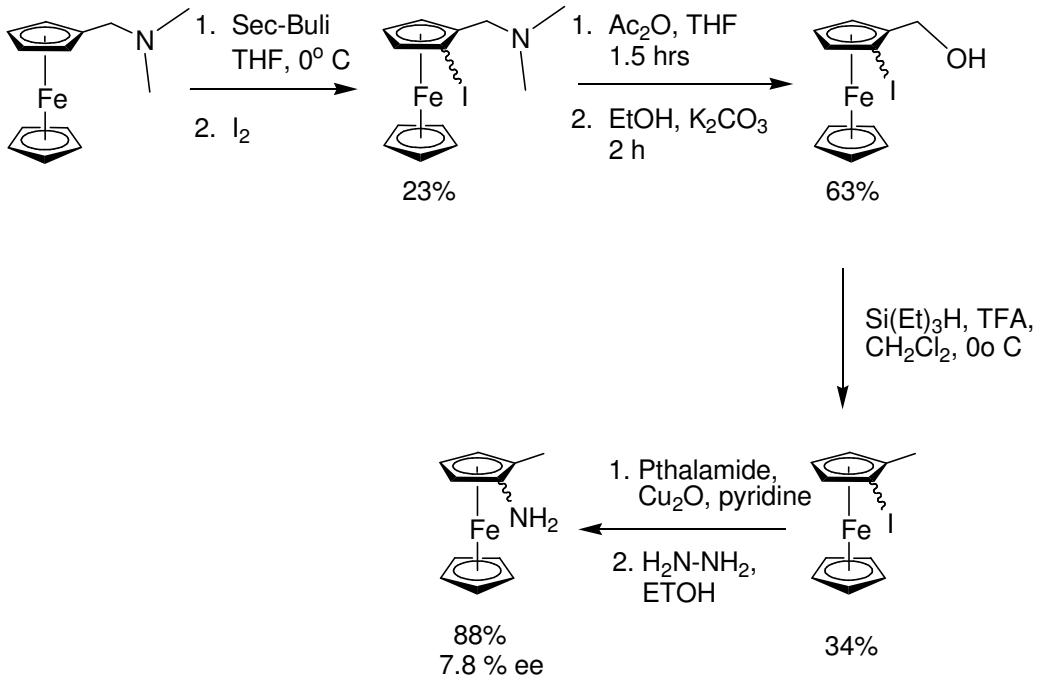


**Scheme 1.3**. Synthesis of Racemic Methyl-aminoferrocene

For establishing the optical purity of the described compounds, a chiral HPLC was performed. For these queries, the chiral/racemic amine was used since the absolute chirality of the metallocene will not change after the installation of bromine. From the results of these tests (**Figures 1.6** through **1.8**) it was shown that there was indeed a very high enantioselectivity involved in the installation of the Br. As the figures show the racemate (**Figure 1.6**) shows an approximate 1:1 mixture of the two isomers, while the two chiral versions (**Figures 1.7** and **1.8**) show a very highly

enantioselective reaction where >99% ee was observed. This was expected based on the study of Sammakia et al.[92]

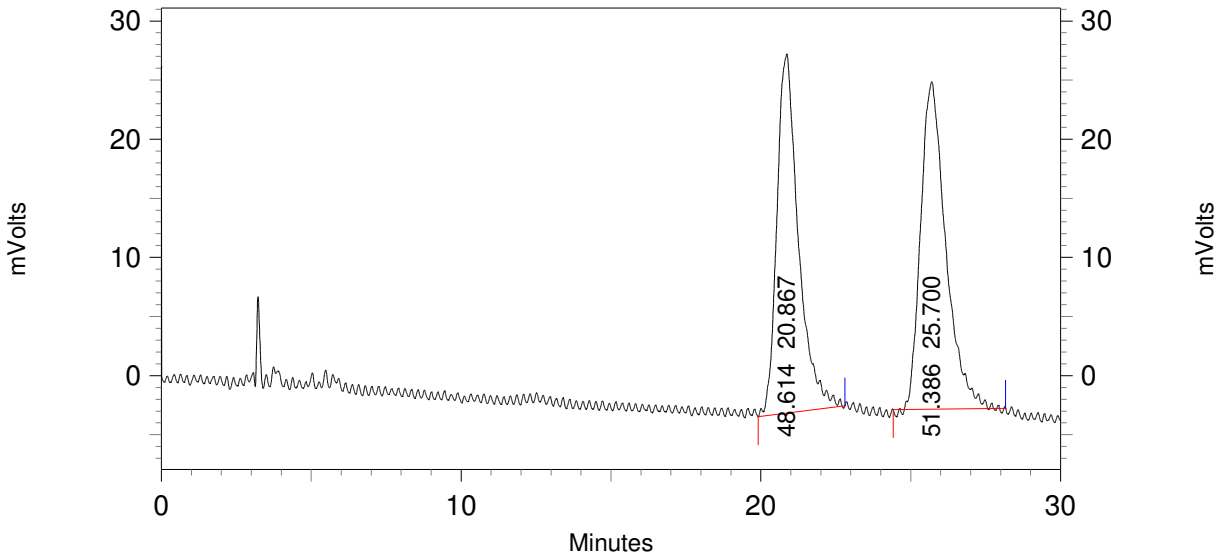


**Figure 1.6.** Chiral HPLC of rac-Amine

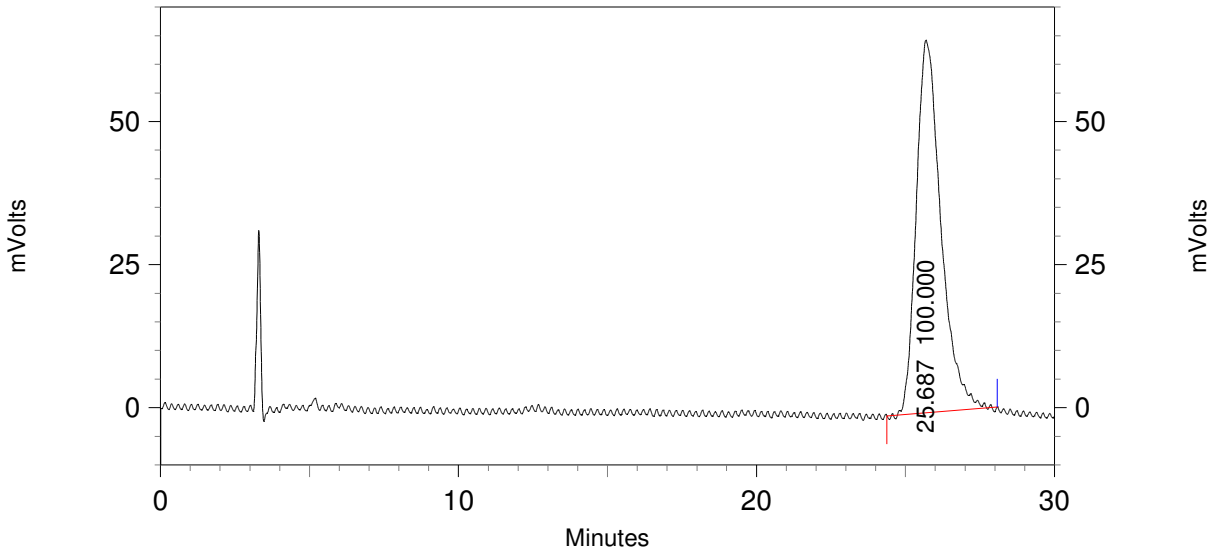


**Figure 1.7**. Chiral HPLC of pS Amine

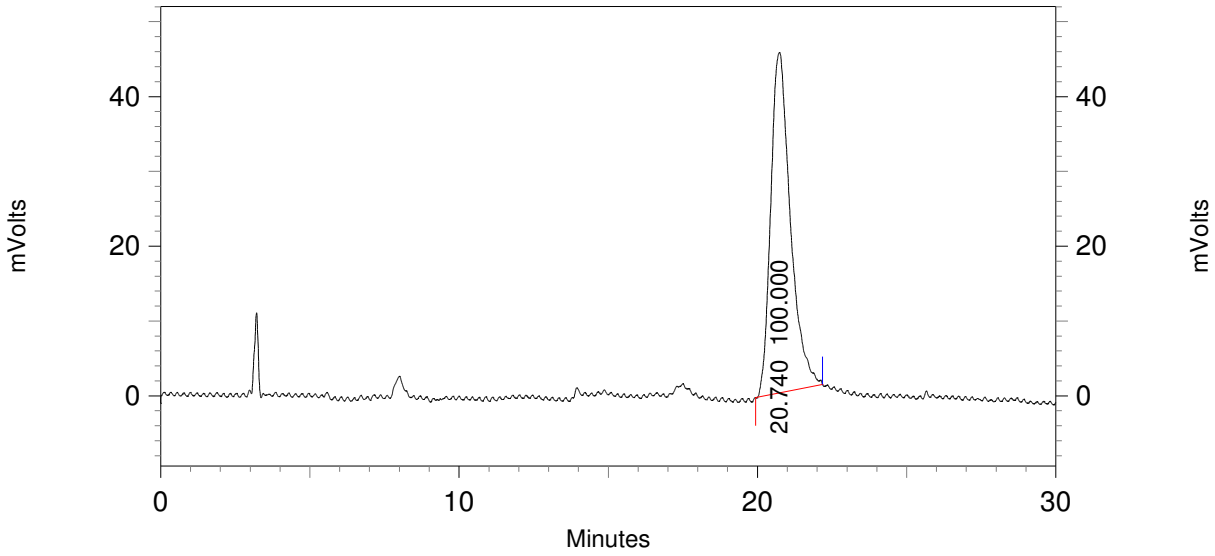


**Figure 1.8**. Chiral HPLC of pR Amine

To unambiguously assess the stereochemistry of ($_p$S)-1-isocyano-2-methyl ferrocene, two equivalents of it were reacted with $PdI_2$, to form $PdI_2$($_p$S)-$(Fc(CH_3)(CN))_2$. The IR spectrum of this complex is one of the most indicative characterization methods, with the $\upsilon_{CN}$ shifting from 2127 $cm^{-1}$ to 2203 $cm^{-1}$. This shift is strong evidence of a bonded isocyanide to Pd where the isocyano ligand is working predominately as a σ donor. The absolute stereochemistry can be determined by X-ray crystallography and will be discussed in more detail below.

### 1.4.2. Synthesis and characterization of 2

The synthesis of the Cr(($_p$S)-1-isocyano-2-methyl ferrocene)$_6$ (**Scheme 1.4**) was performed in order to explore the electrochemical behavior of the chiral isocyanoferrocene in relation to its un-substituted congener as well as to un-substituted isocyanocymentrene. Six equivalents of the chiral isocyanide were

reacted with Cr($\eta^6$-napthalene)$_2$ in THF to afford the homoleptic complex. This was verified through IR, which showed a broad stretch at 1947 cm$^{-1}$, as well as $^1$H NMR to verify the purity of the product.

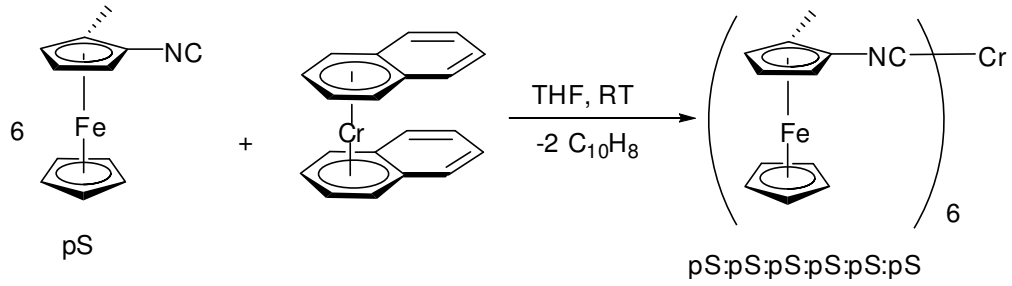


**Scheme 1.4.** Synthesis of Cr((pS)-1-isocyano-2-methyl ferrocene)$_6$

### 1.4.3. Electrochemical and DFT Studies of Organometallic Isocyanocyclopentadienides

The synthesis and characterization of the Cr(CmNC)$_6$ and Cr(FcNC)$_6$ are described in other sources.[43,45] The resulting compounds had their electrochemical properties explored through cyclic voltammetry. The cyclic voltammograms of these two complexes, show two one-electron, quasi-reversible anodic waves[80], that are related to the Cr(0→1$^+$) and Cr(1$^+$→2$^+$) redox potentials (**Figures 1.9** and **1.10**). The values of the peaks at a scan rate of 100 mV/s show $\Delta E_{pc,pa}$= 79-88 mV and a $i_c/i_a \approx 1$, which could be considered reversible since the external Fc/Fc$^+$ shows an $\Delta E_{pc,pa}$= 89 mV under identical experimental conditions. The electrochemical data shown in **Table 1.1** implies that the σ-donor/π-acceptor ratio (looking at the relative contributions of the two bonding interactions based on the ease or difficulty of the reduction/oxidation of the metal center)[23] of the isocyanide ligands goes down substantially in the series of $C_6H_{11}NC$ << FcNC < PhNC << CmNC.

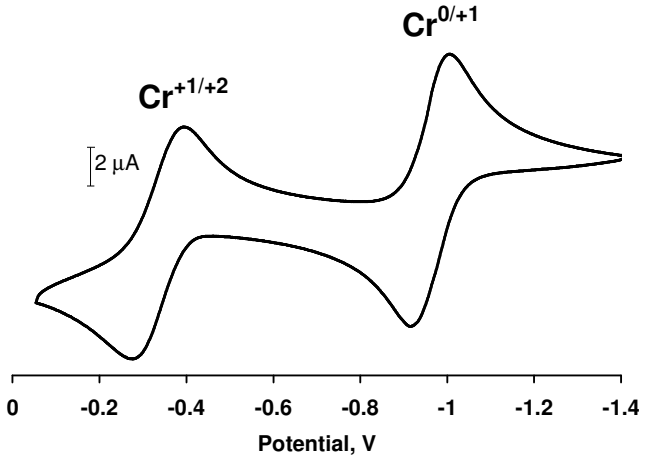


**Figure 1.9** Cyclic voltammogram of $Cr(FcNC)_6$ in 0.1 M $[^nBu_4N][PF_6]/CH_2Cl_2$ vs. $Fc/Fc^+$. Scan rate = 100 mV/s.

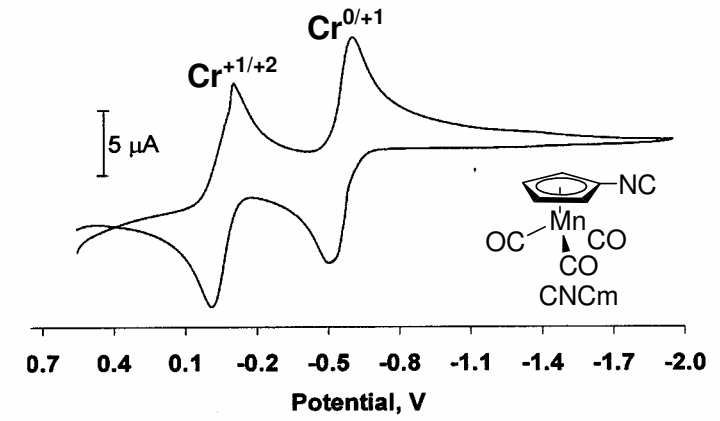


**Figure 1.10.** Cyclic voltammogram of $Cr(CmNC)_6$ in 0.1 M $[^nBu_4N][PF_6]/CH_2Cl_2$ vs. $Fc/Fc^+$. Scan rate = 100 mV/s.

**Table 1.1.** $E_{1/2}$ Potentials[a] for $[Cr(RNC)]^{z/z+1}$ vs. $Fc/Fc^{+}$ [a]

| R | | | | |
|---|---|---|---|---|
| **couple** | **$C_6H_{11}$** [100] | **Fc** | **Ph** [101] | **Cm** |
| **$[Cr(CNR)_6]^{0/1+}$** | -1.54 | -0.97 | -0.83 | -0.53 |
| **$[Cr(CNR)_6]^{1+/2+}$** | -0.77 | -0.35 | -0.21 | -0.04 |

[a]All measurements were performed in $CH_2Cl_2/[^nBu_4N][PF_6]$ to insure quantitative comparison.

The $E_{1/2}$ values of the $Cr^{z/z+1}$ redox couples are influenced by π-back bonding, and the value for these should be highest when the $Cr^0/Cr^I$ is in an electron rich system, also the amount of the σ donation (RNC:→Cr) should be the highest when the chromium metal center is oxidized to its +2 state. Looking at the trend in **Table 1.1**, it can be concluded that CmNC is a much stronger π acceptor, as well as potentially a slightly weaker σ donor than FcNC. To investigate this concept further, density functional theory (DFT)-generated molecular orbitals (MO's) of the two base ligands were generated. **Figure 1.11** shows the virtual MO's that have the ability to π-backbond with the metal center. In the case of the CmNC the lowest unoccupied molecular orbital (LUMO), LUMO+3, LUMO+6 show a much greater stabilization as compared to the corresponding MO's of FcNC (LUMO, LUMO+2, LUMO+3). This shows that CmNC is a stronger π acid than FcNC. Also when looking at the HOMO-7 (HOMO = Highest Occupied Molecular Orbital) of CmNC, the electron density is seen primarily on the terminal carbon atom, its lone pair of electrons, and should be considered anti-bonding with respect to the C–NR bond. To further corroborate this, the HOMO-7 of CmNC is ~ 0.5 eV more stabilized than the similar

molecular orbital (HOMO-7) of FcNC as illustrated in the Figure **1.11**. Thus, CmNC would definitely be a slightly weaker σ-donor than FcNC.

The aforementioned electrochemical analysis shows that the donor/acceptor characteristics of isocyanoferrocene are much more similar to those of aryl isocyanides than to alkyl isocyanides. To further this argument, the $E_{1/2}$ potential of $[Cr(MeNC)_6]^{0/1+}$ couple in $CH_2Cl_2$ was predicted to be -1.67 eV vs. $Fc/Fc^+$,[102] which is 0.7 V more than the $[Cr(FcNC)_6]^{0/1+}$ system. It can be seen that isocyanoferrocene is a much stronger π-acceptor than isocyanomethane, so the previously suggested[47,48] electronic similarities between FcNC and MeNC should only apply to the donor properties of these isocyano ligand systems. The increase in π-acidity of FcNC, as compared to MeNC, is associated with the probability of the electron density via π-back bonding allowing for the delocalization into the ferrocenyl moiety. The LUMO and LUMO+2, as seen in **Figure 1.11**, seem very well suited for this mode of interaction.

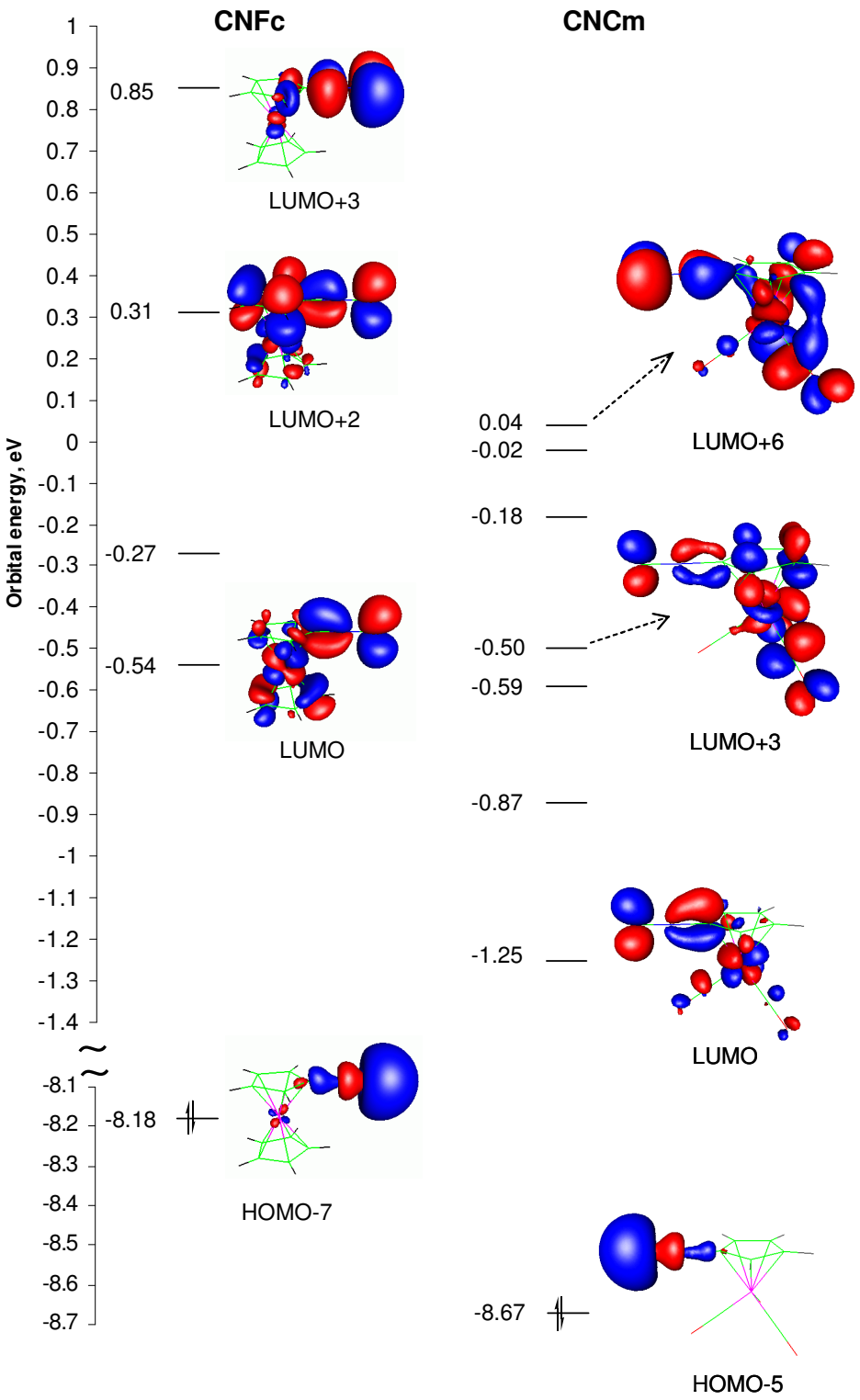


**Figure 1.11.** Selected molecular orbitals of FcNC (left) and CmNC(right) and their corresponding energies calculated at the 6-31 G (D, F) level. For clarity, structures of orbitals with no appreciable density on the isocyano-group are not shown. (Gerry Lushington) Reproduced in part with permission from *Organometallics* **2004**, *23*, 2927-2938. Copyright 2007 American Chemical Society.[43]

With the application of a more positive potential to the solution of FcNC, it produced a very broad anodic peak at ~0.42 V (**Figure 1.12**). The anodic waves shape was indicative for a diffusion controlled process for the oxidation of the six ferrocenyl moieties, with the Cr in a +2 oxidation state.[103] For the reduction half wave, interestingly, a very large response was observed. The symmetric shape of this wave suggests a non-diffusion controlled process for the product of the oxidation either was adsorbed or precipitated onto the platinum electrode surface.[104] A reasonable explanation for this observation is the low solubility of the highly charged cations, i.e. $[Cr(CNFc)_6]^{8+}$, in $CH_2Cl_2$. Once the octa-cation is reduced, the resulting $[Cr(CNFc)_6]^{2+}$ is dissolved into the solution and can then be further reduced, under a diffusion controlled process, generating the mono-cation as well as the neutral species again. Of some note, there was almost no loss of current for the Cr centered reductions when compared to the same oxidations in one red/ox cycle, thus the cyclic voltammogram in **Figure 1.12** stayed essentially the same through the course of several scans of the same sample. The $E_{1/2}$ potential of the Fe center for the II→III redox cycle for $[Cr(CNFc)_6]^{z/z+1}$ is expected to be ~0.26 V, which is very similar to the value of $E_{1/2}$ = 0.25 V ($\Delta E_{pa\text{-}pc}$ = 150 mv at a scan rate of 100 mV/s) for the free FcNC under the same conditions.

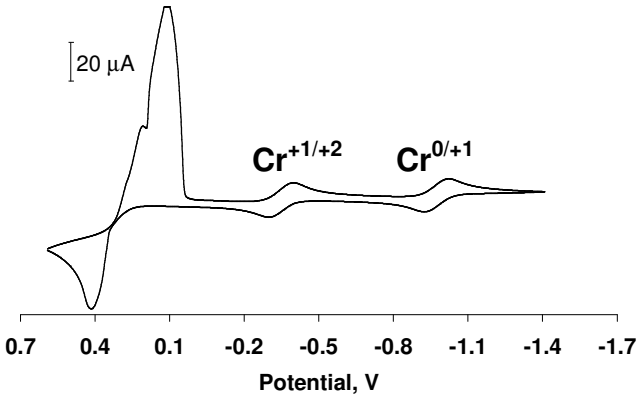


**Figure 1.12.** Cyclic voltammogram of $Cr(FcNC)_6$ in 0.1 M $[^nBu_4N][PF_6]/CH_2Cl_2$ vs. $Fc/Fc^+$ showing all accessible oxidation steps. Scan rate = 100 mV/s.

In **Table 1.2,** the electrochemical properties of the redox couples are shown in relation to the chiral molecule versus it's achiral parent. As was expected, the chiral isocyanoferrocene was a slightly better σ donor than the parent complex. This can be rationalized by the methyl group acting as an electron donor to the Cp ring of the ferrocene, thus making it electron rich. This in turn will make it more difficult for π-back bonding to occur between the metal and the ligand giving rise to the slightly more negative redox potential for the chiral ligand versus its non-optically active parent molecule.

**Table 1.2.** $E_{1/2}$ Potentials (in V) for $[Cr(RNC)_6]^{z/z+1}$ versus $Fc/Fc^+$

| $Cr(CNR)_6$ \ R | S- 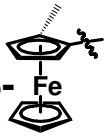 |  |
|---|---|---|
| $E_{1/2}(Cr^{0/1+})$, V | -1.03 | -0.97 |
| $E_{1/2}(Cr^{1+/2+})$, V | -0.32 | -0.36 |
| $E_{p,a}(Fe^{2+/3+})$, V | +0.39 | +0.42 |

The chiral ferrocene, electrochemically, is very similar to the parent ligand, as can be seen in **Figure 1.13**. The cyclic voltammograms's of the chiral ligand shows two one-electron, quasi-reversible anodic waves[80], that are related to the $Cr(0 \rightarrow 1^+)$ and $Cr(1^+ \rightarrow 2^+)$ redox potentials (**Figure 1.13**). The values of the peaks at a scan rate of 100 mV/s show $\Delta E_{pc,pa}$= 87-90 mV and a $i_c/i_a \approx 1$, which could be considered reversible since the external $Fc/Fc^+$ shows an $\Delta E_{pc,pa}$= 89 mV under identical experimental conditions. The phenomenon that was seen in the parent complex, i.e. the anodic wave's shape, which was indicative of a diffusion controlled process for the oxidation of the six ferrocenyl moieties, was observed in the case of the chiral homoleptic compound.[105] Once more for the reduction half wave, a very large response was observed. The symmetric shape of this wave suggests a non-diffusion controlled process for the product of the oxidation again was either adsorbed or precipitated onto the Pt electrode surface.[104]

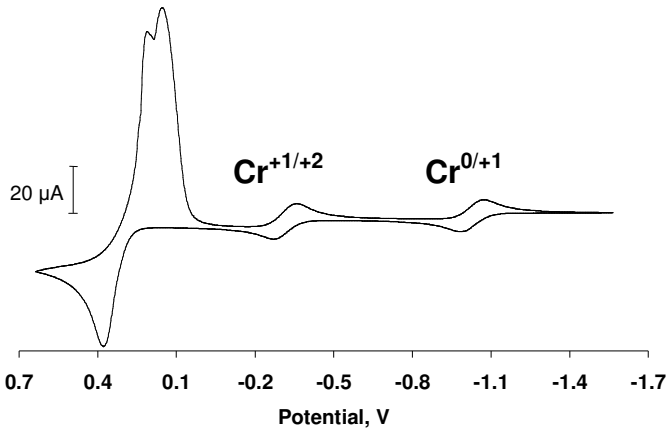


**Figure 1.13.** Cyclic voltammogram of $Cr(Fc(Me)NC)_6$ in 0.1 M $[^nBu_4N][PF_6]/CH_2Cl_2$ vs. $Fc/Fc^+$ showing all accessible oxidation steps. Scan rate = 100 mV/s.

The cyclic voltammograms of $Cr(Fc(Me)NC)_6$ shows a one-electron, quasi-reversible anodic wave[80], that is related to Fe ($2^+ \rightarrow 3^+$) redox potential (**Figure 1.13**). The value of the peak at a scan rate of 100 mV/s show $\Delta E_{pc,pa}$= 87 mV and a $i_c/i_a \approx 1$, which could be considered reversible since the internal $Fc/Fc^+$ shows an $\Delta E_{pc,pa}$= 58 mV under the experimental conditions.

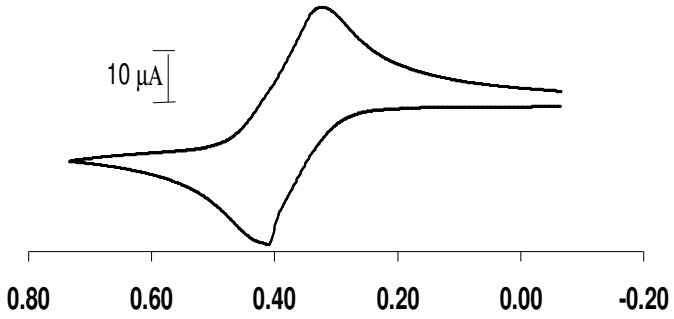


**Figure 1.14.** Cyclic voltammogram of $PdI_2(Fc(Me)NC)_2$ in 0.1 M $[^nBu_4N][PF_6]/CH_2Cl_2$ vs. $Fc/Fc^+$ showing all accessible oxidation steps. Scan rate = 100 mV/s.

### 1.4.4. Crystallographic studies of 1

The ultimate stereo chemistry of the planar chiral isocyanoferrocene is seen in the x-ray structure of its Pd complex. **Figure 1.15** shows the ORTEP Diagram of $PdI_2(_pS)$-$(Fc(CH_3)(NC))_2$ where the two $(_pS)$-$Fc(CH_3)(NC)$ are connected to the Pd metal center. The methyl groups on the chiral isocyanoferrocene are arranged in such a manner that it is indeed the $_pS$ arrangement for the ligand. When the Flack parameter was calculated it was 0.0256, which shows the configuration is correct. If the parameter $\approx$ 1, the stereochemistry of the molecule is reversed, and if the parameter $\approx$ 0.5 then it is a racemic mixture.[87,88] The average Pd-C and C-NFc distances are 1.953(4) Å and 1.156(6) Å respectively, with the average C-N-C angle

of 176.5(4)°. This data, in conjunction with the $\nu_{CN}$ = 2203 $cm^{-1}$ is very indicative of very little back donation to the metal center for this species.

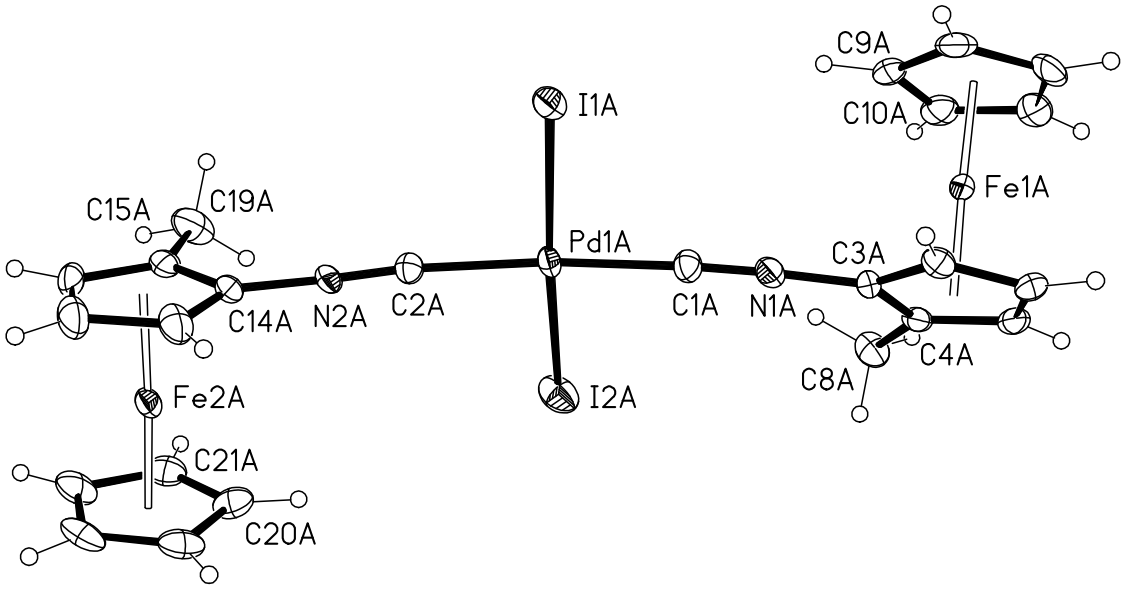


**Figure 1.15**. ORTEP Diagram (50 %) of $PdI_2(_pS)$-$(Fc(CH_3)(CN))_2$

### 1.4.5. Conclusions and future directions

The first planar chiral isocyanide, with its stereochemical cousin and its racemic amine congener have been efficiently synthesized from readily available starting materials and characterized. This expands the library of known planar chiral ferrocene ligands further through the use of an oxazoline fragment, which is an extremely useful tool in developing stereochemistry in metallocenes. Two transition metal complexes using $PdI_2$ and $Cr(C_{10}H_{10})_2$ were synthesized using the described planar chiral ligand system. The Pd complex was characterized by x-ray analysis to confirm the overall stereochemistry of the compound through the synthesis was preserved. In conjunction with x-ray analysis, the ligands were scrutinized using

chiral HPLC to further verify the absolute nature of their optical activity. The $Cr(Fc(Me)NC)_6$ complex was characterized via NMR and CV.

The electrochemical properties of the $[Cr(RNC)_6]^{0,1+,2+}$ (R = Fc and Cm) series indicates that the electronic influences of the ferrocenyl moiety is similar to aryl substituents, rather than alkyl, thus it was seen that the donor/acceptor characteristics of the isocyanoferrocene ligand are much closer to those of aryl isocyanides than they are to alkyl isocyanides, including methylisocyanide, which it had previously been thought to be similar to. Additionally, it was shown that the electronic properties (especially the π-acidity) of the isocyanocyclopentadienide ligand can be tuned, to a very large extent, by changing the nature of the transition metal bound to its ring.

Overall, the work described in this chapter constitutes significant progress towards the synthesis of planar chiral isocyanides and the electrochemical characterization of a series of cyclopentadienyl ligand systems. Further efforts in this project include the exploration of the planar chiral ligand in polymeric studies to form stereospecific helical polymers. It is also feasible to study the use of the ligand systems in the ongoing development of chiral catalysts.

## 1.5. References


1. Ugi, I.; Werner, B.; Dömling, A. *Molecules* **2003**, *8*, 53-66.

2. Weber, L. *Current Medicinal Chemistry* **2002**, *9*, 1241-1253.

3. Dömling, A. *Current Opinion in Chemical Biology* **2002**, *6*, 306-313.

4. Ugi, I. *Pure and Applied Chemistry* **2001**, *73*, 187-191.

5. Dömling, A. *Current Opinion in Chemical Biology* **2000**, *6*, 318-323.

6. Rossen, K.; Pye, P. J.; DiMichele, L. M.; Volante, R. P.; Reider, P. J. *Tetrahedron Letters* **1998**, *39*, 6823-6826.

7. Groeger, H.; Hatam, M.; Martens, J. *Tetrahedron* **1995**, *51*, 7173-80.

8. Ebert, B. M.; Ugi, I. K.; Grosche, M.; Herdtweck, E.; Herrmann, W. A. *Tetrahedron* **1998**, *54*, 11887-11898.

9. Xu, P.; Lin, W.; Zhang, T.; Hu, X.; Zou, X. *Journal of Chinese Pharmaceutical Sciences* **2001**, *10*, 9-13.

10. Endo, A.; Yanagisawa, A.; Abe, M.; Tohma, S.; Kan, T.; Fukuyama, T. *Journal of the American Chemical Society* **2002**, *124*, 6552-6554.

11. Sharma, V.; Piwnica-Worms, D. *Chemical Reviews (Washington, D. C.)* **1999**, *99*, 2545-2560.

12. Wackers, F. J.; Berman, D. S.; Maddahi, J.; Watson, D. D.; Beller, G. A.; Strauss, H. W.; Boucher, C. A.; Picard, M.; Holman, B. L.; Fridrich, R. *Journal of nuclear medicine : official publication, Society of Nuclear Medicine* **1989**, *30*, 301-11.

13. Abrams, M. J.; Davison, A.; Jones, A. G.; Costello, C. E.; Pang, H. *Inorganic Chemistry* **1983**, *22*, 2798-800.

14. Alexandrakis, M. G.; Kyriakou, D. S.; Passam, F. H.; Malliaraki, N.; Christophoridou, A. V.; Karkavitsas, N. *Clinical and laboratory haematology* **2002**, *24*, 155-9.

15. Fonti, R.; Del Vecchio, S.; Zannetti, A.; De Renzo, A.; Di Gennaro, F.; Catalano, L.; Califano, C.; Pace, L.; Rotoli, B.; Salvatore, M. *European journal of nuclear medicine* **2001**, *28*, 214-20.

16. Yildiz, A.; Garipagaoglu, M.; Gungor, F.; Boz, A.; Dalmaz, G. *Cancer biotherapy & radiopharmaceuticals* **2001**, *16*, 163-9.

17. Zhou, J.; Higashi, K.; Ueda, Y.; Kodama, Y.; Guo, D.; Jisaki, F.; Sakurai, A.; Takegami, T.; Katsuda, S.; Yamamoto, I. *Journal of Nuclear Medicine* **2001**, *42*, 1476-1483.

18. Dirlik, A.; Burak, Z.; Goksel, T.; Erinc, R.; Karakus, H.; Ozcan, Z.; Veral, A.; Ozhan, M. *Annals of nuclear medicine* **2002**, *16*, 103-8.

19. Sathekge, M. M.; Mageza, R. B.; Muthuphei, M. N.; Modiba, M. C.; Clauss, R. C. *Head & neck* **2001**, *23*, 305-10.

20. Herman, L. W.; Sharma, V.; Kronauge, J. F.; Barbarics, E.; Herman, L. A.; Piwnica-Worms, D. *Journal of Medicinal Chemistry* **1995**, *38*, 2955-63.

21. Piwnica-Worms, D. R.; (Brigham and Women's Hospital, USA). Application: WO, 1993, p 71 pp.

22. Singleton, E.; Oosthuizen, H. E. *Advances in Organometallic Chemistry* **1983**, *22*, 209-310.

23. Treichel, P. M. *Advances in Organometallic Chemistry* **1973**, *11*, 21-86.

24. Yamamoto, Y. *Coordination Chemistry Reviews* **1980**, *32*, 193-233.

25. Carnahan, E. M.; Protasiewicz, J. D.; Lippard, S. J. *Accounts of Chemical Research* **1993**, *26*, 90-7.

26. Cornelissen, J. L.; Rowan, A. E.; Nolte, R. J. M.; Sommerdijk, N. A. J. M. *Chemical Reviews (Washington, DC, United States)* **2001**, *101*, 4039-4070.

27. Nakano, T.; Okamoto, Y. *Chemical Reviews (Washington, DC, United States)* **2001**, *101*, 4013-4038.

28. Clericuzio, M.; Alagona, G.; Ghio, C.; Salvadori, P. *Journal of the American Chemical Society* **1997**, *119*, 1059-1071.

29. Kollmar, C.; Hoffmann, R. *Journal of the American Chemical Society* **1990**, *112*, 8230-8.

30. Drenth, W.; Nolte, R. J. M. *Accounts of Chemical Research* **1979**, *12*, 30-5.

31. Kauranen, M.; Verbiest, T.; Boutton, C.; Teerenstra, M. N.; Clays, K.; Schouten, A. J.; Nolte, R. J. M.; Persoons, A. *Science (Washington, D. C.)* **1995**, *270*, 966-9.

32. Kauranen, M.; Verbiest, T.; Meijer, E. W.; Havinga, E. E.; Teerenstra, M. N.; Schouten, A. J.; Nolte, R. J. M.; Persoons, A. *Advanced Materials (Weinheim, Germany)* **1995**, *7*, 641-4.

33. Yamagishi, A.; Tanaka, I.; Taniguchi, M.; Takahashi, M. *Journal of the Chemical Society, Chemical Communications* **1994**, 113-14.

34. Malatesta, L. *Progr. in Inorg. Chem. (F. Albert Cotton, editor. Interscience Publishers, Inc.)* **1959**, *1*, 283-379.

35. Meier, M.; Mueller, B.; Ruechardt, C. *Journal of Organic Chemistry* **1987**, *52*, 648-52.

36. Weber, L. *Angewandte Chemie, International Edition* **1998**, *37*, 1515-1517.

37. Hahn, F. E. *Angewandte Chemie* **1993**, *105*, 681-96 (See also Angew Chem , Int Ed Engl , **1993**, 32(5), 650-65.

38. Chen, J.; Calvet, L. C.; Reed, M. A.; Carr, D. W.; Grubisha, D. S.; Bennett, D. W. *Chemical Physics Letters* **1999**, *313*, 741-748.

39. Henderson, J. I.; Feng, S.; Bein, T.; Kubiak, C. P. *Langmuir* **2000**, *16*, 6183-6187.

40. Wagner, N. L.; Laib, F. E.; Bennett, D. W. *Inorganic Chemistry Communications* **2000**, *3*, 87-90.

41. Hanack, M.; Kamenzin, S.; Kamenzin, C.; Subramanian, L. *Synthetic Metals* **2000**, *11*, 93-102.

42. Robinson, R. E.; Holovics, T. C.; Deplazes, S. F.; Powell, D. R.; Lushington, G. H.; Thompson, W. H.; Barybin, M. V. *Organometallics* **2005**, *24*, 2386-2397.

43. Holovics, T. C.; Deplazes, S. F.; Toriyama, M.; Powell, D. R.; Lushington, G. H.; Barybin, M. V. *Organometallics* **2004**, *23*, 2927-2938.

44. Robinson, R. E.; Holovics, T. C.; Deplazes, S. F.; Lushington, G. H.; Powell, D. R.; Barybin, M. V. *Journal of the American Chemical Society* **2003**, *125*, 4432-4433.

45. Barybin, M. V.; Holovics, T. C.; Deplazes, S. F.; Lushington, G. H.; Powell, D. R.; Toriyama, M. *Journal of the American Chemical Society* **2002**, *124*, 13668-13669.

46. Knox, G. R.; Pauson, P. L.; Willison, D.; Solcaniova, E.; Toma, S. *Organometallics* **1990**, *9*, 301-6.

47. El-Shihi, T.; Siglmueller, F.; Herrmann, R.; Fernanda, M.; Carvalho, N. N.; Pombeiro, A. J. L. *Journal of Organometallic Chemistry* **1987**, *335*, 239-47.

48. El-Shihi, T.; Siglmueller, F.; Herrmann, R.; Carvalho, M. F. N. N.; Pombeiro, A. J. L. *Portugaliae Electrochimica Acta* **1987**, *5*, 179-84.

49. van Leusen, D.; Hessen, B. *Organometallics* **2001**, *20*, 224-226.

50. Bildstein, B.; Malaun, M.; Kopacka, H.; Wurst, K.; Mitterböck, M.; Ongania, K.-H.; Opromolla, G.; Zanello, P. *Organometallics* **1999**, *18*, 4325-4336.

51. Kavallieratos, K.; Hwang, S.; Crabtree, R. H. *Inorganic Chemistry* **1999**, *38*, 5184-5186.

52. Shafir, A.; Power, M. P.; Whitener, G. D.; Arnold, J. *Organometallics* **2000**, *19*, 3978-3982.

53. Nesmeyanov, A. N.; Perevalova, E. G.; Gubin, S. P.; Grandberg, I. I.; Kozlovskii, A. G. *Tetrahedron Letters* **1966**, 2381-87.

54. Schlögl, K. *Top. Stereochem* **1967**, *1*, 38-39.

55. Togni, A.; Hayashi, T.; Editors *Ferrocenes: homogeneous catalysis, organic synthesis, materials science*, 1995.

56. Sutcliffe, O. B. B., M. R. *Tetrahedron: Asymmetry* **2003**, *14*, 2297-2325.

57. Delacroix, O. G., J. A *Chemical Communications (Cambridge)* **2003**, 665-675.

58. Colacot, T. J. *Chemical Reviews (Washington, D. C.)* **2003**, *103*, 3101-3118.

59. Blaser, H.-U. B., W.; Pugin, B.; Spindler, F.; Studer, M.; Togni, A *Top. Catal.* **2002**, *19*, 3-16.

60. Blaser, H.-U. *Adv. Synth. Catal.* **2002**, *344*, 17-31.

61. Fu, G. C. *Accounts of Chemical Research* **2000**, *33*, 412-420.

62. Hayashi, T. *Accounts of Chemical Research* **2000**, *33*, 354-362.

63. Boudier, A. B., L. O.; Lotz, M.; Knochel, P *Angew. Chem., Int. Ed.* **2000**, *39*, 4415-4435.

64. Bolm, C. M., K *Chem. Soc. Rev.* **1999**, 51-59.

65. Richards, C. J. L., A. J *Tetrahedron: Asymmetry* **1998**, *9*, 2377-2407.

66. Kagan, H. B. R., O *Adv. Asymmetric Synth.* **1997**, *2*, 189-235.

67. Ito, Y. S., M. *Chem. Rev.* **1992**, *92*, 857-871.

68. Lee, J. H. S., S. U.; Chung. Y. K. *Tetrahedron: Asymmetry* **2003**, *14*, 2109-2113.

69. Son, S. U. P., K. H.; Lee, S. J.; Seo, H.; Chung, Y. K. *Chemical communications* **2002**, 1230-1231.

70. Kudis, S.; Helmchen, G. *Angewandte Chemie, International Edition* **1998**, *37*, 3047-3050.

71. Son, S. U. P., K. H.; Lee, S. J.; Chung, Y. K.; Sweigart, D.A. *Chemical Communications* **2001**, 1290-1291.

72. Bolm, C. M., K *Chem. Soc. Rev.* **1999**, 51-59.

73. Nelson, S. G. H., M. A. *Organic Letters* **1999**, *1*, 1379-1382.

74. Pickett, T. E.; Roca, F. X.; Richards, C. J. *Journal of Organic Chemistry* **2003**, *68*, 2592-2599.

75. Locke, A. J.; Pickett, T. E.; Richards, C. J. *Synlett* **2001**, 141-143.

76. Christopher J. Richards, T. D., David E. Hibbs and Michael B. Hursthouse *Synlett* **1995**, 74-76.

77. Pickett, T. E.; Richards, C. J. *Tetrahedron Letters* **2001**, *42*, 3767-3769.

78. Richards, C. J.; Damalidis, T.; Hibbs, D. E.; Hursthouse, M. B. *Synlett* **1995**, *1*, 74-76.

79. Pomije, M. K.; Kurth, C. J.; Ellis, J. E.; Barybin, M. V. *Organometallics* **1997**, *16*, 3582-3587.

80. Zietlow, T. C.; Klendworth, D. D.; Nimry, T.; Salmon, D. J.; Walton, R. A. *Inorganic Chemistry* **1981**, *20*, 947-9.

81. Connelly, N. G.; Geiger, W. E. *Chemical Reviews (Washington, D. C.)* **1996**, *96*, 877-910.

82. Becke, A. D. *Journal of Chemical Physics* **1993**, *98*, 5648-52.

83. Miehlich, B.; Savin, A.; Stoll, H.; Preuss, H. *Chemical Physics Letters* **1989**, *157*, 200-6.

84. Lee, C.; Yang, W.; Parr, R. G. *Physical Review B: Condensed Matter and Materials Physics* **1988**, *37*, 785-9.

85. Hariharan, P. C.; Pople, J. A. *Molecular Physics* **1974**, *27*, 209-14.

86. Frisch, M. J.; Pople, J. A.; Binkley, J. S. *Journal of Chemical Physics* **1984**, *80*, 3265-9.

87. Flack, H. D. *Acta Crystallographica, Section A: Foundations of Crystallography* **1983**, *A39*, 876-81.

88. Flack, H. D.; Schwarzenbach, D. *Acta Crystallographica, Section A: Foundations of Crystallography* **1988**, *A44*, 499-506.

89. Pickett, T. E.; Richards, C. J. *Tetrahedron: Asymmetry* **1999**, *10*, 4095-4097.

90. Roca, F. X.; Motevalli, M.; Richards, C. J. *Journal of the American Chemical Society* **2005**, *127*, 2388-2389.

91. Vorbrueggen, H.; Krolikiewicz, K. *Tetrahedron Letters* **1981**, *22*, 4471-4.

92. Sammakia, T.; Latham, H. A. *Journal of Organic Chemistry* **1995**, *60*, 6002-3.

93. Tu, T.; Hou, X.-L.; Dai, L.-X. *Journal of Organometallic Chemistry* **2004**, *689*, 3847-3852.

94. Manoury, E.; Fossey, J. S.; Aiet-Haddou, H.; Daran, J.-C.; Balavoine, G. G. A. *Organometallics* **2000**, *19*, 3736-3739.

95. Tu, T.; Deng, W.-P.; Hou, X.-L.; Dai, L.-X.; Dong, X.-C. *Chemistry--A European Journal* **2003**, *9*, 3073-3081.

96. Dai, L.-X.; Tu, T.; You, S.-L.; Deng, W.-P.; Hou, X.-L. *Accounts of Chemical Research* **2003**, *36*, 659-667.

97. Kuwano, R.; Uemura, T.; Saitoh, M.; Ito, Y. *Tetrahedron: Asymmetry* **2004**, *15*, 2263-2271.

98. Peer, M.; de Jong, J. C.; Kiefer, M.; Langer, T.; Rieck, H.; Schell, H.; Sennhenn, P.; Sprinz, J.; Steinhagen, H.; Wiese, B.; Helmchen, G. *Tetrahedron* **1995**, *52*, 7547-7583.

99. Patti, A.; Lambusta, D.; Piattelli, M.; Nicolosi, G. *Tetrahedron: Asymmetry* **1998**, *9*, 3073-3080.

100. Mialki, W. S.; Wigley, D. E.; Wood, T. E.; Walton, R. A. *Inorganic Chemistry* **1982**, *21*, 480-5.

101. Bullock, J. P.; Mann, K. R. *Inorganic Chemistry* **1989**, *28*, 4006-11.

102. Bursten, B. E. *Journal of the American Chemical Society* **1982**, *104*, 1299-304.

103. For the [Cr(CNFc.6]z system, the Cr(II)/Cr(III) oxidation (if it is possible at all) is expected to occur at a much more positive potential as compared to the Fe(II)/Fe(III) processes.

104. Bond, A. M.; Colton, R.; Mahon, P. J.; Snook, G. A.; Tan, W. T. *Journal of Physical Chemistry B* **1998**, *102*, 1229-1234.

105. For the [Cr(CNFc)6]z system, the Cr(II)/Cr(III) oxidation (if it is possible at all) is expected to occur at a much more positive potential as compared to the Fe(II)/Fe(III) processes.

# Chapter Two

Isocyanoazulenes: a Quantitative Organometallic Approach for Probing Electronic Inhomogeneity of the Azulenic Framework

## 2.1. Introduction

Bicyclo[5.3.0]decapentaene, also known as azulene, was isolated from essential oils in the middle of the 19th century. However, its nonbenzenoid nature was not recognized until 1936.[1,2] This dark blue hydrocarbon has the molecular formula of $C_{10}H_8$ and is a constitutional isomer of naphthalene. Azulene is a polar molecule with the dipole moment of 1.08 D (**Figure 2.1**).

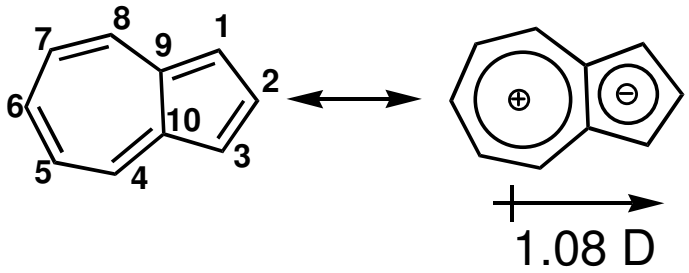


**Figure 2.1**. Azulene, its dipole moment, and carbon atom numbering scheme

The late 1950's marked the beginning of the synthetic chemistry of azulene, primarily through independent work of Hafner and Nozoe.[3-5] After their pioneering contributions, azulene and its derivatives (both natural and synthetic) have found numerous applications in synthesis. Syntheses of highly substituted azulenes,[6-8] as well as the incorporation of the azulenic moiety into porphyrin-like structures called azuliporphyrins,[9] have been demonstrated. Highly substituted azulenes have found use in the medical and pharmaceutical fields.[10-12] In particular, certain naturally occurring azulenes (e.g., chamazulene, guaiazulene, etc)[13] have been shown to exhibit anti-inflammatory, anti-ulcer, and anti-allergy properties. Azulene derivatives have also found their way into cosmetics products.[14]

In the last two decades, azulenic substances have been attracting increasing interest in materials science. In the field of advanced polymers, the azulenic framework has been incorporated into polymeric backbones along with thiophenes to result in stimuli- responsive polymers.[15] In addition, the azulenic motifs have been attached to the backbone of cellulose in attempts to make optoelectronic switches.[16] Biazulene-based polymers, incorporating the 1,1'-biazulenic motif, have also been used in the design of chiroptical switches.[17] Finally, azulenic derivatives have already been used, albeit scarcely, in the design of novel optical materials and liquid crystals.[15-24]

Azulene is a nonalternant aromatic compound. It's π-system constitutes a more general type of aromaticity as compared to the alternant systems, such as benzene or naphthalene, in which the π-electrons are evenly dispersed over even-membered ring(s). Because of this, the properties of azulene are not as straightforward to predict or rationalize.[3,4] **Figure 2.2** qualitatively compares the Frontier molecular orbitals of two isomeric structures: azulene and naphthalene.

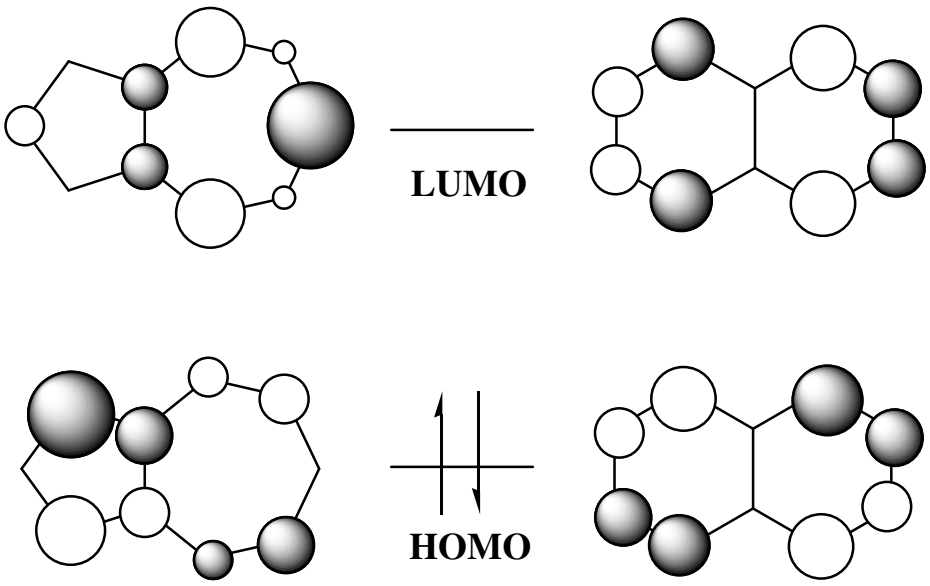


**Figure 2.2:** Frontier molecular orbitals of azulene and naphthalene[25]

From this illustration one can see that, unlike in the case of naphthalene, azulene's Highest Occupied Molecular Orbital (HOMO) and Lowest Unoccupied Molecular Orbital (LUMO) are not superimposable in terms of the squares of the atomic orbital coefficients. In fact, the density coefficients of azulene's HOMO and LUMO are localized in essentially different parts of the molecule. Therefore, the HOMO $\rightarrow$ LUMO excitation would result in substantially lower electron correlation energy in the case of azulene as compared to naphthalene. This phenomenon nicely explains why azulene absorbs in the visible region while naphthalene is colorless. The small HOMO-LUMO gap of azulene is a consequence of its relatively low aromatic stabilization energy (**Figure 2.3**).[26] This nonbenzenoid framework is very attractive for using its $\pi$-system in molecular electron transport systems.[27,28]

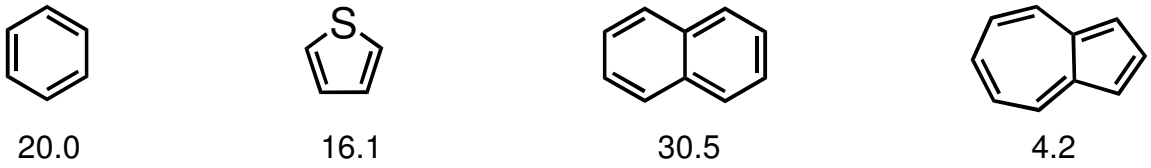


**Figure 2.3**: Comparison of aromatic delocalization energies (kcal/mol) for several aromatic species[26]

Since the discovery of azulene, great progress has been made in understanding its unusual physical and chemical properties, which arise from the electronic inhomogeneity of the nonbenzenoid framework.[6-24] However, the structure-property relationships in azulene chemistry are somewhat fragile,[6] and some are currently being debated.[27,29-31] While the azulene scaffold has been at the forefront in the development of several advanced organic materials,[6-24] its use in functional organometallic systems has been rather limited, primarily due to the propensity of the azulenic nucleus to undergo multi-hapto and, frequently, unpredictable bonding with transition metal atoms and ions (e.g., **Figure 2.4**).[32-34]

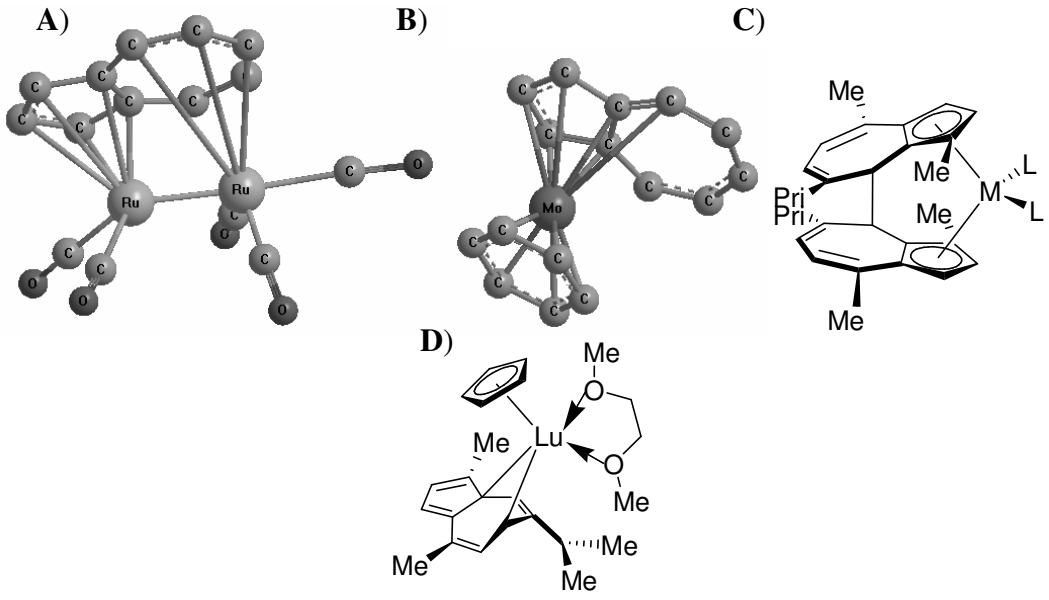


**Figure 2.4.** (Courtesy of Prof. M. V. Barybin). Examples of the multihapto coordination of azulene: A) $\eta^5$-$\eta^3$ [35] B) $\eta^6$ [34] C) $\eta^5$ [36] D) $\eta^2$ [36]

For example, interaction of azulene with $Mo(\eta^6\text{-}C_6H_6)_2$ affords complex $(\eta^6\text{-}C_{10}H_8)Mo(\eta^6\text{-}C_6H_6)$, in which the azulenic moiety undergoes coordination to the Mo-center via the carbon atoms 1, 2, 3, 4, 9 and 10 (**Figure 2.4.B**).[31] Azulene-containing complexes of transition metals with no direct interactions between the metal and the azulenic fragment are very uncommon and, typically, have metal ions bound to porphyrin-like rings[37,38] or "sandwiched" between $\eta^4$-cyclobutadienyl and/or $\eta^5$-cyclopentadienyl rings (e.g., **Figure 2.5**).[21,39-41] Azulene-based ligands are also known to undergo relatively facile C-C coupling reactions (e.g., Figure 1.4c)[32,36] and C-H activation transformations.[41,42]

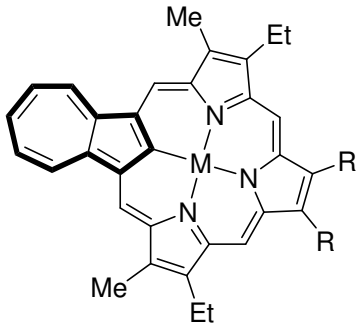


**Figure 2.5.** Example of azulene incorporated into a metal bound porphyrin (M = Ni,Pt or Pd; R = Et or Ph)[41]

The Barybin group has recently overcome the above challenge of constructing well-defined metal-azulene hybrid compounds by employing "alligator clips" between the metal atoms/ions and the azulenic scaffold. In particular, the isocyanide junction group proved exceptionally effective in this regard. An isocyanide (CNR) possesses cylindrical symmetry of the C≡N- bond. This is important for mediating electronic interaction between the metal orbitals of π-symmetry and the aromatic

moiety of azulene (because the coplanarity of these is no longer an absolute requirement for the maximum interaction between the π-systems to occur).[43]

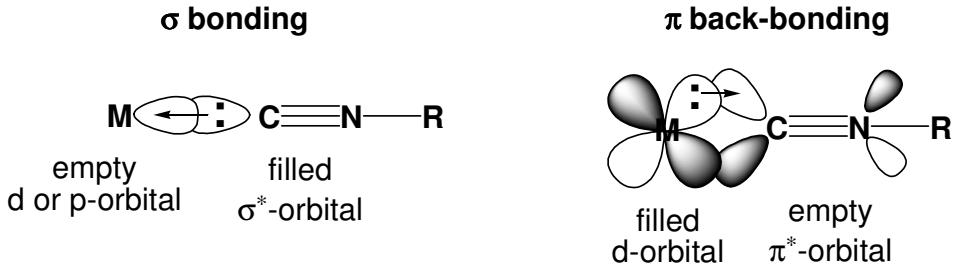


**Figure 2.6.** Representation of bonding interactions of organic isocyanides and transition metal ions (courtesy of Prof. M. V. Barybin).

Being similar to carbon monoxide as a ligand, the isocyanide is more versatile as it tends to stabilize metals in both high and low oxidation states.[44,45] The electronic and steric properties of isocyanides (CNR) are tunable by means of varying the substituent R. Two types of bonding interactions between a transition metal ion and an organic isocyanide are schematically shown in **Figure 2.6**. Notably, π-backbonding (**Figure 2.6**, right) may facilitate electronic communication between the electron–rich metal center and the π-system of the substituent R, if R is an aryl group.[46-49]

Incorporating the isocyanide substituent at the azulenic core would allow systematic exploration of the electronic nature of the azulenic π-system, as five different isomeric isocyanoazulenes might be considered (**Figure 2.7**).[27] Given the dipolar nature of the azulenic moiety, the isocyanoazulenes may be formally viewed as derivatives of hypothetical isocyanocyclopentadienyl ($CN^1Az$ and $CN^2Az$) or isocyanocycloheptatrienyl ($CN^4Az$, $CN^5Az$, and $CN^6Az$) rings. The atom of

attachment of the isocyanide will likely play a profound role in determining the electronic characteristics of the isocyanoazulenes as ligands. Recently, Dr. R. E. Robinson of the Barybin group was successful in the regioselective synthesis of all five possible isocyanoazulenes, which represent the first examples of nonbenzenoid organic isocyanides, as well as of many derivatives thereof.[27]

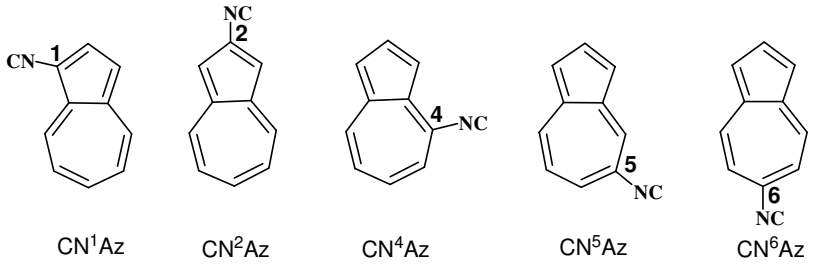


**Figure 2.7**. The five possible isomers of isocyanoazulene

With the ability to install a single isocyano group at every position of the azulenic core, one can envision various diisocyanoazulene motifs that could be used to bridge metal atoms and ions. Such architectures would be extremely attractive for molecular electronics applications. Indeed, the azulenic motif (a combination of fused 5- and 7-membered $sp^2$-hybridized carbon rings) occurs naturally as a defect in carbon nanotubes and has been demonstrated to be responsible for the unusually high conductivity of these inorganic systems.[50-54] Moreover, a structure made exclusively of carbon pentagons and heptagons has been predicted to exhibit metallic behavior.[55] Finally, it has been theorized that a 2,6-azulenic bridge between two electron reservoirs (**Figure 2.8**) should have remarkably facile charge transport characteristics.[56] Because of its asymmetric nature, this linker is also expected to have the asymmetric *I/V* profile, which is an important prerequisite in molecular switching applications.[56]

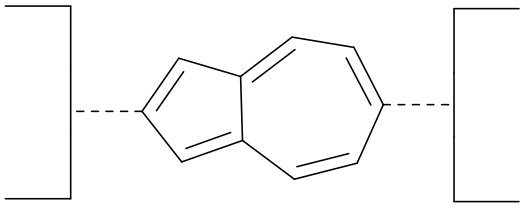

**Figure 2.8.** Schematic of a 2,6-azulenic bridge between two electron reservoirs[56]

The analytical technique known as Cyclic Voltammetry (CV) may prove useful in experimental determination of the HOMO-LUMO gaps of various azulene derivatives as the energy of the HOMO should correlate with the oxidation potential of the molecule whereas the energy of the LUMO may be related to its first reduction potential. Such an approach was used by chemists in the past and has been summarized by Naya *et al*. in 2005.[57] Furthermore, binary chromium isocyanide complexes of the type $[Cr(CNR)_6]^Z$ were shown by Mann *et al*.[58-61] and Treichel *et al.*[62-67] to have well-behaved, reversible CV profiles (**Figure 2.9**), which reflected the relative electron donor/acceptor properties of the CNR ligands depending on the substituent R. In addition, Lever explored isocyanides, along with other ligands, to compile an electrochemical series of ligands based upon the potential of the Ru (II/III) couple for their ruthenium complexes.[68]

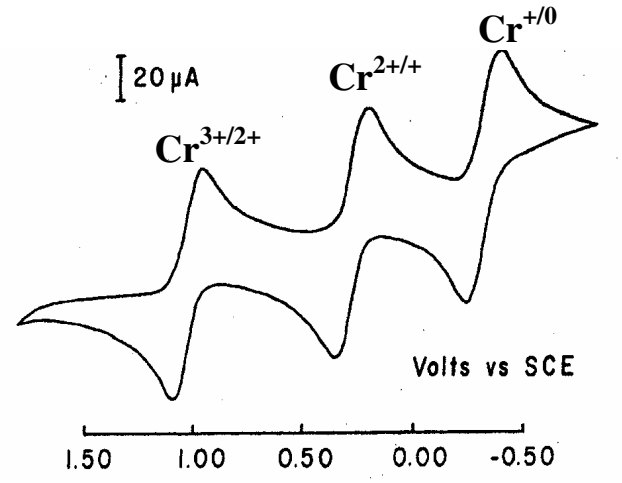


**Figure 2.9**: Cyclic Voltammogram of $[Cr(CNC_6H_5)_6]^+[PF_6]^-$ Reproduced in part with permission from *Inorganic Chemistry* **1976**, *15*, 146-150. Copyright 2007 American Chemical Society [63]

## 2.2. Work Described in Chapter Two

This chapter deals with the electrochemistry of azulene, its isocyanide derivatives, and chromium(0) and tungsten(0) complexes thereof. The first systematic investigation of the electronic inhomogeneity of the azulenic scaffold is presented. The electrochemical results are compared with those obtained through UV-vis and theoretical (DFT) studies. Determination and chemical consequences of the σ-donor/π-acceptor ratios of the isocyanoazulene ligands are described.[62] In addition, an electrochemical investigation of the first azulene-bridged bimetallic ensembles is reported.

## 2.3. Experimental Section

### 2.3.1. General Procedures

Methylene chloride was freed of impurities by standard procedures and stored under argon. Tetrabutylammonium hexafluorophosphate was purified by recrystalization from tetrahydrofuran/pentane. Cyclic voltammetric (CV) experiments on $2\times10^{-3}$ M solutions in $CH_2Cl_2$ were conducted at room temperature using an EPSILON electrochemical workstation. The electrochemical cell was placed in an argon-filled Vacuum Atmospheres dry-box. Tetrabutylammonium hexafluorophosphate (0.1 M solution in $CH_2Cl_2$) was used as a supporting electrolyte in all cases. Cyclic voltammograms were recorded at 22 ± 2 °C using a three component system consisting of a platinum working electrode, a platinum wire auxiliary electrode, and a glass encased non-aqueous silver/silver chloride reference electrode. The reference $Ag/Ag^+$ electrode was monitored with the ferrocene/ferrocenium couple. Under the experimental conditions employed, $\Delta E_{pa,pc}$ of the $Fc^+/Fc$ couple was 89 mV at the scan rate of 100 mV/s. This peak-to-peak separation is identical to that previously observed for the $Fc^+/Fc$ couple at 100 mV/s in a very similar electrochemical setup, which employed a 0.2 M solution of $[^nBu_4N][PF_6]$ in $CH_2Cl_2$ as a supporting electrolyte.[69] IR compensation was achieved before each CV run by measuring the uncompensated solution resistance followed by incremental compensation and circuit stability testing. Background cyclic voltammograms of the electrolyte solution were recorded before adding the analytes. The half-wave potentials ($E_{1/2}$) were determined as averages of the cathodic and

anodic peak potentials of reversible couples and are referenced to the $Fc^+/Fc$ couple. No significant difference (< 0.01 V) between external and internal referencing with $Fc^+/Fc$ was documented. The compounds that were subject to the CV experiments are listed in **Table 2.1**.

**Table 2.1**. List of compounds and figure numbers of the corresponding cyclic voltammograms reported in this Chapter

| **Compound** | **Figure # and designation** |
|---|---|
| Azulene | Figure 2.15 (**1**) |
| 1-Isocyanoazulene | Figure 2.16 (**2**) |
| 2-Isocyanoazulene | Figure 2.17 (**3**) |
| 4-Isocyanoazulene | Figure 2.18 (**4**) |
| 6-Isocyanoazulene | Figure 2.19 (**5**) |
| 1,3-Di-*tert*-butylazulene | Figure 2.20 (**6**) |
| 1,3-Di-*Tert*-butyl-5-isocyanoazulene | Figure 2.21 (**7**) |
| $[Cr(CN^{1}Az)_6]^+[BF_4]^-$ | Figure 2.22 (**8**) |
| $[Cr(CN^{2}Az)_6]^+[BF_4]^-$ | Figure 2.23 (**9**) |
| $[Cr(CN^{4}Az)_6]^+[\ SbF_6]^-$ | Figure 2.24 (**10**) |
| $Cr(5\text{-}CN\text{-}1,3\text{-}di\text{-}t\text{-}butyl\text{-}C_{10}H_5)_6$ | Figure 2.25 (**11**) |
| $[Cr(CN^{6}Az)_6]^+[\ BF_4]^-$ | Figure 2.26(**12**) |
| $[Cr(2\text{-}CN\text{-}1,3\text{-}CO_2Et\text{-}C_{10}H_5)_6]^+[BF_4]^-$ | Figure 2.28 (**13**) |
| $2,6\text{-}(CN)_2\text{-}1,3\text{-}(CO_2Et)_2\text{-}C_{10}H_4$ | Figure 2.35 (**14**) |
| $[Cr(CO)_5]_2(2\text{-}CN\text{-}1,3\text{-}CO_2Et\text{-}C_{10}H_5)$ | Figure 2.36 (**15**) |
| $[Cr(CO)_5]_2(\ 2\text{-}CN\text{-}1,3\text{-}CO_2Et\text{-}C_{10}H_5)$ | Figure 2.37 (**16**) |
| $[W(CO)_5]_2(2\text{-}CN^{2}\text{-}1,3\text{-}CO_2Et\text{-}C_{10}H_5)$ | Figure 2.38 (**17**) |

### 2.3.2. Computational Work

Computational work was accomplished with the help of by Prof. Ward. H Thompson and Dr. Gerald H. Lushington of the University of Kansas. Electronic structure calculations were performed at the all-electron density functional theory (DFT) level using the Gaussian 98 program.[70] The computations were performed using Becke's three parameter hybrid exchange functional[71] with the LYP (B3-LYP) correlation functional.[72,73]

For calculations on the isocyanoazulenes $CN^xAz$ (x = 1, 2, 4, 5, 6), the standard 6-31G split valence basis set[74] was employed, augmented by a single d polarization function on each heavy atom and a single p function on each hydrogen.[75] The approximate starting molecular geometry of azulene was generated at the molecular mechanics level, using the Tripos force field.[76] This geometry was subsequently refined through quantum chemical optimization at the level of theory described above. Identification of the minimum for the geometry of each $CN^xAz$ was confirmed by a frequency calculation. The peripheral C-C distances of the azulenyl fragment did not show appreciable alternation and were ca. 0.1 Å shorter than the C-C bonds at the 5- and 7-membered ring junctions. The above C-C bond lengths are very similar to the corresponding parameters for the azulenyl moieties in $[Cr(CN^xAz)_6]^+$ (x = 1, 2, 4, 6) determined by X-ray crystallography (*vide supra*). In addition, they are virtually identical to the corresponding distances calculated for isomeric 1, 2, 4, 5, and 6-cyanoazulenes.[77] Vertical excitation energies for each $CN^xAz$ were obtained using time-dependent DFT[78,79] with the Q-Chem program.[80]

Electronic structure calculations on the low-spin $d^5$ complexes $[Cr(CN^1Az)_6]^+$ and $[Cr(CN^6Az)_6]^+$ were also effected at the same density function B3-LYP level used for the free ligands. However, the STO-3G basis set was employed for these larger systems.[81] The counter-ions were included explicitly in the calculations in order to provide a reasonable description of electrostatic environment effects. The geometries used for the complex calculations corresponded to those of the crystal structures reported herein (*vide supra*), and no subsequent geometry optimization was performed. All parameters not explicitly specified above were set to their default values. The orbital plots provided are isosurfaces defined by orbital intensities corresponding to +0.03 a.u. (red or yellow) and –0.03 a.u. (blue) respectively.

## 2.4. Results and Discussion

### 2.4.1. UV-vis and Time Dependent Density Functional Theory (TD-DFT) Studies of Isocyanoazulenes

In order to quantitatively assess the electronic inhomogeneity of the azulenic framework, several techniques were employed. The first method involved analysis of the isocyanoazulenes **2** – **6** in solution by electronic spectroscopy. All of these species exhibit a characteristic structural band in the visible region with $\lambda_{max}$ ranging from 565 to 609 nm in pentane. This transition corresponds to the $^1A \rightarrow {}^1L_b$ excitation (HOMO → LUMO) of the azulenic framework. For the unsubstituted azulene, the transition of this nature occurs at 579 nm in the same solvent (**Figure 2.10**).

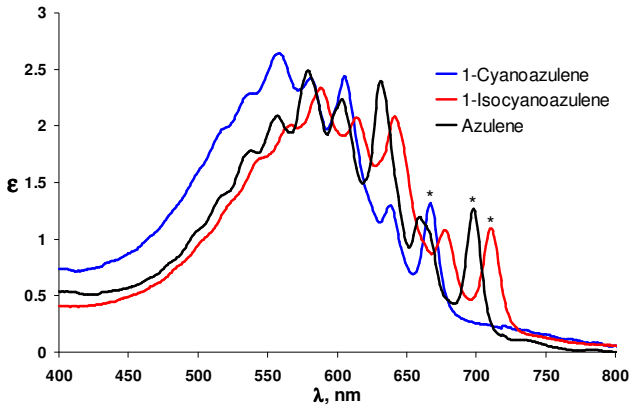


**Figure 2.10**. The long-wave absorption bands of 1-cyanoazulene, 1-isocyanoazulene, and azulene, all recorded in pentane at 24 °C. The 0→0 transitions are labeled with asterisks.[27]

For substituted azulenes, the value of $\lambda_{max}$ for the HOMO→LUMO excitation is known to be a function of the position of attachment of the substituent to the azulenic framework, as well as the electronic nature of that substituent.[18] These two factors determine either widening or shrinking of azulene's HOMO-LUMO gap

because of the uneven electron density distribution around the azulenic core for its HOMO's and LUMO's (**Figure 2.11**). This is in sharp contrast to the alternant aromatics, such as naphthalene, which have symmetric HOMO and LUMO (e.g., **Figure 2.2**).[3,82]

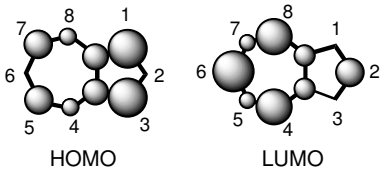


**Figure 2.11.** Schematic representation of azulene's HOMO and LUMO. The circles indicate squares of atomic orbital coefficients.[27]

It further has been suggested that by adding an unsaturated electron-withdrawing group (EWG) at the 2, 4 or 6 positions of the azulenic structure, there should be a red (bathochromic) shift of the azulenes $^1A \rightarrow {}^1L_b$ band due to the stabilization of the LUMO through conjugation and inductive effects, while not causing any change in the HOMO energy, to a first approximation.[18] Conversely, by adding an EWG to an odd numbered carbon, the HOMO will be affected, but not the LUMO (**Figure 2.12**).[3,82] This is due to the stabilization caused by the substituent's positive inductive effects and destabilization due to conjugation with the substituent. For strongly EWG's, the inductive effect is more prevalent, thus resulting in a blue (hypsochromic) shift of the $^1A \rightarrow {}^1L_b$ band.[3,82] This has been shown experimentally to be true by using five isomeric formylazulenes (**Figure 2.13.A**).[82] The very same hypothesis apparently holds true for 1-, 2-, 4-, and 6-cyanoazulenes ($NC^xAz$, x = 1, 2, 4, 6) (**Figure 2.13.B**). 5-Cyanoazulene is currently unknown. Since the isocyanide moiety is considered a strong EWG,[83,84] it was surprising to find that the long-held

theory discussed above does not work consistently in the case of isocyanoazulenes. In particular, it fails to predict directions of the shifts in the HOMO→LUMO electronic transitions with respect to azulene for $CN^1Az$ and $CN^2Az$ (**Figure 2.13.C**). While the red shift of the low energy band for $CN^1Az$ vs. azulene can be still rationalized by invoking dominance of the conjugation effect, in the case of $CN^2Az$ neither resonance nor inductive arguments can explain the blue shift of the the $^1A \rightarrow {}^1L_b$ band for this species versus the corresponding transition observed for azulene.

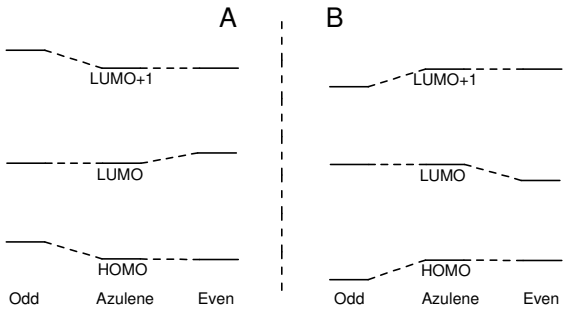


**Figure 2.12**. Substituent effects on azulene's HOMO, LUMO and LUMO+1. A) Electron donating substituents. B)Electron withdrawing substituents.[18]

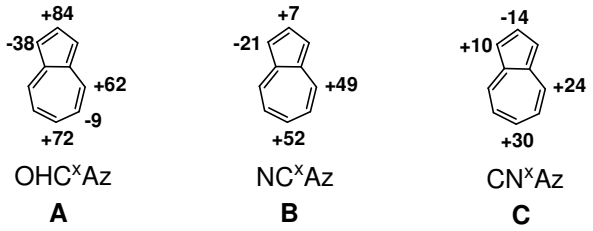


**Figure 2.13** Shifts (in nm) of $\lambda_{max}$ of the $^1A \rightarrow {}^1L_b$ band upon substitution of azulene with (A) formyl, (B) cyano, and (C) isocyano groups at various positions.[85]

When comparing the energies of the long-wavelength transitions for $CN^xAz$ vs. the equivalent $NC^xAz$, the *relative* difference in inductive strengths of the cyanide and isocyanide moieties should be approximately the same. This is due to a very close structural relationship between the –NC and –CN groups, assuming all other factors being approximately equal. In order to confirm this hypothesis, the fine structures of

the $S_0 \rightarrow S_1$ bands for $CN^xAz$ (x = 1, 2, 4, 6) were considered, which turned out to be very similar to those observed for the corresponding cyanoazulenes (e.g., **Figure 2.13**). The long-wavelength absorptions for $CN^xAz$ (x = 2, 4 and 6) were all blue-shifted by similar amounts in relation to the corresponding $NC^xAz$ analogues (**Table 2.3**). This can be rationalized by invoking less pronounced stabilization of the LUMOs of the $CN^xAz$ species vs. $NC^xAz$ due to the weaker polarity of the isocyanide vs. cyanide groups. In addition, due to the smaller inductive stabilization of $CN^1Az$'s HOMO compared to that of $NC^1Az$, the HOMO $\rightarrow$ LUMO transition of $CN^1Az$ is red-shifted with respect to that of $NC^1Az$.[27]

The apparent discrepancy between the qualitative theoretical expectations and the experimental electronic spectroscopic data was addressed through time dependent DFT (TD-DFT) and cyclic voltammetry studies of isocyanoazulenes. The DFT analysis of $CN^xAz$ (x = 1, 2, 4 and 6) is summarized in **Figure 2.14** and **Table 2.2.** The relative magnitudes of the HOMO-LUMO gaps and the TD-DFT excitation energies for $CN^xAz$ predict decrease in the energy of the long-wave transitions in the order of $CN^2Az > CN^1Az > CN^4Az \approx CN^6Az$. The same trend was observed in our electronic spectroscopy studies of $CN^xAz$ as can be clearly seen in **Table 2.3**. Among the isomeric $CN^xAz$, $CN^1Az$ has the highest HOMO energy. Thus, it appears that the conjugation effect is dominant in affecting the HOMO-LUMO separation upon –NC substitution of azulene. Also, stabilization of the HOMO of $CN^2Az$ vs. those of $CN^4Az$ and $CN^6Az$ is indicated, which is not at all obvious from the qualitative considerations described by Liu et al.[18]

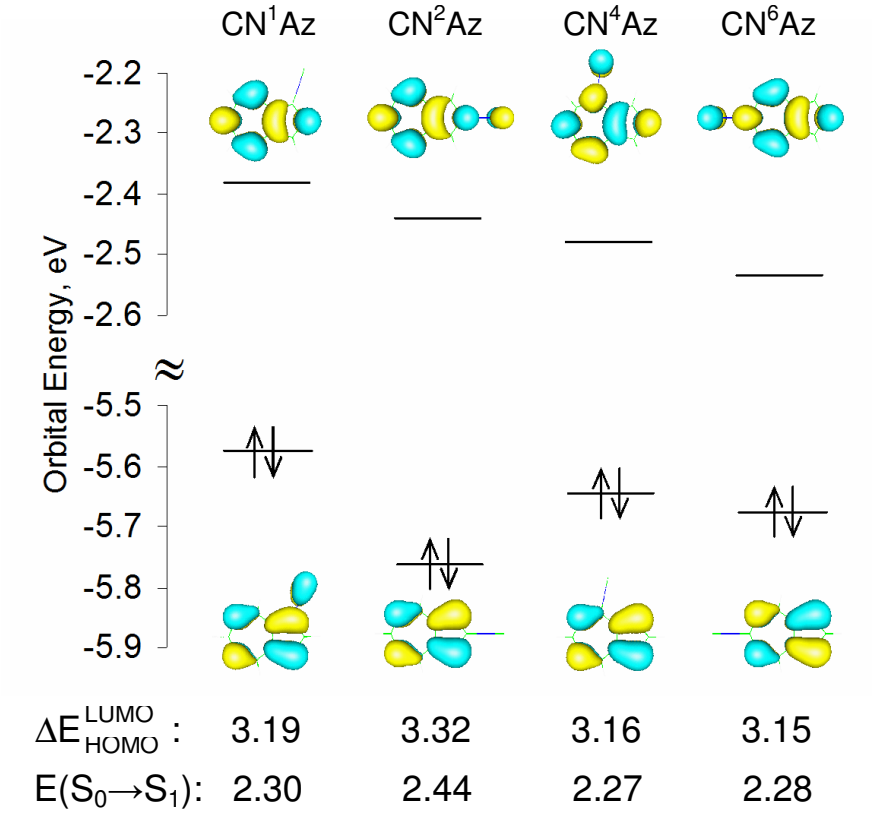


**Figure 2.14.** From left to right: HOMO's and LUMO's of $CN^1Az$, $CN^2Az$, $CN^4Az$, and $CN^6Az$. The corresponding HOMO-LUMO gaps (eV) and TD-DFT excitation energies ($S_0 \rightarrow S_1$, eV) are listed at the bottom of the diagram Reproduced in part with permission from *Journal of the American Chemical Society* **2006**, *128*, 2300-2309. Copyright 2007 American Chemical Society.[27,86]

**Table 2.2.** Calculated energies of the frontier molecular orbitals, the corresponding HOMO-LUMO gaps, and TD-DFT $S_0 \rightarrow S_1$ excitation energies for $CN^xAz$ (x = 1, 2, 4, 5, 6)

| Molecule | E(HOMO) eV | E(LUMO) eV | HOMO-LUMO Gap eV | $E(S_0 \rightarrow S_1)$ eV |
|---|---|---|---|---|
| **$CN^1Az$** | -5.57 | -2.38 | 3.19 | 2.3 |
| **$CN^2Az$** | -5.76 | -2.44 | 3.32 | 2.44 |
| **$CN^4Az$** | -5.64 | -2.48 | 3.16 | 2.27 |
| **$CN^5Az$** | -5.63 | -2.39 | 3.24 | 2.36 |
| **$CN^6Az$** | -5.68 | -2.53 | 3.15 | 2.28 |

**Table 2.3.** Comparison of energies ($\lambda$ in nm, $\nu$ in $cm^{-1}$) of the long-wave transitions for $CN^1Az$, $CN^2Az$, $CN^4Az$, and $CN^6Az$ vs. those for the corresponding cyanoazulenes.

| x | $CN^xAz$ $\lambda_{max}$ ($\nu_{max}$) | $NC^xAz$ $\lambda_{max}$ ($\nu_{max}$) | $\Delta\lambda_{max}$ ($\Delta\nu_{max}$)[a] |
|---|---|---|---|
| 1 | 589 (16978)[b] | 558 (17921)[b] | +31 (-943) |
| 2 | 565 (17699)[b] | 586 (17065)[c] | -21 (+634) |
| 4 | 603 (16584)[b] | 628 (15924)[d] | -25 (+660) |
| 6 | 609 (16420)[b] | 631 (15847)[e] | -22 (+573) |

[a] $\Delta\lambda_{max} = \lambda_{max}(CN^xAz) - \lambda_{max}(NC^xAz)$, $\Delta\nu_{max} = \nu_{max}(CN^xAz) - \nu_{max}(NC^xAz)$. [b] In pentane[27]. [c] In $C_6H_{12}$.[87] [d] In hexane.[88] [e] In $C_6H_{12}$.[89]

In order to obtain additional independent experimental support for the above TD-DFT results, the isocyanoazulenes were subject to cyclic voltammetry studies. First, the oxidation potential of $CN^2Az$ is 90 mV higher than that of $CN^4Az$ (**Table 2.4**), which is in accord with the DFT prediction. Second, the electrochemically estimated HOMO-LUMO gap of $CN^2Az$ is somewhat wider than that of azulene (**Table 2.4),** as well as of those of the other isocyanoazulenes considered. While this nicely explains the unexpected blue shift of the $^1A \rightarrow {}^1L_b$ band upon the -NC substitution of azulene at carbon atom 2, the result should only be treated qualitatively because some of the redox processes involved in the estimations are irreversible.[90] Likewise, the redox properties of $CN^4Az$ correlate nicely with its red-shifted, low-energy band in relation to azulene since the difference between its reduction and oxidation potentials is ca. 2.61 V, which is less than the corresponding value associated with azulene itself (2.70 V). Notably, both $CN^4Az$ and $CN^6Az$ show fully reversible one-electron reductions at -1.79 and -1.80 V, respectively (**Table 2.4** and **Figures 2.18** and **2.19**), which makes chemical pursuit of the radical-anions of these species feasible.

Since the parent $CN^5Az$ species has yet to be synthesized, the electrochemical behavior of its 1,3-di-tert-butyl derivative is treated separately and compared to that of 1,3-di-*tert*-butylazulene. The HOMO-LUMO gap of this species appears to shrink upon installation of the isocyanide substituent at 5-position of 1,3-di-*tert*-butylazulene (**Table 2.4**). This observation parallels that documented for 1-isocyanoazulene when compared to azulene itself. Such a behavior is consistent with both 1- and 5-positions of the azulenic framework having nodes in the LUMO and sizable coefficients in the HOMO.

**Table 2.4.** Oxidation and reduction potentials of isocyanoazulenes vs. $Fc^+/Fc$ in $CH_2Cl_2$.[a]

| Compound | $E_{p,c}$(red), V | $E_{p,a}$(ox), V | $E_{p,a}(ox) - E_{p,c}(red)$ |
|---|---|---|---|
| Azulene | -2.16 (i) | 0.54 (i) | 2.70 |
| $CN^1Az$ | -1.87 (i) | e | – |
| $CN^2Az$ | -1.86 (i) | 0.92 (i) | 2.77 |
| $CN^4Az$ | -1.80 I[b] | 0.83 (i) | 2.61 |
| $CN^6Az$ | -1.79 I[c] | e | – |
| 1,3-Di-*tert*-butylazulene | -2.36 (i) | 0.41I[d] | 2.77 |
| 1,3-Di-t*ert*-butyl-5-isocyanoazulene | -2.06 (i) | 0.63 (i) | 2.69 |

[a] Scan rate = 100 mV/s, i = irreversible, I = reversible. [b] $E_{1/2}$ = -1.76 V, $i_{p,c}/ i_{p,a}$ = 1.1 $\Delta E_{p,c-p,a}$ = 81 mV. [c] $E_{1/2}$ = -1.75 V, $i_{p,c}/ i_{p,a}$ = 1.1 $\Delta E_{p,c-p,a}$ = 83 mV. [d] $E_{1/2}$ = 0.37 V, $i_{p,c}/ i_{p,a}$ = 1.0 $\Delta E_{p,c-p,a}$ = 88 mV. [e] Not clearly defined.

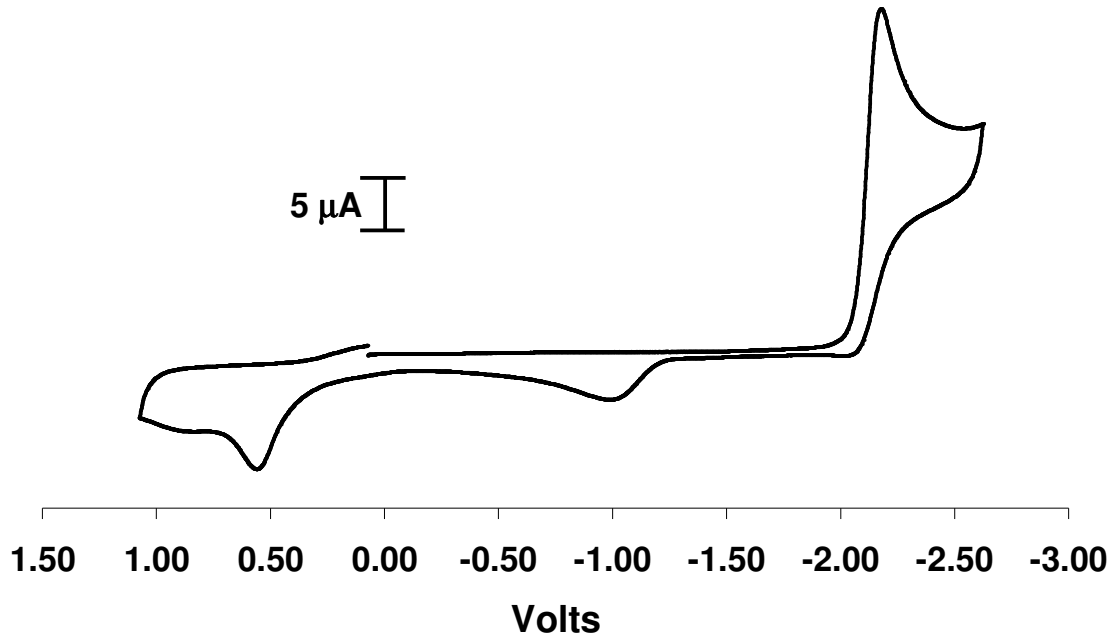


**Figure 2.15**. Cyclic voltammogram of azulene (**1**) in 0.1 M [$^{n}Bu_4N$][$PF_6$]/$CH_2Cl_2$ vs. Fc/$Fc^+$. Scan rate = 100 mV/s.

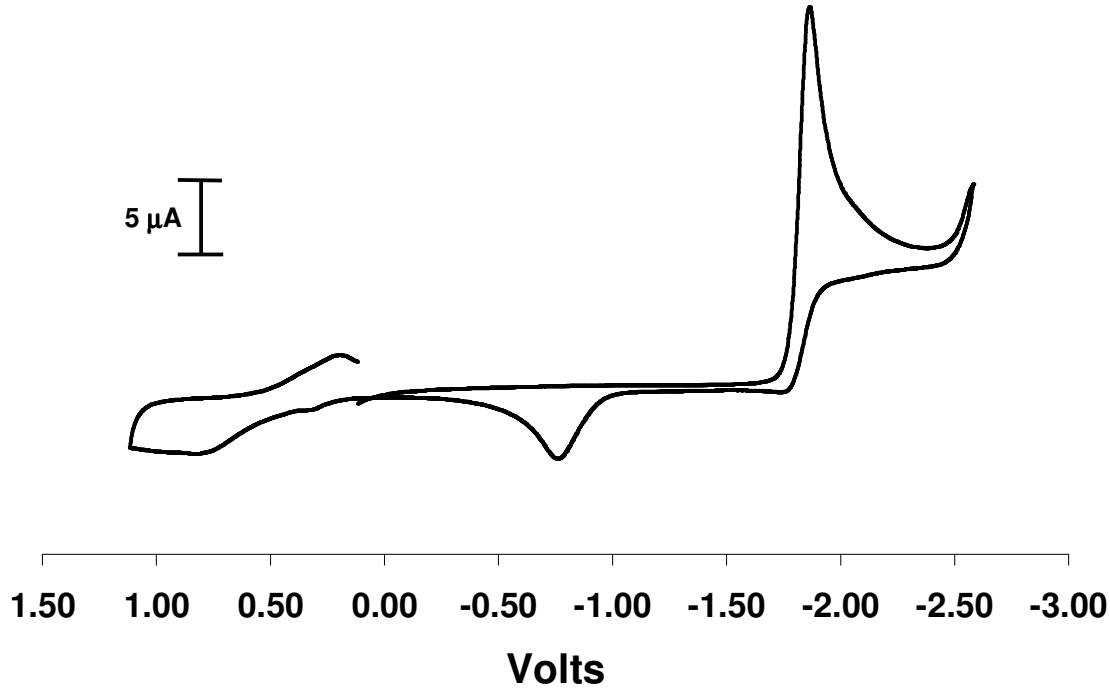


**Figure 2.16**. Cyclic voltammogram of 1-isocyanoazulene (**2**) in 0.1 M [$^{n}Bu_4N$][$PF_6$]/$CH_2Cl_2$ vs. Fc/$Fc^+$. Scan rate = 100 mV/s.

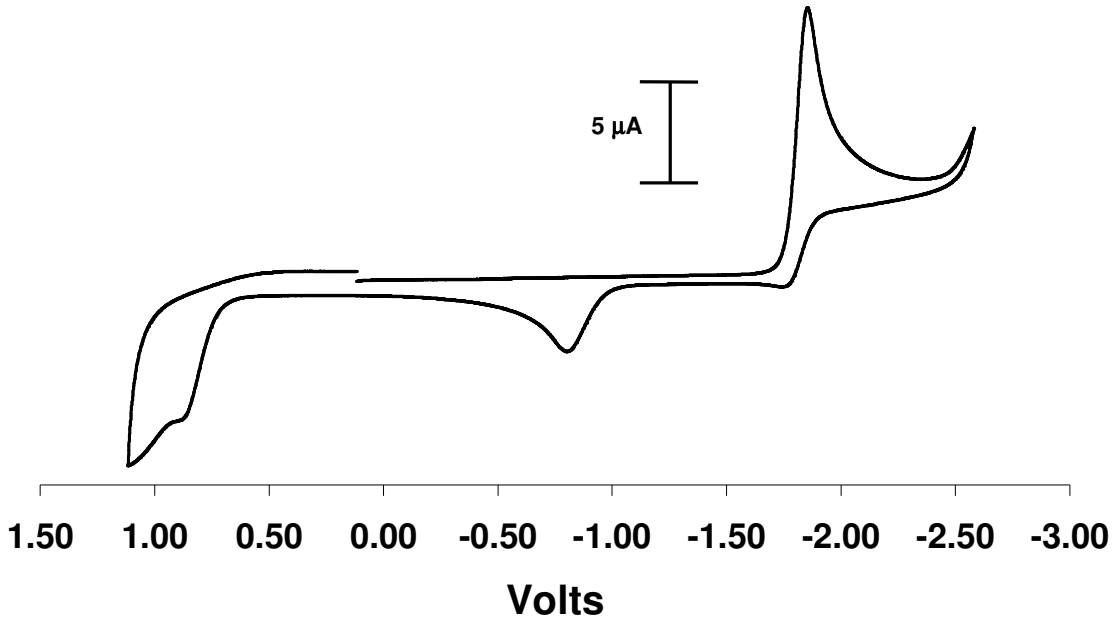


**Figure 2.17**. Cyclic voltammogram of 2-isocyanoazulene (**3**) in 0.1 M [$^{n}Bu_4N$][$PF_6$]/$CH_2Cl_2$ vs. $Fc/Fc^+$. Scan rate = 100 mV/s.

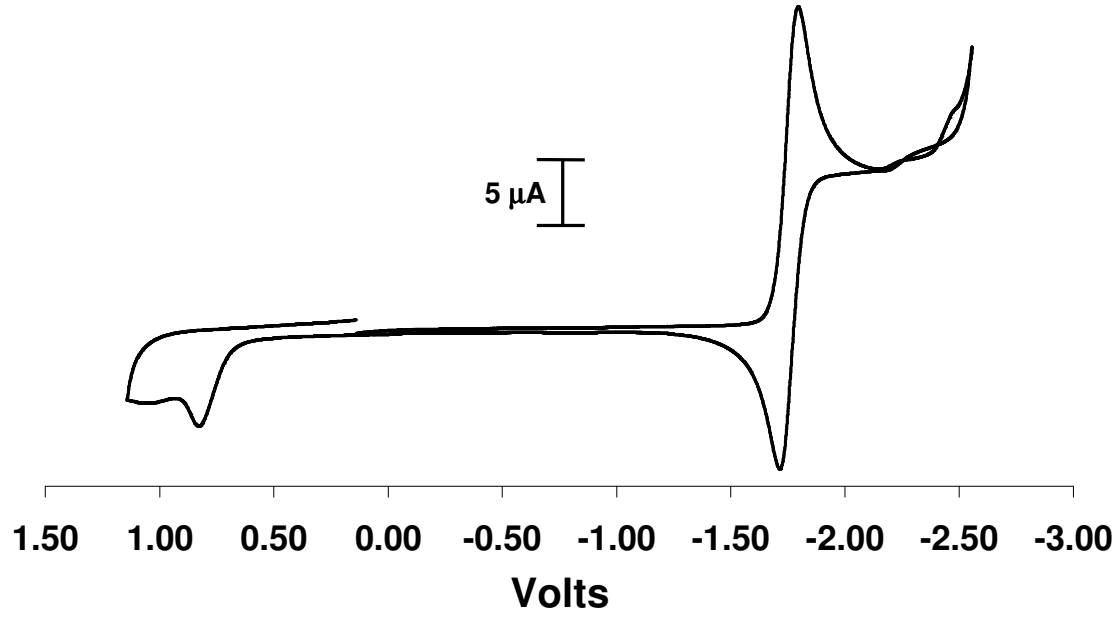


**Figure 2.18**. Cyclic voltammogram of 4-isocyanoazulene (**4**) in 0.1 M [$^{n}Bu_4N$][$PF_6$]/$CH_2Cl_2$ vs. $Fc/Fc^+$. Scan rate = 100 mV/s.

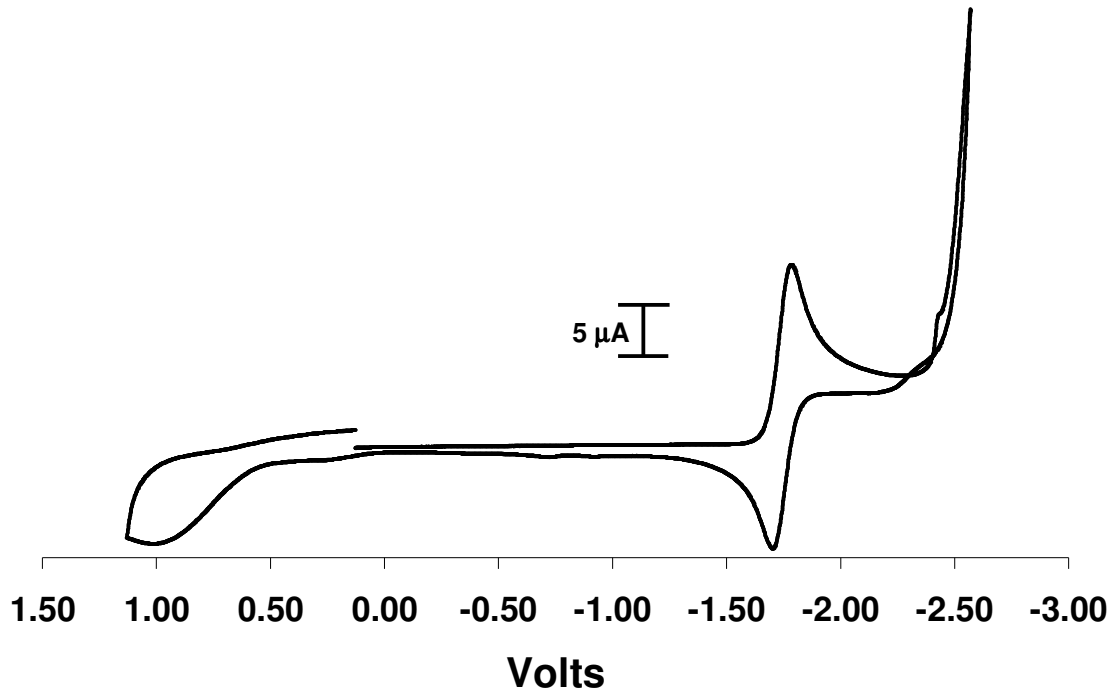


**Figure 2.19**. Cyclic voltammogram of 6-isocyanoazulene (**5**) in 0.1 M [$^{n}Bu_4N$][$PF_6$]/$CH_2Cl_2$ vs. $Fc/Fc^+$. Scan rate = 100 mV/s.

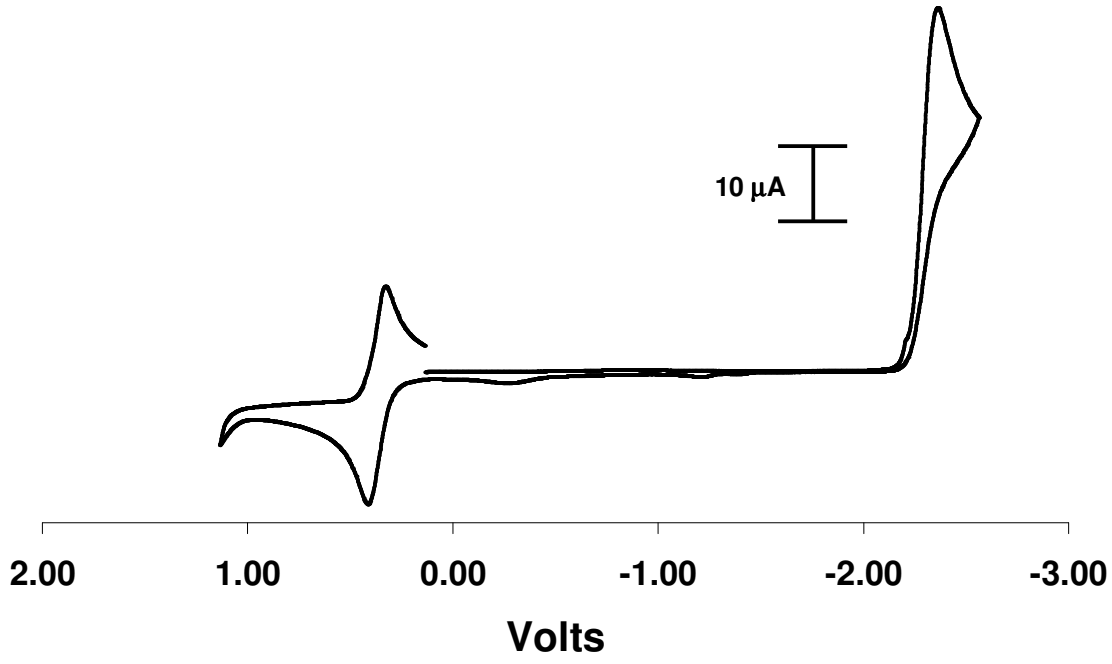


**Figure 2.20**. Cyclic voltammogram of 1,3-tert-butylazulene (**6**) in 0.1 M [$^{n}Bu_4N$][$PF_6$]/$CH_2Cl_2$ vs. $Fc/Fc^+$. Scan rate = 100 mV/s.

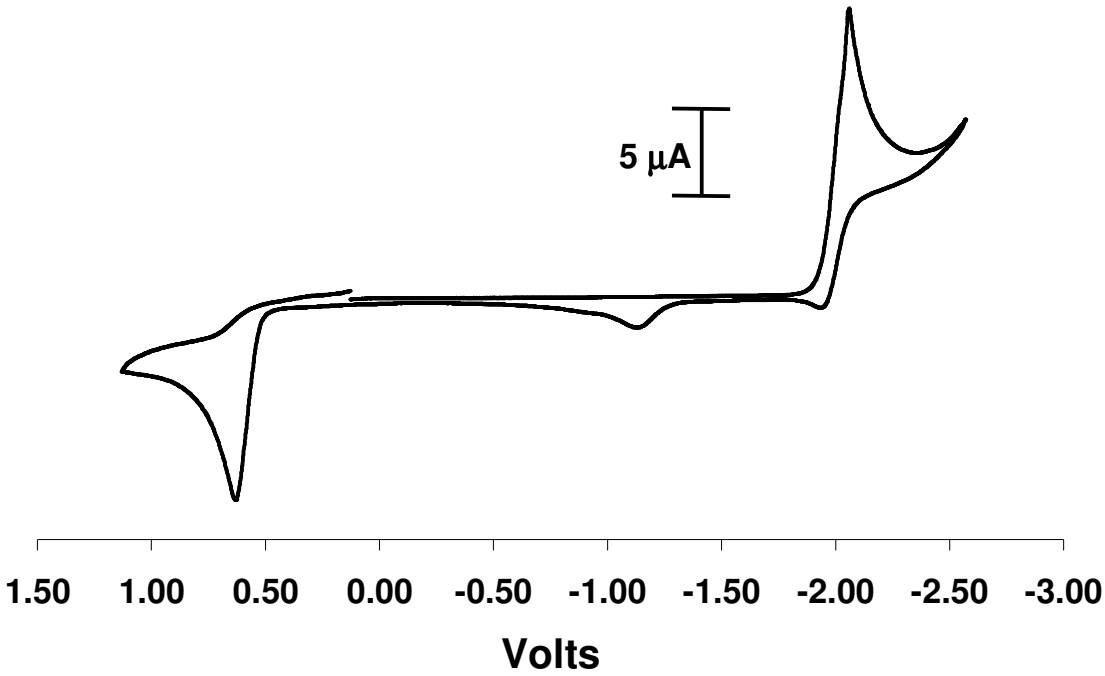


**Figure 2.21**. Cyclic voltammogram of 1,3-tert-butyl-5-isocyanoazulene (**7**) in 0.1 M $[^{n}Bu_4N][PF_6]/CH_2Cl_2$ vs. $Fc/Fc^{+}$. Scan rate = 100 mV/s.

### 2.4.2. Electrochemical and DFT Studies of Hexakis(isocyanoazulene)chromium Complexes

To systematically and quantitatively assess the electronic inhomogeneity of the azulenic framework, the homoleptic systems $[Cr(CN^{x}Az)_6]^{z/z+1}$ (z = 0, 1) were studied electrochemically. These studies involved determination of the isocyanoazulene ligands' σ-donor/π-acceptor ratios.[62] It has been qualitatively observed by Dr. Thomas Holovics of the Barybin group that, while $Cr(CN^{1}Az)_6$ was readily oxidized by $V(CO)_6$ to give $[Cr(CN^{1}Az)_6]^{+}$ $[V(CO)_6]^{-}$, the $Cr(CN^{4}Az)_6$ and $Cr(CN^{6}Az)_6$ species were essentially unperturbed by this 17-electron mild oxidizing reagent. Also, treatment of $Cr(CN^{2}Az)_6$ with one equivalent of $V(CO)_6$ produced an equilibrium mixture of $Cr(CN^{2}Az)_6$, $V(CO)_6$, and $[Cr(CN^{1}Az)_6]^{+}[V(CO)_6]^{-}$.

Complexes $[Cr(CN^xAz)_6]^{z/z+1}$ (z = 0, 1) were subject to cyclic voltammetry experiments and exhibited at least two quasi-reversible waves. These data are summarized in **Table 2.5**. The half-wave potentials reported in this Table correspond to the Cr-centered redox processes. From Table 1.5 it is readily apparent that changing the location of attachment of the isocyanide "alligator clip" to the azulene moiety alters electron richness of the Cr center in the "$Cr(CN)_6$" core. The CV data clearly imply that the σ-donor/π-acceptor ratio[62] of the isocyanide ligands decreases in the order $CN^1Az < CN^5Az < CNPh < CN^2Az < CN^6Az < CN^4Az$.

**Table 2.5.** $E_{1/2}$ potentials (in V) for $[Cr(CNR)_6]^{z/z+1}$ versus $Fc^0/Fc^+$. [a]

| | R | | | | | |
|---|---|---|---|---|---|---|
| **z/z+1** | **$^1$Az** | **$^5$Az$^*$** [b] | **Ph** [c] | **$^2$Az** | **$^6$Az** | **$^4$Az** |
| **0/+1** | -0.98 | -0.87 | -0.83 | -0.69 | -0.49 | -0.44 |
| **+1/+2** | -0.42 | -0.29 | -0.21 | -0.16 | -0.03 | +0.02 |

[a] All measurements were performed in $CH_2Cl_2/[^nBu_4N][PF_6]$ to ensure quantitative comparison, scan rate = 100 mV/s. [b] $Az^*$ = 1,3-$^tBu_2$-azulenyl. [c] [63,91].

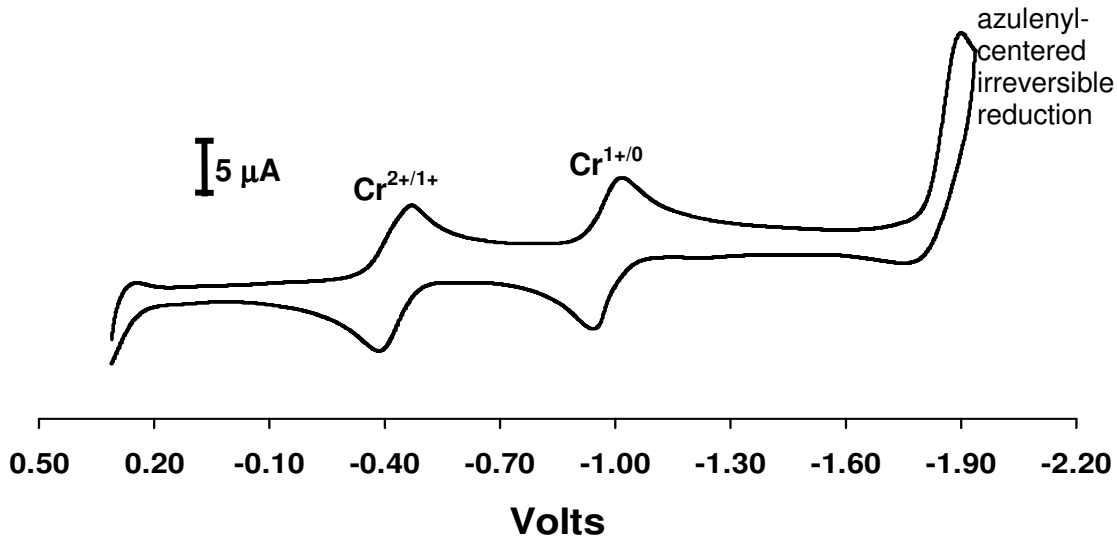


**Figure 2.22**. Cyclic Voltammogram of $[Cr(CN^1Az)_6]^+[BF_4]^-$ (**8**) in 0.1 M $[^nBu_4N][PF_6]/CH_2Cl_2$ vs. $Fc/Fc^+$. Scan rate = 100 mV/s.

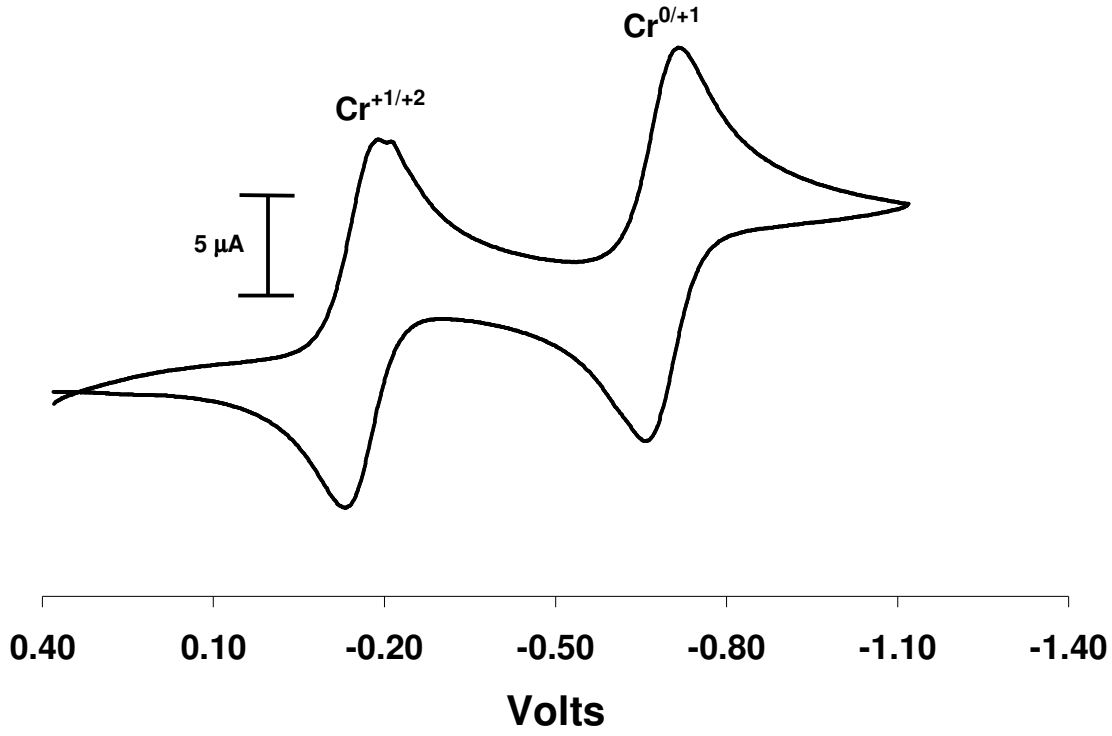


**Figure 2.23**. Cyclic Voltammogram of $[Cr(CN^2Az)_6]^+[BF_4]^-$(**9**) in 0.1 M $[^nBu_4N][PF_6]/CH_2Cl_2$ vs. $Fc/Fc^+$. Scan rate = 100 mV/s.

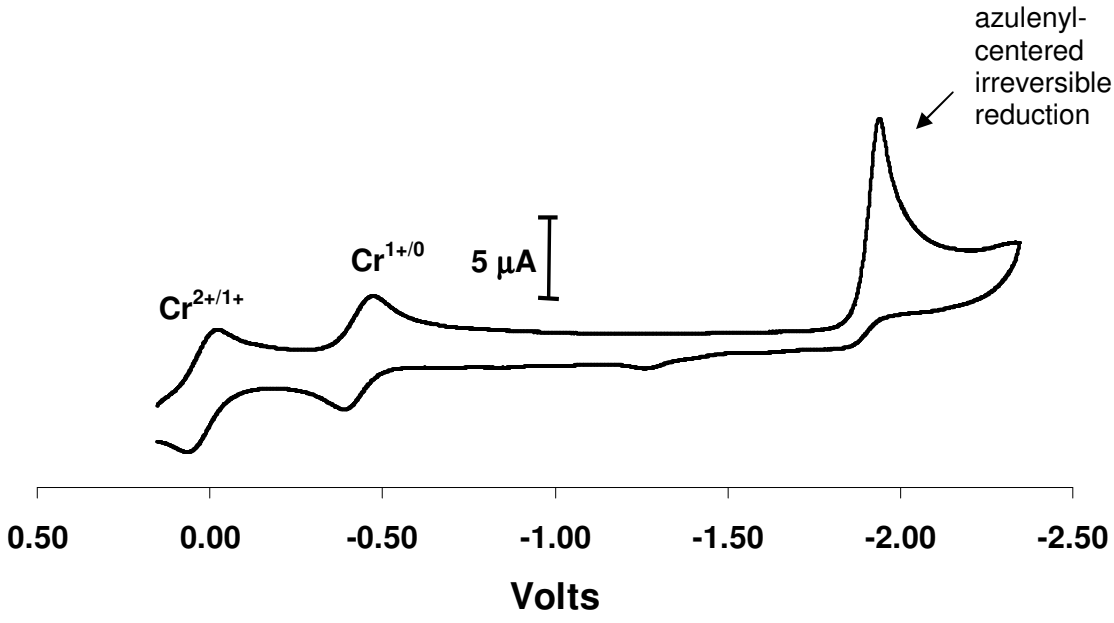


**Figure 2.24**. Cyclic Voltammogram of $[Cr(CN^4Az)_6]^+[SbF_6]^-$(**10**) in 0.1 M $[^nBu_4N][PF_6]/CH_2Cl_2$ vs. $Fc/Fc^+$. Scan rate = 100 mV/s.

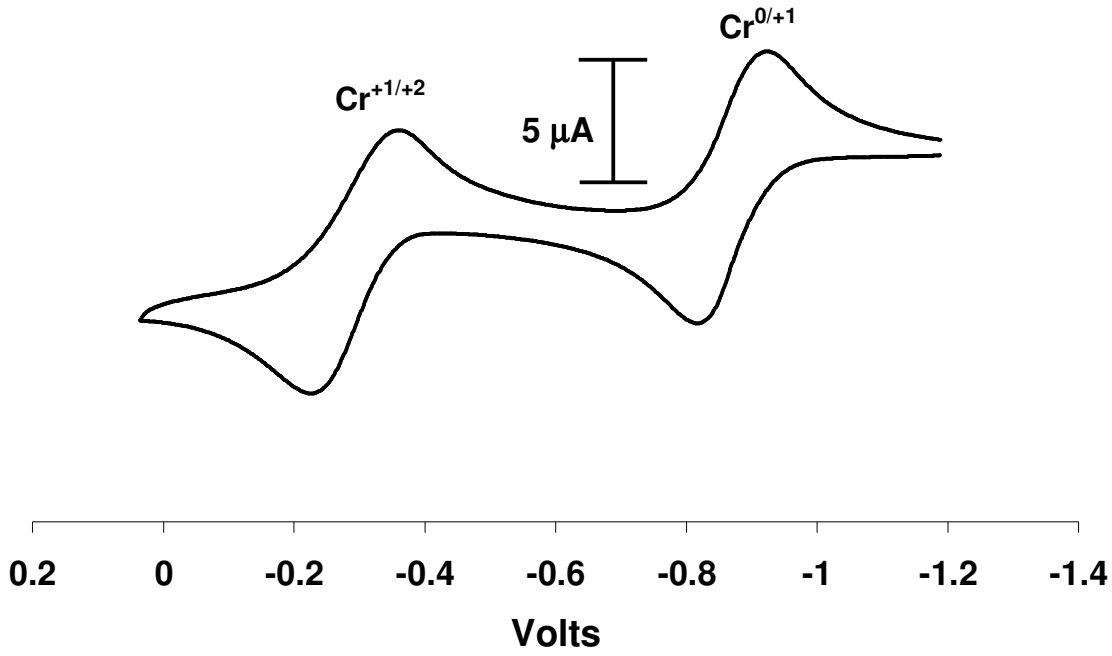


**Figure 2.25**. Cyclic Voltammogram of $Cr(CN^5Az\text{-}1,3\text{-}t\text{-}Bu)_6$(**11**) in 0.1 M $[^nBu_4N][PF_6]/CH_2Cl_2$ vs. $Fc/Fc^+$. Scan rate = 100 mV/s.

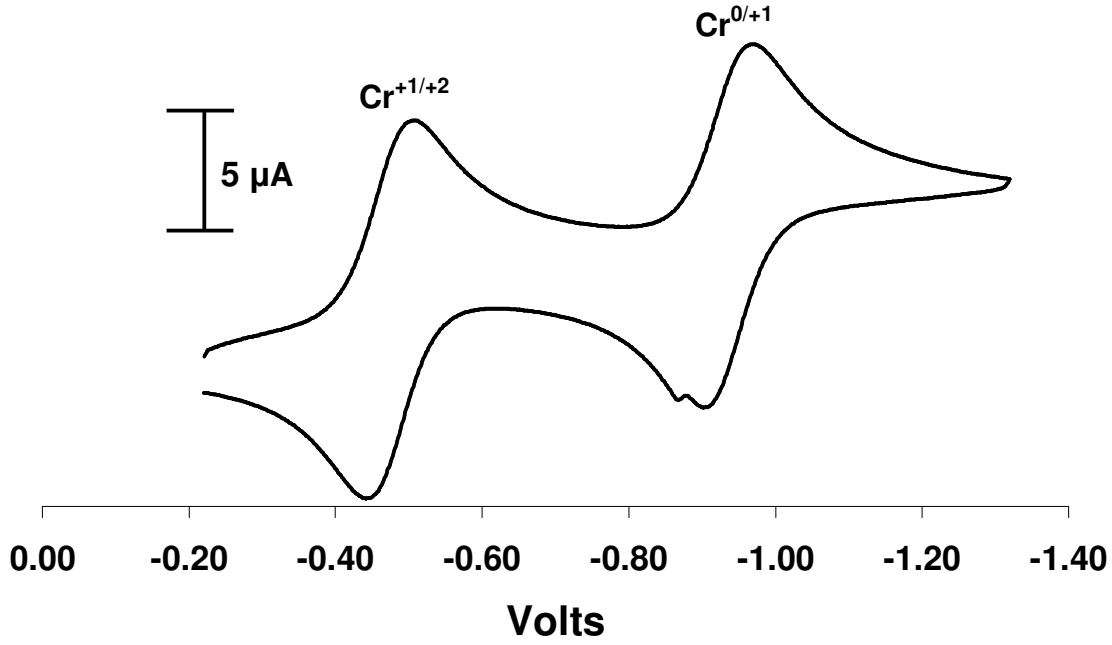


**Figure 2.26**. Cyclic Voltammogram of $[Cr(CN^6Az)_6]^+[BF_4]^-$(**12**) in 0.1 M $[^nBu_4N][PF_6]/CH_2Cl_2$ vs. $Fc/Fc^+$. Scan rate = 100 mV/s.

Remarkably, the $E_{1/2}$ value for the $Cr(CN^4Az)_6^{0/+1}$ couple (-0.44 V) is approximately the same as that for $Cr(CN^1Az)_6^{+1/+2}$ couple (-0.42V). This indicates

that the Cr(I) center in $Cr(CN^1Az)_6$ is as electron rich as the Cr(0) in $Cr(CN^4Az)_6$. The large variations in redox potential for the isomeric $Cr(CN^xAz)_6$ complexes is a direct consequence of the electronic inhomogeneity of the azulenic framework in the isocyanoazulene ligands. Notably, the $E_{1/2}$ potential of the $[Cr(CN^1Az)_6]^{0/+1}$couple is virtually equal to that of $[Cr(CNFc)_6]^{0/+1}$ (-0.97 V)[92] suggesting that the $CN^1Az$ and CNFc ligands have nearly identical donor/acceptor characteristics. Thus, the "electrochemical series" described in **Table 2.5** constitutes the first quantitative measure of the electronic inhomogeneity of the azulenic scaffold. Interestingly, this series correlates well with the trend in $pK_a$ values measured for azuloic acids: 6.99 $\{HO_2C^1Az\}$ > 5.86 $\{HO_2C^2Az\}$ > 5.21 $\{HO_2C^6Az\}$(**Figure 2.27**).[93] However, $HO_2C^4Az$ is unknown and the quantitative interpretation of its acidity, as well as that of $HO_2C^1Az$, would be compromised by the expected intramolecular hydrogen bonding interaction involving the carbonyl oxygen atom of the carboxylate group and the H-1 (in the case of $HO_2C^4Az$) or H-4 (in the case of $HO_2C^1Az$) atoms of the azulenic scaffold.[93]

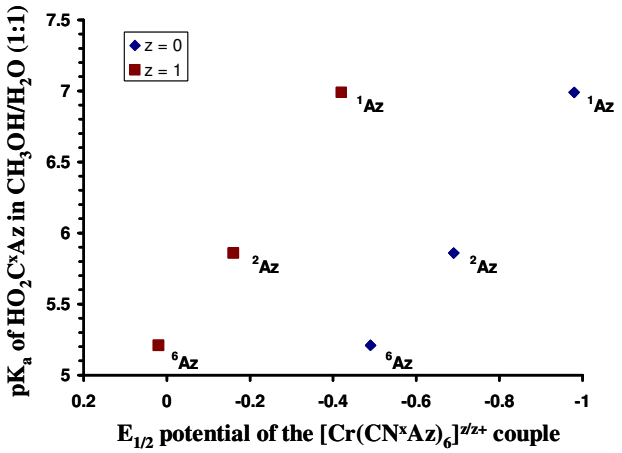


**Figure 2.27**. $pK_a$ values for $HO_2C^xAz$ acids plotted against the $E_{1/2}$ potentials of the $[Cr(CN^xAz)_6]^{z/z+}$ couples (x= 1, 2, 6; z= 0–2) vs. ferrocene/ferrocenium

The electrochemical data summarized in Table 2.5 nicely explain the differences in the reactivity of $Cr(CN^xAz)_6$ toward $V(CO)_6$ as described in the beginning of this section. Indeed, since the $E_{1/2}$ potential for the $[V(CO)_6]^{0/-}$ couple (-0.54 V, **Figure 2.28**) is very similar to that of the $[Cr(CN^2Az)_6]^{0/+}$ couple, combining $V(CO)_6$ with $Cr(CN^2Az)_6$ results in the equilibrium mixture containing about a half of these neutral reactants and the $[Cr(CN^2Az)_6][V(CO)_6]$ product. The qualitative position of the equilibrium inferred from the FTIR studies in the $\nu_{CN}$ region (Dr. Tom Holovics, *vide supra*) is in accord with that predicted by the Nernst equation for this system.[90] The $E_{1/2}$ values for the $[Cr(CN^xAz)_6]^{0/+}$ (x = 4, 6) are more than 50 mV greater than that for the $[V(CO)_6]^{-/0}$ couple, which, according to the Nernst equation, should result in essentially no reaction of $Cr(CN^xAz)_6$ when combined with $V(CO)_6$, which was indeed observed. On the contrary, the $E_{1/2}$ value for the $[Cr(CN^1Az)_6]^{0/+}$ is ca. 440 mV more negative than that documented for the $[V(CO)_6]^{0/-}$ couple, which

should lead to the practically complete electron transfer from $Cr(CN^1Az)_6$ to $V(CO)_6$, which was documented crystallographically.[27]

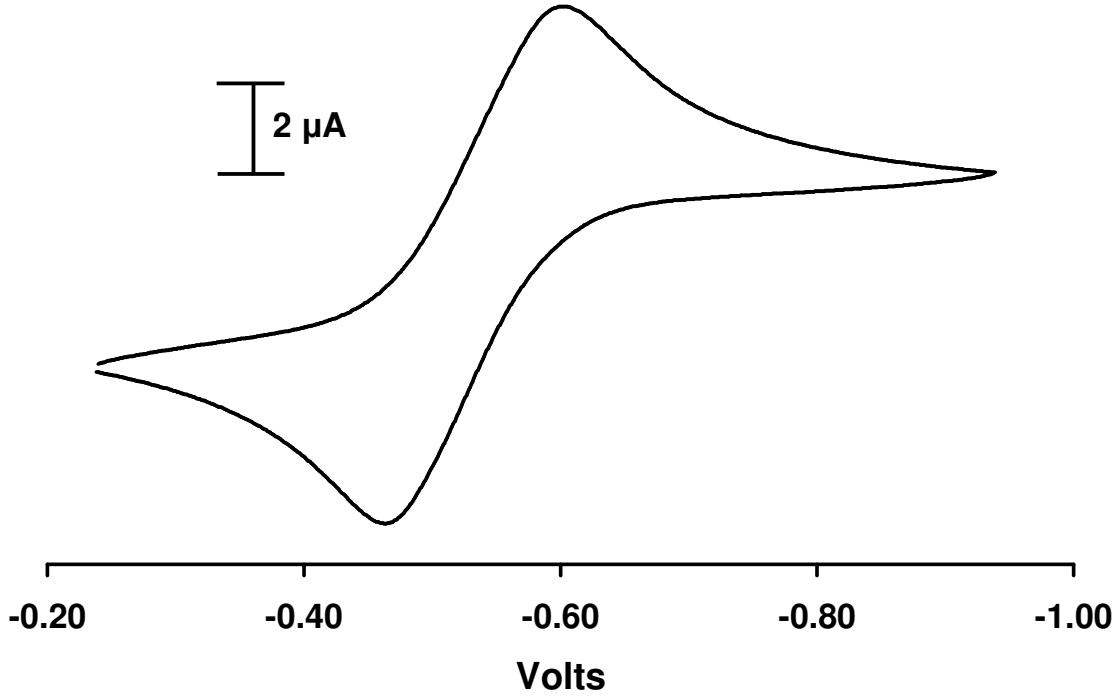


**Figure 2.28.** Cyclic Voltammogram of $V(CO)^-$ in 0.1 M $[^nBu_4N][PF_6]/CH_2Cl_2$ vs. $Fc/Fc^+$. Scan rate = 100 mV/s.

In our efforts to improve solubility properties of the azulenic ligands and their complexes, substitution of the azulenic framework with ester groups was considered. The choice of the ester substituents was driven by their relative compatibility with a diverse set of reaction conditions and functional groups, as well as the potential for varying the length (size) of the R fragment within the $–CO_2R$ unit. Since the LUMO of the azulenic framework lacks electron density at positions 1 and 3 (e.g., **Figure 2.29**), attaching substituents to these carbon atoms should not affect the electronics of its $\pi^*$ system. Therefore, the 1,3-diester substitution of the azulenic nucleus is an attractive solution for modulating solubility of the metal-isocyanoazulene materials

for which maintaining electronics of the ligand's LUMO is important. The success of above approach was unambiguously demonstrated by recording and comparing cyclic voltammograms for $[Cr(CN^2Az)_6]^+$ (**9**) and its 1,3-diethoxycarbonyl-substituted analogue, $[Cr(2\text{-}CN\text{-}1,3\text{-}(CO_2Et)_2C_{10}H_5)_6]^+$ (**13**) (**Figures 2.23** and **2.30**). Indeed, the $E_{1/2}$ potentials for the chromium-centered couples $Cr^{0/+}$ and $Cr^{+/2+}$ change by only 20 mV in both cases upon going from **9** to **13** (**Table 2.6**). This implies that the electronic characteristics of the ligands in **9** and **13** are essentially identical. Thus, the 1,3-diester substitution of the azulenic scaffold would be a convenient tool to employ in the design of new isocyanoazulenic ligands, including diisocyanoazulenes (*vide infra*).

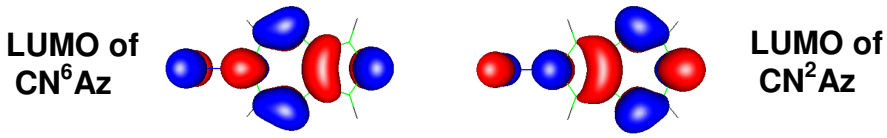


**Figure 2.29.** DFT-calculated LUMO's for 2- and 6-isocyanoazulenes

**Table 2.6.** $E^{1/2}$ potentials (in V) for $[Cr(CNR)_6]^{z/z+1}$ versus $Fc/Fc^+$

| R | 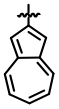 | 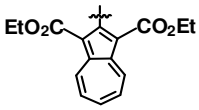 |
|---|---|---|
| $E_{1/2}(0/1+)$ | -0.69 | -0.67 |
| $E_{1/2}(1+/2+)$ | -0.16 | -0.14 |

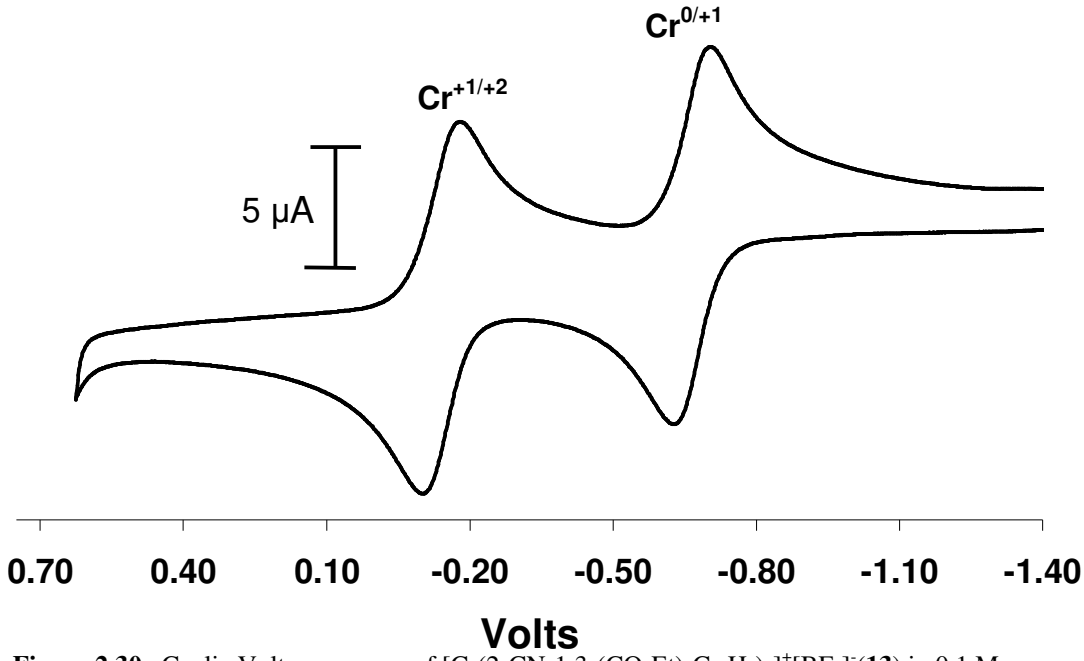


**Figure 2.30**. Cyclic Voltammogram of $[Cr(2\text{-}CN\text{-}1,3\text{-}(CO_2Et)_2C_{10}H_5)_6]^+[BF_4]^-$(**13**) in 0.1 M $[^nBu_4N][PF_6]/CH_2Cl_2$ vs. $Fc/Fc^+$. Scan rate = 100 mV/s.

The substantial differences in the redox characteristics of isomeric $[Cr(CN^xAz)_6]^z$ can be rationalized by the effect of the azulenic dipole (vide supra) on the basicity of the isocyanide carbon's lone pair and on the M(dπ)→L(pπ*) backbonding interaction (e.g., **Figure 2.31**).[27] The variations in the latter interaction would certainly be more important in the case of electron-rich complexes, such as that shown in **Figure 2.31**. This Figure illustrates DFT-calculated shapes of the three HOMOs of $[Cr(CN^6Az)_6]^+$ and clearly indicates substantial electron delocalization from the Cr(I) center onto the 6-azulenyl fragment by means of backbonding with the isocyanide alligator clip. Notably, the cylindrical symmetry of the –NC junction ensures optimal interaction between the Cr(dπ) orbitals and the π*-system of the azulenic scaffold, and depending on the atom of attachment of the azulenyl group to the isocyanide "alligator clip". As shown by Dr. Holovics of the Barybin group, the

nature and extent of the unpaired electron delocalization within $[Cr(CN^6Az)_6]^+$ can be quantitatively addressed by analyzing NMR spectra of these paramagnetic species (e.g., **2.32, 2.33**).[27]

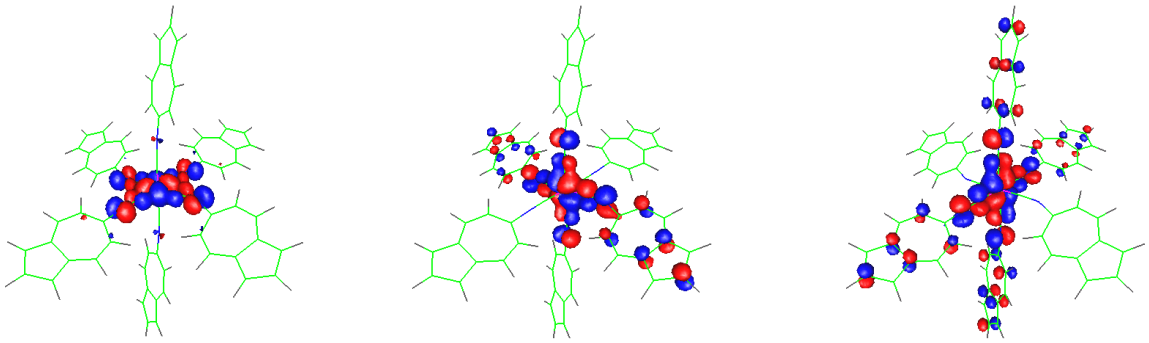


**Figure 2.31**. The nearly degenerate set of the highest occupied MO's of **12** (solid state structure, the $[BF_4]^-$ counter-ion is omitted for clarity). Reproduced in part with permission from *Journal of the American Chemical Society* **2006**, *128*, 2300-2309. Copyright 2007 American Chemical Society [27]

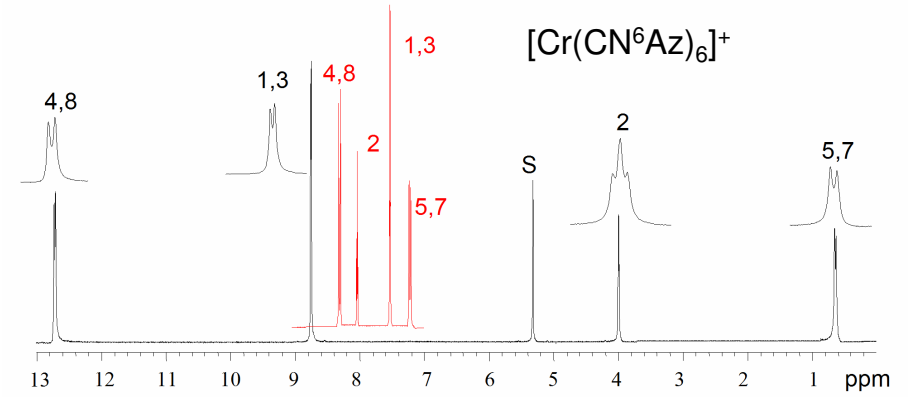


**Figure 2.32.** $^1$H Paramagnetic NMR of **12** in $CD_2Cl_2$ at 25 $^oC$. The red insert is the $^1$H NMR patterns of the corresponding diamagnetic $Cr(CN^6Az)_6$ which was recorded under the same conditions. Reproduced in part with permission from *Journal of the American Chemical Society* **2006**, *128*, 2300-2309. Copyright 2007 American Chemical Society [27]

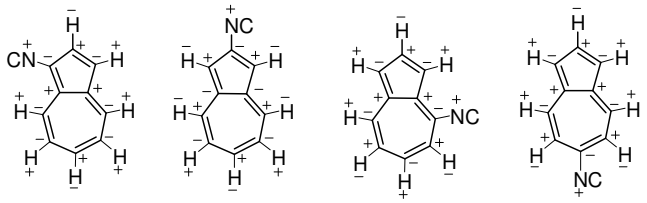


**Figure 2.33.** The observed directions of the $^{1}H$, $^{13}C$, and $^{14}N$ paramagnetic shifts for the nuclei in A)$[Cr(CN^{1}Az)_6]^+$, B)$[Cr(CN^{2}Az)_6]^+$, C)$[Cr(CN^{4}Az)_6]^+$, and D)$[Cr(CN^{6}Az)_6]^+$. The symbols "-" and "+" denote upfield and downfield shifts, respectively, relative to chemical shifts of the nuclei in the corresponding diamagnetic $[Cr(CN^{x}Az)_6]^+$ [27]

### 2.4.3. Electrochemical Studies of Diisocyanoazulene-Bridged Metal Complexes

Recently, Dr. Robinson and Mr. Weintrob of the Barybin group have developed the synthesis of 2,6-diisocyano-1,3-diethoxycarbonylazulene (**14**), which may be considered the azulenic analogue of the ditopic linear linker 1,4-diisocyanobenzene frequently used in organometallic and surface chemistry. This diisocyanoazulene can be regioselectively complexed with one or two 16-electron $M(CO)_5$ (M = Cr, W) units.[28] The mono and bimetallic complexes of **14** have been subjected to electrochemical investigations by the author of this Thesis.

The X-ray structure of $[Cr(CO)_5]_2(\mu$-**14**) was used to probe the electronic structure of this bimetallic complex by DFT. These calculations showed that the LUMO of the complex (**Figure 2.34**) looks very similar to the LUMO of the free ligand. The HOMO of the dinuclear complex constitutes a mixture of the $Cr(CO)_5$ fragments with the $Cr(CO)_5$ unit on the side of the five-membered ring of the bridge providing a greater contribution. Thus, the 2,6-diisocyanoazulene linker is nicely set up to mediate electron transport by means of $M(d\pi)\rightarrow$bridge($p\pi^*$) interactions.

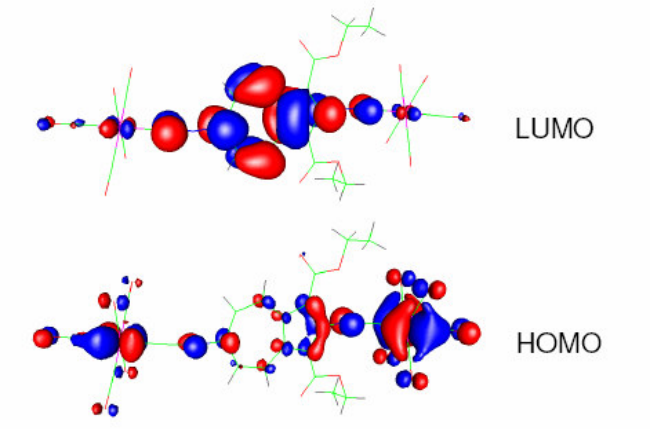


**Figure 2.34**. DFT-calculated Frontier Molecular Orbitals of $[Cr(CO)_5]_2(\mu$-**14**)

To quantify the redox characteristics of $[Cr(CO)_5]_2(\mu$-**14**), it was subjected to the CV and DPV (Differential Pulse Voltammetry) studies detailed below. The results are tabulated in **Table 2.7**, with selected examples of the CVs and DPVs shown in **Figures 2.35 - 2.38**.

**Table 2.7**. $E_{1/2}$ Values of $Cr^{0/+1}$ or $W^{0/+1}$ and reduction potentials of azulene bridge vs. $Fc^{+}/Fc$ in $CH_2Cl_2$

| | $E_{1/2}$ $Cr^{0/+1}$ or $E_{ox}$ $W^{0/+1}$ | $E_{red}$ Azulene |
|---|---|---|
| 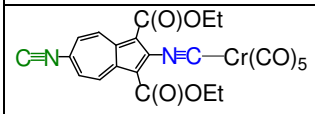 | 0.82 | -1.16 |
| 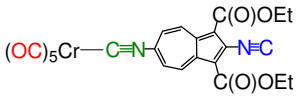 | 0.84 | -1.15 |
| 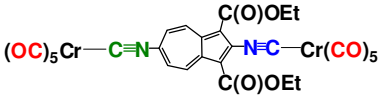 | 0.85 | -1.16 |
| 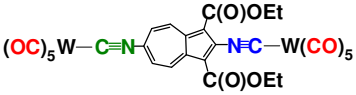 | 1.04 V | -1.10 V |
| **14** | - | -1.15 V |

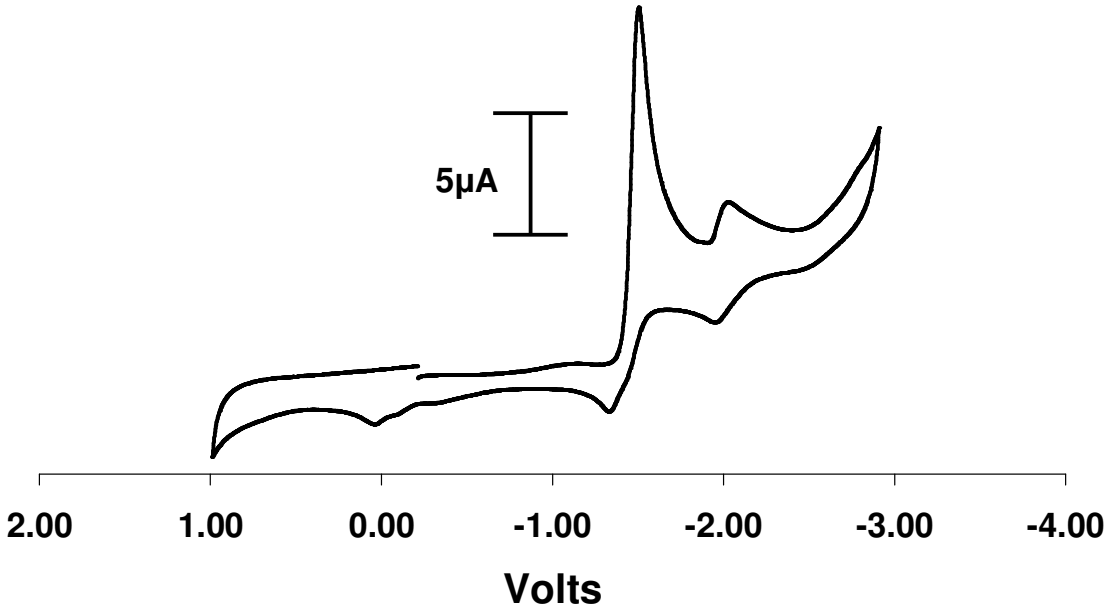


**Figure 2.35.** Cyclic voltammogram of 2,6-diisocyano-1,3-diethoxycarbonylazulene (**14**) in 0.1 M $[^{n}Bu_4N][PF_6]/CH_2Cl_2$ vs. $Fc/Fc^{+}$. Scan rate = 100 mV/s.

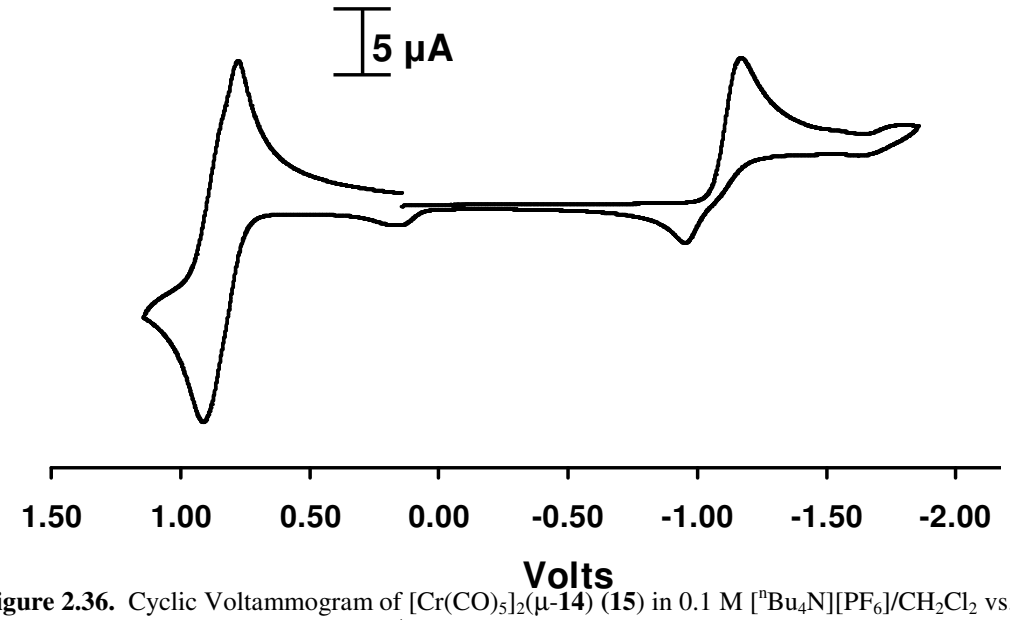


**Figure 2.36.** Cyclic Voltammogram of $[Cr(CO)_5]_2$(µ-**14**) (**15**) in 0.1 M $[^nBu_4N][PF_6]/CH_2Cl_2$ vs. $Fc/Fc^+$. Scan rate = 100 mV/s.

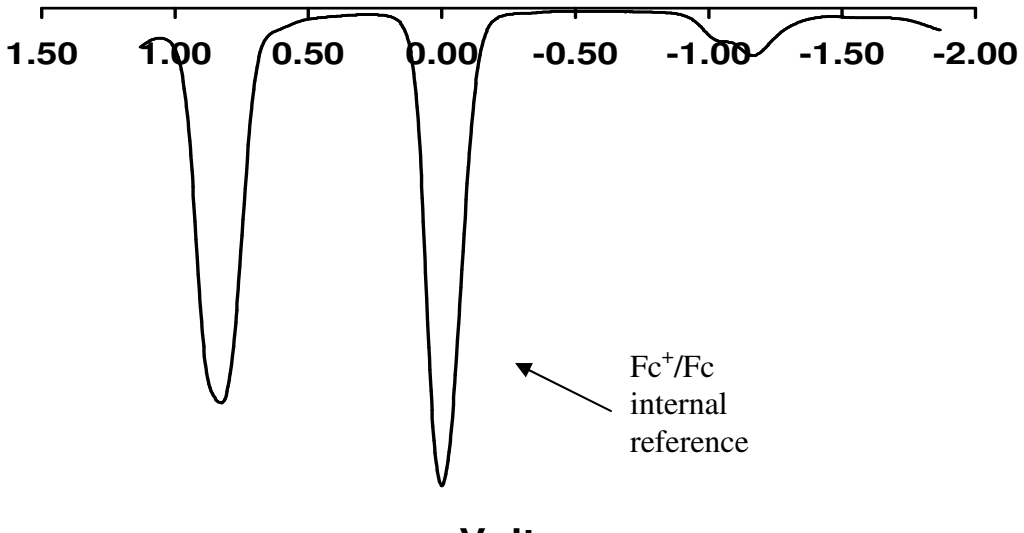


**Figure 2.37.** Differential Pulse Voltammogram of $[Cr(CO)_5]_2$(µ-**14**) (**15**) in 0.1 M $[^nBu_4N][PF_6]/CH_2Cl_2$ vs. $Fc/Fc^+$. Scan rate = 100 mV/s.

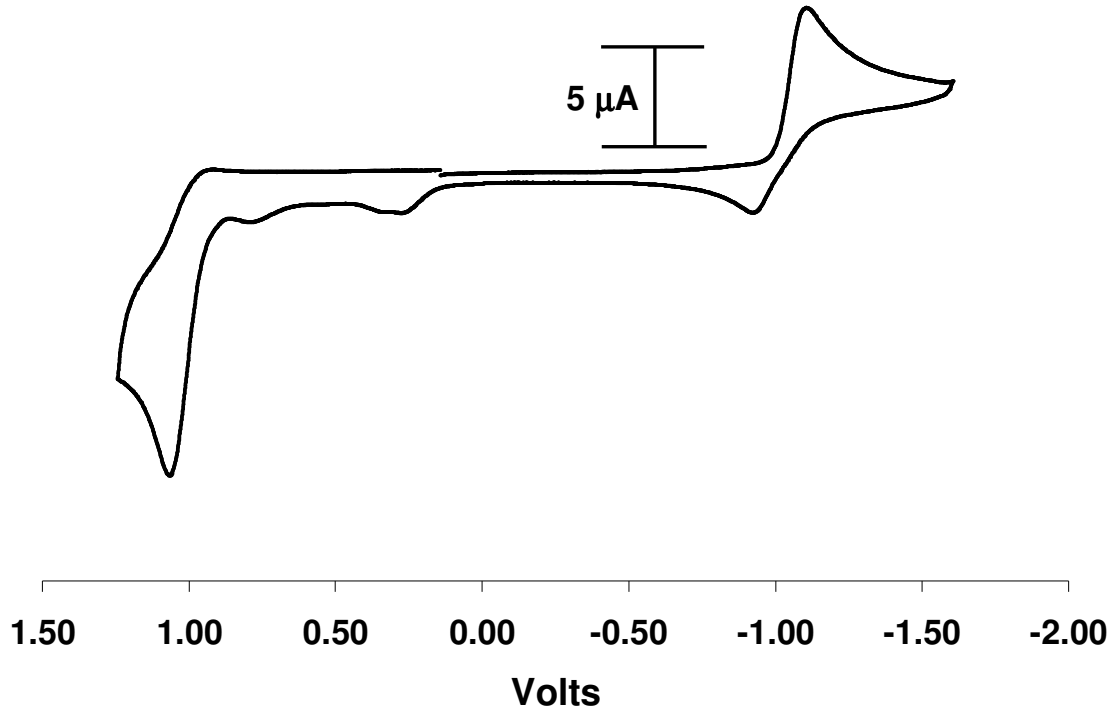


**Figure 2.38.** Cyclic Voltammogram of $[W(CO)_5]_2(\mu$-**14**$)$ (**16**) in 0.1 M $[^nBu_4N][PF_6]/CH_2Cl_2$ vs. $Fc/Fc^+$. Scan rate = 100 mV/s.

From the above cyclic voltammograms it can be seen that the $E_{Red}$ of the azulenic bridge was approximately the same for all systems, i.e., the free ligand and the complexes involving $Cr(CO)_5$ have a reduction potential of approximately -1.15 V. When the metal carbonyl unit(s) is (are) changed from $Cr(CO)_5$ to $W(CO)_5$, the reduction potential of the system (**Table 2.7**) shifts slightly to -1.10 V. This minor change can be rationalized by the more diffuse (greater size) nature of the tungsten d-orbitals vs. those of chromium, which results in greater extent of conjugation within the bridged ensemble. At the same time, the $M(CO)_5$-centered oxidation is harder to achieve in the case of M = W, which nicely parallels the oxidation potential trend documented for Group 6 metal hexacarbonyls.[28]

The CV of $[Cr(CO)_5]_2(\mu$-14) shows two overlapping fully reversible redox couples, with no apparent coupling between the two metal centers. This was not unexpected due to the highly π-acidic nature of the ancillary carbonyl ligands associated with the chromium metal centers. Since CO is a stronger π-accepting ligand than the isocyanide, the metal centers' electron density is predominantly delocalized into the carbonyl moieties by means of Cr(dπ)→CO(pπ*) backbonding. Thus, upon oxidation of the chromium termini, there is even less electron density available for delocalization into the bridge's π*-system. To increase the likelihood of observing electron communication within the above scaffolds, it would be necessary to change the ancillary ligands to less π-acidic and/or more σ-donating groups such as a $CrL_5$-Bridge- $CrL_5$ (L = CNXyl, $PR_3$, etc.). This should give more electron rich metal termini, thereby allowing for the potential to document the long-range coupling (*vide infra*).

Recently, the groups of Barybin and Chisholm have reported on a second type of the 2,6-azulene-bridged metal system that involves carboxylate rather isocyanide "alligator clips" and metal-metal quadruple bonds (tungsten or molybdenum) as the metal termini (**Figure 2.39**).[94] While complexes of this type deteriorate rapidly upon exposure to air and/or moisture (and, therefore, would be difficult to incorporate in the design of devices), they are much better than the $t_{2g}$-bridge-$t_{2g}$ system described above in terms of quantitative electron delocalization considerations. Indeed the $t_{2g}$-bridge-$t_{2g}$ system that involves single metal ions as the termini necessarily lends a greater complexity due to multiple possible $d_\pi$-orbital ($d_{xy}$, $d_{xz}$ and $d_{yz}$) interactions

with the bridge and spin-orbit coupling. These interactions give rise to numerous electronic transitions in the low energy region.[94] The situation is simplified dramatically in the case of complexes such as those shown in **Figure 2.39** because of the single M(dδ)→L(pπ*) interaction responsible for electron delocalization.

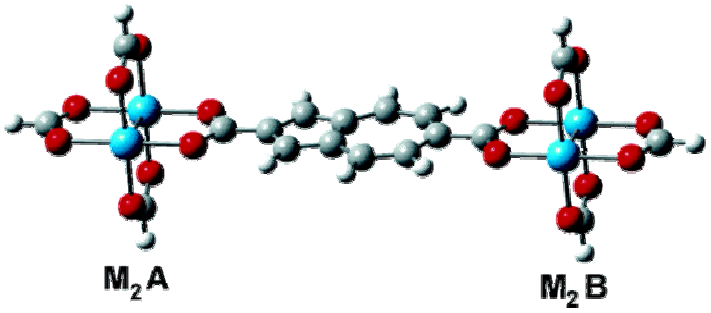


**Figure 2.39.** Model Diagram of $[(HCO_2)_3M_2]_2(\mu\text{-}O_2CC_{10}H_6CO_2)$ (M = Mo, W)(Blue= Metal, Red = Oxygen, Grey = Carbon) Reproduced in part with permission from *Journal of the American Chemical Society* **2005**, *127*, 15182-15190. Copyright 2007 American Chemical Society.[94]

A notable limitation of the Barybin-Chisholm 2,6-azulenedicarboxylate bridged structure is associated with potential rotation of the 2,6-azulenic unit with respect to the δ-systems of the quadruply-bonded metal units that may result in reduction or even complete cessation of the electronic interaction between the metal termini. Given the cylindrical symmetry of the -N≡C "alligator clips", the 2,6-diisocyanoazule linker does not possess this limitation. In addition, the latter bridge appears to form complexes that are reasonably stable under ambient environmental conditions, which is an important prerequisite for its use in the design of devices.

### 2.4.4. Conclusions and Future Work

In this chapter, the systematic electrochemical investigation of the first isocyanoazulene ligands and their electron-rich complexes has been presented. The

electronic properties of azulene and its isocyanide derivatives have been investigated by electronic spectroscopy, cyclic voltammetry, and theoretical calculations. Through this work, the properties of the Frontier molecular orbitals of isocyanoazulenes were determined quantitatively. The previous qualitative theory predicting the effect of substituents on the magnitude of azulene's HOMO-LUMO gap (and, hence, its optical properties) popularized by Liu *et al.*[82] does not hold in the case of the isocyanide substituent. The unexpected directions of the shifts of the $S_0 \rightarrow S_1$ transition for $CN^1Az$ and $CN^2Az$ have been fully rationalized by considering, together the electronic spectra, electrochemical properties, and the TD-DFT structures of these species. Furthermore, the first comprehensive quantitative electrochemical assessment of electronic inhomogeneity of the azulenic scaffold has been performed by analyzing the redox properties of the complexes $Cr(CN^xAz)_6$. The quantitative series of the donor/acceptor ratios of the isocyanoazulene ligands has been obtained. Also, through this work it was shown, both experimentally and theoretically, that 1,3-substitution of the isocyanoazulene ligands $CN^xAz$ (x = 2 and/or 6) has minimal effect on the electronics of the $\pi^*$-system of the isocyanoazulenes.

As more ligands involving the isocyanoazulene motif are developed, there will be a continued need to explore properties using the methodology detailed in this chapter. In particular, the group's work toward the 2,6-azulene-bridged materials will rely on extensive electrochemical interrogations to assess the extent of electronic transport in these systems. In particular, the 2,6-azulenic bridges also incorporating –

C≡C- units within the bridge are currently under investigation. The organometallic chemistry of biazulenic linkers (3 types) is in progress as well.

Overall, the work described in this chapter provides a solid foundation toward quantitative understanding of the electronic inhomogeneity of the azulenic framework and the consequences of this phenomenon on the properties of hybrid metal/azulene systems involving the isocyanide junctions. The results and conclusions obtained in these studies have already been[28,95] and will be instrumental in guiding the design of new and more sophisticated metal/azulenic ensembles for electronics and/or optical purposes.

## 2.5. References


1. Hansen, H. J. *Chimia* **1997**, *51*, 147-159.

2. Hansen, H. J. *Chimia* **1996**, *50*, 489-496.

3. Heilbronner, E. In *Non-Benzenoid Aromatic Compounds*; Ginsburg, D., Ed.; Interscience Publishers: New York, 1959, p 171-276.

4. Lloyd, D. *NonBenzenoid Conjugated Carbocyclic Compounds*; Elsevier: New York, 1984.

5. Mochalin, V. B.; Porshnev, Y. N. *Uspekhi Khimii* **1977**, *46*, 1002-40.

6. Crombie, A. L.; Kane, J. L.; Shea, K. M.; Danheiser, R. L. *Journal of Organic Chemistry* **2004**, *69*, 8652-8667.

7. Ito, S.; Okujima, T.; Kabuto, C.; Morita, N. *Tetrahedron* **2003**, *59*, 4651-4659.

8. Lu, Y.; Lemal, D. M.; Jasinski, J. P. *Journal of the American Chemical Society* **2000**, *122*, 2440-2445.

9. Lash, T. D.; Colby, D. A.; Graham, S. R.; Chaney, S. T. *Journal of Organic Chemistry* **2004**, *69*, 8851-8864.

10. Asato, A. E.; Peng, A.; Hossain, M. Z.; Mirzadegan, T.; Bertram, J. S. *Journal of Medicinal Chemistry* **1993**, *36*, 3137-47.

11. Noguchi, K.; Kase, J.; Saitoh, M.; Masumiya, H.; Saitoh, M.; Nakazawa, T.; Tanaka, Y.; Tanaka, H.; Hashimoto, K.; Shigenobu, K. *Pharmacology* **2002**, *64*, 36-42.

12. Tanaka, Y.; Shigenobu, K. *Cardiovascular Drug Reviews* **2001**, *19*, 297-312.

13. Rekka, E.; Chrysselis, M.; Siskou, I.; Kourounakis, A. *Chemical & pharmaceutical bulletin* **2002**, *50*, 904-7.

14. Bennett, S. *Chemistry and Manufacture of Cosmetics (3rd Edition)* **2002**, *3*, 243.

15. Wang, F.; Lai, Y.-H.; Han, M.-Y. *Macromolecules* **2004**, *37*, 3222-3230.

16. Redl, F. X.; Kothe, O.; Rockl, K.; Bauer, W.; Daub, J. *Macromolecular Chemistry and Physics* **2000**, *201*, 2091-2100.

17. Feringa, B. L.; van Delden, R. A.; Koumura, N.; Geertsema, E. M. *Chemical Reviews* **2000**, *100*, 1789-1816.

18. Liu, R. S. H.; Asato, A. E. *Journal of Photochemistry and Photobiology, C: Photochemistry Reviews* **2003**, *4*, 179-194.

19. Lambert, C.; Noell, G.; Zabel, M.; Hampel, F.; Schmaelzlin, E.; Braeuchle, C.; Meerholz, K. *Chemistry--A European Journal* **2003**, *9*, 4232-4239.

20. Lacroix, P. G.; Malfant, I.; Iftime, G.; Razus, A. C.; Nakatani, K.; Delaire, J. A. *Chemistry--A European Journal* **2000**, *6*, 2599-2608.

21. Herrmann, R.; Pedersen, B.; Wagner, G.; Youn, J.-H. *Journal of Organometallic Chemistry* **1998**, *571*, 261-266.

22. Cristian, L.; Sasaki, I.; Lacroix, P. G.; Donnadieu, B.; Asselberghs, I.; Clays, K.; Razus, A. C. *Chemistry of Materials* **2004**, *16*, 3543-3551.

23. Estdale, S. E.; Brettle, R.; Dummur, D. A.; Marson, C. M. *Journal of Materials Chemistry* **1997**, *7*, 391-401.

24. Ito, S.; Inabe, H.; Morita, N.; Ohta, K.; Kitamura, T.; Imafuku, K. *Journal of the American Chemical Society* **2003**, *125*, 1669-1680.

25. Liu, R. S. H. *Journal of Chemical Education* **2002**, *79*, 183-185.

26. Dewar, M. J. S. *The Molecular Orbital Theory of Organic Chemistry*; McGraw-Hill: New York, 1969.

27. Robinson, R. E.; Holovics, T. C.; Deplazes, S. F.; Powell, D. R.; Lushington, G. H.; Thompson, W. H.; Barybin, M. V. *Organometallics* **2005**, *24*, 2386-2397.

28. Holovics, T. C.; Robinson, R. E.; Weintrob, E. C.; Toriyama, M.; Lushington, G. H.; Barybin, M. V. *Journal of the American Chemical Society* **2006**, *128*, 2300-2309.

29. Moellerstedt, H.; Piqueras, M. C.; Crespo, R.; Ottosson, H. *Journal of the American Chemical Society* **2004**, *126*, 13938-13939.

30. Stirling, A.; Iannuzzi, M.; Laio, A.; Parrinello, M. *Chemphyschem : a European journal of chemical physics and physical chemistry* **2004**, *5*, 1558-68.

31. Alder Roger, W.; East Stephen, P.; Harvey Jeremy, N.; Oakley Mark, T. *Journal of the American Chemical Society* **2003**, *125*, 5375-87.

32. Churchill, M. R. *Progress in Inorganic Chemistry* **1970**, *11*, 53-98.

33. Wang, F.; Lai, Y.-H.; Han, M. Y. *Organic Letters* **2003**, *5*, 4791-4794.

34. Toefke, S.; Behrens, U. *Angewandte Chemie* **1987**, *99*, 134-5.

35. Arce, A. J.; De Sanctis, Y.; Galarza, E.; Garland, M. T.; Gobetto, R.; Machado, R.; Manzur, J.; Russo, A.; Spodine, E.; Stchedroff, M. J. *Organometallics* **2001**, *20*, 359-362.

36. Fedushkin, I. L.; Bochkarev, M. N.; Muehle, S.; Schumann, H. *Russian Chemical Bulletin (Translation of Izvestiya Akademii Nauk, Seriya Khimicheskaya)* **2003**, *52*, 2005-2011.

37. Colby, D. A.; Ferrence, G. M.; Lash, T. D. *Angewandte Chemie, International Edition* **2004**, *43*, 1346-1349.

38. Yeow, E. K. L.; Ziolek, M.; Karolczak, J.; Shevyakov, S. V.; Asato, A. E.; Maciejewski, A.; Steer, R. P. *Journal of Physical Chemistry A* **2004**, *108*, 10980-10988.

39. Fabian, K. H. H.; Elwahy, A. H. M.; Hafner, K. *Tetrahedron Letters* **2000**, *41*, 2855-2858.

40. Farrell, T.; Meyer-Friedrichsen, T.; Malessa, M.; Haase, D.; Saak, W.; Asselberghs, I.; Wostyn, K.; Clays, K.; Persoons, A.; Heck, J.; Manning, A. R. *Journal of the Chemical Society, Dalton Transaction* **2001**, 29-36.

41. Lash, T. D.; Colby, D. A.; Graham, S. R.; Ferrence, G. M.; Szczepura, L. F. *Inorganic Chemistry* **2003**, *42*, 7326-7338.

42. De Sanctis, Y.; Arce, A. J.; Canavera, F.; Machado, R.; Deeming, A. J.; Gonzalez, T.; Galarza, E. *Journal of Organometallic Chemistry* **2004**, *689*, 2025-2028.

43. Nakatsuji, H.; Ushio, J.; Han, S.; Yonezawa, T. *Journal of the American Chemical Society* **1983**, *105*, 426-34.

44. Barybin, M. V.; Young, V. G., Jr.; Ellis, J. E. *Organometallics* **1999**, *18*, 2744-2746.

45. Barybin, M. V.; Young, V. G., Jr.; Ellis, J. E. *Journal of the American Chemical Society* **2000**, *122*, 4678-4691.

46. Murphy, A. R.; Frechet, J. M. J.; Chang, P. C.; Lee, J.; Subramanian, V. *Journal of the American Chemical Society* **2004**, *126*, 1596-1597.

47. Murphy, K. L.; Tysoe, W. T.; Bennett, D. W. *Langmuir* **2004**, *20*, 1732-1738.

48. Swanson, S. A.; McClain, R.; Lovejoy, K. S.; Alamdari, N. B.; Hamilton, J. S.; Scott, J. C. *Langmuir* **2005**, *21*, 5034-5039.

49. Stapleton, J. J.; Daniel, T. A.; Uppili, S.; Cabarcos, O. M.; Naciri, J.; Shashidhar, R.; Allara, D. L. *Langmuir* **2005**, *21*, 11061-11070.

50. Chico, L.; Benedict, L. X.; Louie, S. G.; Cohen, M. L. *Physical Review B: Condensed Matter* **1996**, *54*, 2600-2628.

51. Chico, L.; Crespi, V. H.; Benedict, L. X.; Louie, S. G.; Cohen, M. L. *Physical Review Letters* **1996**, *76*, 971-4.

52. Lambin, P.; Fonseca, A.; Vigneron, J. P.; Nagy, J. B.; Lucas, A. A. *Chemical Physics Letters* **1995**, *245*, 85-9.

53. Han, J.; Anantram, M. P.; Jaffe, R. L.; Kong, J.; Dai, H. *Physical Review B: Condensed Matter and Materials Physics* **1998**, *57*, 14983-14989.

54. Lambin, P.; Biro, L. P. *New Journal of Physics* **2003**, *5*, 1-14, Paper No 141.

55. Crespi, V. H.; Benedict, L. X.; Cohen, M. L.; Louie, S. G. *Physical Review B: Condensed Matter* **1996**, *53*, R13303-R13305.

56. Treboux, G.; Lapstun, P.; Silverbrook, K. *Journal of Physical Chemistry B* **1998**, *102*, 8978-8980.

57. Naya, S.-i.; Yoda, K.; Nitta, M. *Tetrahedron* **2005**, *61*, 8616-8624.

58. Bohling, D. A.; Mann, K. R. *Inorganic Chemistry* **1983**, *22*, 1561-3.

59. Bohling, D. A.; Evans, J. F.; Mann, K. R. *Inorganic Chemistry* **1982**, *21*, 3546-51.

60. Gray, H. B.; Mann, K. R.; Lewis, N. S.; Thich, J. A.; Richman, R. M. *Advances in Chemistry Series* **1978**, *168*, 44-56.

61. Bohling, D. A.; Mann, K. R. *Inorganic Chemistry* **1984**, *23*, 1426-32.

62. Treichel, P. M. *Advances in Organometallic Chemistry* **1973**, *11*, 21-86.

63. Treichel, P. M.; Essenmacher, G. J. *Inorganic Chemistry* **1976**, *15*, 146-50.

64. Treichel, P. M.; Firsich, D. W.; Essenmacher, G. P. *Inorganic Chemistry* **1979**, *18*, 2405-9.

65. Treichel, P. M.; Shaw, D. B. *Journal of Organometallic Chemistry* **1977**, *139*, 21-30.

66. Treichel, P. M.; Shaw, D. B. *Inorganica Chimica Acta* **1976**, *16*, 199-202.

67. Treichel, P. M.; Dirreen, G. E. *Journal of Organometallic Chemistry* **1972**, *39*, C20-C22.

68. Lever, A. B. P. *Inorganic Chemistry* **1990**, *29*, 1271-85.

69. Mialki, W. S.; Wigley, D. E.; Wood, T. E.; Walton, R. A. *Inorganic Chemistry* **1982**, *21*, 480-5.

70. Vicente, J.; Chicote, M.-T.; Alvarez-Falcon, M. M.; Jones, P. G. *Organometallics* **2005**, *24*, 4666-4675.

71. Becke, A. D. *Journal of Chemical Physics* **1993**, *98*, 5648-52.

72. Miehlich, B.; Savin, A.; Stoll, H.; Preuss, H. *Chemical Physics Letters* **1989**, *157*, 200-6.

73. Lee, C.; Yang, W.; Parr, R. G. *Physical Review B: Condensed Matter and Materials Physics* **1988**, *37*, 785-9.

74. Hariharan, P. C.; Pople, J. A. *Molecular Physics* **1974**, *27*, 209-14.

75. Frisch, M. J.; Pople, J. A.; Binkley, J. S. *Journal of Chemical Physics* **1984**, *80*, 3265-9.

76. Clark, M. C. I., R. D.; van Opdenbosch, N. *J. Comp. Chem* **1989**, *10*, 982-1012.

77. Howard, S. T.; Fallis, I. A.; Willock, D. J. *Molecular Physics* **1999**, *97*, 913-918.

78. Runge, E.; Gross, E. K. U. *Physical Review Letters* **1984**, *52*, 997-1000.

79. Hirata, S.; Head-Gordon, M. *Chemical Physics Letters* **1999**, *302*, 375-382.

80. Kong, J.; White, C. A.; Krylov, A. I.; Sherrill, D.; Adamson, R. D.; Furlani, T. R.; Lee, M. S.; Lee, A. M.; Gwaltney, S. R.; Adams, T. R.; Ochsenfeld, C.; Gilbert, A. T. B.; Kedziora, G. S.; Rassolov, V. A.; Maurice, D. R.; Nair, N.; Shao, Y.; Besley, N. A.; Maslen, P. E.; Dombroski, J. P.; Daschel, H.; Zhang, W.; Korambath, P. P.; Baker, J.; Byrd, E. F. C.; Van Voorhis, T.; Oumi, M.; Hirata, S.; Hsu, C.-P.; Ishikawa, N.; Florian, J.; Warshel, A.; Johnson, B. G.;

Gill, P. M. W.; Head-Gordon, M.; Pople, J. A. *Journal of Computational Chemistry* **2000**, *21*, 1532-1548.

81. Stewart, R. F. *Journal of Chemical Physics* **1970**, *52*, 431-8.

82. Shevyakov, S. V.; Li, H.; Muthyala, R.; Asato, A. E.; Croney, J. C.; Jameson, D. M.; Liu, R. S. H. *Journal of Physical Chemistry A* **2003**, *107*, 3295-3299.

83. El-Shihi, T.; Siglmueller, F.; Herrmann, R.; Fernanda, M.; Carvalho, N. N.; Pombeiro, A. J. L. *Journal of Organometallic Chemistry* **1987**, *335*, 239-47.

84. Ugi, I. *Isonitrile Chemistry*; Academic Press: New York, 1971.

85. The shifts are calculated from the UV-Vis data reported in this work and in ref. 24, 45-48

86. For CNXAz (and azulene derivatives in general), the S0→S1 excitation energies are significantly smaller than the corresponding HOMO-LUMO separations because of the electron correlation effect: Liu, R. S. H. J. Chem. Ed. 2002, 79, 183-185.

87. Vicente, J.; Chicote, M.-T.; Alvarez-Falcon, M. M.; Jones, P. G. *Organometallics* **2005**, *24*, 5956-5963.

88. Nozoe, T.; Seto, S.; Matsumura, S. *Bulletin of the Chemical Society of Japan* **1962**, *35*, 1990-8.

89. Huenig, S.; Hafner, K.; Ort, B.; Mueller, M. *Liebigs Annalen der Chemie* **1986**, 1222-40.

90. Connelly, N. G.; Geiger, W. E. *Chemical Reviews (Washington, D. C.)* **1996**, *96*, 877-910.

91. Bullock, J. P.; Mann, K. R. *Inorganic Chemistry* **1989**, *28*, 4006-11.

92. Holovics, T. C.; Deplazes, S. F.; Toriyama, M.; Powell, D. R.; Lushington, G. H.; Barybin, M. V. *Organometallics* **2004**, *23*, 2927-2938.

93. McDonald, R. N.; Reitz, R. R. *Journal of Organic Chemistry* **1972**, *37*, 2703-5.

94. Barybin, M. V.; Chisholm, M. H.; Dalal, N. S.; Holovics, T. H.; Patmore, N. J.; Robinson, R. E.; Zipse, D. J. *Journal of the American Chemical Society* **2005**, *127*, 15182-15190.

95. DuBose, D. L.; Robinson, R. E.; Holovics, T. C.; Moody, D. R.; Weintrob, E. C.; Berrie, C. L.; Barybin, M. V. *Langmuir* **2006**, *22*, 4599-4606.

# Chapter Three

Non-Benzenoid Aryl Isocyanide Complexes of Gold (I): Toward New Classes of Metallomesogens

## 3.1. Introduction

In recent years, a new class of mesogens, or molecules that show liquid crystalline behavior, involving simple coordination complexes of aryl isocyanides with gold(I), silver(I), paladium(II), platinum(II), copper(I), iron(0), etc. has emerged.[1,2] Remarkably, even non-mesogenic simple aryl isocyanide ligands with only one aromatic ring often produce liquid crystalline systems when coordinated to the aforementioned transition metals.[3,4] The growing interest in metal-containing liquid crystals is driven by the fact that such systems can bring about additional useful properties (optical, electrical, and magnetic) compared to their organic counterparts.

Mesogens were first discovered in 1888 when Friedrick Reinitzer observed two melting points for cholesteryl benzoate, a fact that is now considered an indication of the formation of a mesophase or an intermediate phase between the liquid and solid phase. From that time forward, there have been many advances in the field, including the discovery of the first organometallic mesogen, or metallomesogen, by Daniel Vorlander in 1923. He observed mesogenic behavior in diarylmercury derivatives.[5] In 1956, the first gold(I) isocyanide complex was described.[6] However, it was not until much later that the compounds of this nature were shown to exhibit mesogenic properties under certain conditions.[7]

Liquid crystalline behavior arises from the non-random orientation of molecules of a substance in its liquid phase. Generally, in order to exhibit liquid crystalline behavior molecules must be reasonably rigid in the liquid state and be longer in one direction than another, or anisotropic. The most common class of

mesogens is called “calamitic” (e.g., **Figure 3.1.A**), where molecules of a substance have a “rigid-rod” shape in the liquid state and are substantially longer in one direction than the others. The other common type of mesogens is called “discotic”. In these, the disk-like molecules undergo stacking on top of each other (e.g., **Figure 3.1.B**). Beyond these two types, polymeric and colloidal suspensions can exhibit liquid crystalline behavior as well, depending on concentration. The latter systems are known as lytropic liquid crystals.[8]

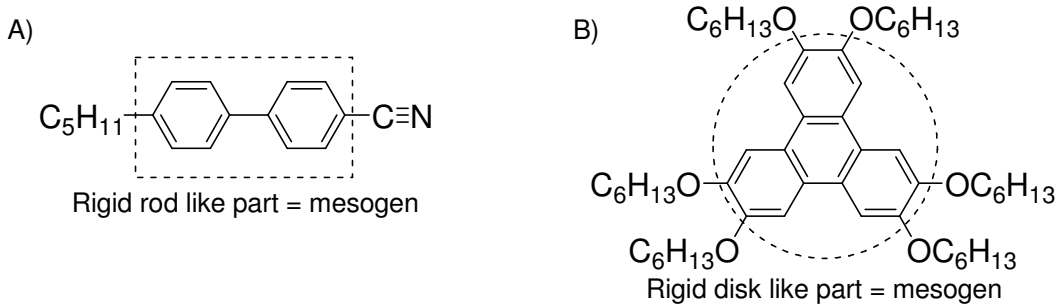


**Figure 3.1.** Examples of mesogens: A) Calamitic B) Discotic

Certain types of complexes of metal ions with the $d^{10}$ electron configuration are now known to exhibit liquid crystalline behavior. In such systems, no crystal field stabilization is possible, so the molecular geometry is determined primarily by the steric requirements of the ligands and the size and polarizability of the metal center. In the case of the $ML_2$ general motif, this leads to the linear arrangement of the ligands,[2] which is highly suitable for the design and development of mesogenic materials (**Scheme 3.1**).[9]

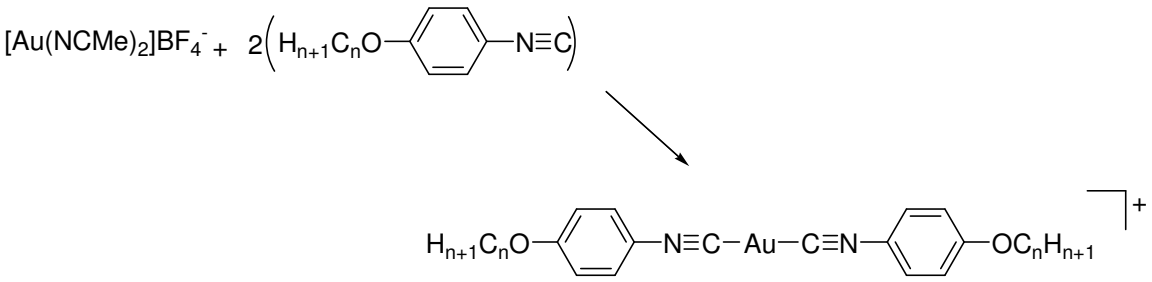


**Scheme 3.1.** Assembly of a gold(I) ionic isocyanide complex which displays liquid crystalline behavior (n = 4,8,12)[9]

In addition to the linear arrangement of the ligands in [$AuL_2$] complexes, the gold-based systems have another important quality that is very attractive in terms of achieving potential mesogenic properties, the ability to undergo molecular aggregation through "metallophilic" interactions.[10] Such interactions have been observed for many late transition metal complexes, including those of silver, mercury, palladium, and, very commonly, gold.[10] Due to its frequent occurrence in the gold-based systems, especially gold-isocyanide gold complexes, this behavior was termed "aurophilic interactions" in the case of gold complexes. (e.g., **Figure 3.2**).[10]

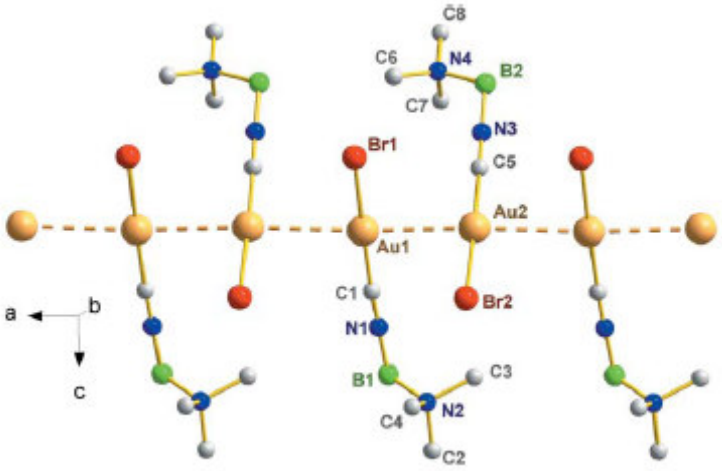


**Figure 3.2.** Example of aurophilic interaction in a gold-isocyanide complex (dashed line represents gold-gold bond) *Dalton Transactions* **2005**, 439-446. Copyright 2007 Royal Society of Chemists.[10]

The Au···Au interactions have been calculated to be worth between 8 – 13 kcal/mol, which is similar to a hydrogen bond in strength.[10] This weak bonding phenomenon allows for the self-assembly of crystalline lattices.[10] Furthermore, materials featuring Au···Au interactions can undergo facile rearrangements "in response to even mild changes in temperature, pressure or concentration."[10] This is why gold-based complexes have recently been at the center of the research efforts targeting new metallomesogens.

Due to its unique chiroptical and electronic characteristics, the azulenic scaffold is extremely attractive for incorporation into liquid crystal materials.[11] The potential of using the azulene nucleus as a core or a subunit in mesogenic molecules has been contemplated for about a decade.[12] To date, only a few organic azulene-based liquid crystalline systems have been described,[11-16] with one example shown in **Figure 3.3**. The main obstacle in the design of azulenic liquid crystals is associated with synthetic difficulties in preparing suitable azulene derivatives. The linear 2,6-substituted azulenic motif appears to be the most suitable fragment for the liquid crystal design, because the transition moment of the azulenic framework is polarized perpendicular to the molecular axis passing though carbon atoms 2 & 6 (**Figure 3.4**).[11] This allows for the construction of the calamitic style of liquid crystals due to its ability to become functionally rod like as the alkyl chain associated with the mesogen is increased in length.

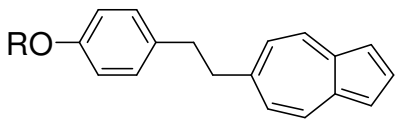


**Figure 3.3.** Example of a mesogen containing the azulenic nucleus (R= $C_6H_{13}$ or $C_{10}H_{21}$)[11]

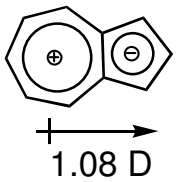


**Figure 3.4.** Azulene and the direction of its dipole moment

Since azulene is highly colored and its absorption properties can be tuned in the entire visible range through substitution at the aromatic ring,[17] the use of azulene derivatives as highly polarizable and colored components in liquid crystal devices is feasible. It may be possible to prepare azulene-containing liquid crystals of various colors that would exhibit either positive or negative linear dichroism.[11] The recently discovered isocyanoazulenes, and 2- and 6-isocyanoazulenes in particular,[18-20]are poised for solving the synthetic challenge of incorporating azulenes into novel liquid crystalline materials.

The incorporation of the ferrocene unit in the design of liquid crystals has led to several calamitic mesogens containing the ferrocenyl group as the terminal moiety (e.g., **Figure 3.5 A**).[5,21] In addition, through symmetrical or unsymmetrical 1,1'-(**Figure 3.5 B**)[22-26] or 1,3-disubstitution (**Figure 3.5 C**),[25,27-29] calamitic mesogens have been generated as well. In studies where the 1,1'- and 1,3-disubstituted mesogens were synthesized, the 1,3 disubstituted mesogens showed the greatest potential for the use in liquid crystalline materials.

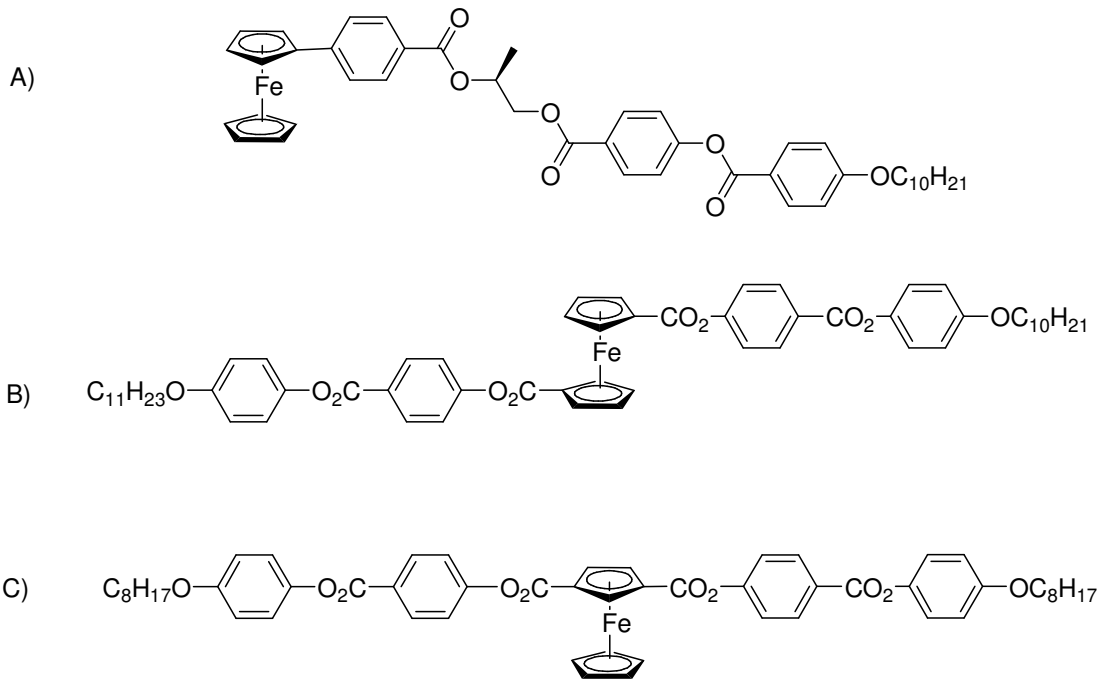


**Figure 3.5.** Selected examples of different mesogenic compounds containing ferrocene: A) ferrocenyl as a terminal moiety[21]; B) 1,1' disubstitituted ferrocene[26]; C) 1,3 disubstitiuted[25]

The ferrocene unit in liquid crystalline materials has been shown to act as a redox- active switch (**Figure 3.6**).[30,31] For example, Deschenaux *et al.* have described a compound that does not display any liquid crystalline behavior when the ferrocene fragment is in its neutral form, i.e., containing $Fe^{II}$. However, upon oxidation of the iron center to its ferric form, the substance begins to exhibit liquid crystalline properties.[31] The reason for such a dramatic change in the mesogenic behavior is associated with the ionic interactions that are introduced following the oxidation.[31] It has also been noted that by simply adding another aromatic ring to a promesogenic rod, the system may be forced to exhibit liquid crystalline behavior.[31]

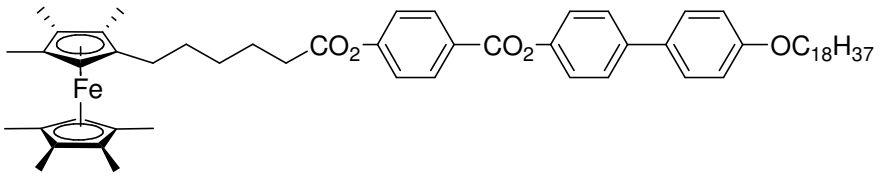


**Figure 3.6.** Example of a redox switchable, ferrocene-based liquid crystalline material[31]

Thus far, there has been very little work targeting the combination of azulene and ferrocene in the same molecule. In fact, the only known example has been investigated for its potential non-linear optical properties.[32] Herrmann *et al.* have reported on such a system featuring either an alkene or an imine bridge (e.g., **Scheme 3.2**) The resulting molecules do display interesting non-linear optical properties but undergo photochemical degradation over the course of a week in solution.[32]

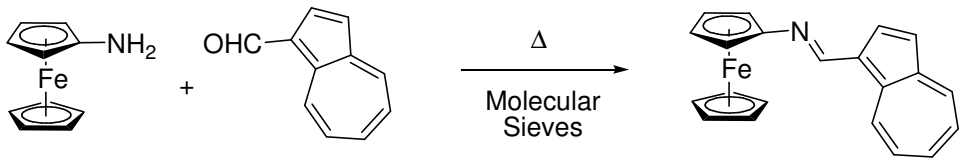


**Scheme 3.2.** Example of mixed azulene-ferrocene system that displays non-linear optical properties[32]

Finally, within the last decade, several gold(I)-containing liquid crystals have been developed.[33,34] Recently, such compounds that incorporate an azo-linkage have been of particular interest (e.g., **Figure 3.7**).[35] The azo-linkage has the flexibility to shift reversibly between its *cis* and *trans* configuration upon exposure to UV light, which is easily verifiable through UV-vis spectroscopy. When silver(I) is added to the system shown in Figure **3.7**, the photoisomerization reactions are prevented because of the steric hindrance associated with the Ag(I) ion being encapsulated within the framework. This behavior could be reversed by adding *tetra*-n-butylammonium chloride, which allows for the photoisomerization process to take

place again.[35] The above system constitutes an important step toward the design of a molecular dual input logic photoswitch.

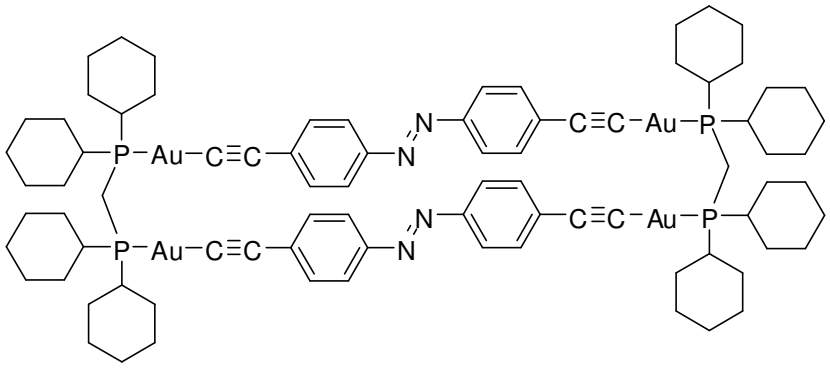


**Figure 3.7.** Example of a gold macrocycle used as a molecular dual input logic photoswitch[35]

## 3.2. Work Described in Chapter Three

The chemistry of a large gold(I) coordination macrocycle containing the diisocyanoferrocene unit is discussed in this chapter. In addition, nonbenzenoid isocyanide complexes of gold(I) containing either 1,3-diethoxycarbonyl-2-isocyanoazulene or isocyanoferrocene ligands are examined. The assembly of the above systems was investigated with the future aim of elaborating the "parent" structures into novel metallomesogens.

## 3.3. Experimental Section

### 3.3.1. General Procedures and Starting Materials

Unless specified otherwise, all procedures were performed under Ar atmosphere (99.5% purified by passage through columns of activated BASF catalyst and molecular sieves). All connections involving the gas purification system were made of glass, metal or other materials impermeable to air. Standard schlenk techniques were employed using a double-manifold vacuum line. Solvents, including dueterated solvents, were freed of impurities by standard procedures and stored under argon. Syntheses of 1,1'-ferrocene-dicarboxylic acid,[36] 1,1'-diisocyanoferrocene,[37] 2-isocyano-1,3-diethoxycarbonyl azulene,[19,20] and bis(dicyclohexylphosphinomethyl)-gold(I)dichloride[33] (**1**) were prepared according to literature methods. Infrared spectra were collected on a Shimadzu FTIR-8400S FTIR spectrometer with samples sealed in a 0.1 mm gastight NaCl cells. NMR samples were analyzed on Bruker DRX-400 and Bruker Avance 500 Spectrometers. $^{1}H$ and $^{13}C$ chemical shifts are given with reference to residual solvent resonances relative to $SiMe_4$. $^{31}P$ NMR shifts are given in reference to ortho-phosporic acid and $^{19}F$ NMR shifts are referenced to α,α,α-trifluorotoluene. Melting points are uncorrected and were determined for samples in sealed capillary tubes.

### 3.3.2. Synthesis of [(dcpm)$Au^{I}_2$(1,1'-diisocyanoferrocene)]$^{2+}$ ([OTf]$^-$)$_2$ (2), bis(dicyclohexylphosphinomethyl) = dcpm

To a clear, colorless solution of (dcpm)$Au^{I}_2Cl_2$ (200 mg, 0.229 mmol) in $CH_2Cl_2$, AgOTf (117 mg, 0.458 mmol) dissolved in 0.6 mL of acetone was added with stirring the resulting mixture turned cloudy white. After 15 minutes, the reaction turned dark blue. This solution/slurry was then filtered through a Schlenk frit to provide a clear colorless filtrate. The solvent was removed under vacuum to provide a white solid. This solid was then redissolved in 40 mL of $CH_2Cl_2$. To this stirring clear, colorless solution, 1,1'-diisocyanoferrocene (54.0 mg, 0.229 mmol) dissolved in 100 mL of $CH_2Cl_2$ was transferred over a five-minute period. During the course of the addition, the solution color changed to orange. After stirring for one hour, an FTIR spectrum of the reaction mixture indicated lack of the free diisocyanoferrocene. The solution was concentrated under vacuum and an orange solid was precipitated after the addition of pentane. The solvent was then removed via cannula and the product was washed with 2 x 30 mL of pentane and dried under vacuum to give a 83% yield of **2** (232 mg, 0.190 mmol) as an orange solid. MP = decomposes above 185 °C. FTIR ($CH_2Cl_2$): $\nu_{CN}$ 2240 $cm^{-1}$. Anal. Calcd. For $C_{39}H_{54}N_2F_6FeAu_2O_6P_2S_2$: C 35.04, H 4.07, N 2.10. Found: C 37.41, H 4.29, N 2.04. $^1$H NMR (400 MHz, $CD_2Cl_2$, 25 $^o$C): δ 1.38 (m, 22 H), 1.77 (d, 4 H), 1.93 (d, 8 H), 2.06 (s, 8H), 2.35(s, 4 H), 2.59 (t, 2H), 4.57 (t, 4H), 5.18(t, 4H) ppm. $^{13}$C NMR(100.6 MHz, $CD_2Cl_2$, 25 ºC): δ 26.00, 27.00, 27.07, 27.14, 29.99, 30.62, 36.18,

36.34, 36.50, 70.56, 72.14 ppm. $^{31}$P NMR(161.9 MHz, $CD_2Cl_2$, 25 ºC): δ 50.69 (s) ppm. $^{19}$F NMR(376.5 MHz, $CD_2Cl_2$, 25 ºC): δ -16.08 (s) ppm.

### 3.3.3. Synthesis of [(dcpm) $Au^I_2$bis(1,3-diethoxycarbonyl-2-isocyanoazulene)]$^{2+}$ ($[OTf]^-$)$_2$ (3)

To a clear, colorless solution of (dcpm)$Au^I_2Cl_2$ (125 mg, 0.114 mmol) in $CH_2Cl_2$, AgOTf (58.7 mg, 0.228 mmol) dissolved in 0.5 mL of acetone was added with stirring. The resulting mixture turned cloudy white. After 15 minutes, the solution color changed to dark blue. This solution was then filtered through a Schlenk frit to provide a clear, colorless filtrate. The solvent was evaporated from the filtrate under vacuum, leaving a white solid. This solid was then redissolved in 30 mL of $CH_2Cl_2$. To this stirring clear, colorless solution isocyanoazulene (51.5 mg, 0.228 mmol) dissolved in 30 mL of $CH_2Cl_2$ was transferred over a five-minute period. During the course of the addition, the reaction mixture acquired a light red colored. After one hour of stirring, an FTIR spectrum of the mixture indicated complete consumption of the free isocyanoazulene. The solution was concentrated under vacuum and a red solid was precipitated after the addition of pentane. The solvent was then removed via cannula, the solid was washed with 2 x 20 mL of pentane and then dried under vacuum to afford a 58% yield of **3** (185 mg, 0.111 mmol) as a maroon-red solid. MP = 97-101 °C. FTIR ($CH_2Cl_2$): $\nu_{CN}$ 2233 cm$^{-1}$. Anal. Calcd. For $C_{59}H_{76}N_2F_8FeAu_2O_8P_2B_2 \cdot CH_2Cl_2$: C 43.53, H 4.75, N 1.69. Found: C 43.40, H 4.77, N 1.64. $^1$H NMR (400 MHz, $CD_2Cl_2$, 25 $^o$C): δ 1.52 (t, 20 H), 1.65 (m, 10 H), 1.84 (d, 4 H), 2.00 (d, 8H), 2.19 (m, 8H), 2.56 (m, 4H), 2.90 (t, 2H), 4.46 (q, 8H), 7.78 (t,

4H), 8.18 (t, 2H), 9.30 (d, 4H) ppm. $^{13}C\{^{1}H\}$ NMR(100.6 MHz, $CD_2Cl_2$, 25 ºC): δ 14.95, 26.00, 26.95, 30.14, 30.48, 36.15, 36.32, 62.14, 113.59, 133.98, 139.92, 143.48, 146.67, 162.17 ppm. $^{31}P$ NMR(161.9 MHz, $CD_2Cl_2$, 25 ºC): δ 50.5 (s) ppm. $^{19}F$ NMR(376.5 MHz, $CD_2Cl_2$, 25 ºC): δ -16.49 (s) ppm.

### 3.3.4. Synthesis of (1,3-diethoxycarbonyl-2-isocyanoazulene)$Au^{I}Cl$ (4)

To a clear, colorless solution of $S(Me)_2AuCl$ (75.0 mg, 0.253 mmol) in 10 mL of $CH_2Cl_2$, a red solution of 1,3-diethoxyxarbonyl-2-isocyanoazulene (75.3 mg, 0.253 mmol) in 5 mL of $CH_2Cl_2$ was added with stirring. Upon the addition, a pink solid precipitated. An FTIR spectrum of the reaction mixture taken after 1.5 hours showed no free isocyanide present. The solution was then concentrated to approximately 5 mL and 10 mL of pentane was added. The liquid was cannulated off and the pink solid was washed with 2 x 10 mL portions of pentane. The resulting solid was then dried under vacuum to give a 67 % (90.0 mg, 0.170 mmol) yield of neon pink **4**. MP = decomposes above 207 °C Anal. Calcd. For $C_{17}H_{15}NO_4AuCl$: C 38.23, H 2.49, N 2.67. Found: C 38.54, H 2.85, N 2.64. IR ($CH_2Cl_2$): $\nu_{CN}$ 2225 $cm^{-1}$. $^{1}H$ NMR (400 MHz, $CD_2Cl_2$, 25 $^{o}$C): δ 1.45 (t, 6H), 4.43 ppm (q, 4H), 7.90 (t, 2H), 8.16 (t, 1H), 9.90 (d, 2H). $^{13}C\{^{1}H\}$ NMR(100.6 MHz, $CD_2Cl_2$, 25 ºC): δ 14.91, 61.89, 113.63, 133.35, 141.64, 142.99, 144.88, 162.88 ppm.

### 3.3.5. Synthesis of (CNFc)$Au^{I}Cl$ (5), Fc = ferrocenyl

To a clear, colorless solution of $S(Me)_2AuCl$ (150 mg, 0.507 mmol) in 15 mL of $CH_2Cl_2$, an orange solution of 114 mg (0.507 mmol) of isocyanoferrocene in 5 mL

of $CH_2Cl_2$ was added with stirring. Upon addition, the solution changed to an orange/brown and was allowed to stir for 1.5 hours at room temperature. After this time, an FTIR spectrum of the reaction mixture was taken and indicated complete consumption of the free isocyanoferrocene. The solution was then concentrated down to approximately 5 mL and 10 mL of pentane was added to precipitate an orange solid. The colorless liquid was cannulated off and the orange solid was washed with 2 x 10 mL portions of pentane. The resulting solid was then dried under vacuum to afford a 91 % (204 mg, 0.170 mmol) yield of orange **5**. MP = decomposes above 134 °C. $C_{11}H_9NI_2FePdAuCl$: C 29.79, H 2.05, N 3.16. Found: C 29.58, H 1.80, N 3.16. IR ($CH_2Cl_2$): $\nu_{CN}$ 2225 $cm^{-1}$. $^1H$ NMR (400 MHz, $CD_2Cl_2$, 25 $^oC$): δ 4.32 (t, 2H), 4.38 (s, 5H), 4.78 (t, 2H) ppm. $^{13}C\{^1H\}$ NMR(100.6 MHz, $CD_2Cl_2$, 25 ºC): δ 68.17, 69.05, 71.82 ppm.

### 3.3.6. Synthesis of [(1,3-diethoxycarbonyl-2-isocyanoazulene)$_2$Au$^I$]$^{2+}$([BF$_4$]$^-$)$_2$ (6)

To a neon pink solution of **4** (40.0 mg, 0.075 mmol) in 80 mL of $CH_2Cl_2$, $AgBF_4$ (14.6 mg, 0.075 mmol) dissolved in 0.5 mL of acetone was added with stirring. After 15 minutes, the solution color turned dark blue and the mixture was allowed to stir for an additional three hours. This solution was then filtered through a Schlenk frit to afford a pink filtrate. The solvent was evaporated under vacuum to afford a red solid. This solid was then dissolved in 40 mL of $CH_2Cl_2$. To this stirring red solution 1,3-diethoxycarbonyl-2-isocyanoazulene (22.4 mg, 0.075 mmol) dissolved in 10 mL of $CH_2Cl_2$ was canulated in over a 5 minute period. During the

course of the addition the solution changed to a darker red color. After one hour of stirring, an FTIR spectrum of the mixture indicated complete consumption of the free isocyanoazulene. The solution was concentrated under vacuum and a red solid was precipitated after the addition of pentane. The solvent was then removed via cannula, the solid was washed with 2 x 20 mL of pentane and then dried under vacuum to afford a yield of 65% of **6** (40.6 mg, 0.049 mmol) a red solid. MP = decomposes above 116 °C. IR ($CH_2Cl_2$): $\upsilon_{CN}$ 2225 $cm^{-1}$. $^1H$ NMR (400 MHz, $CD_2Cl_2$, 25 $^oC$): δ 1.60 (t, 6H), 4.61 (q, 4H), 8.11 (t, 2H), 8.38 (t, 2H), 10.02 (d, 2H) ppm. $^{13}C\{^1H\}$ NMR(100.6 MHz, $CD_2Cl_2$, 25 ºC): δ 15.00, 62.28, 114.57, 134.02, 141.11, 144.38, 146.56, 162.64 ppm $^{19}F$ NMR(376.5 MHz, $CD_2Cl_2$, 25 ºC): δ -90.97 (s) ppm.

### 3.3.7. X-ray Analysis of 2

X-ray quality crystals were grown by placing the orange/brown solid in a solution of $CH_2Cl_2$ and then canulated into a Schlenk tube. To this, pentane was then slowly layered on and the solution was allowed to slowly diffuse at 4 $^oC$, after two weeks the solution was then placed into freezer and stored at -12 $^oC$. X-ray analysis was performed by Dr. Victor Day at the University of Kansas.

Golden yellow crystals of **2** are, at 100(2) K, monoclinic, space group C2/c - $C_{2h}^6$ (No. 15)[38] with **a** = 15.712(1) **b** = 14.752(1) Å, **c** = 19.890(1) Å, **β** = 105.151(1)°, V = 4450.1(5) $Å^3$ and Z = 8 asymmetric (½ dication, 1 anion) units {$d_{calcd}$ = 1.995 $g/cm^3$, $\mu_a$(MoKα) = 7.137 $mm^{-1}$}. A full hemisphere of diffracted intensities (1850 10-second frames with a ω scan width of 0.30°) was measured for a

single-domain specimen using graphite-monochromated MoKα radiation (λ= 0.71073 Å) on a Bruker SMART APEX CCD Single Crystal Diffraction System. [39] X-rays were provided by a fine-focus sealed x-ray tube operated at 50kV and 35mA. Lattice constants were determined with the Bruker SAINT software package using peak centers for 7196 reflections. A total of 25732 integrated reflection intensities having $2\theta(MoK\alpha) < 60.06°$ were produced using the Bruker program SAINT[40]; 6478 of these were unique and gave $R_{int} = 0.032$ with a coverage which was 99.6% complete. The data were corrected empirically for variable absorption effects using 6459 equivalent reflections; the relative transmission factors ranged from 0.717 to 1.000. The Bruker software package SHELXTL was used to solve the structure using "direct methods" techniques. All stages of weighted full-matrix least-squares refinement were conducted using $F_o^2$ data with the SHELXTL Version 6.10 software package.[41,42]

All hydrogen atoms were located from a single difference Fourier and included in the structural model as independent isotropic atoms whose positional parameters were allowed to vary during least-squares refinement cycles. The final structural model incorporated anisotropic thermal parameters for all nonhydrogen atoms and isotropic thermal parameters for all hydrogen atoms. A total of 380 parameters were refined using no restraints, 6478 data and weights of $w = 1/ [\sigma^2(F^2) + (0.0260\ P)^2]$, where $P = [F_o^2 + 2F_c^2] / 3$. Final agreement factors at convergence are: $R_1$(unweighted, based on F) = 0.020 for 5701 independent absorption-corrected "observed" reflections having $2\theta(MoK\alpha) < 60.06°$ and $I > 2\sigma(I)$; $R_1$(unweighted,

based on F) = 0.024 and $wR_2$(weighted, based on $F^2$) = 0.048 for all 6478 independent absorption-corrected reflections having $2\theta(MoK\alpha) < 60.06°$. The largest shift/s.u. was 0.002 in the final refinement cycle. The top four peaks (1.79 – 1.00 $e^-$/Å) in the final difference Fourier map were within 0.83 Å of the Au atom; there were no other peaks above the background level (0.92 $e^-/Å^3$). The final difference Fourier had a minimum of -1.30 $e^-/Å^3$, respectively. Complete crystallographic data for **2** are provided in Appendix B.

### 3.3.8. X-ray Analysis of 4

X-ray quality crystals were grown by placing the neon pink solid **4** in a solution of $CH_2Cl_2$. The solution was allowed to slowly crystallize at 4 °C, after two weeks the solution was then placed into freezer and stored at -12 °C. X-ray analysis was performed by Dr. Victor Day at the University of Kansas.

Orange crystals of **4** are, at 100(2) K, monoclinic, space group $P2_1/c - C_{2h}^5$ (No. 14)[38] with **a** = 14.311(1) Å, **b** = 15.779(1) Å, **c** = 7.194(6) Å, $\beta$ = 93.600(1)°, V = 1621.3(2) $Å^3$ and Z = 4 molecules {$d_{calcd}$ = 2.170 g/$cm^3$; $\mu_a(MoK\alpha)$ = 9.260 $mm^{-1}$}. A full hemisphere of diffracted intensities (1850 20-second frames with a $\omega$ scan width of 0.30°) was measured for a single-domain specimen using graphite-monochromated MoK$\alpha$ radiation ($\lambda$= 0.71073 Å) on a Bruker SMART APEX CCD Single Crystal Diffraction System.[39] X-rays were provided by a fine-focus sealed x-ray tube operated at 50kV and 30mA. Lattice constants were determined with the Bruker SAINT software package using peak centers for 8458 reflections. A total of

19433 integrated reflection intensities having $2\theta((MoK\alpha) < 61.10°$ were produced using the Bruker program SAINT[40]; 4966 of these were unique and gave $R_{int} = 0.040$ with a coverage which was 99.8% complete. The data were corrected empirically for variable absorption effects using equivalent reflections.[40] The relative transmission factors ranged from 0.631 to 1.000. The Bruker software package SHELXTL was used to solve the structure using "direct methods" techniques. All stages of weighted full-matrix least-squares refinement were conducted using $F_o^2$ data with the SHELXTL Version 6.10 software package.[41]

Both methyl groups were incorporated into the structural model as rigid groups (using idealized $sp^3$-hybridized geometry and a C-H bond length of 0.98 Å) which were allowed to rotate about their C-C bonds in least-squares refinement cycles. The remaining hydrogen atoms were included into the structural model as idealized atoms (assuming $sp^2$- or $sp^3$-hybridization of the carbon atoms and C-H bond lengths of 0.95 – 0.99 Å). The isotropic thermal parameters of all hydrogen atoms were fixed at values 1.2 (nonmethyl) or 1.5 (methyl) times the equivalent isotropic thermal parameter of the carbon atom to which they are covalently bonded.

The final structural model incorporated anisotropic thermal parameters for all nonhydrogen atoms and isotropic thermal parameters for all hydrogen atoms. A total of 219 parameters were refined using no restraints, 4966 data and weights of $w = 1/ [\sigma^2(F^2) + (0.0409\ P)^2]$, where $P = [F_O^2 + 2F_C^2] / 3$. Final agreement factors at convergence are: $R_1$(unweighted, based on F) = 0.029 for 4274 independent absorption-corrected "observed" reflections having $2\theta(MoK\alpha) < 61.10°$ and $I>2\sigma(I)$;

$R_1$(unweighted, based on F) = 0.036 and $wR_2$(weighted, based on $F^2$) = 0.071 for all 4966 independent absorption-corrected reflections having $2\theta(MoK\alpha) < 61.10°$. The largest shift/s.u. was 0.000 in the final refinement cycle. The 4 largest peaks in the final difference Fourier map (5.55 – 1.06 $e^-/Å^3$) were within 0.90 Å of the Au atom; the next highest peak (0.90 $e^-/Å^3$) was 1.62 Å away from the Au atom. This final difference Fourier map had a minimum of –1.75 $e^-/Å^3$. Complete crystallographic data for **4** are provided in Appendix C.

### 3.4. Results and Discussion

The structures of our targeted metallomesogens, that contain both azulenic and ferrocene frameworks, are illustrated in **Figure 3.8**. Such systems would not only be color-tunable but also redox-addressable and may prove instrumental in the Barybin group's quest for novel switchable supramolecular devices.

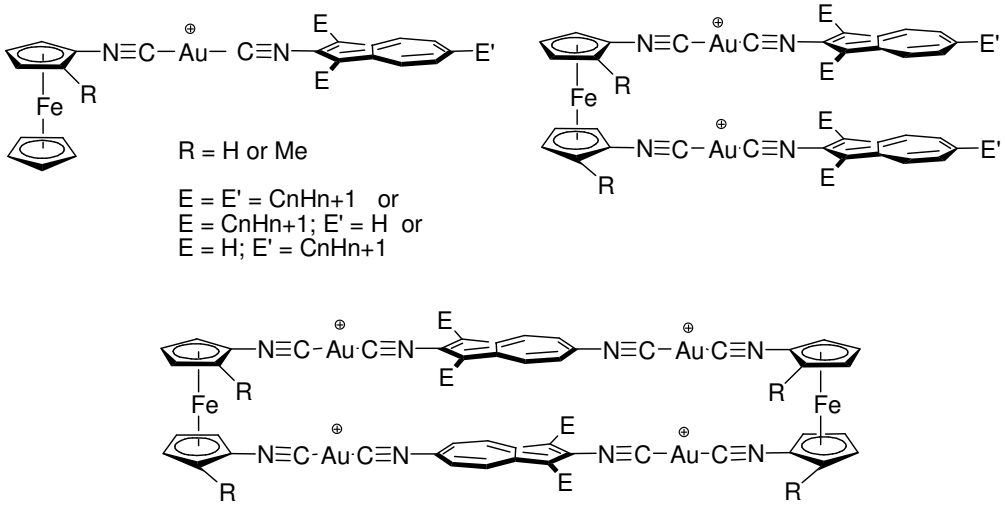


**Figure 3.8.** Proposed azulene/ferrocene metallomesogens.

#### 3.4.1. Synthesis and characterization of 2

Recently, 1,1'-diisocyanoferrocene has been shown to form a stable bis-AuCl polymeric complex (**Figure 3.9**)[44] that features the 3,4-diaura-[6]-ferrocenophane motif. The polymetic nature of this substance arises from the intermolecular Au···Au interactions. In our quest for well-defined gold complexes incorporating the ferrocene unit, non-polymeric, macrocyclic digold adduct of this μ-diisocyanide ligand has been sought. As illustrated in **Scheme 3.3**, treatment of $Me_2SAuCl$, which

contains a very labile $Me_2S$ ligand, with bis(dicyclohexylphosphino)methane (dcpm) afforded white complex **1** in a near quantitative yield.[33] This species was then reacted with silver triflate, dissolved in acetone, to precipitate AgCl. The resulting bis(triflate) intermediate was isolated and treated with 1,1'-diisocyanferrocene to afford macrocycle **2** in an excellent yield (**Scheme 3.3**)**.** This procedure was inspired by a report by Irwin and coworkers[33,45] on the chemistry of gold macrocycles involving linear aryl diisocyanide ligands.

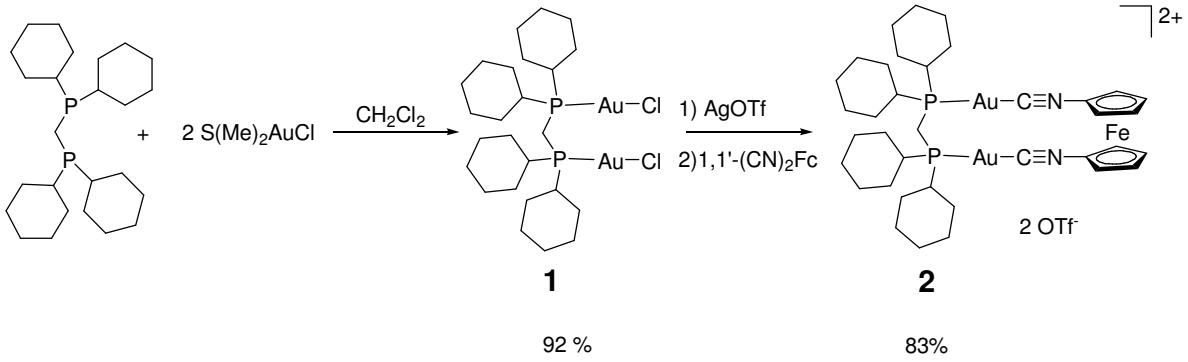


**Scheme 3.3**. Synthesis of gold(I) macrocycle **2** containing 1,1'-diisocyanoferrocene

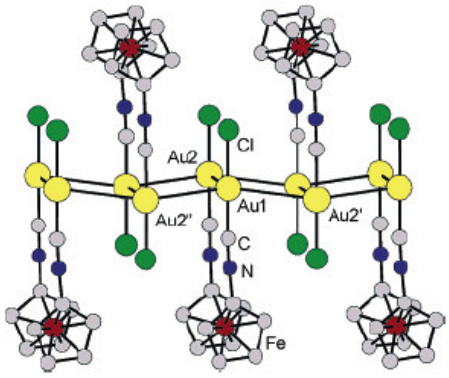


**Figure 3.9.** Polymeric1,1'-diisocyanoferrocene complex of $Au^{I}Cl$ Reproduced in part with permission from *Journal of the American Chemical Society* **2005**, *127*, 1102-1103. Copyright 2007 American Chemical Society..[44]

Given that the isocyanide has a lone pair of electrons on its terminal carbon atom, which is somewhat anti-bonding in the C≡N region, the difference between the $\nu_{CN}$ values for the metal-bound and free isocyanides may increase or decrease depending on the relative contributions of the RNC(σ)→M and M(dπ)→CNR(pπ$^*$) interactions. Since the RNC(σ)→M interaction is expected to be dominant in complexes of $Au^I$, the $\nu_{CN}$ stretching frequency should increase upon complexation of the isocyanide ligand to $Au^I$. This is indeed what was observed for **2**: the $\nu_{CN}$ value recorded for **2** is 2240 $cm^{-1}$, while that for free 1,1'-diisocyanoferrocene is 2128 $cm^{-1}$. Thus, the diisocyanoferrocene ligand in **2** functions essentially as a σ-donor only in **2**. Notably, no formation of the oligomeric complexes was observed. The assembly of the thermodynamically favored cyclic product was facilitated by the perfect match between the Au···Au interaction within the digold precursor and the interplanar separation involving the isocyanocyclopentadienyl rings in diisocyanoferrocene. In addition, the lack of backbonding in the $Au^I$-CNR unit allows for reversible complexation of the isocyanide ligand to occur. This is in sharp contrast to the kinetic control of the isocyanide complexation involving the systems with significant extents of backbonding.[20]

The single crystal X-ray analysis of **2** confirmed the cyclic nature of this complex (**Figure 3.10**). The Au···Au distance of 3.0469(2) Å (**Table 3.1**) is consistent with the presence of an aurophilic interaction between the two gold centers. Without the Au-Au bonding, the Au···Au separation might be expected to be similar to the

non-bonded distances P···P' (3.155 Å) and C(3)···C(3)' (3.325 Å). In addition, the C(1)-Au-Au' and P-Au-Au' angles of nearly 90° each support the conclusion about the aurophilic interaction in **2** as well.

**Table 3.1.** Selected bond distances (Å) and angles (°) in the X-ray structure of **2**

| | Bond distance (Å) | Bond Angle (°) |
|---|---|---|
| Au-Au | 3.0469(2) | |
| Au-Cl | 1.999(2) | |
| Au-P | 2.2853(6) | |
| C(1)-Au-P | | 169.05(7) |
| C(1)-N(1)-C(3) | | 176.0(2) |
| N(1)-C(1)-Au | | 174.7(2) |
| C(1)-Au-Au' | | 92.70(6) |
| P-Au-Au' | | 89.535(14) |

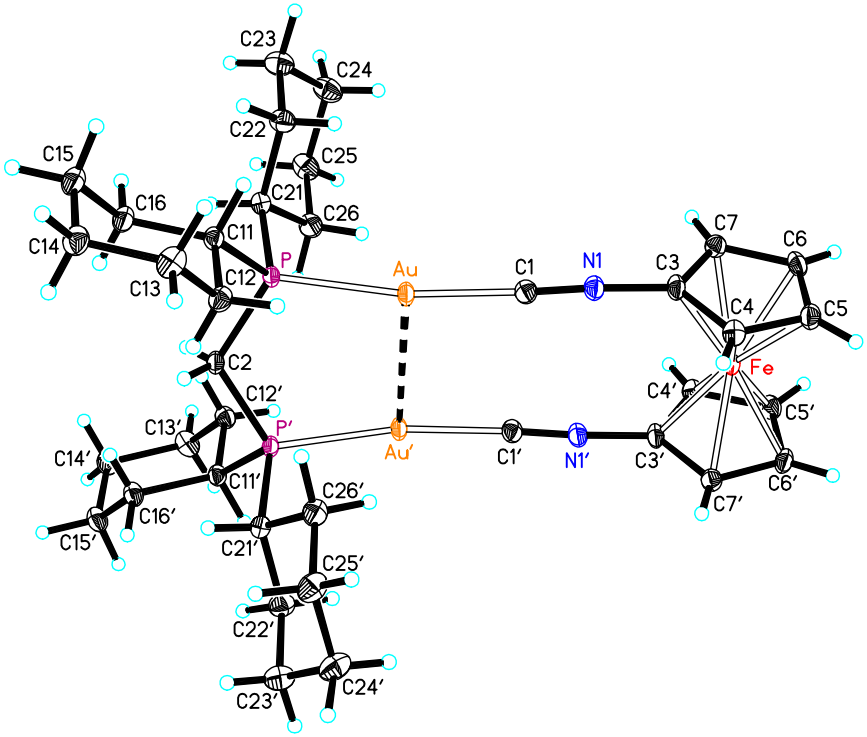


**Figure 3.10.** ORTEP Diagram (50 %) of $[\{((C_6H_{11})_2P)_2CH_2\}\{Au(CNC_5H_4)\}_2Fe][O_3SCF_3]_2$

The compound **2** constitutes the first example of a polygold macrocycle containing the ferrocene moiety. The pre-established gold-gold interaction within the

acyclic digold precursor is important for the success in the assembly of **2**. Indeed, it has been previously shown that the attempts co complex ditopic linkers using gold reactants without such interactions invariably resulted in the formation of coordination polymers form rather than rings.[33] Again, the highly selective ring formation leading to **2** is a consequence of two factors: the U-shaped geometry of the digold precursor and the relatively labile nature of the gold-isocyanide bond.

### 3.4.2 Synthesis and Characterization of 3

Following the methodology established for the preparation of **2**, the synthesis shown in **Scheme 3.4** was conducted to provide a reasonable yield of the bis(2-diisocyanoazulene) complex **3**. This synthesis was performed in an effort to ascertain whether the aurophilic interaction is stronger than the perceived repulsion of the *syn*-azuleneophane arrangement where the negative and positive dipoles of the five and seven membered rings were stacked on top of each other. This is in part because of a theoretical study reported by Grimme *et al*. where it was shown that the *syn* orientation was the highest energy arrangement for stacked azulene dimers.[48]

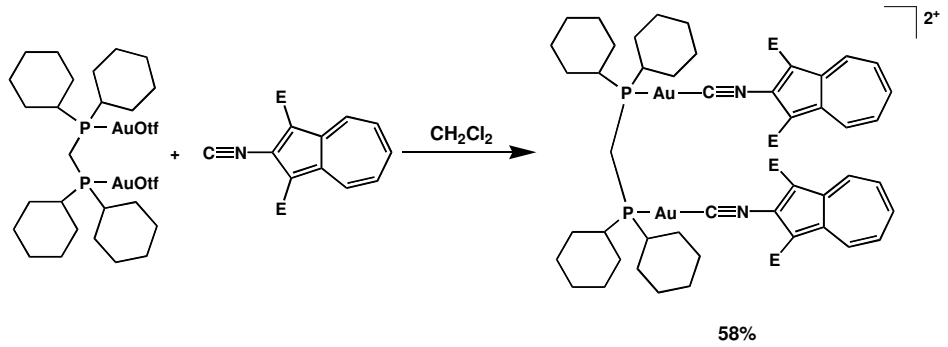


**Scheme 3.4.** Synthesis of **3** (E = ethylester).

The NMR data documented for **3** were compared to those recorded for **4** and **6**. Large shifts in the $^1$H NMR resonances were observed for the protons at the 4, 5 and 6 positions (**Table 3.2**). The most noticeable shift occurs for the H-atom at position 4, (a shift of 0.6 ppm versus **4** and a shift of 0.8 ppm compared to **6**). This large shift could be attributed to the protons at the 4 and 8 positions being in the cone of shielding of an adjacent azulene ring, with the 5-7 positions sitting at the periphery (**Figure 3.11**). These shifts suggest that the aurophilic interactions are strong enough to maintain the two azulenic frameworks positioned on top one another.

**Table 3.2** NMR shifts (in ppm) for Carbons 4,5 and 6 in $CH_2Cl_2$

| | Position 4 | Position 5 | Position 6 |
|---|---|---|---|
| **3** | 9.30 | 7.78 | 8.18 |
| **4** | 9.90 | 7.90 | 8.16 |
| **6** | 10.02 | 8.11 | 8.38 |

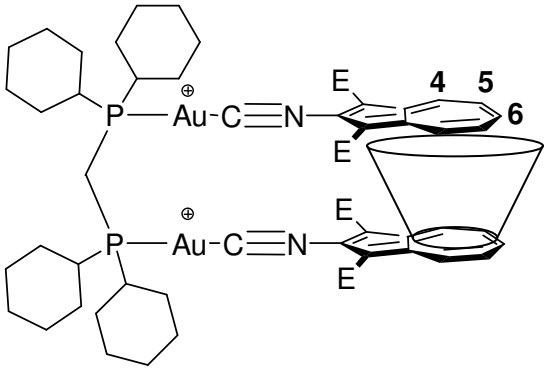


**Figure 3.11**. Representation of **3** (E = ethyl ester) with a cones of shielding associated with the five and seven membered rings

### 3.4.3 2-Isocyanoazulene and Isocyanoferrocene Adducts of Gold Chloride (**4** and **5**, respectively)

Treatment of $S(Me)_2AuCl$ with one equivalent of 1,3-diethoxycarbonyl-2-isocyanoazulene afforded the corresponding neutral monoisocyanide adduct **4**. The

reaction proceeded very quickly, with a pink solid precipitating out of solution immediately (**Scheme 3.5**). This product has very limited solubility in common organic solvents. In $CH_2Cl_2$ (apparently the best solvent), its solubility is approximately 0.5mg/mL. In coordinating solvents, such as DMSO and DMF, the isocyanide ligand was displaced readily as observed by IR, to produce yellow to red solutions. It should be noted that following the reaction sequence shown in Scheme 3.5 but using isocyanoferrocene instead of the isocyanoazulene, the corresponding isocyanoferrocene adduct **5** was obtained. Unlike **4**, orange **5** is very soluble in non- or weakly coordinating organic solvents.

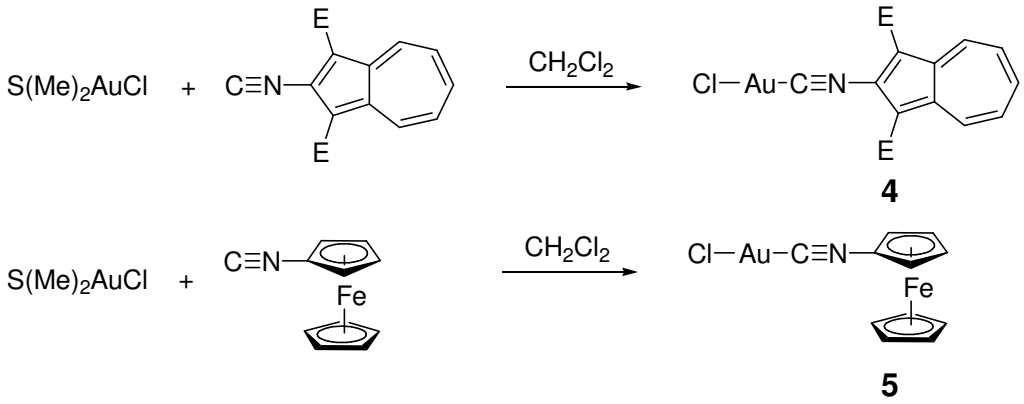


**Scheme 3.5.** Synthesis of **4** (E = ethyl ester group) and **5**.

Unlike the polymeric adduct of 1,1'-diisocyanoferrocene with $Au^{I}Cl$, the molecular structure of **4** shows discrete AuCl(isocyanide) units and does not feature aurophilic interactions (**Figure 3.12**). The average distance between the gold atoms in **4** is 7.17 Å. However, the crystal packing of **4** reveals intermolecular π-stacking interactions between the azulenyl groups. As **Figure 3.13** illustrates, these interactions result in an anti-azulenophane arrangement of the azulenyl substituents. The distance between the centroids of either 5- or 7-membered rings of the interacting

azulenyl substituents is *ca.* 3.79 Å**.** Similar intermolecular anti-azulenophane π-interactions were also documented by Dr. Thomas Holovics[18] for the crystal structures of $[Cr(CN^{1}Az)_6]^+$ and $Cr[(CN^{4}Az)_6]^+$. In addition, this phenomenon has been suspected to occur in azulene-based liquid crystalline materials, very few of which are currently known.[11] It should also be noted that in the calculations by Grimme, the off-centered arrangement of the π-stacked azulenic units has an even lower energy than that of the perfect anti-azulenophane dimer.[48] In the instance of **4**, it can be envisioned that the sterics associated with the ethylester "arms" could be the determining factor in causing the staggered alignment of the azulenyl groups.

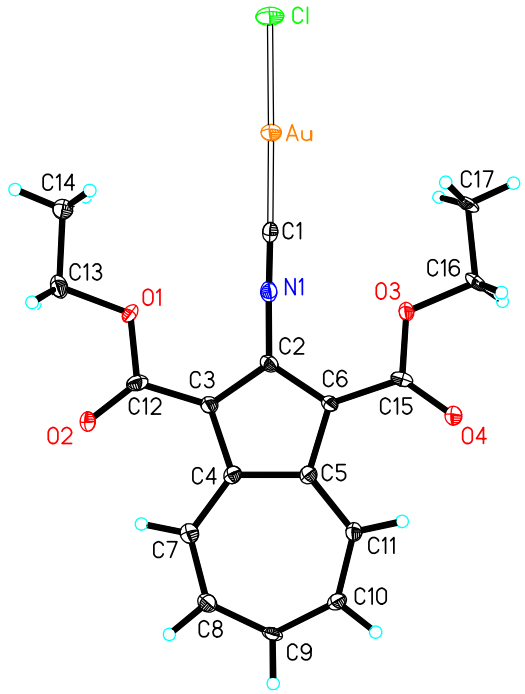


**Figure 3.12.** Molecular structure of **4** (50% thermal ellipsoids).

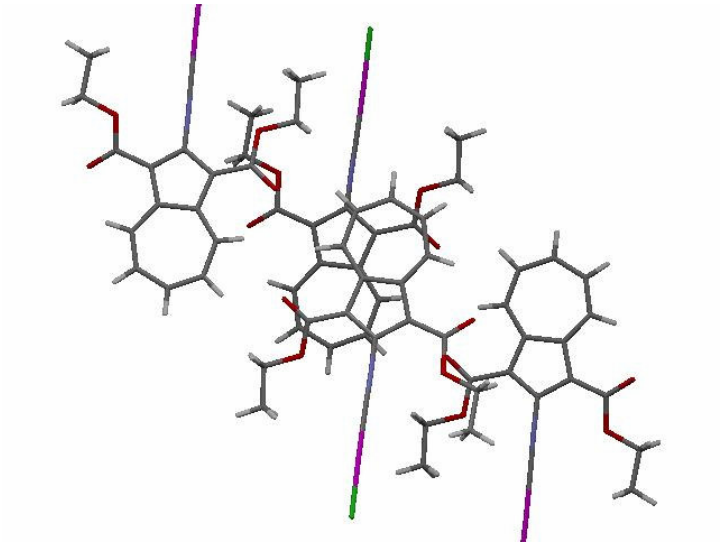

**Figure 3.13**. A crystal packing illustration of **4,** showing π stacking interactions. Atom coordinates were extracted from the .CIF file

### 3.4.4 Homoleptic Bis(2-isocyanoazulene) Adduct of $Au^{I}$ (6)

Treatment of a solution of the gold chloride adduct **4** described above with one equivalent of silver triflate results in the precipitation of AgCl. The intermediate gold triflate complex left in solution reacts with an additional equivalent of 1,3-diethoxycarbonyl-2-isocyanoazulene ligand to afford the homoleptic bis(isocyanide) adduct **6** in a good yield (**Scheme 3.6**). It should be noted that the solubility of **6** in methylene chloride is much better than that of its neutral precursor. A similar behavior has been documented by the Barybin group for the systems $[Cr(CN^{x}Az)_6]^{0/+}$ (x = 2,6).[18] Indeed, while neutral $Cr(CN^{x}Az)_6$ (x = 2,6) species are essentially insoluble, introduction of the counterions resuts in a dramatic increase in the complex solubility, presumably due to the partial disruption of the close packing of the molecular units in the crystalline lattice.

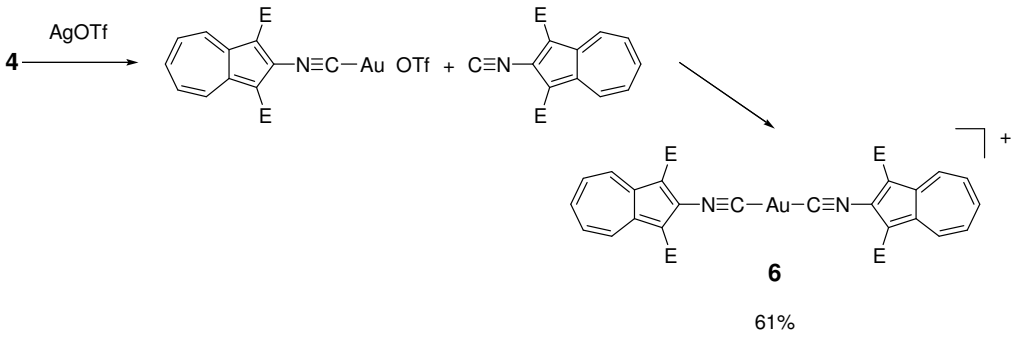


**Scheme 3.6**. Synthesis of **6** (E =ethylester)

Unfortunately, this above reaction sequence would not work for preparing the homoleptic diisocyanoferrocene analogue of **6**, because the iron(II) center of ferrocene unit in the precursor **5** would be oxidized to iron(III) in the presence silver(I). In principle, this obstacle can be overcome by employing $NaBPh_4$ instead of AgOTf to precipitate the cholide ion.[53]

### 3.4.5 Attempted synthesis of [( 1,3-$CO_2$Et-2-CN-$C_{10}H_5$) $Au^I$(CNFc)]$^+$[OTf]$^-$

After the successful syntheses of the neutral intermediate adducts **4** and **5**, as well the bis(isocyanoazulene)gold(I) complex **6**, attempts were made to isolate the mixed isocyanide complexes shown in **Figure 3.8** (top left). The first attempt at isolating such compounds involved starting with **4** and proceeding to introduce the isocyanoferrocene ligand instead of the second isocyanoazulene ligand (**Scheme 3.7**). This reaction appeared to work on the basis of the observation of an IR stretch of 2225 $cm^{-1}$. However, on closer examination the reaction solution appeared to contain a mixture of products. This was confirmed through a partial X-ray structural analysis of [bis(isocyanoferrocene)$Au^I$]$^+$[OTf]$^-$.(Deplazes, S.F., unpublished work)

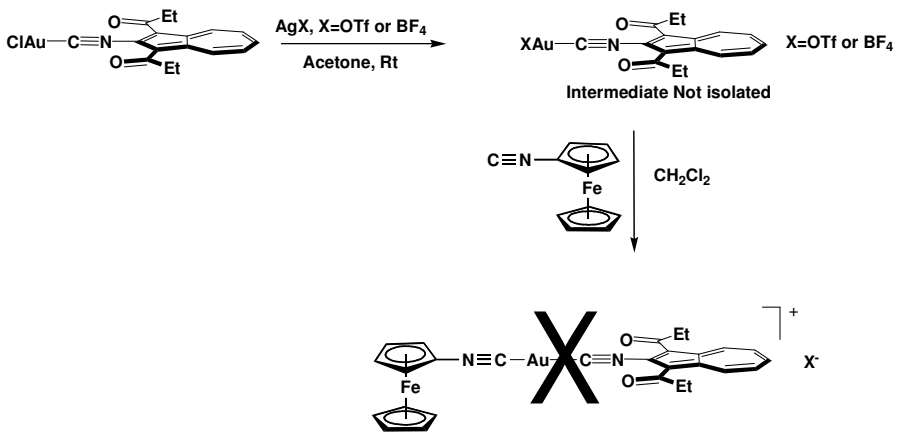


**Scheme 3.7**. Attempted synthesis of a mixed diisocyanide-gold(I) complex.

The production of a mixture of products in the above reaction can be related to the previous studies that involved the reversible binding of thiolate and cyanide ligands to Au(I). It was found by NMR, that a thiolate ligand would displace a cyanide ligand to give a mixed thiolate/cyanide complex.[54] Furthermore, the authors found that in addition to the above substitution, the mixed-ligand complex may disproportionate to give a mixture of the dithiol- and dicyanide-gold complexes.[54]

These findings are further corroborated by Shaw *et al*. who investigated the ligand scrambling reactions involving various phosphine ligands in Au(I)-cyanide complexes.[55] The authors determined that there are multiple factors that affect the ligand scrambling reaction. The first depends on the polarity and ionic strength of the solution: increasing both will make the ligand scrambling reaction occur faster. It was also shown that as the σ-donating strength or Lewis basicity of the ligand increases, the scrambling was suppressed.[55] These factors, especially the difference in the σ-donating abilities of the two ligands used in **Scheme 3.7**, likely played the critical role in the failure to produce the desired mixed isocyanide complex. Indeed,

1,3-diethoxycarbonyl-2-isocyanoazulene is a substantially weaker σ-donor as compared to isocyanoferrocene (see Chapter Two for the discussion on this issue). Thus, the fact that the coordinated 2-isocyanoazulene ligand ended up being displaced by isocyanoferrocene from the Au(I) complex is not too surprising. The above obstacle in isolating the mixed diisocyanide-gold(I) complexes is likely to be difficult to overcome, so a new strategy needs to be developed in order to construct a system similar to that proposed earlier in Section **3.4**

### 3.4.6. Conclusions and Future Work

The first gold macrocycle incorporating the redox-active ferrocene unit has been isolated and characterized. The 1,1'-diisocyanoferrocene ligand employed in this study undergoes $\mu_2$ coordination to a pair of $Au^I$ ions under the thermodynamic control, i.e., no oligomeric structures are produced at all. Formation of the cyclic product is facilitated by the near perfect match between the interplanar distance involving the five-membered rings of the diisocyanoferrocene ligand and the Au·· Au separation within the di-gold precursor that features an aurophilic interaction. Thus, 1,1'-diisocyanoferrocene can be used to obtain well-defined coordination ensembles in gold(I) chemistry, especially, if the aurophilic interaction(s) is/are already in place in the gold reactant.

In this chapter, formation of stable isocyanoazulene complexes of Au(I) has been demonstrated. It appears that in the case of the di-gold species **3** in solution, the pre-established aurophilic interaction between the two gold(I) ions is strong enough to override the somewhat unfavorable *syn*-azulenophane stacking interactions between the azulenic groups. On the contrary, the reaction between $Me_2SAuCl$ and the 2-isocyanoazulene derivative results in *discrete* mono-Au species. In this latter case, the stacking of the azulenic rings is best described as an off-centered *anti*-azulenophane arrangement.

Finally, attempts to isolate a mixed gold complexes featuring two different isocyanide ligands proved unsuccessful to date. This was likely due to the ligand

scrambling phenomenon that occurs in the gold(I) systems considered, in which the isocyanide ligands function as σ-donors only. To overcome this problem and install both the azulene and the ferrocene scaffolds into the same gold complex, this project needs to be redirected to proceed in either of the following three directions. The first route will involve covalent linking of both pieces within a single ligand. One example of such a system that has been recently synthesized in the Barybin group is shown in **Figure 3.14**. This ligand contains both ferrocene and azulene moieties connected together through an acetylene linker. The isocyanide alligator clip is positioned at carbon atom #2 of the azulenic nucleus. This design will allow for the coordination of the entire assembly to the gold center to afford a redox addressable hybrid gold/azulene material with potentially unique optical properties and electronic characteristics. It may also be possible to elaborate the "parent" design to achieve liquid crystalline behavior of the ligand and/or its complexes.

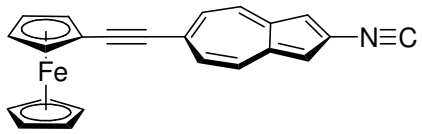


**Figure 3.14**. Recently synthesized ligand featuring both azulene and ferrocene motifs.

The second possible approach would involve complexation of the gold(I) center with an acetylide followed by the reaction with an isocyanide.[45] This reaction sequence is particularly attractive given that the Barybin group now possesses acetylenes with both ferrocenyl or azulenyl substituents (e.g., **Figure 3.15**). This procedure does not involve displacement of the chloride from the [AuCl] fragment, so the choice of which substituted acetylene to use is not critically important. One

caution associated with this preparation stems from the observations that some gold acetylides have been shown to be explosive, so they should only be produced in small quantities and should not be subject to shock before their properties are fully understood.[45]

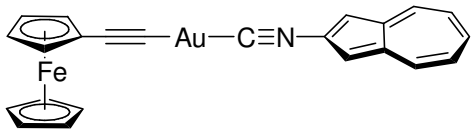


**Figure 3.15**. Proposed framework of Au containing mesogen incorporating an isocyanide and an alkyne

The third method of incorporating both ferrocene and azulene units into a possible liquid crystalline material would be based on the methodology introduced by Espinet *et al.*, which involves installation of the ferrocenyl group directly attached to the gold(I) ion followed by addition of the desired isocyanide.[4,51,56] This method forgoes the precipitation of the chloride using silver(I) and, thus, could prove very convenient for incorporating both the ferrocene and azulene fragments into the gold complex (e.g., **Figure 3.16**).

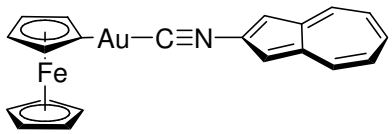


**Figure 3.16**. A potential framework towards a gold containing metallomesogen using azulene and ferrocene

Overall, the work described in this chapter constitutes significant progress toward the development of "parent" motifs to be incorporated in the potential novel mesogenic materials containing both ferrocene and azulene units. This chapter has furthered the group's knowledge of the reactivity of gold isocyanides and uncovered the reasons for challenges in isolating gold complexes with mixed isocyanide ligands.

## 3.5. References


1. Gimenez, R.; Lydon, D. R.; Serrano, J.-L. *Current Opinion in Solid State and Materials Science* **2002**, *6*, 527-535.

2. Espinet, P.; Esteruelas, M. A.; Oro, L. A.; Serrano, J. L.; Sola, E. *Coordination Chemistry Reviews* **1992**, *117*, 215-74.

3. Benouazzabe, M.; Coco, S.; Espinet, P.; Martin-Alvarez, J. M. *Journal of Materials Chemistry* **1999**, *9*, 2327-2332.

4. Bayon, R.; Coco, S.; Espinet, P.; Fernandez-Mayordomo, C.; Martin-Alvarez, J. M. *Inorganic Chemistry* **1997**, *36*, 2329-2334.

5. Imrie, C.; Engelbrecht, P.; Loubser, C.; McCleland, C. W. *Applied Organometallic Chemistry* **2001**, *15*, 1-15.

6. Sacco, A.; Freni, M. *Gazzetta Chimica Italiana* **1956**, *86*, 195-8.

7. Adams, H.; Bailey, N. A.; Bruce, D. W.; Dhillon, R.; Dunmur, D. A.; Hunt, S. E.; Lalinde, E.; Maggs, A. A.; Orr, R.; et al. *Polyhedron* **1988**, *7*, 1861-7.

8. Chandrasekhar, S. *Liquid Crystals. 2nd Ed*, 1995.

9. Benouazzane, M.; Coco, S.; Espinet, P.; Martin-Alvarez, J. M.; Barbera, J. *Journal of Materials Chemistry* **2002**, *12*, 691-696.

10. Humphrey, S. M.; Mack, H.-G.; Redshaw, C.; Elsegood, M. R. J.; Young, K. J. H.; Mayer, H. A.; Kaska, W. C. *Dalton Transactions* **2005**, 439-446.

11. Estdale, S. E.; Brettle, R.; Dummur, D. A.; Marson, C. M. *Journal of Materials Chemistry* **1997**, *7*, 391-401.

12. Brettle, R.; Dunmur, D. A.; Estdale, S.; Marson, C. M. *Journal of Materials Chemistry* **1993**, *3*, 327-31.

13. Ito, S.; Inabe, H.; Morita, N.; Ohta, K.; Kitamura, T.; Imafuku, K. *Journal of the American Chemical Society* **2003**, *125*, 1669-1680.

14. Hussain, Z.; Hopf, H.; Pohl, L.; Rantanen, T. *Synthetic Communications* **2006**, *36*, 559-571.

15. Morita, T.; Kaneko, M.; (Mitsubishi Kasei Corp., Japan). Application: JP, 1991, p 4 pp.

16. Morita, T.; Kaneko, M.; (Mitsubishi Kasei Corp., Japan). Application: JP, 1991, p 4 pp.

17. Liu, R. S. H.; Asato, A. E. *Journal of Photochemistry and Photobiology, C: Photochemistry Reviews* **2003**, *4*, 179-194.

18. Robinson, R. E.; Holovics, T. C.; Deplazes, S. F.; Powell, D. R.; Lushington, G. H.; Thompson, W. H.; Barybin, M. V. *Organometallics* **2005**, *24*, 2386-2397.

19. DuBose, D. L.; Robinson, R. E.; Holovics, T. C.; Moody, D. R.; Weintrob, E. C.; Berrie, C. L.; Barybin, M. V. *Langmuir* **2006**, *22*, 4599-4606.

20. Holovics, T. C.; Robinson, R. E.; Weintrob, E. C.; Toriyama, M.; Lushington, G. H.; Barybin, M. V. *Journal of the American Chemical Society* **2006**, *128*, 2300-2309.

21. Imrie, C.; Loubser, C. *Journal of the Chemical Society, Chemical Communications* **1994**, 2740.

22. Bhatt, J. C. Synthesis and Structure-Property Relationships of Ferrocene-Containing Liquid Crystals, **1991**. University of Oklahoma.

23. Bhatt, J.; Fung, B. M.; Nicholas, K. M.; Poon, C. D. *Journal of the Chemical Society, Chemical Communications* **1988**, 1439.

24. Deschenaux, R.; Rama, M.; Santiago, J. *Tetrahedron Letters* **1993**, *34*, 3293-6.

25. Deschenaux, R.; Marendaz, J. L. *Journal of the Chemical Society, Chemical Communications* **1991**, 909-10.

26. Deschenaux, R.; Marendaz, J. L.; Santiago, J. *Helvetica Chimica Acta* **1993**, *76*, 865-76.

27. Deschenaux, R.; Santiago, J. *Tetrahedron Letters* **1994**, *35*, 2169-72.

28. Deschenaux, R.; Kosztics, I.; Marendaz, J. L.; Stoeckli-Evans, H. *Chimia* **1993**, *47*, 206-10.

29. Deschenaux, R.; Santiago, J.; Guillon, D.; Heinrich, B. *Journal of Materials Chemistry* **1994**, *4*, 679-82.

30. Chuard, T.; Deschenaux, R. *Chimia* **2003**, *57*, 597-600.

31. Deschenaux, R.; Schweissguth, M.; Vilches, M.-T.; Levelut, A.-M.; Hautot, D.; Long, G. J.; Luneau, D. *Organometallics* **1999**, *18*, 5553-5559.

32. Herrmann, R.; Pedersen, B.; Wagner, G.; Youn, J.-H. *Journal of Organometallic Chemistry* **1998**, *571*, 261-266.

33. Irwin, M. J.; Rendina, L. M.; Vittal, J. J.; Puddephatt, R. J. *Chemical Communications (Cambridge)* **1996**, 1281-1282.

34. Puddephatt, R. J. *Coordination Chemistry Reviews* **2001**, *216-217*, 313-332.

35. Tang, H.-S.; Zhu, N.; Yam, V. W.-W. *Organometallics* **2007**, *26*, 22-25.

36. Carroll, M. A.; Widdowson, D. A.; Williams, D. J. *Synlett* **1994**, 1025-6.

37. van Leusen, D.; Hessen, B. *Organometallics* **2001**, *20*, 224-226.

38. Hahn, T.; Editor *International Tables for Crystallography, Vol. A: Space-Group Symmetry, Fourth, Revised Edition*, 1995.

39. *Data Collection: SMART Software Reference Manual* Bruker-AXS: 5465 E. Cheryl Parkway, Madison, WI 53711-5373 USA, 1998.

40. *Data Reduction: SAINT Software Reference Manual* Bruker-AXS: 6300 Enterprise Dr., Madison, WI 53719-1173, USA, 1998.

41. Sheldrick, G. M. *SHELXLT Version 6.10 Reference Manual*; Bruker-AXS: Madison, WI, 2000.

42. Wilson, A. J. C.; Editor *International Tables for Crystallography, Vol. C; Mathematical, Physical and Chemical Tables*, 1992.

43. Benouazzabe, M.; Coco, S.; Espinet, P.; Martin-Alvarez, J. M.; Barberá, J. *Journal of Materials Chemistry* **2002**, *12*, 691-696.

44. Siemeling, U.; Rother, D.; Bruhn, C.; Fink, H.; Weidner, T.; Traeger, F.; Rothenberger, A.; Fenske, D.; Priebe, A.; Maurer, J.; Winter, R. *Journal of the American Chemical Society* **2005**, *127*, 1102-1103.

45. Irwin, M. J.; Jia, G.; Payne, N. C.; Puddephatt, R. J. *Organometallics* **1996**, *15*, 51-7.

46. Irwin, M. J.; Vittal, J. J.; Yap, G. P. A.; Puddephatt, R. J. *Journal of the American Chemical Society* **1996**, *118*, 13101-13102.

47. Mathieson, T. J.; Langdon, A. G.; Milestone, N. B.; Nicholson, B. K. *Journal of the Chemical Society, Dalton Transactions: Inorganic Chemistry* **1999**, 201-208.

48. Piacenza, M.; Grimme, S. *Journal of the American Chemical Society* **2005**, *127*, 14841-14848.

49. Benouazzabe, M.; Coco, S.; Espinet, P.; Martin-Alvarez, J. M. *Journal of Materials Chemistry* **1995**, *5*, 441-445.

50. Coco, S.; Espinet, P.; Falagan, S.; Martin-Alvarez, J. M. *New Journal of Chemistry* **1995**, *19*, 959-964.

51. Coco, S.; Cordovilla, C.; Espinet, P.; Martin-Alvarez, J.; Munoz, P. *Inorganic Chemistry* **2006**, *45*, 10180-10187.

52. Bayon, R.; Coco, S.; Espinet, P. *Chemistry of Materials* **2002**, *14*, 3515-3518.

53. Tong, Y.-Y.; Frausto da Silva, J. J. R.; Pombeiro, A. J. L.; Wagner, G.; Herrmann, R. *Journal of Organometallic Chemistry* **1998**, *552*, 17-21.

54. Lewis, G.; Shaw, C. F., III *Inorganic Chemistry* **1986**, *25*, 58-62.

55. Hormann-Arendt, A. L.; Shaw, C. F., III *Inorganic Chemistry* **1990**, *29*, 4683-7.

56. Coco, S.; Espinet, P.; Martin-Alvarez, J. M.; Levelut, A.-M. *Journal of Materials Chemistry* **1997**, *7*, 19-23.

# Appendix A.

Crystallography Data for $\{(C_5H_5)Fe(C_5H_3(NC)(CH_3)\}_2\ PdI_2$

**Table A.1.** Crystal data and structure refinement for $\{(C_5H_5)Fe(C_5H_3(NC)(CH_3))\}_2PdI_2$

| | | |
|---|---|---|
| Empirical formula | $C_{24}\ H_{22}\ Fe_2\ I_2\ N_2\ Pd$ | |
| Formula weight | 810.34 | |
| Crystal system | Monoclinic | |
| Space group | $P2_1$ | |
| Unit cell dimensions | $a$ = 10.742(4) Å | α= 90° |
| | $b$ = 7.473(3) Å | β= 90.942(6)° |
| | $c$ = 31.028(6) Å | γ= 90° |
| Volume | 2490.4(14) $Å^3$ | |
| Z, Z' | 4, 2 | |
| Density (calculated) | 2.161 $Mg/m^3$ | |
| Wavelength | 0.71073 Å | |
| Temperature | 100(2) K | |
| $F$(000) | 1536 | |
| Absorption coefficient | 4.357 $mm^{-1}$ | |
| Absorption correction | Semi-empirical from equivalents | |
| Max. and min. transmission | 0.8804 and 0.3453 | |
| Theta range for data collection | 1.97 to 26.00° | |
| Reflections collected | 21789 | |
| Independent reflections | 9762 [R(int) = 0.0272] | |
| Data / restraints / parameters | 9762 / 1 / 559 | |
| $wR(F^2$ all data) | $wR2$ = 0.0637 | |
| $R$($F$ obsd data) | $R1$ = 0.0256 | |
| Goodness-of-fit on $F^2$ | 1.006 | |
| Observed data [I > 2□(I)] | 9520 | |
| Absolute structure parameter | -0.015(14) | |
| Largest and mean shift / s.u. | 0.003and 0.000 | |
| Largest diff. peak and hole | 1.827 and -0.449 e/$Å^3$ | |

**Table A.2.** Atomic coordinates and equivalent isotropic displacement parameters for $\{(C_5H_5)Fe(C_5H_3(NC)(CH_3))\}_2PdI_2$. U(eq) is defined as one third of the trace of the orthogonalized $U_{ij}$ tensor

| | x | y | z | U(eq) |
|---|---|---|---|---|
| I(1A) | 0.20801(3) | 0.22496(4) | 0.088132(9) | 0.02560(7) |
| I(2A) | 0.51529(3) | 0.73216(5) | 0.130934(9) | 0.03209(8) |
| Pd(1A) | 0.35331(3) | 0.48266(4) | 0.113989(9) | 0.01709(7) |
| Fe(1A) | 0.20881(5) | 0.78983(8) | -0.056464(18) | 0.01686(12) |
| Fe(2A) | 0.50038(6) | 0.29387(8) | 0.295181(19) | 0.01990(13) |
| N(1A) | 0.2545(3) | 0.7206(5) | 0.03878(11) | 0.0204(7) |
| N(2A) | 0.4147(3) | 0.2824(5) | 0.19980(10) | 0.0196(7) |
| C(1A) | 0.2934(4) | 0.6290(6) | 0.06581(15) | 0.0207(9) |
| C(2A) | 0.3985(4) | 0.3488(6) | 0.16695(14) | 0.0193(9) |
| C(3A) | 0.2110(4) | 0.8376(6) | 0.00716(14) | 0.0192(9) |
| C(4A) | 0.2871(4) | 0.9681(6) | -0.01383(13) | 0.0185(8) |
| C(5A) | 0.2079(4) | 1.0574(6) | -0.04284(14) | 0.0227(10) |
| C(6A) | 0.0857(4) | 0.9851(6) | -0.04035(14) | 0.0236(9) |
| C(7A) | 0.0862(4) | 0.8479(6) | -0.00925(14) | 0.0194(9) |
| C(8A) | 0.4212(4) | 1.0034(7) | -0.00395(15) | 0.0276(10) |
| C(9A) | 0.2798(4) | 0.5408(6) | -0.06718(16) | 0.0273(10) |
| C(10A) | 0.3503(4) | 0.6725(6) | -0.08944(16) | 0.0282(11) |
| C(11A) | 0.2693(4) | 0.7636(7) | -0.11816(13) | 0.0293(10) |
| C(12A) | 0.1466(4) | 0.6900(7) | -0.11411(14) | 0.0300(11) |
| C(13A) | 0.1546(5) | 0.5517(6) | -0.08266(16) | 0.0282(11) |
| C(14A) | 0.4275(4) | 0.1958(6) | 0.23940(14) | 0.0201(9) |
| C(15A) | 0.5341(5) | 0.0925(6) | 0.25229(15) | 0.0253(10) |
| C(16A) | 0.5047(5) | 0.0218(7) | 0.29298(16) | 0.0329(12) |
| C(17A) | 0.3841(5) | 0.0817(7) | 0.30550(17) | 0.0369(13) |
| C(18A) | 0.3362(4) | 0.1917(7) | 0.27196(15) | 0.0281(10) |
| C(19A) | 0.6476(5) | 0.0620(8) | 0.22593(17) | 0.0389(13) |
| C(20A) | 0.5630(4) | 0.5502(6) | 0.28644(18) | 0.0289(11) |
| C(21A) | 0.6618(4) | 0.4374(6) | 0.30060(16) | 0.0264(10) |
| C(22A) | 0.6311(4) | 0.3629(7) | 0.34061(16) | 0.0312(11) |
| C(23A) | 0.5112(5) | 0.4318(7) | 0.35204(16) | 0.0317(11) |
| C(24A) | 0.4712(5) | 0.5451(7) | 0.31925(17) | 0.0305(11) |
| I(1B) | 0.02855(3) | 0.26775(4) | 0.340269(9) | 0.02701(7) |
| I(2B) | 0.26334(3) | 0.76917(4) | 0.424252(10) | 0.03202(8) |
| Pd(1B) | 0.14573(3) | 0.51734(4) | 0.382529(10) | 0.01789(7) |
| Fe(1B) | 0.22031(5) | 0.23134(8) | 0.559524(18) | 0.01820(12) |
| Fe(2B) | 0.00073(6) | 0.76516(9) | 0.209260(18) | 0.02256(13) |
| N(1B) | 0.1718(3) | 0.2703(5) | 0.46260(11) | 0.0222(7) |
| N(2B) | 0.1062(3) | 0.7536(5) | 0.30099(10) | 0.0191(7) |
| C(1B) | 0.1634(4) | 0.3586(6) | 0.43256(14) | 0.0216(9) |
| C(2B) | 0.1241(4) | 0.6695(6) | 0.33205(14) | 0.0195(9) |
| C(3B) | 0.1934(4) | 0.1581(6) | 0.49804(14) | 0.0196(9) |

| | | | | |
|---|---|---|---|---|
| C(4B) | 0.3160(4) | 0.1059(6) | 0.51131(14) | 0.0200(9) |
| C(5B) | 0.2962(4) | -0.0138(6) | 0.54680(14) | 0.0248(9) |
| C(6B) | 0.1669(5) | -0.0311(6) | 0.55390(15) | 0.0279(10) |
| C(7B) | 0.1016(4) | 0.0756(6) | 0.52341(15) | 0.0247(10) |
| C(8B) | 0.4345(4) | 0.1612(7) | 0.49146(16) | 0.0305(11) |
| C(9B) | 0.2417(12) | 0.4987(8) | 0.5640(2) | 0.089(4) |
| C(10B) | 0.3323(6) | 0.4203(9) | 0.5863(2) | 0.0538(19) |
| C(11B) | 0.2840(6) | 0.3153(7) | 0.61806(18) | 0.0465(16) |
| C(12B) | 0.1560(7) | 0.3322(12) | 0.6155(3) | 0.082(3) |
| C(13B) | 0.1325(9) | 0.4524(15) | 0.5809(4) | 0.105(5) |
| C(14B) | 0.0876(4) | 0.8499(6) | 0.26356(14) | 0.0214(9) |
| C(15B) | 0.1719(5) | 0.8507(7) | 0.22920(16) | 0.0306(11) |
| C(16B) | 0.1172(7) | 0.9740(8) | 0.19846(17) | 0.0520(19) |
| C(17B) | 0.0033(8) | 1.0372(7) | 0.2142(2) | 0.0539(19) |
| C(18B) | -0.0174(5) | 0.9604(7) | 0.25474(17) | 0.0372(13) |
| C(19B) | 0.2896(4) | 0.7468(9) | 0.22705(18) | 0.0488(16) |
| C(20B) | -0.0618(4) | 0.5096(6) | 0.21707(16) | 0.0278(10) |
| C(21B) | 0.0290(5) | 0.5151(7) | 0.18433(17) | 0.0305(11) |
| C(22B) | -0.0163(5) | 0.6336(7) | 0.15166(16) | 0.0301(11) |
| C(23B) | -0.1332(5) | 0.6989(7) | 0.16442(16) | 0.0327(11) |
| C(24B) | -0.1620(5) | 0.6206(6) | 0.20457(17) | 0.0292(11) |

**Table A.3.** Bond lengths [Å] and angles [°] for $\{(C_5H_5)Fe(C_5H_3(NC)(CH_3))\}_2PdI_2$

| | | | |
|---|---|---|---|
| I(1A)-Pd(1A) | 2.5975(8) | Fe(2A)-C(24A) | 2.047(5) |
| I(2A)-Pd(1A) | 2.5981(8) | Fe(2A)-C(17A) | 2.047(5) |
| Pd(1A)-C(1A) | 1.953(4) | Fe(2A)-C(20A) | 2.049(5) |
| Pd(1A)-C(2A) | 1.977(4) | N(1A)-C(1A) | 1.156(6) |
| Fe(1A)-C(3A) | 2.006(4) | N(1A)-C(3A) | 1.389(5) |
| Fe(1A)-C(7A) | 2.033(4) | N(2A)-C(2A) | 1.144(5) |
| Fe(1A)-C(6A) | 2.037(4) | N(2A)-C(14A) | 1.394(5) |
| Fe(1A)-C(13A) | 2.037(5) | C(3A)-C(7A) | 1.429(6) |
| Fe(1A)-C(12A) | 2.040(4) | C(3A)-C(4A) | 1.436(6) |
| Fe(1A)-C(9A) | 2.041(4) | C(4A)-C(5A) | 1.398(6) |
| Fe(1A)-C(11A) | 2.041(4) | C(4A)-C(8A) | 1.491(6) |
| Fe(1A)-C(10A) | 2.044(5) | C(5A)-C(6A) | 1.424(6) |
| Fe(1A)-C(5A) | 2.044(4) | C(5A)-H(5A) | 0.9500 |
| Fe(1A)-C(4A) | 2.048(4) | C(6A)-C(7A) | 1.408(6) |
| Fe(2A)-C(14A) | 2.025(4) | C(6A)-H(6A) | 0.9500 |
| Fe(2A)-C(16A) | 2.035(5) | C(7A)-H(7A) | 0.9500 |
| Fe(2A)-C(22A) | 2.039(5) | C(8A)-H(8A1) | 0.9799 |
| Fe(2A)-C(18A) | 2.042(5) | C(8A)-H(8A2) | 0.9800 |
| Fe(2A)-C(21A) | 2.044(4) | C(8A)-H(8A3) | 0.9801 |
| Fe(2A)-C(23A) | 2.045(5) | C(9A)-C(13A) | 1.423(7) |
| Fe(2A)-C(15A) | 2.045(5) | C(9A)-C(10A) | 1.427(7) |

| | | | |
|---|---|---|---|
| C(9A)-H(9A) | 0.9500 | Fe(2B)-C(20B) | 2.041(5) |
| C(10A)-C(11A) | 1.410(7) | Fe(2B)-C(18B) | 2.041(5) |
| C(10A)-H(10A) | 0.9500 | Fe(2B)-C(22B) | 2.046(5) |
| C(11A)-C(12A) | 1.435(7) | Fe(2B)-C(23B) | 2.046(5) |
| C(11A)-H(11A) | 0.9500 | Fe(2B)-C(21B) | 2.047(5) |
| C(12A)-C(13A) | 1.423(7) | Fe(2B)-C(24B) | 2.058(5) |
| C(12A)-H(12A) | 0.9500 | N(1B)-C(1B) | 1.144(6) |
| C(13A)-H(13A) | 0.9500 | N(1B)-C(3B) | 1.400(6) |
| C(14A)-C(18A) | 1.419(6) | N(2B)-C(2B) | 1.164(6) |
| C(14A)-C(15A) | 1.433(6) | N(2B)-C(14B) | 1.378(6) |
| C(15A)-C(16A) | 1.409(7) | C(3B)-C(7B) | 1.413(6) |
| C(15A)-C(19A) | 1.497(7) | C(3B)-C(4B) | 1.428(6) |
| C(16A)-C(17A) | 1.431(8) | C(4B)-C(5B) | 1.437(6) |
| C(16A)-H(16A) | 0.9500 | C(4B)-C(8B) | 1.482(6) |
| C(17A)-C(18A) | 1.416(7) | C(5B)-C(6B) | 1.415(7) |
| C(17A)-H(17A) | 0.9500 | C(5B)-H(5B) | 0.9500 |
| C(18A)-H(18A) | 0.9500 | C(6B)-C(7B) | 1.414(7) |
| C(19A)-H(19A) | 0.9800 | C(6B)-H(6B) | 0.9500 |
| C(19A)-H(19B) | 0.9800 | C(7B)-H(7B) | 0.9500 |
| C(19A)-H(19C) | 0.9801 | C(8B)-H(8B1) | 0.9799 |
| C(20A)-C(21A) | 1.419(7) | C(8B)-H(8B2) | 0.9800 |
| C(20A)-C(24A) | 1.430(7) | C(8B)-H(8B3) | 0.9799 |
| C(20A)-H(20A) | 0.9500 | C(9B)-C(10B) | 1.321(11) |
| C(21A)-C(22A) | 1.405(7) | C(9B)-C(13B) | 1.339(14) |
| C(21A)-H(21A) | 0.9500 | C(9B)-H(9B) | 0.9500 |
| C(22A)-C(23A) | 1.437(7) | C(10B)-C(11B) | 1.369(9) |
| C(22A)-H(22A) | 0.9500 | C(10B)-H(10B) | 0.9500 |
| C(23A)-C(24A) | 1.386(8) | C(11B)-C(12B) | 1.381(10) |
| C(23A)-H(23A) | 0.9500 | C(11B)-H(11B) | 0.9500 |
| C(24A)-H(24A) | 0.9500 | C(12B)-C(13B) | 1.418(14) |
| I(1B)-Pd(1B) | 2.5939(7) | C(12B)-H(12B) | 0.9500 |
| I(2B)-Pd(1B) | 2.6000(7) | C(13B)-H(13B) | 0.9500 |
| Pd(1B)-C(2B) | 1.946(4) | C(14B)-C(15B) | 1.410(7) |
| Pd(1B)-C(1B) | 1.961(4) | C(14B)-C(18B) | 1.421(6) |
| Fe(1B)-C(3B) | 2.001(4) | C(15B)-C(16B) | 1.444(8) |
| Fe(1B)-C(9B) | 2.016(6) | C(15B)-C(19B) | 1.486(8) |
| Fe(1B)-C(13B) | 2.020(7) | C(16B)-C(17B) | 1.406(10) |
| Fe(1B)-C(10B) | 2.025(5) | C(16B)-H(16B) | 0.9500 |
| Fe(1B)-C(12B) | 2.025(6) | C(17B)-C(18B) | 1.404(9) |
| Fe(1B)-C(11B) | 2.030(5) | C(17B)-H(17B) | 0.9500 |
| Fe(1B)-C(5B) | 2.046(5) | C(18B)-H(18B) | 0.9500 |
| Fe(1B)-C(7B) | 2.047(5) | C(19B)-H(19D) | 0.9800 |
| Fe(1B)-C(6B) | 2.050(5) | C(19B)-H(19E) | 0.9802 |
| Fe(1B)-C(4B) | 2.055(4) | C(19B)-H(19F) | 0.9800 |
| Fe(2B)-C(14B) | 2.015(4) | C(20B)-C(24B) | 1.409(7) |
| Fe(2B)-C(16B) | 2.032(5) | C(20B)-C(21B) | 1.420(7) |
| Fe(2B)-C(15B) | 2.033(5) | C(20B)-H(20B) | 0.9500 |
| Fe(2B)-C(17B) | 2.039(5) | C(21B)-C(22B) | 1.425(8) |

| | | | |
|---|---|---|---|
| C(21B)-H(21B) | 0.9500 | C(23B)-C(24B) | 1.415(7) |
| C(22B)-C(23B) | 1.410(7) | C(23B)-H(23B) | 0.9500 |
| C(22B)-H(22B) | 0.9500 | C(24B)-H(24B) | 0.9500 |

| | | | |
|---|---|---|---|
| C(1A)-Pd(1A)-C(2A) | 173.09(18) | C(6A)-Fe(1A)-C(4A) | 68.72(18) |
| C(1A)-Pd(1A)-I(1A) | 89.43(13) | C(13A)-Fe(1A)-C(4A) | 159.62(19) |
| C(2A)-Pd(1A)-I(1A) | 91.12(13) | C(12A)-Fe(1A)-C(4A) | 158.28(19) |
| C(1A)-Pd(1A)-I(2A) | 87.94(13) | C(9A)-Fe(1A)-C(4A) | 123.22(18) |
| C(2A)-Pd(1A)-I(2A) | 92.32(13) | C(11A)-Fe(1A)-C(4A) | 122.32(18) |
| I(1A)-Pd(1A)-I(2A) | 172.549(16) | C(10A)-Fe(1A)-C(4A) | 107.56(18) |
| C(3A)-Fe(1A)-C(7A) | 41.42(17) | C(5A)-Fe(1A)-C(4A) | 39.94(18) |
| C(3A)-Fe(1A)-C(6A) | 68.17(17) | C(14A)-Fe(2A)-C(16A) | 67.57(18) |
| C(7A)-Fe(1A)-C(6A) | 40.46(18) | C(14A)-Fe(2A)-C(22A) | 159.13(19) |
| C(3A)-Fe(1A)-C(13A) | 123.14(19) | C(16A)-Fe(2A)-C(22A) | 105.1(2) |
| C(7A)-Fe(1A)-C(13A) | 106.84(19) | C(14A)-Fe(2A)-C(18A) | 40.85(18) |
| C(6A)-Fe(1A)-C(13A) | 122.75(19) | C(16A)-Fe(2A)-C(18A) | 68.6(2) |
| C(3A)-Fe(1A)-C(12A) | 157.86(19) | C(22A)-Fe(2A)-C(18A) | 156.8(2) |
| C(7A)-Fe(1A)-C(12A) | 120.21(18) | C(14A)-Fe(2A)-C(21A) | 125.17(19) |
| C(6A)-Fe(1A)-C(12A) | 105.81(19) | C(16A)-Fe(2A)-C(21A) | 120.5(2) |
| C(13A)-Fe(1A)-C(12A) | 40.8(2) | C(22A)-Fe(2A)-C(21A) | 40.3(2) |
| C(3A)-Fe(1A)-C(9A) | 108.92(19) | C(18A)-Fe(2A)-C(21A) | 162.2(2) |
| C(7A)-Fe(1A)-C(9A) | 124.09(19) | C(14A)-Fe(2A)-C(23A) | 159.30(19) |
| C(6A)-Fe(1A)-C(9A) | 159.90(19) | C(16A)-Fe(2A)-C(23A) | 122.1(2) |
| C(13A)-Fe(1A)-C(9A) | 40.85(19) | C(22A)-Fe(2A)-C(23A) | 41.19(19) |
| C(12A)-Fe(1A)-C(9A) | 69.0(2) | C(18A)-Fe(2A)-C(23A) | 122.0(2) |
| C(3A)-Fe(1A)-C(11A) | 160.29(19) | C(21A)-Fe(2A)-C(23A) | 68.2(2) |
| C(7A)-Fe(1A)-C(11A) | 156.39(18) | C(14A)-Fe(2A)-C(15A) | 41.21(17) |
| C(6A)-Fe(1A)-C(11A) | 121.13(19) | C(16A)-Fe(2A)-C(15A) | 40.4(2) |
| C(13A)-Fe(1A)-C(11A) | 68.6(2) | C(22A)-Fe(2A)-C(15A) | 120.6(2) |
| C(12A)-Fe(1A)-C(11A) | 41.16(19) | C(18A)-Fe(2A)-C(15A) | 69.9(2) |
| C(9A)-Fe(1A)-C(11A) | 68.5(2) | C(21A)-Fe(2A)-C(15A) | 106.3(2) |
| C(3A)-Fe(1A)-C(10A) | 124.91(19) | C(23A)-Fe(2A)-C(15A) | 157.5(2) |
| C(7A)-Fe(1A)-C(10A) | 161.51(19) | C(14A)-Fe(2A)-C(24A) | 125.77(19) |
| C(6A)-Fe(1A)-C(10A) | 157.13(19) | C(16A)-Fe(2A)-C(24A) | 158.8(2) |
| C(13A)-Fe(1A)-C(10A) | 68.62(19) | C(22A)-Fe(2A)-C(24A) | 67.9(2) |
| C(12A)-Fe(1A)-C(10A) | 68.87(19) | C(18A)-Fe(2A)-C(24A) | 109.6(2) |
| C(9A)-Fe(1A)-C(10A) | 40.89(19) | C(21A)-Fe(2A)-C(24A) | 67.87(19) |
| C(11A)-Fe(1A)-C(10A) | 40.40(19) | C(23A)-Fe(2A)-C(24A) | 39.6(2) |
| C(3A)-Fe(1A)-C(5A) | 67.81(17) | C(15A)-Fe(2A)-C(24A) | 160.4(2) |
| C(7A)-Fe(1A)-C(5A) | 68.70(18) | C(14A)-Fe(2A)-C(17A) | 67.97(19) |
| C(6A)-Fe(1A)-C(5A) | 40.83(18) | C(16A)-Fe(2A)-C(17A) | 41.0(2) |
| C(13A)-Fe(1A)-C(5A) | 159.2(2) | C(22A)-Fe(2A)-C(17A) | 120.2(2) |
| C(12A)-Fe(1A)-C(5A) | 122.4(2) | C(18A)-Fe(2A)-C(17A) | 40.5(2) |
| C(9A)-Fe(1A)-C(5A) | 158.3(2) | C(21A)-Fe(2A)-C(17A) | 155.9(2) |
| C(11A)-Fe(1A)-C(5A) | 106.90(19) | C(23A)-Fe(2A)-C(17A) | 106.4(2) |
| C(10A)-Fe(1A)-C(5A) | 121.96(19) | C(15A)-Fe(2A)-C(17A) | 69.3(2) |
| C(3A)-Fe(1A)-C(4A) | 41.46(16) | C(24A)-Fe(2A)-C(17A) | 123.8(2) |
| C(7A)-Fe(1A)-C(4A) | 70.11(17) | C(14A)-Fe(2A)-C(20A) | 110.4(2) |

| | | | |
|---|---|---|---|
| C(16A)-Fe(2A)-C(20A) | 157.1(2) | C(13A)-C(9A)-C(10A) | 107.6(4) |
| C(22A)-Fe(2A)-C(20A) | 68.4(2) | C(13A)-C(9A)-Fe(1A) | 69.4(3) |
| C(18A)-Fe(2A)-C(20A) | 125.9(2) | C(10A)-C(9A)-Fe(1A) | 69.7(3) |
| C(21A)-Fe(2A)-C(20A) | 40.57(19) | C(13A)-C(9A)-H(9A) | 126.2 |
| C(23A)-Fe(2A)-C(20A) | 68.2(2) | C(10A)-C(9A)-H(9A) | 126.2 |
| C(15A)-Fe(2A)-C(20A) | 122.7(2) | Fe(1A)-C(9A)-H(9A) | 126.3 |
| C(24A)-Fe(2A)-C(20A) | 40.9(2) | C(11A)-C(10A)-C(9A) | 108.2(4) |
| C(17A)-Fe(2A)-C(20A) | 161.3(2) | C(11A)-C(10A)-Fe(1A) | 69.7(2) |
| C(1A)-N(1A)-C(3A) | 177.2(4) | C(9A)-C(10A)-Fe(1A) | 69.5(3) |
| C(2A)-N(2A)-C(14A) | 176.4(4) | C(11A)-C(10A)-H(10A) | 125.9 |
| N(1A)-C(1A)-Pd(1A) | 176.5(4) | C(9A)-C(10A)-H(10A) | 125.9 |
| N(2A)-C(2A)-Pd(1A) | 172.4(4) | Fe(1A)-C(10A)-H(10A) | 126.5 |
| N(1A)-C(3A)-C(7A) | 126.1(4) | C(10A)-C(11A)-C(12A) | 108.5(4) |
| N(1A)-C(3A)-C(4A) | 124.1(4) | C(10A)-C(11A)-Fe(1A) | 69.9(3) |
| C(7A)-C(3A)-C(4A) | 109.9(4) | C(12A)-C(11A)-Fe(1A) | 69.4(2) |
| N(1A)-C(3A)-Fe(1A) | 125.6(3) | C(10A)-C(11A)-H(11A) | 125.7 |
| C(7A)-C(3A)-Fe(1A) | 70.3(2) | C(12A)-C(11A)-H(11A) | 125.7 |
| C(4A)-C(3A)-Fe(1A) | 70.8(2) | Fe(1A)-C(11A)-H(11A) | 126.5 |
| C(5A)-C(4A)-C(3A) | 105.8(4) | C(13A)-C(12A)-C(11A) | 107.1(4) |
| C(5A)-C(4A)-C(8A) | 128.6(4) | C(13A)-C(12A)-Fe(1A) | 69.5(3) |
| C(3A)-C(4A)-C(8A) | 125.6(4) | C(11A)-C(12A)-Fe(1A) | 69.4(2) |
| C(5A)-C(4A)-Fe(1A) | 69.9(2) | C(13A)-C(12A)-H(12A) | 126.5 |
| C(3A)-C(4A)-Fe(1A) | 67.7(2) | C(11A)-C(12A)-H(12A) | 126.5 |
| C(8A)-C(4A)-Fe(1A) | 129.2(3) | Fe(1A)-C(12A)-H(12A) | 126.2 |
| C(4A)-C(5A)-C(6A) | 109.6(4) | C(12A)-C(13A)-C(9A) | 108.6(4) |
| C(4A)-C(5A)-Fe(1A) | 70.2(2) | C(12A)-C(13A)-Fe(1A) | 69.7(3) |
| C(6A)-C(5A)-Fe(1A) | 69.3(2) | C(9A)-C(13A)-Fe(1A) | 69.7(3) |
| C(4A)-C(5A)-H(5A) | 125.2 | C(12A)-C(13A)-H(13A) | 125.7 |
| C(6A)-C(5A)-H(5A) | 125.2 | C(9A)-C(13A)-H(13A) | 125.7 |
| Fe(1A)-C(5A)-H(5A) | 126.9 | Fe(1A)-C(13A)-H(13A) | 126.5 |
| C(7A)-C(6A)-C(5A) | 108.7(4) | N(2A)-C(14A)-C(18A) | 125.3(4) |
| C(7A)-C(6A)-Fe(1A) | 69.6(2) | N(2A)-C(14A)-C(15A) | 124.3(4) |
| C(5A)-C(6A)-Fe(1A) | 69.8(2) | C(18A)-C(14A)-C(15A) | 110.4(4) |
| C(7A)-C(6A)-H(6A) | 125.7 | N(2A)-C(14A)-Fe(2A) | 128.1(3) |
| C(5A)-C(6A)-H(6A) | 125.7 | C(18A)-C(14A)-Fe(2A) | 70.2(3) |
| Fe(1A)-C(6A)-H(6A) | 126.5 | C(15A)-C(14A)-Fe(2A) | 70.2(2) |
| C(6A)-C(7A)-C(3A) | 106.1(4) | C(16A)-C(15A)-C(14A) | 105.2(4) |
| C(6A)-C(7A)-Fe(1A) | 69.9(2) | C(16A)-C(15A)-C(19A) | 129.0(5) |
| C(3A)-C(7A)-Fe(1A) | 68.3(2) | C(14A)-C(15A)-C(19A) | 125.7(4) |
| C(6A)-C(7A)-H(7A) | 127.0 | C(16A)-C(15A)-Fe(2A) | 69.4(3) |
| C(3A)-C(7A)-H(7A) | 127.0 | C(14A)-C(15A)-Fe(2A) | 68.6(2) |
| Fe(1A)-C(7A)-H(7A) | 126.4 | C(19A)-C(15A)-Fe(2A) | 128.5(4) |
| C(4A)-C(8A)-H(8A1) | 109.5 | C(15A)-C(16A)-C(17A) | 110.1(4) |
| C(4A)-C(8A)-H(8A2) | 109.5 | C(15A)-C(16A)-Fe(2A) | 70.2(3) |
| H(8A1)-C(8A)-H(8A2) | 109.5 | C(17A)-C(16A)-Fe(2A) | 69.9(3) |
| C(4A)-C(8A)-H(8A3) | 109.5 | C(15A)-C(16A)-H(16A) | 125.0 |
| H(8A1)-C(8A)-H(8A3) | 109.5 | C(17A)-C(16A)-H(16A) | 125.0 |
| H(8A2)-C(8A)-H(8A3) | 109.5 | Fe(2A)-C(16A)-H(16A) | 126.5 |

| | | | |
|---|---|---|---|
| C(18A)-C(17A)-C(16A) | 107.5(5) | C(2B)-Pd(1B)-C(1B) | 178.11(18) |
| C(18A)-C(17A)-Fe(2A) | 69.5(3) | C(2B)-Pd(1B)-I(1B) | 87.87(13) |
| C(16A)-C(17A)-Fe(2A) | 69.0(3) | C(1B)-Pd(1B)-I(1B) | 90.29(13) |
| C(18A)-C(17A)-H(17A) | 126.2 | C(2B)-Pd(1B)-I(2B) | 91.63(13) |
| C(16A)-C(17A)-H(17A) | 126.2 | C(1B)-Pd(1B)-I(2B) | 90.21(13) |
| Fe(2A)-C(17A)-H(17A) | 126.8 | I(1B)-Pd(1B)-I(2B) | 179.484(17) |
| C(17A)-C(18A)-C(14A) | 106.8(4) | C(3B)-Fe(1B)-C(9B) | 110.6(2) |
| C(17A)-C(18A)-Fe(2A) | 69.9(3) | C(3B)-Fe(1B)-C(13B) | 118.5(3) |
| C(14A)-C(18A)-Fe(2A) | 68.9(2) | C(9B)-Fe(1B)-C(13B) | 38.7(4) |
| C(17A)-C(18A)-H(18A) | 126.6 | C(3B)-Fe(1B)-C(10B) | 131.1(2) |
| C(14A)-C(18A)-H(18A) | 126.6 | C(9B)-Fe(1B)-C(10B) | 38.2(3) |
| Fe(2A)-C(18A)-H(18A) | 126.1 | C(13B)-Fe(1B)-C(10B) | 64.7(3) |
| C(15A)-C(19A)-H(19A) | 109.5 | C(3B)-Fe(1B)-C(12B) | 150.9(3) |
| C(15A)-C(19A)-H(19B) | 109.5 | C(9B)-Fe(1B)-C(12B) | 67.2(3) |
| H(19A)-C(19A)-H(19B) | 109.5 | C(13B)-Fe(1B)-C(12B) | 41.0(4) |
| C(15A)-C(19A)-H(19C) | 109.5 | C(10B)-Fe(1B)-C(12B) | 66.2(2) |
| H(19A)-C(19A)-H(19C) | 109.5 | C(3B)-Fe(1B)-C(11B) | 168.2(2) |
| H(19B)-C(19A)-H(19C) | 109.5 | C(9B)-Fe(1B)-C(11B) | 66.1(3) |
| C(21A)-C(20A)-C(24A) | 106.6(5) | C(13B)-Fe(1B)-C(11B) | 66.7(3) |
| C(21A)-C(20A)-Fe(2A) | 69.5(3) | C(10B)-Fe(1B)-C(11B) | 39.5(3) |
| C(24A)-C(20A)-Fe(2A) | 69.5(3) | C(12B)-Fe(1B)-C(11B) | 39.8(3) |
| C(21A)-C(20A)-H(20A) | 126.7 | C(3B)-Fe(1B)-C(5B) | 67.84(17) |
| C(24A)-C(20A)-H(20A) | 126.7 | C(9B)-Fe(1B)-C(5B) | 148.8(4) |
| Fe(2A)-C(20A)-H(20A) | 125.9 | C(13B)-Fe(1B)-C(5B) | 170.1(5) |
| C(22A)-C(21A)-C(20A) | 108.9(4) | C(10B)-Fe(1B)-C(5B) | 117.9(3) |
| C(22A)-C(21A)-Fe(2A) | 69.7(3) | C(12B)-Fe(1B)-C(5B) | 129.9(3) |
| C(20A)-C(21A)-Fe(2A) | 69.9(3) | C(11B)-Fe(1B)-C(5B) | 108.7(2) |
| C(22A)-C(21A)-H(21A) | 125.6 | C(3B)-Fe(1B)-C(7B) | 40.84(18) |
| C(20A)-C(21A)-H(21A) | 125.6 | C(9B)-Fe(1B)-C(7B) | 132.1(3) |
| Fe(2A)-C(21A)-H(21A) | 126.4 | C(13B)-Fe(1B)-C(7B) | 110.8(3) |
| C(21A)-C(22A)-C(23A) | 107.5(5) | C(10B)-Fe(1B)-C(7B) | 169.1(3) |
| C(21A)-C(22A)-Fe(2A) | 70.0(3) | C(12B)-Fe(1B)-C(7B) | 117.6(2) |
| C(23A)-C(22A)-Fe(2A) | 69.6(3) | C(11B)-Fe(1B)-C(7B) | 149.7(2) |
| C(21A)-C(22A)-H(22A) | 126.3 | C(5B)-Fe(1B)-C(7B) | 68.37(19) |
| C(23A)-C(22A)-H(22A) | 126.3 | C(3B)-Fe(1B)-C(6B) | 67.74(18) |
| Fe(2A)-C(22A)-H(22A) | 125.7 | C(9B)-Fe(1B)-C(6B) | 170.3(4) |
| C(24A)-C(23A)-C(22A) | 107.8(5) | C(13B)-Fe(1B)-C(6B) | 132.8(4) |
| C(24A)-C(23A)-Fe(2A) | 70.3(3) | C(10B)-Fe(1B)-C(6B) | 150.0(3) |
| C(22A)-C(23A)-Fe(2A) | 69.2(3) | C(12B)-Fe(1B)-C(6B) | 109.3(3) |
| C(24A)-C(23A)-H(23A) | 126.1 | C(11B)-Fe(1B)-C(6B) | 117.5(2) |
| C(22A)-C(23A)-H(23A) | 126.1 | C(5B)-Fe(1B)-C(6B) | 40.43(19) |
| Fe(2A)-C(23A)-H(23A) | 126.0 | C(7B)-Fe(1B)-C(6B) | 40.38(19) |
| C(23A)-C(24A)-C(20A) | 109.2(5) | C(3B)-Fe(1B)-C(4B) | 41.19(17) |
| C(23A)-C(24A)-Fe(2A) | 70.1(3) | C(9B)-Fe(1B)-C(4B) | 116.4(3) |
| C(20A)-C(24A)-Fe(2A) | 69.7(3) | C(13B)-Fe(1B)-C(4B) | 148.7(5) |
| C(23A)-C(24A)-H(24A) | 125.4 | C(10B)-Fe(1B)-C(4B) | 108.4(2) |
| C(20A)-C(24A)-H(24A) | 125.4 | C(12B)-Fe(1B)-C(4B) | 167.4(3) |
| Fe(2A)-C(24A)-H(24A) | 126.4 | C(11B)-Fe(1B)-C(4B) | 128.8(2) |

| | | | |
|---|---|---|---|
| C(5B)-Fe(1B)-C(4B) | 41.03(18) | C(1B)-N(1B)-C(3B) | 174.5(4) |
| C(7B)-Fe(1B)-C(4B) | 69.91(18) | C(2B)-N(2B)-C(14B) | 178.2(4) |
| C(6B)-Fe(1B)-C(4B) | 69.17(18) | N(1B)-C(1B)-Pd(1B) | 177.6(4) |
| C(14B)-Fe(2B)-C(16B) | 67.58(19) | N(2B)-C(2B)-Pd(1B) | 176.1(4) |
| C(14B)-Fe(2B)-C(15B) | 40.78(19) | N(1B)-C(3B)-C(7B) | 126.2(4) |
| C(16B)-Fe(2B)-C(15B) | 41.6(2) | N(1B)-C(3B)-C(4B) | 122.0(4) |
| C(14B)-Fe(2B)-C(17B) | 67.6(2) | C(7B)-C(3B)-C(4B) | 111.7(4) |
| C(16B)-Fe(2B)-C(17B) | 40.4(3) | N(1B)-C(3B)-Fe(1B) | 127.2(3) |
| C(15B)-Fe(2B)-C(17B) | 69.7(3) | C(7B)-C(3B)-Fe(1B) | 71.3(3) |
| C(14B)-Fe(2B)-C(20B) | 110.11(19) | C(4B)-C(3B)-Fe(1B) | 71.4(2) |
| C(16B)-Fe(2B)-C(20B) | 160.7(3) | C(3B)-C(4B)-C(5B) | 104.1(4) |
| C(15B)-Fe(2B)-C(20B) | 123.8(2) | C(3B)-C(4B)-C(8B) | 126.8(4) |
| C(17B)-Fe(2B)-C(20B) | 158.2(3) | C(5B)-C(4B)-C(8B) | 129.1(4) |
| C(14B)-Fe(2B)-C(18B) | 41.00(18) | C(3B)-C(4B)-Fe(1B) | 67.4(2) |
| C(16B)-Fe(2B)-C(18B) | 68.3(3) | C(5B)-C(4B)-Fe(1B) | 69.1(3) |
| C(15B)-Fe(2B)-C(18B) | 70.2(2) | C(8B)-C(4B)-Fe(1B) | 128.2(3) |
| C(17B)-Fe(2B)-C(18B) | 40.2(3) | C(6B)-C(5B)-C(4B) | 109.5(4) |
| C(20B)-Fe(2B)-C(18B) | 123.5(2) | C(6B)-C(5B)-Fe(1B) | 69.9(3) |
| C(14B)-Fe(2B)-C(22B) | 156.3(2) | C(4B)-C(5B)-Fe(1B) | 69.8(2) |
| C(16B)-Fe(2B)-C(22B) | 105.8(2) | C(6B)-C(5B)-H(5B) | 125.2 |
| C(15B)-Fe(2B)-C(22B) | 119.0(2) | C(4B)-C(5B)-H(5B) | 125.2 |
| C(17B)-Fe(2B)-C(22B) | 123.1(2) | Fe(1B)-C(5B)-H(5B) | 126.6 |
| C(20B)-Fe(2B)-C(22B) | 68.2(2) | C(7B)-C(6B)-C(5B) | 108.7(4) |
| C(18B)-Fe(2B)-C(22B) | 160.0(2) | C(7B)-C(6B)-Fe(1B) | 69.7(3) |
| C(14B)-Fe(2B)-C(23B) | 162.9(2) | C(5B)-C(6B)-Fe(1B) | 69.6(3) |
| C(16B)-Fe(2B)-C(23B) | 120.1(2) | C(7B)-C(6B)-H(6B) | 125.6 |
| C(15B)-Fe(2B)-C(23B) | 154.9(2) | C(5B)-C(6B)-H(6B) | 125.6 |
| C(17B)-Fe(2B)-C(23B) | 107.5(2) | Fe(1B)-C(6B)-H(6B) | 126.6 |
| C(20B)-Fe(2B)-C(23B) | 68.0(2) | C(3B)-C(7B)-C(6B) | 106.0(4) |
| C(18B)-Fe(2B)-C(23B) | 124.7(2) | C(3B)-C(7B)-Fe(1B) | 67.8(2) |
| C(22B)-Fe(2B)-C(23B) | 40.3(2) | C(6B)-C(7B)-Fe(1B) | 69.9(3) |
| C(14B)-Fe(2B)-C(21B) | 122.2(2) | C(3B)-C(7B)-H(7B) | 127.0 |
| C(16B)-Fe(2B)-C(21B) | 122.9(3) | C(6B)-C(7B)-H(7B) | 127.0 |
| C(15B)-Fe(2B)-C(21B) | 105.3(2) | Fe(1B)-C(7B)-H(7B) | 126.8 |
| C(17B)-Fe(2B)-C(21B) | 159.5(3) | C(4B)-C(8B)-H(8B1) | 109.5 |
| C(20B)-Fe(2B)-C(21B) | 40.7(2) | C(4B)-C(8B)-H(8B2) | 109.5 |
| C(18B)-Fe(2B)-C(21B) | 158.5(2) | H(8B1)-C(8B)-H(8B2) | 109.5 |
| C(22B)-Fe(2B)-C(21B) | 40.8(2) | C(4B)-C(8B)-H(8B3) | 109.5 |
| C(23B)-Fe(2B)-C(21B) | 68.2(2) | H(8B1)-C(8B)-H(8B3) | 109.5 |
| C(14B)-Fe(2B)-C(24B) | 127.2(2) | H(8B2)-C(8B)-H(8B3) | 109.5 |
| C(16B)-Fe(2B)-C(24B) | 156.4(2) | C(10B)-C(9B)-C(13B) | 108.8(7) |
| C(15B)-Fe(2B)-C(24B) | 161.7(2) | C(10B)-C(9B)-Fe(1B) | 71.3(4) |
| C(17B)-Fe(2B)-C(24B) | 122.6(3) | C(13B)-C(9B)-Fe(1B) | 70.8(5) |
| C(20B)-Fe(2B)-C(24B) | 40.21(19) | C(10B)-C(9B)-H(9B) | 125.6 |
| C(18B)-Fe(2B)-C(24B) | 109.5(2) | C(13B)-C(9B)-H(9B) | 125.6 |
| C(22B)-Fe(2B)-C(24B) | 67.8(2) | Fe(1B)-C(9B)-H(9B) | 123.9 |
| C(23B)-Fe(2B)-C(24B) | 40.3(2) | C(9B)-C(10B)-C(11B) | 110.3(7) |
| C(21B)-Fe(2B)-C(24B) | 68.0(2) | C(9B)-C(10B)-Fe(1B) | 70.6(4) |

| | | | |
|---|---|---|---|
| C(11B)-C(10B)-Fe(1B) | 70.5(3) | C(14B)-C(18B)-Fe(2B) | 68.5(3) |
| C(9B)-C(10B)-H(10B) | 124.9 | C(17B)-C(18B)-H(18B) | 127.1 |
| C(11B)-C(10B)-H(10B) | 124.9 | C(14B)-C(18B)-H(18B) | 127.1 |
| Fe(1B)-C(10B)-H(10B) | 125.7 | Fe(2B)-C(18B)-H(18B) | 126.2 |
| C(10B)-C(11B)-C(12B) | 107.1(6) | C(15B)-C(19B)-H(19D) | 109.5 |
| C(10B)-C(11B)-Fe(1B) | 70.1(3) | C(15B)-C(19B)-H(19E) | 109.5 |
| C(12B)-C(11B)-Fe(1B) | 69.9(3) | H(19D)-C(19B)-H(19E) | 109.5 |
| C(10B)-C(11B)-H(11B) | 126.4 | C(15B)-C(19B)-H(19F) | 109.5 |
| C(12B)-C(11B)-H(11B) | 126.4 | H(19D)-C(19B)-H(19F) | 109.5 |
| Fe(1B)-C(11B)-H(11B) | 125.2 | H(19E)-C(19B)-H(19F) | 109.5 |
| C(11B)-C(12B)-C(13B) | 105.4(7) | C(24B)-C(20B)-C(21B) | 108.5(4) |
| C(11B)-C(12B)-Fe(1B) | 70.3(3) | C(24B)-C(20B)-Fe(2B) | 70.6(3) |
| C(13B)-C(12B)-Fe(1B) | 69.3(4) | C(21B)-C(20B)-Fe(2B) | 69.9(3) |
| C(11B)-C(12B)-H(12B) | 127.3 | C(24B)-C(20B)-H(20B) | 125.8 |
| C(13B)-C(12B)-H(12B) | 127.3 | C(21B)-C(20B)-H(20B) | 125.8 |
| Fe(1B)-C(12B)-H(12B) | 124.8 | Fe(2B)-C(20B)-H(20B) | 125.3 |
| C(9B)-C(13B)-C(12B) | 108.3(6) | C(20B)-C(21B)-C(22B) | 107.3(4) |
| C(9B)-C(13B)-Fe(1B) | 70.5(4) | C(20B)-C(21B)-Fe(2B) | 69.4(3) |
| C(12B)-C(13B)-Fe(1B) | 69.7(4) | C(22B)-C(21B)-Fe(2B) | 69.6(3) |
| C(9B)-C(13B)-H(13B) | 125.9 | C(20B)-C(21B)-H(21B) | 126.4 |
| C(12B)-C(13B)-H(13B) | 125.9 | C(22B)-C(21B)-H(21B) | 126.4 |
| Fe(1B)-C(13B)-H(13B) | 125.6 | Fe(2B)-C(21B)-H(21B) | 126.2 |
| N(2B)-C(14B)-C(15B) | 123.6(4) | C(23B)-C(22B)-C(21B) | 108.1(4) |
| N(2B)-C(14B)-C(18B) | 124.7(4) | C(23B)-C(22B)-Fe(2B) | 69.8(3) |
| C(15B)-C(14B)-C(18B) | 111.7(4) | C(21B)-C(22B)-Fe(2B) | 69.7(3) |
| N(2B)-C(14B)-Fe(2B) | 126.8(3) | C(23B)-C(22B)-H(22B) | 126.0 |
| C(15B)-C(14B)-Fe(2B) | 70.3(3) | C(21B)-C(22B)-H(22B) | 126.0 |
| C(18B)-C(14B)-Fe(2B) | 70.5(3) | Fe(2B)-C(22B)-H(22B) | 126.1 |
| C(14B)-C(15B)-C(16B) | 104.0(5) | C(22B)-C(23B)-C(24B) | 108.2(5) |
| C(14B)-C(15B)-C(19B) | 126.1(5) | C(22B)-C(23B)-Fe(2B) | 69.8(3) |
| C(16B)-C(15B)-C(19B) | 129.9(5) | C(24B)-C(23B)-Fe(2B) | 70.3(3) |
| C(14B)-C(15B)-Fe(2B) | 68.9(3) | C(22B)-C(23B)-H(23B) | 125.9 |
| C(16B)-C(15B)-Fe(2B) | 69.1(3) | C(24B)-C(23B)-H(23B) | 125.9 |
| C(19B)-C(15B)-Fe(2B) | 126.0(4) | Fe(2B)-C(23B)-H(23B) | 125.6 |
| C(17B)-C(16B)-C(15B) | 109.4(5) | C(20B)-C(24B)-C(23B) | 108.0(4) |
| C(17B)-C(16B)-Fe(2B) | 70.1(3) | C(20B)-C(24B)-Fe(2B) | 69.2(3) |
| C(15B)-C(16B)-Fe(2B) | 69.3(3) | C(23B)-C(24B)-Fe(2B) | 69.4(3) |
| C(17B)-C(16B)-H(16B) | 125.3 | C(20B)-C(24B)-H(24B) | 126.0 |
| C(15B)-C(16B)-H(16B) | 125.3 | C(23B)-C(24B)-H(24B) | 126.0 |
| Fe(2B)-C(16B)-H(16B) | 127.0 | Fe(2B)-C(24B)-H(24B) | 127.0 |
| C(18B)-C(17B)-C(16B) | 109.0(5) | | |
| C(18B)-C(17B)-Fe(2B) | 70.0(3) | | |
| C(16B)-C(17B)-Fe(2B) | 69.5(3) | | |
| C(18B)-C(17B)-H(17B) | 125.5 | | |
| C(16B)-C(17B)-H(17B) | 125.5 | | |
| Fe(2B)-C(17B)-H(17B) | 126.6 | | |
| C(17B)-C(18B)-C(14B) | 105.9(5) | | |
| C(17B)-C(18B)-Fe(2B) | 69.8(3) | | |

**Table A.4**. Anisotropic displacement parameters ($Å^2 x\ 10^3$ ) for $\{(C_5H_5)Fe(C_5H_3(NC)(CH_3))\}_2PdI_2$. The anisotropic displacement factor exponent takes the form: $-2\ \pi^2[\ h^2\ a^{*2}\ U_{11} + ... + 2\ h\ k\ a^*\ b^*\ U_{12}\ ]$

| | $U_{11}$ | $U_{22}$ | $U_{33}$ | $U_{23}$ | $U_{13}$ | $U_{12}$ |
|---|---|---|---|---|---|---|
| I(1A) | 32(1) | 24(1) | 20(1) | -1(1) | -4(1) | -5(1) |
| I(2A) | 30(1) | 40(1) | 26(1) | -3(1) | 1(1) | -13(1) |
| Pd(1A) | 19(1) | 20(1) | 12(1) | 2(1) | -3(1) | 2(1) |
| Fe(1A) | 23(1) | 14(1) | 14(1) | 0(1) | -2(1) | 2(1) |
| Fe(2A) | 25(1) | 21(1) | 13(1) | 1(1) | -4(1) | -3(1) |
| N(1A) | 24(2) | 22(2) | 16(2) | -1(2) | -2(1) | -1(2) |
| N(2A) | 25(2) | 20(2) | 14(2) | -2(2) | -7(1) | 3(2) |
| C(1A) | 20(2) | 21(2) | 21(2) | 3(2) | -4(2) | -2(2) |
| C(2A) | 20(2) | 20(2) | 18(2) | 1(2) | -2(2) | 2(2) |
| C(3A) | 28(2) | 15(2) | 14(2) | 1(2) | -5(2) | 2(2) |
| C(4A) | 26(2) | 15(2) | 14(2) | -2(2) | 2(2) | -5(2) |
| C(5A) | 38(3) | 14(2) | 16(2) | -1(2) | 5(2) | 1(2) |
| C(6A) | 31(2) | 17(2) | 22(2) | -5(2) | -1(2) | 9(2) |
| C(7A) | 19(2) | 23(2) | 16(2) | -3(2) | 4(2) | 1(2) |
| C(8A) | 28(2) | 32(3) | 23(2) | 1(2) | 0(2) | -6(2) |
| C(9A) | 36(3) | 18(2) | 28(2) | -8(2) | -5(2) | 11(2) |
| C(10A) | 30(2) | 26(2) | 29(3) | -8(2) | 4(2) | 6(2) |
| C(11A) | 46(3) | 28(2) | 15(2) | 0(2) | 8(2) | 1(2) |
| C(12A) | 39(3) | 35(3) | 16(2) | -11(2) | -5(2) | 8(2) |
| C(13A) | 32(3) | 19(2) | 33(3) | -12(2) | -2(2) | -1(2) |
| C(14A) | 26(2) | 19(2) | 16(2) | -1(2) | -8(2) | -2(2) |
| C(15A) | 35(3) | 19(2) | 21(2) | -4(2) | -12(2) | 1(2) |
| C(16A) | 55(3) | 20(2) | 23(2) | 6(2) | -20(2) | -8(2) |
| C(17A) | 54(3) | 34(3) | 22(3) | 8(2) | -8(2) | -21(3) |
| C(18A) | 30(2) | 32(3) | 22(2) | 3(2) | -6(2) | -13(2) |
| C(19A) | 40(3) | 45(3) | 31(3) | -13(2) | -12(2) | 20(2) |
| C(20A) | 30(2) | 20(2) | 37(3) | -4(2) | 2(2) | -5(2) |
| C(21A) | 23(2) | 27(2) | 30(3) | -8(2) | 0(2) | -6(2) |
| C(22A) | 29(2) | 39(3) | 25(3) | -11(2) | -10(2) | -1(2) |
| C(23A) | 32(2) | 42(3) | 21(2) | -15(2) | -2(2) | -7(2) |
| C(24A) | 28(2) | 29(3) | 35(3) | -15(2) | -5(2) | -4(2) |
| I(1B) | 38(1) | 23(1) | 20(1) | -2(1) | -3(1) | -6(1) |
| I(2B) | 39(1) | 31(1) | 26(1) | -5(1) | -11(1) | -6(1) |
| Pd(1B) | 23(1) | 20(1) | 11(1) | 1(1) | -2(1) | 1(1) |
| Fe(1B) | 24(1) | 17(1) | 14(1) | -1(1) | 0(1) | 2(1) |
| Fe(2B) | 36(1) | 16(1) | 15(1) | 0(1) | -8(1) | -2(1) |
| N(1B) | 27(2) | 24(2) | 15(2) | -1(2) | -4(1) | -3(2) |
| N(2B) | 23(2) | 19(2) | 15(2) | -4(2) | -1(1) | 0(2) |
| C(1B) | 25(2) | 24(2) | 16(2) | -1(2) | -2(2) | 0(2) |

| | | | | | | |
|---|---|---|---|---|---|---|
| C(2B) | 18(2) | 21(2) | 20(2) | -2(2) | 0(2) | -3(2) |
| C(3B) | 27(2) | 17(2) | 15(2) | -1(2) | -3(2) | -1(2) |
| C(4B) | 27(2) | 17(2) | 16(2) | -10(2) | -2(2) | 4(2) |
| C(5B) | 36(2) | 20(2) | 18(2) | -2(2) | -7(2) | 5(2) |
| C(6B) | 45(3) | 20(2) | 19(2) | 2(2) | 2(2) | -4(2) |
| C(7B) | 24(2) | 31(2) | 20(2) | -2(2) | -2(2) | -7(2) |
| C(8B) | 24(2) | 39(3) | 29(3) | -6(2) | 2(2) | 0(2) |
| C(9B) | 219(12) | 11(3) | 35(4) | -8(3) | -17(6) | 17(5) |
| C(10B) | 56(4) | 44(3) | 62(4) | -38(3) | 29(3) | -31(3) |
| C(11B) | 82(5) | 27(3) | 30(3) | -13(2) | -25(3) | 10(3) |
| C(12B) | 77(5) | 105(6) | 66(5) | -69(5) | 58(4) | -60(5) |
| C(13B) | 86(6) | 125(9) | 101(7) | -99(7) | -67(6) | 84(6) |
| C(14B) | 31(2) | 16(2) | 16(2) | -2(2) | -7(2) | 4(2) |
| C(15B) | 38(3) | 31(3) | 23(2) | 0(2) | -4(2) | -22(2) |
| C(16B) | 100(5) | 39(3) | 17(2) | 12(2) | -17(3) | -47(4) |
| C(17B) | 102(6) | 17(3) | 42(4) | -5(2) | -37(4) | 2(3) |
| C(18B) | 58(3) | 25(3) | 28(3) | -10(2) | -21(2) | 17(2) |
| C(19B) | 37(3) | 68(4) | 42(3) | -27(3) | 14(2) | -26(3) |
| C(20B) | 40(3) | 18(2) | 25(2) | 0(2) | -3(2) | -7(2) |
| C(21B) | 34(2) | 23(2) | 35(3) | -14(2) | 0(2) | -5(2) |
| C(22B) | 40(3) | 35(3) | 14(2) | -11(2) | -2(2) | -16(2) |
| C(23B) | 41(3) | 33(3) | 24(2) | 2(2) | -13(2) | -5(2) |
| C(24B) | 26(2) | 27(2) | 34(3) | 1(2) | -3(2) | -2(2) |

**Table A.5.** Hydrogen coordinates and isotropic displacement parameters for $\{(C_5H_5)Fe(C_5H_3(NC)(CH_3))\}_2PdI_2$

| | x | y | z | U(eq) |
|---|---|---|---|---|
| H(5A) | 0.2320 | 1.1520 | -0.0614 | 0.027 |
| H(6A) | 0.0154 | 1.0230 | -0.0569 | 0.028 |
| H(7A) | 0.0174 | 0.7767 | -0.0009 | 0.023 |
| H(8A1) | 0.4626 | 1.0435 | -0.0302 | 0.041 |
| H(8A2) | 0.4608 | 0.8933 | 0.0066 | 0.041 |
| H(8A3) | 0.4283 | 1.0965 | 0.0182 | 0.041 |
| H(9A) | 0.3109 | 0.4603 | -0.0459 | 0.033 |
| H(10A) | 0.4368 | 0.6950 | -0.0856 | 0.034 |
| H(11A) | 0.2920 | 0.8578 | -0.1370 | 0.035 |
| H(12A) | 0.0739 | 0.7267 | -0.1295 | 0.036 |
| H(13A) | 0.0875 | 0.4789 | -0.0735 | 0.034 |
| H(16A) | 0.5573 | -0.0545 | 0.3097 | 0.039 |
| H(17A) | 0.3434 | 0.0529 | 0.3316 | 0.044 |
| H(18A) | 0.2581 | 0.2513 | 0.2714 | 0.034 |
| H(19A) | 0.7164 | 0.0225 | 0.2448 | 0.058 |
| H(19B) | 0.6707 | 0.1737 | 0.2116 | 0.058 |
| H(19C) | 0.6300 | -0.0301 | 0.2042 | 0.058 |

| | | | | |
|---|---|---|---|---|
| H(20A) | 0.5587 | 0.6161 | 0.2603 | 0.035 |
| H(21A) | 0.7365 | 0.4159 | 0.2855 | 0.032 |
| H(22A) | 0.6805 | 0.2817 | 0.3571 | 0.037 |
| H(23A) | 0.4672 | 0.4047 | 0.3775 | 0.038 |
| H(24A) | 0.3948 | 0.6092 | 0.3187 | 0.037 |
| H(5B) | 0.3600 | -0.0723 | 0.5630 | 0.030 |
| H(6B) | 0.1301 | -0.1025 | 0.5756 | 0.034 |
| H(7B) | 0.0140 | 0.0890 | 0.5206 | 0.030 |
| H(8B1) | 0.4573 | 0.0744 | 0.4693 | 0.046 |
| H(8B2) | 0.5004 | 0.1662 | 0.5137 | 0.046 |
| H(8B3) | 0.4243 | 0.2797 | 0.4783 | 0.046 |
| H(9B) | 0.2524 | 0.5754 | 0.5399 | 0.106 |
| H(10B) | 0.4186 | 0.4348 | 0.5810 | 0.065 |
| H(11B) | 0.3298 | 0.2441 | 0.6381 | 0.056 |
| H(12B) | 0.0964 | 0.2754 | 0.6331 | 0.099 |
| H(13B) | 0.0529 | 0.4931 | 0.5714 | 0.126 |
| H(16B) | 0.1526 | 1.0073 | 0.1718 | 0.062 |
| H(17B) | -0.0509 | 1.1186 | 0.1997 | 0.065 |
| H(18B) | -0.0872 | 0.9786 | 0.2726 | 0.045 |
| H(19D) | 0.3555 | 0.8101 | 0.2431 | 0.073 |
| H(19E) | 0.3136 | 0.7336 | 0.1969 | 0.073 |
| H(19F) | 0.2772 | 0.6282 | 0.2398 | 0.073 |
| H(20B) | -0.0559 | 0.4423 | 0.2430 | 0.033 |
| H(21B) | 0.1056 | 0.4516 | 0.1842 | 0.037 |
| H(22B) | 0.0251 | 0.6633 | 0.1258 | 0.036 |
| H(23B) | -0.1839 | 0.7813 | 0.1488 | 0.039 |
| H(24B) | -0.2359 | 0.6396 | 0.2203 | 0.035 |

**Table A. 6**. Torsion angles [°] for $\{(C_5H_5)Fe(C_5H_3(NC)(CH_3))\}_2PdI_2$.

| | |
|---|---|
| C(3A)-N(1A)-C(1A)-Pd(1A) | 68(12) |
| C(2A)-Pd(1A)-C(1A)-N(1A) | 11(7) |
| I(1A)-Pd(1A)-C(1A)-N(1A) | 106(6) |
| I(2A)-Pd(1A)-C(1A)-N(1A) | -81(6) |
| C(14A)-N(2A)-C(2A)-Pd(1A) | 74(8) |
| C(1A)-Pd(1A)-C(2A)-N(2A) | -3(4) |
| I(1A)-Pd(1A)-C(2A)-N(2A) | -97(3) |
| I(2A)-Pd(1A)-C(2A)-N(2A) | 90(3) |
| C(1A)-N(1A)-C(3A)-C(7A) | -138(9) |
| C(1A)-N(1A)-C(3A)-C(4A) | 42(9) |
| C(1A)-N(1A)-C(3A)-Fe(1A) | 132(9) |
| C(7A)-Fe(1A)-C(3A)-N(1A) | 120.8(5) |
| C(6A)-Fe(1A)-C(3A)-N(1A) | 159.1(4) |
| C(13A)-Fe(1A)-C(3A)-N(1A) | 43.4(4) |
| C(12A)-Fe(1A)-C(3A)-N(1A) | 81.0(6) |
| C(9A)-Fe(1A)-C(3A)-N(1A) | 0.4(4) |
| C(11A)-Fe(1A)-C(3A)-N(1A) | -78.7(7) |

| | |
|---|---|
| C(10A)-Fe(1A)-C(3A)-N(1A) | -42.3(4) |
| C(5A)-Fe(1A)-C(3A)-N(1A) | -156.7(4) |
| C(4A)-Fe(1A)-C(3A)-N(1A) | -118.8(5) |
| C(6A)-Fe(1A)-C(3A)-C(7A) | 38.3(3) |
| C(13A)-Fe(1A)-C(3A)-C(7A) | -77.5(3) |
| C(12A)-Fe(1A)-C(3A)-C(7A) | -39.8(6) |
| C(9A)-Fe(1A)-C(3A)-C(7A) | -120.5(3) |
| C(11A)-Fe(1A)-C(3A)-C(7A) | 160.5(5) |
| C(10A)-Fe(1A)-C(3A)-C(7A) | -163.1(3) |
| C(5A)-Fe(1A)-C(3A)-C(7A) | 82.5(3) |
| C(4A)-Fe(1A)-C(3A)-C(7A) | 120.4(4) |
| C(7A)-Fe(1A)-C(3A)-C(4A) | -120.4(4) |
| C(6A)-Fe(1A)-C(3A)-C(4A) | -82.1(3) |
| C(13A)-Fe(1A)-C(3A)-C(4A) | 162.1(3) |
| C(12A)-Fe(1A)-C(3A)-C(4A) | -160.3(5) |
| C(9A)-Fe(1A)-C(3A)-C(4A) | 119.1(3) |
| C(11A)-Fe(1A)-C(3A)-C(4A) | 40.1(6) |
| C(10A)-Fe(1A)-C(3A)-C(4A) | 76.4(3) |
| C(5A)-Fe(1A)-C(3A)-C(4A) | -37.9(3) |
| N(1A)-C(3A)-C(4A)-C(5A) | -179.6(4) |
| C(7A)-C(3A)-C(4A)-C(5A) | 0.1(5) |
| Fe(1A)-C(3A)-C(4A)-C(5A) | 59.8(3) |
| N(1A)-C(3A)-C(4A)-C(8A) | -2.6(7) |
| C(7A)-C(3A)-C(4A)-C(8A) | 177.1(4) |
| Fe(1A)-C(3A)-C(4A)-C(8A) | -123.2(4) |
| N(1A)-C(3A)-C(4A)-Fe(1A) | 120.6(4) |
| C(7A)-C(3A)-C(4A)-Fe(1A) | -59.7(3) |
| C(3A)-Fe(1A)-C(4A)-C(5A) | -117.6(4) |
| C(7A)-Fe(1A)-C(4A)-C(5A) | -80.2(3) |
| C(6A)-Fe(1A)-C(4A)-C(5A) | -36.9(3) |
| C(13A)-Fe(1A)-C(4A)-C(5A) | -165.1(5) |
| C(12A)-Fe(1A)-C(4A)-C(5A) | 42.3(6) |
| C(9A)-Fe(1A)-C(4A)-C(5A) | 161.4(3) |
| C(11A)-Fe(1A)-C(4A)-C(5A) | 77.3(3) |
| C(10A)-Fe(1A)-C(4A)-C(5A) | 119.1(3) |
| C(7A)-Fe(1A)-C(4A)-C(3A) | 37.4(2) |
| C(6A)-Fe(1A)-C(4A)-C(3A) | 80.7(3) |
| C(13A)-Fe(1A)-C(4A)-C(3A) | -47.5(6) |
| C(12A)-Fe(1A)-C(4A)-C(3A) | 159.9(4) |
| C(9A)-Fe(1A)-C(4A)-C(3A) | -81.0(3) |
| C(11A)-Fe(1A)-C(4A)-C(3A) | -165.1(3) |
| C(10A)-Fe(1A)-C(4A)-C(3A) | -123.3(3) |
| C(5A)-Fe(1A)-C(4A)-C(3A) | 117.6(4) |
| C(3A)-Fe(1A)-C(4A)-C(8A) | 118.5(5) |
| C(7A)-Fe(1A)-C(4A)-C(8A) | 155.9(4) |
| C(6A)-Fe(1A)-C(4A)-C(8A) | -160.8(4) |
| C(13A)-Fe(1A)-C(4A)-C(8A) | 71.0(7) |
| C(12A)-Fe(1A)-C(4A)-C(8A) | -81.6(6) |
| C(9A)-Fe(1A)-C(4A)-C(8A) | 37.5(5) |

| | |
|---|---|
| C(11A)-Fe(1A)-C(4A)-C(8A) | -46.6(5) |
| C(10A)-Fe(1A)-C(4A)-C(8A) | -4.8(4) |
| C(5A)-Fe(1A)-C(4A)-C(8A) | -123.9(5) |
| C(3A)-C(4A)-C(5A)-C(6A) | -0.2(5) |
| C(8A)-C(4A)-C(5A)-C(6A) | -177.1(4) |
| Fe(1A)-C(4A)-C(5A)-C(6A) | 58.2(3) |
| C(3A)-C(4A)-C(5A)-Fe(1A) | -58.4(3) |
| C(8A)-C(4A)-C(5A)-Fe(1A) | 124.7(5) |
| C(3A)-Fe(1A)-C(5A)-C(4A) | 39.3(2) |
| C(7A)-Fe(1A)-C(5A)-C(4A) | 84.1(3) |
| C(6A)-Fe(1A)-C(5A)-C(4A) | 121.2(4) |
| C(13A)-Fe(1A)-C(5A)-C(4A) | 165.4(5) |
| C(12A)-Fe(1A)-C(5A)-C(4A) | -162.8(3) |
| C(9A)-Fe(1A)-C(5A)-C(4A) | -46.2(6) |
| C(11A)-Fe(1A)-C(5A)-C(4A) | -120.5(3) |
| C(10A)-Fe(1A)-C(5A)-C(4A) | -79.0(3) |
| C(3A)-Fe(1A)-C(5A)-C(6A) | -81.8(3) |
| C(7A)-Fe(1A)-C(5A)-C(6A) | -37.1(3) |
| C(13A)-Fe(1A)-C(5A)-C(6A) | 44.3(6) |
| C(12A)-Fe(1A)-C(5A)-C(6A) | 76.0(3) |
| C(9A)-Fe(1A)-C(5A)-C(6A) | -167.4(5) |
| C(11A)-Fe(1A)-C(5A)-C(6A) | 118.3(3) |
| C(10A)-Fe(1A)-C(5A)-C(6A) | 159.9(3) |
| C(4A)-Fe(1A)-C(5A)-C(6A) | -121.2(4) |
| C(4A)-C(5A)-C(6A)-C(7A) | 0.2(5) |
| Fe(1A)-C(5A)-C(6A)-C(7A) | 58.9(3) |
| C(4A)-C(5A)-C(6A)-Fe(1A) | -58.7(3) |
| C(3A)-Fe(1A)-C(6A)-C(7A) | -39.2(3) |
| C(13A)-Fe(1A)-C(6A)-C(7A) | 77.1(3) |
| C(12A)-Fe(1A)-C(6A)-C(7A) | 118.3(3) |
| C(9A)-Fe(1A)-C(6A)-C(7A) | 46.4(6) |
| C(11A)-Fe(1A)-C(6A)-C(7A) | 160.3(3) |
| C(10A)-Fe(1A)-C(6A)-C(7A) | -168.7(4) |
| C(5A)-Fe(1A)-C(6A)-C(7A) | -120.0(4) |
| C(4A)-Fe(1A)-C(6A)-C(7A) | -83.9(3) |
| C(3A)-Fe(1A)-C(6A)-C(5A) | 80.9(3) |
| C(7A)-Fe(1A)-C(6A)-C(5A) | 120.0(4) |
| C(13A)-Fe(1A)-C(6A)-C(5A) | -162.9(3) |
| C(12A)-Fe(1A)-C(6A)-C(5A) | -121.7(3) |
| C(9A)-Fe(1A)-C(6A)-C(5A) | 166.4(5) |
| C(11A)-Fe(1A)-C(6A)-C(5A) | -79.7(3) |
| C(10A)-Fe(1A)-C(6A)-C(5A) | -48.7(6) |
| C(4A)-Fe(1A)-C(6A)-C(5A) | 36.1(3) |
| C(5A)-C(6A)-C(7A)-C(3A) | -0.1(5) |
| Fe(1A)-C(6A)-C(7A)-C(3A) | 59.0(3) |
| C(5A)-C(6A)-C(7A)-Fe(1A) | -59.1(3) |
| N(1A)-C(3A)-C(7A)-C(6A) | 179.7(4) |
| C(4A)-C(3A)-C(7A)-C(6A) | 0.0(5) |
| Fe(1A)-C(3A)-C(7A)-C(6A) | -60.1(3) |

| | |
|---|---|
| N(1A)-C(3A)-C(7A)-Fe(1A) | -120.2(4) |
| C(4A)-C(3A)-C(7A)-Fe(1A) | 60.0(3) |
| C(3A)-Fe(1A)-C(7A)-C(6A) | 117.6(4) |
| C(13A)-Fe(1A)-C(7A)-C(6A) | -121.1(3) |
| C(12A)-Fe(1A)-C(7A)-C(6A) | -78.7(3) |
| C(9A)-Fe(1A)-C(7A)-C(6A) | -162.5(3) |
| C(11A)-Fe(1A)-C(7A)-C(6A) | -46.1(6) |
| C(10A)-Fe(1A)-C(7A)-C(6A) | 166.1(5) |
| C(5A)-Fe(1A)-C(7A)-C(6A) | 37.4(3) |
| C(4A)-Fe(1A)-C(7A)-C(6A) | 80.2(3) |
| C(6A)-Fe(1A)-C(7A)-C(3A) | -117.6(4) |
| C(13A)-Fe(1A)-C(7A)-C(3A) | 121.4(3) |
| C(12A)-Fe(1A)-C(7A)-C(3A) | 163.8(3) |
| C(9A)-Fe(1A)-C(7A)-C(3A) | 79.9(3) |
| C(11A)-Fe(1A)-C(7A)-C(3A) | -163.7(4) |
| C(10A)-Fe(1A)-C(7A)-C(3A) | 48.6(7) |
| C(5A)-Fe(1A)-C(7A)-C(3A) | -80.2(3) |
| C(4A)-Fe(1A)-C(7A)-C(3A) | -37.4(2) |
| C(3A)-Fe(1A)-C(9A)-C(13A) | 119.2(3) |
| C(7A)-Fe(1A)-C(9A)-C(13A) | 75.6(3) |
| C(6A)-Fe(1A)-C(9A)-C(13A) | 41.1(7) |
| C(12A)-Fe(1A)-C(9A)-C(13A) | -37.4(3) |
| C(11A)-Fe(1A)-C(9A)-C(13A) | -81.7(3) |
| C(10A)-Fe(1A)-C(9A)-C(13A) | -119.0(4) |
| C(5A)-Fe(1A)-C(9A)-C(13A) | -163.4(5) |
| C(4A)-Fe(1A)-C(9A)-C(13A) | 162.9(3) |
| C(3A)-Fe(1A)-C(9A)-C(10A) | -121.9(3) |
| C(7A)-Fe(1A)-C(9A)-C(10A) | -165.4(3) |
| C(6A)-Fe(1A)-C(9A)-C(10A) | 160.0(5) |
| C(13A)-Fe(1A)-C(9A)-C(10A) | 119.0(4) |
| C(12A)-Fe(1A)-C(9A)-C(10A) | 81.6(3) |
| C(11A)-Fe(1A)-C(9A)-C(10A) | 37.3(3) |
| C(5A)-Fe(1A)-C(9A)-C(10A) | -44.5(6) |
| C(4A)-Fe(1A)-C(9A)-C(10A) | -78.1(3) |
| C(13A)-C(9A)-C(10A)-C(11A) | 0.2(5) |
| Fe(1A)-C(9A)-C(10A)-C(11A) | -59.1(3) |
| C(13A)-C(9A)-C(10A)-Fe(1A) | 59.3(3) |
| C(3A)-Fe(1A)-C(10A)-C(11A) | -162.0(3) |
| C(7A)-Fe(1A)-C(10A)-C(11A) | 160.7(5) |
| C(6A)-Fe(1A)-C(10A)-C(11A) | -42.8(6) |
| C(13A)-Fe(1A)-C(10A)-C(11A) | 81.7(3) |
| C(12A)-Fe(1A)-C(10A)-C(11A) | 37.7(3) |
| C(9A)-Fe(1A)-C(10A)-C(11A) | 119.6(4) |
| C(5A)-Fe(1A)-C(10A)-C(11A) | -78.2(3) |
| C(4A)-Fe(1A)-C(10A)-C(11A) | -119.6(3) |
| C(3A)-Fe(1A)-C(10A)-C(9A) | 78.4(3) |
| C(7A)-Fe(1A)-C(10A)-C(9A) | 41.1(7) |
| C(6A)-Fe(1A)-C(10A)-C(9A) | -162.4(4) |
| C(13A)-Fe(1A)-C(10A)-C(9A) | -37.9(3) |

| | |
|---|---|
| C(12A)-Fe(1A)-C(10A)-C(9A) | -81.9(3) |
| C(11A)-Fe(1A)-C(10A)-C(9A) | -119.6(4) |
| C(5A)-Fe(1A)-C(10A)-C(9A) | 162.2(3) |
| C(4A)-Fe(1A)-C(10A)-C(9A) | 120.8(3) |
| C(9A)-C(10A)-C(11A)-C(12A) | 0.2(5) |
| Fe(1A)-C(10A)-C(11A)-C(12A) | -58.8(3) |
| C(9A)-C(10A)-C(11A)-Fe(1A) | 59.0(3) |
| C(3A)-Fe(1A)-C(11A)-C(10A) | 48.6(7) |
| C(7A)-Fe(1A)-C(11A)-C(10A) | -164.9(4) |
| C(6A)-Fe(1A)-C(11A)-C(10A) | 162.0(3) |
| C(13A)-Fe(1A)-C(11A)-C(10A) | -81.7(3) |
| C(12A)-Fe(1A)-C(11A)-C(10A) | -119.9(4) |
| C(9A)-Fe(1A)-C(11A)-C(10A) | -37.7(3) |
| C(5A)-Fe(1A)-C(11A)-C(10A) | 119.8(3) |
| C(4A)-Fe(1A)-C(11A)-C(10A) | 78.9(3) |
| C(3A)-Fe(1A)-C(11A)-C(12A) | 168.5(5) |
| C(7A)-Fe(1A)-C(11A)-C(12A) | -44.9(6) |
| C(6A)-Fe(1A)-C(11A)-C(12A) | -78.0(3) |
| C(13A)-Fe(1A)-C(11A)-C(12A) | 38.2(3) |
| C(9A)-Fe(1A)-C(11A)-C(12A) | 82.2(3) |
| C(10A)-Fe(1A)-C(11A)-C(12A) | 119.9(4) |
| C(5A)-Fe(1A)-C(11A)-C(12A) | -120.3(3) |
| C(4A)-Fe(1A)-C(11A)-C(12A) | -161.2(3) |
| C(10A)-C(11A)-C(12A)-C(13A) | -0.4(5) |
| Fe(1A)-C(11A)-C(12A)-C(13A) | -59.5(3) |
| C(10A)-C(11A)-C(12A)-Fe(1A) | 59.1(3) |
| C(3A)-Fe(1A)-C(12A)-C(13A) | -51.4(6) |
| C(7A)-Fe(1A)-C(12A)-C(13A) | -80.7(3) |
| C(6A)-Fe(1A)-C(12A)-C(13A) | -122.1(3) |
| C(9A)-Fe(1A)-C(12A)-C(13A) | 37.4(3) |
| C(11A)-Fe(1A)-C(12A)-C(13A) | 118.4(4) |
| C(10A)-Fe(1A)-C(12A)-C(13A) | 81.3(3) |
| C(5A)-Fe(1A)-C(12A)-C(13A) | -163.4(3) |
| C(4A)-Fe(1A)-C(12A)-C(13A) | 165.8(4) |
| C(3A)-Fe(1A)-C(12A)-C(11A) | -169.7(4) |
| C(7A)-Fe(1A)-C(12A)-C(11A) | 160.9(3) |
| C(6A)-Fe(1A)-C(12A)-C(11A) | 119.5(3) |
| C(13A)-Fe(1A)-C(12A)-C(11A) | -118.4(4) |
| C(9A)-Fe(1A)-C(12A)-C(11A) | -81.0(3) |
| C(10A)-Fe(1A)-C(12A)-C(11A) | -37.0(3) |
| C(5A)-Fe(1A)-C(12A)-C(11A) | 78.2(3) |
| C(4A)-Fe(1A)-C(12A)-C(11A) | 47.5(6) |
| C(11A)-C(12A)-C(13A)-C(9A) | 0.5(5) |
| Fe(1A)-C(12A)-C(13A)-C(9A) | -59.0(3) |
| C(11A)-C(12A)-C(13A)-Fe(1A) | 59.5(3) |
| C(10A)-C(9A)-C(13A)-C(12A) | -0.4(5) |
| Fe(1A)-C(9A)-C(13A)-C(12A) | 59.0(3) |
| C(10A)-C(9A)-C(13A)-Fe(1A) | -59.4(3) |
| C(3A)-Fe(1A)-C(13A)-C(12A) | 159.4(3) |

| | |
|---|---|
| C(7A)-Fe(1A)-C(13A)-C(12A) | 117.0(3) |
| C(6A)-Fe(1A)-C(13A)-C(12A) | 75.6(3) |
| C(9A)-Fe(1A)-C(13A)-C(12A) | -120.0(4) |
| C(11A)-Fe(1A)-C(13A)-C(12A) | -38.5(3) |
| C(10A)-Fe(1A)-C(13A)-C(12A) | -82.0(3) |
| C(5A)-Fe(1A)-C(13A)-C(12A) | 42.7(7) |
| C(4A)-Fe(1A)-C(13A)-C(12A) | -164.9(4) |
| C(3A)-Fe(1A)-C(13A)-C(9A) | -80.6(3) |
| C(7A)-Fe(1A)-C(13A)-C(9A) | -123.1(3) |
| C(6A)-Fe(1A)-C(13A)-C(9A) | -164.4(3) |
| C(12A)-Fe(1A)-C(13A)-C(9A) | 120.0(4) |
| C(11A)-Fe(1A)-C(13A)-C(9A) | 81.5(3) |
| C(10A)-Fe(1A)-C(13A)-C(9A) | 38.0(3) |
| C(5A)-Fe(1A)-C(13A)-C(9A) | 162.7(5) |
| C(4A)-Fe(1A)-C(13A)-C(9A) | -44.9(7) |
| C(2A)-N(2A)-C(14A)-C(18A) | -53(7) |
| C(2A)-N(2A)-C(14A)-C(15A) | 124(7) |
| C(2A)-N(2A)-C(14A)-Fe(2A) | -145(7) |
| C(16A)-Fe(2A)-C(14A)-N(2A) | -157.4(5) |
| C(22A)-Fe(2A)-C(14A)-N(2A) | -84.4(7) |
| C(18A)-Fe(2A)-C(14A)-N(2A) | 119.9(5) |
| C(21A)-Fe(2A)-C(14A)-N(2A) | -45.0(5) |
| C(23A)-Fe(2A)-C(14A)-N(2A) | 80.3(7) |
| C(15A)-Fe(2A)-C(14A)-N(2A) | -118.6(5) |
| C(24A)-Fe(2A)-C(14A)-N(2A) | 41.5(5) |
| C(17A)-Fe(2A)-C(14A)-N(2A) | 158.1(5) |
| C(20A)-Fe(2A)-C(14A)-N(2A) | -1.9(4) |
| C(16A)-Fe(2A)-C(14A)-C(18A) | 82.7(3) |
| C(22A)-Fe(2A)-C(14A)-C(18A) | 155.7(5) |
| C(21A)-Fe(2A)-C(14A)-C(18A) | -164.9(3) |
| C(23A)-Fe(2A)-C(14A)-C(18A) | -39.6(7) |
| C(15A)-Fe(2A)-C(14A)-C(18A) | 121.5(4) |
| C(24A)-Fe(2A)-C(14A)-C(18A) | -78.4(3) |
| C(17A)-Fe(2A)-C(14A)-C(18A) | 38.2(3) |
| C(20A)-Fe(2A)-C(14A)-C(18A) | -121.8(3) |
| C(16A)-Fe(2A)-C(14A)-C(15A) | -38.8(3) |
| C(22A)-Fe(2A)-C(14A)-C(15A) | 34.1(7) |
| C(18A)-Fe(2A)-C(14A)-C(15A) | -121.5(4) |
| C(21A)-Fe(2A)-C(14A)-C(15A) | 73.6(3) |
| C(23A)-Fe(2A)-C(14A)-C(15A) | -161.2(5) |
| C(24A)-Fe(2A)-C(14A)-C(15A) | 160.1(3) |
| C(17A)-Fe(2A)-C(14A)-C(15A) | -83.3(3) |
| C(20A)-Fe(2A)-C(14A)-C(15A) | 116.7(3) |
| N(2A)-C(14A)-C(15A)-C(16A) | -176.7(4) |
| C(18A)-C(14A)-C(15A)-C(16A) | 1.3(5) |
| Fe(2A)-C(14A)-C(15A)-C(16A) | 60.1(3) |
| N(2A)-C(14A)-C(15A)-C(19A) | 0.4(7) |
| C(18A)-C(14A)-C(15A)-C(19A) | 178.4(5) |
| Fe(2A)-C(14A)-C(15A)-C(19A) | -122.8(5) |

| | |
|---|---|
| N(2A)-C(14A)-C(15A)-Fe(2A) | 123.2(4) |
| C(18A)-C(14A)-C(15A)-Fe(2A) | -58.8(3) |
| C(14A)-Fe(2A)-C(15A)-C(16A) | -116.6(4) |
| C(22A)-Fe(2A)-C(15A)-C(16A) | 76.8(4) |
| C(18A)-Fe(2A)-C(15A)-C(16A) | -80.2(3) |
| C(21A)-Fe(2A)-C(15A)-C(16A) | 118.2(3) |
| C(23A)-Fe(2A)-C(15A)-C(16A) | 46.0(7) |
| C(24A)-Fe(2A)-C(15A)-C(16A) | -172.3(5) |
| C(17A)-Fe(2A)-C(15A)-C(16A) | -36.8(3) |
| C(20A)-Fe(2A)-C(15A)-C(16A) | 159.3(3) |
| C(16A)-Fe(2A)-C(15A)-C(14A) | 116.6(4) |
| C(22A)-Fe(2A)-C(15A)-C(14A) | -166.6(3) |
| C(18A)-Fe(2A)-C(15A)-C(14A) | 36.4(3) |
| C(21A)-Fe(2A)-C(15A)-C(14A) | -125.2(3) |
| C(23A)-Fe(2A)-C(15A)-C(14A) | 162.6(5) |
| C(24A)-Fe(2A)-C(15A)-C(14A) | -55.7(7) |
| C(17A)-Fe(2A)-C(15A)-C(14A) | 79.8(3) |
| C(20A)-Fe(2A)-C(15A)-C(14A) | -84.0(3) |
| C(14A)-Fe(2A)-C(15A)-C(19A) | 119.3(5) |
| C(16A)-Fe(2A)-C(15A)-C(19A) | -124.0(6) |
| C(22A)-Fe(2A)-C(15A)-C(19A) | -47.2(5) |
| C(18A)-Fe(2A)-C(15A)-C(19A) | 155.8(5) |
| C(21A)-Fe(2A)-C(15A)-C(19A) | -5.9(5) |
| C(23A)-Fe(2A)-C(15A)-C(19A) | -78.0(7) |
| C(24A)-Fe(2A)-C(15A)-C(19A) | 63.7(8) |
| C(17A)-Fe(2A)-C(15A)-C(19A) | -160.9(5) |
| C(20A)-Fe(2A)-C(15A)-C(19A) | 35.3(5) |
| C(14A)-C(15A)-C(16A)-C(17A) | -1.0(5) |
| C(19A)-C(15A)-C(16A)-C(17A) | -177.9(5) |
| Fe(2A)-C(15A)-C(16A)-C(17A) | 58.7(4) |
| C(14A)-C(15A)-C(16A)-Fe(2A) | -59.6(3) |
| C(19A)-C(15A)-C(16A)-Fe(2A) | 123.4(5) |
| C(14A)-Fe(2A)-C(16A)-C(15A) | 39.6(3) |
| C(22A)-Fe(2A)-C(16A)-C(15A) | -119.8(3) |
| C(18A)-Fe(2A)-C(16A)-C(15A) | 83.8(3) |
| C(21A)-Fe(2A)-C(16A)-C(15A) | -79.1(3) |
| C(23A)-Fe(2A)-C(16A)-C(15A) | -161.1(3) |
| C(24A)-Fe(2A)-C(16A)-C(15A) | 172.8(5) |
| C(17A)-Fe(2A)-C(16A)-C(15A) | 121.3(4) |
| C(20A)-Fe(2A)-C(16A)-C(15A) | -49.9(6) |
| C(14A)-Fe(2A)-C(16A)-C(17A) | -81.7(3) |
| C(22A)-Fe(2A)-C(16A)-C(17A) | 118.9(3) |
| C(18A)-Fe(2A)-C(16A)-C(17A) | -37.5(3) |
| C(21A)-Fe(2A)-C(16A)-C(17A) | 159.6(3) |
| C(23A)-Fe(2A)-C(16A)-C(17A) | 77.6(3) |
| C(15A)-Fe(2A)-C(16A)-C(17A) | -121.3(4) |
| C(24A)-Fe(2A)-C(16A)-C(17A) | 51.5(6) |
| C(20A)-Fe(2A)-C(16A)-C(17A) | -171.2(5) |
| C(15A)-C(16A)-C(17A)-C(18A) | 0.2(6) |

| | |
|---|---|
| Fe(2A)-C(16A)-C(17A)-C(18A) | 59.1(3) |
| C(15A)-C(16A)-C(17A)-Fe(2A) | -58.8(4) |
| C(14A)-Fe(2A)-C(17A)-C(18A) | -38.5(3) |
| C(16A)-Fe(2A)-C(17A)-C(18A) | -119.2(4) |
| C(22A)-Fe(2A)-C(17A)-C(18A) | 162.9(3) |
| C(21A)-Fe(2A)-C(17A)-C(18A) | -166.6(4) |
| C(23A)-Fe(2A)-C(17A)-C(18A) | 120.4(3) |
| C(15A)-Fe(2A)-C(17A)-C(18A) | -82.9(3) |
| C(24A)-Fe(2A)-C(17A)-C(18A) | 80.7(4) |
| C(20A)-Fe(2A)-C(17A)-C(18A) | 50.2(8) |
| C(14A)-Fe(2A)-C(17A)-C(16A) | 80.7(3) |
| C(22A)-Fe(2A)-C(17A)-C(16A) | -77.9(3) |
| C(18A)-Fe(2A)-C(17A)-C(16A) | 119.2(4) |
| C(21A)-Fe(2A)-C(17A)-C(16A) | -47.5(6) |
| C(23A)-Fe(2A)-C(17A)-C(16A) | -120.4(3) |
| C(15A)-Fe(2A)-C(17A)-C(16A) | 36.3(3) |
| C(24A)-Fe(2A)-C(17A)-C(16A) | -160.1(3) |
| C(20A)-Fe(2A)-C(17A)-C(16A) | 169.3(6) |
| C(16A)-C(17A)-C(18A)-C(14A) | 0.6(5) |
| Fe(2A)-C(17A)-C(18A)-C(14A) | 59.3(3) |
| C(16A)-C(17A)-C(18A)-Fe(2A) | -58.7(3) |
| N(2A)-C(14A)-C(18A)-C(17A) | 176.8(4) |
| C(15A)-C(14A)-C(18A)-C(17A) | -1.2(5) |
| Fe(2A)-C(14A)-C(18A)-C(17A) | -60.0(3) |
| N(2A)-C(14A)-C(18A)-Fe(2A) | -123.2(4) |
| C(15A)-C(14A)-C(18A)-Fe(2A) | 58.8(3) |
| C(14A)-Fe(2A)-C(18A)-C(17A) | 118.1(4) |
| C(16A)-Fe(2A)-C(18A)-C(17A) | 38.0(3) |
| C(22A)-Fe(2A)-C(18A)-C(17A) | -40.1(7) |
| C(21A)-Fe(2A)-C(18A)-C(17A) | 162.1(6) |
| C(23A)-Fe(2A)-C(18A)-C(17A) | -77.3(4) |
| C(15A)-Fe(2A)-C(18A)-C(17A) | 81.3(3) |
| C(24A)-Fe(2A)-C(18A)-C(17A) | -119.5(3) |
| C(20A)-Fe(2A)-C(18A)-C(17A) | -162.3(3) |
| C(16A)-Fe(2A)-C(18A)-C(14A) | -80.0(3) |
| C(22A)-Fe(2A)-C(18A)-C(14A) | -158.1(5) |
| C(21A)-Fe(2A)-C(18A)-C(14A) | 44.0(8) |
| C(23A)-Fe(2A)-C(18A)-C(14A) | 164.6(3) |
| C(15A)-Fe(2A)-C(18A)-C(14A) | -36.7(3) |
| C(24A)-Fe(2A)-C(18A)-C(14A) | 122.5(3) |
| C(17A)-Fe(2A)-C(18A)-C(14A) | -118.1(4) |
| C(20A)-Fe(2A)-C(18A)-C(14A) | 79.7(3) |
| C(14A)-Fe(2A)-C(20A)-C(21A) | -120.7(3) |
| C(16A)-Fe(2A)-C(20A)-C(21A) | -40.3(6) |
| C(22A)-Fe(2A)-C(20A)-C(21A) | 36.9(3) |
| C(18A)-Fe(2A)-C(20A)-C(21A) | -164.1(3) |
| C(23A)-Fe(2A)-C(20A)-C(21A) | 81.4(3) |
| C(15A)-Fe(2A)-C(20A)-C(21A) | -76.4(3) |
| C(24A)-Fe(2A)-C(20A)-C(21A) | 117.7(4) |

| | |
|---|---|
| C(17A)-Fe(2A)-C(20A)-C(21A) | 157.9(6) |
| C(14A)-Fe(2A)-C(20A)-C(24A) | 121.6(3) |
| C(16A)-Fe(2A)-C(20A)-C(24A) | -158.0(4) |
| C(22A)-Fe(2A)-C(20A)-C(24A) | -80.8(3) |
| C(18A)-Fe(2A)-C(20A)-C(24A) | 78.2(4) |
| C(21A)-Fe(2A)-C(20A)-C(24A) | -117.7(4) |
| C(23A)-Fe(2A)-C(20A)-C(24A) | -36.3(3) |
| C(15A)-Fe(2A)-C(20A)-C(24A) | 165.9(3) |
| C(17A)-Fe(2A)-C(20A)-C(24A) | 40.2(8) |
| C(24A)-C(20A)-C(21A)-C(22A) | 0.9(5) |
| Fe(2A)-C(20A)-C(21A)-C(22A) | -59.0(3) |
| C(24A)-C(20A)-C(21A)-Fe(2A) | 59.9(3) |
| C(14A)-Fe(2A)-C(21A)-C(22A) | -159.5(3) |
| C(16A)-Fe(2A)-C(21A)-C(22A) | -76.8(3) |
| C(18A)-Fe(2A)-C(21A)-C(22A) | 166.7(6) |
| C(23A)-Fe(2A)-C(21A)-C(22A) | 38.6(3) |
| C(15A)-Fe(2A)-C(21A)-C(22A) | -118.3(3) |
| C(24A)-Fe(2A)-C(21A)-C(22A) | 81.5(3) |
| C(17A)-Fe(2A)-C(21A)-C(22A) | -42.6(6) |
| C(20A)-Fe(2A)-C(21A)-C(22A) | 120.2(4) |
| C(14A)-Fe(2A)-C(21A)-C(20A) | 80.3(3) |
| C(16A)-Fe(2A)-C(21A)-C(20A) | 163.1(3) |
| C(22A)-Fe(2A)-C(21A)-C(20A) | -120.2(4) |
| C(18A)-Fe(2A)-C(21A)-C(20A) | 46.6(8) |
| C(23A)-Fe(2A)-C(21A)-C(20A) | -81.6(3) |
| C(15A)-Fe(2A)-C(21A)-C(20A) | 121.5(3) |
| C(24A)-Fe(2A)-C(21A)-C(20A) | -38.7(3) |
| C(17A)-Fe(2A)-C(21A)-C(20A) | -162.8(5) |
| C(20A)-C(21A)-C(22A)-C(23A) | -0.7(5) |
| Fe(2A)-C(21A)-C(22A)-C(23A) | -59.8(3) |
| C(20A)-C(21A)-C(22A)-Fe(2A) | 59.1(3) |
| C(14A)-Fe(2A)-C(22A)-C(21A) | 53.4(7) |
| C(16A)-Fe(2A)-C(22A)-C(21A) | 119.7(3) |
| C(18A)-Fe(2A)-C(22A)-C(21A) | -169.7(5) |
| C(23A)-Fe(2A)-C(22A)-C(21A) | -118.4(5) |
| C(15A)-Fe(2A)-C(22A)-C(21A) | 78.9(3) |
| C(24A)-Fe(2A)-C(22A)-C(21A) | -81.4(3) |
| C(17A)-Fe(2A)-C(22A)-C(21A) | 161.4(3) |
| C(20A)-Fe(2A)-C(22A)-C(21A) | -37.2(3) |
| C(14A)-Fe(2A)-C(22A)-C(23A) | 171.9(5) |
| C(16A)-Fe(2A)-C(22A)-C(23A) | -121.9(3) |
| C(18A)-Fe(2A)-C(22A)-C(23A) | -51.3(7) |
| C(21A)-Fe(2A)-C(22A)-C(23A) | 118.4(4) |
| C(15A)-Fe(2A)-C(22A)-C(23A) | -162.7(3) |
| C(24A)-Fe(2A)-C(22A)-C(23A) | 37.0(3) |
| C(17A)-Fe(2A)-C(22A)-C(23A) | -80.2(4) |
| C(20A)-Fe(2A)-C(22A)-C(23A) | 81.2(3) |
| C(21A)-C(22A)-C(23A)-C(24A) | 0.2(5) |
| Fe(2A)-C(22A)-C(23A)-C(24A) | -59.9(3) |

| | |
|---|---|
| C(21A)-C(22A)-C(23A)-Fe(2A) | 60.1(3) |
| C(14A)-Fe(2A)-C(23A)-C(24A) | -52.8(7) |
| C(16A)-Fe(2A)-C(23A)-C(24A) | -165.6(3) |
| C(22A)-Fe(2A)-C(23A)-C(24A) | 119.0(4) |
| C(18A)-Fe(2A)-C(23A)-C(24A) | -82.3(3) |
| C(21A)-Fe(2A)-C(23A)-C(24A) | 81.2(3) |
| C(15A)-Fe(2A)-C(23A)-C(24A) | 161.0(5) |
| C(17A)-Fe(2A)-C(23A)-C(24A) | -123.6(3) |
| C(20A)-Fe(2A)-C(23A)-C(24A) | 37.4(3) |
| C(14A)-Fe(2A)-C(23A)-C(22A) | -171.8(5) |
| C(16A)-Fe(2A)-C(23A)-C(22A) | 75.4(4) |
| C(18A)-Fe(2A)-C(23A)-C(22A) | 158.8(3) |
| C(21A)-Fe(2A)-C(23A)-C(22A) | -37.8(3) |
| C(15A)-Fe(2A)-C(23A)-C(22A) | 42.0(7) |
| C(24A)-Fe(2A)-C(23A)-C(22A) | -119.0(4) |
| C(17A)-Fe(2A)-C(23A)-C(22A) | 117.4(3) |
| C(20A)-Fe(2A)-C(23A)-C(22A) | -81.6(3) |
| C(22A)-C(23A)-C(24A)-C(20A) | 0.4(5) |
| Fe(2A)-C(23A)-C(24A)-C(20A) | -58.9(3) |
| C(22A)-C(23A)-C(24A)-Fe(2A) | 59.2(3) |
| C(21A)-C(20A)-C(24A)-C(23A) | -0.8(5) |
| Fe(2A)-C(20A)-C(24A)-C(23A) | 59.1(3) |
| C(21A)-C(20A)-C(24A)-Fe(2A) | -59.9(3) |
| C(14A)-Fe(2A)-C(24A)-C(23A) | 159.7(3) |
| C(16A)-Fe(2A)-C(24A)-C(23A) | 35.8(7) |
| C(22A)-Fe(2A)-C(24A)-C(23A) | -38.5(3) |
| C(18A)-Fe(2A)-C(24A)-C(23A) | 116.8(3) |
| C(21A)-Fe(2A)-C(24A)-C(23A) | -82.1(3) |
| C(15A)-Fe(2A)-C(24A)-C(23A) | -158.2(5) |
| C(17A)-Fe(2A)-C(24A)-C(23A) | 74.0(4) |
| C(20A)-Fe(2A)-C(24A)-C(23A) | -120.5(4) |
| C(14A)-Fe(2A)-C(24A)-C(20A) | -79.8(3) |
| C(16A)-Fe(2A)-C(24A)-C(20A) | 156.2(5) |
| C(22A)-Fe(2A)-C(24A)-C(20A) | 82.0(3) |
| C(18A)-Fe(2A)-C(24A)-C(20A) | -122.7(3) |
| C(21A)-Fe(2A)-C(24A)-C(20A) | 38.4(3) |
| C(23A)-Fe(2A)-C(24A)-C(20A) | 120.5(4) |
| C(15A)-Fe(2A)-C(24A)-C(20A) | -37.7(7) |
| C(17A)-Fe(2A)-C(24A)-C(20A) | -165.6(3) |
| C(3B)-N(1B)-C(1B)-Pd(1B) | -140(8) |
| C(2B)-Pd(1B)-C(1B)-N(1B) | -110(10) |
| I(1B)-Pd(1B)-C(1B)-N(1B) | -124(10) |
| I(2B)-Pd(1B)-C(1B)-N(1B) | 56(10) |
| C(14B)-N(2B)-C(2B)-Pd(1B) | -85(16) |
| C(1B)-Pd(1B)-C(2B)-N(2B) | 1(10) |
| I(1B)-Pd(1B)-C(2B)-N(2B) | 15(6) |
| I(2B)-Pd(1B)-C(2B)-N(2B) | -165(6) |
| C(1B)-N(1B)-C(3B)-C(7B) | -157(4) |
| C(1B)-N(1B)-C(3B)-C(4B) | 19(5) |

| | |
|---|---|
| C(1B)-N(1B)-C(3B)-Fe(1B) | 109(5) |
| C(9B)-Fe(1B)-C(3B)-N(1B) | -9.6(6) |
| C(13B)-Fe(1B)-C(3B)-N(1B) | 32.3(6) |
| C(10B)-Fe(1B)-C(3B)-N(1B) | -47.7(5) |
| C(12B)-Fe(1B)-C(3B)-N(1B) | 70.1(7) |
| C(11B)-Fe(1B)-C(3B)-N(1B) | -81.2(11) |
| C(5B)-Fe(1B)-C(3B)-N(1B) | -156.1(4) |
| C(7B)-Fe(1B)-C(3B)-N(1B) | 121.8(5) |
| C(6B)-Fe(1B)-C(3B)-N(1B) | 160.1(4) |
| C(4B)-Fe(1B)-C(3B)-N(1B) | -116.6(5) |
| C(9B)-Fe(1B)-C(3B)-C(7B) | -131.4(5) |
| C(13B)-Fe(1B)-C(3B)-C(7B) | -89.5(5) |
| C(10B)-Fe(1B)-C(3B)-C(7B) | -169.5(4) |
| C(12B)-Fe(1B)-C(3B)-C(7B) | -51.7(6) |
| C(11B)-Fe(1B)-C(3B)-C(7B) | 157.0(9) |
| C(5B)-Fe(1B)-C(3B)-C(7B) | 82.1(3) |
| C(6B)-Fe(1B)-C(3B)-C(7B) | 38.3(3) |
| C(4B)-Fe(1B)-C(3B)-C(7B) | 121.6(4) |
| C(9B)-Fe(1B)-C(3B)-C(4B) | 107.0(5) |
| C(13B)-Fe(1B)-C(3B)-C(4B) | 148.9(5) |
| C(10B)-Fe(1B)-C(3B)-C(4B) | 68.9(4) |
| C(12B)-Fe(1B)-C(3B)-C(4B) | -173.3(6) |
| C(11B)-Fe(1B)-C(3B)-C(4B) | 35.4(11) |
| C(5B)-Fe(1B)-C(3B)-C(4B) | -39.5(3) |
| C(7B)-Fe(1B)-C(3B)-C(4B) | -121.6(4) |
| C(6B)-Fe(1B)-C(3B)-C(4B) | -83.4(3) |
| N(1B)-C(3B)-C(4B)-C(5B) | -177.3(4) |
| C(7B)-C(3B)-C(4B)-C(5B) | -0.4(5) |
| Fe(1B)-C(3B)-C(4B)-C(5B) | 59.9(3) |
| N(1B)-C(3B)-C(4B)-C(8B) | 1.2(7) |
| C(7B)-C(3B)-C(4B)-C(8B) | 178.1(4) |
| Fe(1B)-C(3B)-C(4B)-C(8B) | -121.7(4) |
| N(1B)-C(3B)-C(4B)-Fe(1B) | 122.8(4) |
| C(7B)-C(3B)-C(4B)-Fe(1B) | -60.2(3) |
| C(9B)-Fe(1B)-C(4B)-C(3B) | -91.7(4) |
| C(13B)-Fe(1B)-C(4B)-C(3B) | -60.9(6) |
| C(10B)-Fe(1B)-C(4B)-C(3B) | -132.2(3) |
| C(12B)-Fe(1B)-C(4B)-C(3B) | 164.9(10) |
| C(11B)-Fe(1B)-C(4B)-C(3B) | -171.3(3) |
| C(5B)-Fe(1B)-C(4B)-C(3B) | 116.1(4) |
| C(7B)-Fe(1B)-C(4B)-C(3B) | 36.4(3) |
| C(6B)-Fe(1B)-C(4B)-C(3B) | 79.6(3) |
| C(3B)-Fe(1B)-C(4B)-C(5B) | -116.1(4) |
| C(9B)-Fe(1B)-C(4B)-C(5B) | 152.2(4) |
| C(13B)-Fe(1B)-C(4B)-C(5B) | -177.1(5) |
| C(10B)-Fe(1B)-C(4B)-C(5B) | 111.6(4) |
| C(12B)-Fe(1B)-C(4B)-C(5B) | 48.8(12) |
| C(11B)-Fe(1B)-C(4B)-C(5B) | 72.6(4) |
| C(7B)-Fe(1B)-C(4B)-C(5B) | -79.8(3) |

| | |
|---|---|
| C(6B)-Fe(1B)-C(4B)-C(5B) | -36.6(3) |
| C(3B)-Fe(1B)-C(4B)-C(8B) | 119.8(5) |
| C(9B)-Fe(1B)-C(4B)-C(8B) | 28.2(6) |
| C(13B)-Fe(1B)-C(4B)-C(8B) | 58.9(7) |
| C(10B)-Fe(1B)-C(4B)-C(8B) | -12.4(5) |
| C(12B)-Fe(1B)-C(4B)-C(8B) | -75.3(12) |
| C(11B)-Fe(1B)-C(4B)-C(8B) | -51.4(5) |
| C(5B)-Fe(1B)-C(4B)-C(8B) | -124.0(5) |
| C(7B)-Fe(1B)-C(4B)-C(8B) | 156.2(5) |
| C(6B)-Fe(1B)-C(4B)-C(8B) | -160.6(5) |
| C(3B)-C(4B)-C(5B)-C(6B) | 0.1(5) |
| C(8B)-C(4B)-C(5B)-C(6B) | -178.3(4) |
| Fe(1B)-C(4B)-C(5B)-C(6B) | 58.8(3) |
| C(3B)-C(4B)-C(5B)-Fe(1B) | -58.7(3) |
| C(8B)-C(4B)-C(5B)-Fe(1B) | 122.9(5) |
| C(3B)-Fe(1B)-C(5B)-C(6B) | -81.2(3) |
| C(9B)-Fe(1B)-C(5B)-C(6B) | -174.7(5) |
| C(13B)-Fe(1B)-C(5B)-C(6B) | 50.2(15) |
| C(10B)-Fe(1B)-C(5B)-C(6B) | 152.8(3) |
| C(12B)-Fe(1B)-C(5B)-C(6B) | 71.5(4) |
| C(11B)-Fe(1B)-C(5B)-C(6B) | 110.8(3) |
| C(7B)-Fe(1B)-C(5B)-C(6B) | -37.0(3) |
| C(4B)-Fe(1B)-C(5B)-C(6B) | -120.9(4) |
| C(3B)-Fe(1B)-C(5B)-C(4B) | 39.7(3) |
| C(9B)-Fe(1B)-C(5B)-C(4B) | -53.8(5) |
| C(13B)-Fe(1B)-C(5B)-C(4B) | 171.1(14) |
| C(10B)-Fe(1B)-C(5B)-C(4B) | -86.3(3) |
| C(12B)-Fe(1B)-C(5B)-C(4B) | -167.6(3) |
| C(11B)-Fe(1B)-C(5B)-C(4B) | -128.3(3) |
| C(7B)-Fe(1B)-C(5B)-C(4B) | 83.8(3) |
| C(6B)-Fe(1B)-C(5B)-C(4B) | 120.9(4) |
| C(4B)-C(5B)-C(6B)-C(7B) | 0.2(5) |
| Fe(1B)-C(5B)-C(6B)-C(7B) | 58.9(3) |
| C(4B)-C(5B)-C(6B)-Fe(1B) | -58.7(3) |
| C(3B)-Fe(1B)-C(6B)-C(7B) | -38.7(3) |
| C(9B)-Fe(1B)-C(6B)-C(7B) | 43.4(15) |
| C(13B)-Fe(1B)-C(6B)-C(7B) | 70.1(5) |
| C(10B)-Fe(1B)-C(6B)-C(7B) | -174.1(4) |
| C(12B)-Fe(1B)-C(6B)-C(7B) | 110.2(4) |
| C(11B)-Fe(1B)-C(6B)-C(7B) | 152.9(3) |
| C(5B)-Fe(1B)-C(6B)-C(7B) | -120.2(4) |
| C(4B)-Fe(1B)-C(6B)-C(7B) | -83.1(3) |
| C(3B)-Fe(1B)-C(6B)-C(5B) | 81.5(3) |
| C(9B)-Fe(1B)-C(6B)-C(5B) | 163.6(14) |
| C(13B)-Fe(1B)-C(6B)-C(5B) | -169.7(4) |
| C(10B)-Fe(1B)-C(6B)-C(5B) | -53.9(5) |
| C(12B)-Fe(1B)-C(6B)-C(5B) | -129.6(4) |
| C(11B)-Fe(1B)-C(6B)-C(5B) | -86.9(3) |
| C(7B)-Fe(1B)-C(6B)-C(5B) | 120.2(4) |

| | |
|---|---|
| C(4B)-Fe(1B)-C(6B)-C(5B) | 37.1(3) |
| N(1B)-C(3B)-C(7B)-C(6B) | 177.2(4) |
| C(4B)-C(3B)-C(7B)-C(6B) | 0.4(5) |
| Fe(1B)-C(3B)-C(7B)-C(6B) | -59.8(3) |
| N(1B)-C(3B)-C(7B)-Fe(1B) | -122.9(4) |
| C(4B)-C(3B)-C(7B)-Fe(1B) | 60.3(3) |
| C(5B)-C(6B)-C(7B)-C(3B) | -0.4(5) |
| Fe(1B)-C(6B)-C(7B)-C(3B) | 58.5(3) |
| C(5B)-C(6B)-C(7B)-Fe(1B) | -58.8(3) |
| C(9B)-Fe(1B)-C(7B)-C(3B) | 71.2(5) |
| C(13B)-Fe(1B)-C(7B)-C(3B) | 109.9(5) |
| C(10B)-Fe(1B)-C(7B)-C(3B) | 46.4(12) |
| C(12B)-Fe(1B)-C(7B)-C(3B) | 154.5(4) |
| C(11B)-Fe(1B)-C(7B)-C(3B) | -170.9(4) |
| C(5B)-Fe(1B)-C(7B)-C(3B) | -80.7(3) |
| C(6B)-Fe(1B)-C(7B)-C(3B) | -117.8(4) |
| C(4B)-Fe(1B)-C(7B)-C(3B) | -36.7(3) |
| C(3B)-Fe(1B)-C(7B)-C(6B) | 117.8(4) |
| C(9B)-Fe(1B)-C(7B)-C(6B) | -171.0(5) |
| C(13B)-Fe(1B)-C(7B)-C(6B) | -132.4(5) |
| C(10B)-Fe(1B)-C(7B)-C(6B) | 164.2(11) |
| C(12B)-Fe(1B)-C(7B)-C(6B) | -87.7(4) |
| C(11B)-Fe(1B)-C(7B)-C(6B) | -53.1(5) |
| C(5B)-Fe(1B)-C(7B)-C(6B) | 37.1(3) |
| C(4B)-Fe(1B)-C(7B)-C(6B) | 81.1(3) |
| C(3B)-Fe(1B)-C(9B)-C(10B) | -131.2(4) |
| C(13B)-Fe(1B)-C(9B)-C(10B) | 118.6(7) |
| C(12B)-Fe(1B)-C(9B)-C(10B) | 80.1(5) |
| C(11B)-Fe(1B)-C(9B)-C(10B) | 36.6(4) |
| C(5B)-Fe(1B)-C(9B)-C(10B) | -50.3(7) |
| C(7B)-Fe(1B)-C(9B)-C(10B) | -172.6(3) |
| C(6B)-Fe(1B)-C(9B)-C(10B) | 150.5(13) |
| C(4B)-Fe(1B)-C(9B)-C(10B) | -86.5(5) |
| C(3B)-Fe(1B)-C(9B)-C(13B) | 110.2(5) |
| C(10B)-Fe(1B)-C(9B)-C(13B) | -118.6(7) |
| C(12B)-Fe(1B)-C(9B)-C(13B) | -38.5(5) |
| C(11B)-Fe(1B)-C(9B)-C(13B) | -82.0(5) |
| C(5B)-Fe(1B)-C(9B)-C(13B) | -168.9(5) |
| C(7B)-Fe(1B)-C(9B)-C(13B) | 68.8(6) |
| C(6B)-Fe(1B)-C(9B)-C(13B) | 31.9(17) |
| C(4B)-Fe(1B)-C(9B)-C(13B) | 154.9(5) |
| C(13B)-C(9B)-C(10B)-C(11B) | 1.7(8) |
| Fe(1B)-C(9B)-C(10B)-C(11B) | -59.5(4) |
| C(13B)-C(9B)-C(10B)-Fe(1B) | 61.2(5) |
| C(3B)-Fe(1B)-C(10B)-C(9B) | 69.2(6) |
| C(13B)-Fe(1B)-C(10B)-C(9B) | -37.4(5) |
| C(12B)-Fe(1B)-C(10B)-C(9B) | -82.7(6) |
| C(11B)-Fe(1B)-C(10B)-C(9B) | -121.0(6) |
| C(5B)-Fe(1B)-C(10B)-C(9B) | 153.2(5) |

| | |
|---|---|
| C(7B)-Fe(1B)-C(10B)-C(9B) | 30.2(13) |
| C(6B)-Fe(1B)-C(10B)-C(9B) | -170.4(5) |
| C(4B)-Fe(1B)-C(10B)-C(9B) | 109.5(5) |
| C(3B)-Fe(1B)-C(10B)-C(11B) | -169.8(3) |
| C(9B)-Fe(1B)-C(10B)-C(11B) | 121.0(6) |
| C(13B)-Fe(1B)-C(10B)-C(11B) | 83.6(6) |
| C(12B)-Fe(1B)-C(10B)-C(11B) | 38.2(4) |
| C(5B)-Fe(1B)-C(10B)-C(11B) | -85.8(4) |
| C(7B)-Fe(1B)-C(10B)-C(11B) | 151.2(10) |
| C(6B)-Fe(1B)-C(10B)-C(11B) | -49.4(6) |
| C(4B)-Fe(1B)-C(10B)-C(11B) | -129.5(4) |
| C(9B)-C(10B)-C(11B)-C(12B) | -0.9(7) |
| Fe(1B)-C(10B)-C(11B)-C(12B) | -60.4(4) |
| C(9B)-C(10B)-C(11B)-Fe(1B) | 59.5(4) |
| C(3B)-Fe(1B)-C(11B)-C(10B) | 40.8(12) |
| C(9B)-Fe(1B)-C(11B)-C(10B) | -35.4(5) |
| C(13B)-Fe(1B)-C(11B)-C(10B) | -77.8(6) |
| C(12B)-Fe(1B)-C(11B)-C(10B) | -117.8(6) |
| C(5B)-Fe(1B)-C(11B)-C(10B) | 111.5(4) |
| C(7B)-Fe(1B)-C(11B)-C(10B) | -169.6(4) |
| C(6B)-Fe(1B)-C(11B)-C(10B) | 154.6(4) |
| C(4B)-Fe(1B)-C(11B)-C(10B) | 70.1(5) |
| C(3B)-Fe(1B)-C(11B)-C(12B) | 158.6(10) |
| C(9B)-Fe(1B)-C(11B)-C(12B) | 82.4(6) |
| C(13B)-Fe(1B)-C(11B)-C(12B) | 40.0(6) |
| C(10B)-Fe(1B)-C(11B)-C(12B) | 117.8(6) |
| C(5B)-Fe(1B)-C(11B)-C(12B) | -130.7(5) |
| C(7B)-Fe(1B)-C(11B)-C(12B) | -51.8(6) |
| C(6B)-Fe(1B)-C(11B)-C(12B) | -87.6(5) |
| C(4B)-Fe(1B)-C(11B)-C(12B) | -172.1(5) |
| C(10B)-C(11B)-C(12B)-C(13B) | -0.3(7) |
| Fe(1B)-C(11B)-C(12B)-C(13B) | -60.7(4) |
| C(10B)-C(11B)-C(12B)-Fe(1B) | 60.5(4) |
| C(3B)-Fe(1B)-C(12B)-C(11B) | -171.2(4) |
| C(9B)-Fe(1B)-C(12B)-C(11B) | -79.6(5) |
| C(13B)-Fe(1B)-C(12B)-C(11B) | -116.0(7) |
| C(10B)-Fe(1B)-C(12B)-C(11B) | -37.9(4) |
| C(5B)-Fe(1B)-C(12B)-C(11B) | 69.5(5) |
| C(7B)-Fe(1B)-C(12B)-C(11B) | 153.4(4) |
| C(6B)-Fe(1B)-C(12B)-C(11B) | 110.1(4) |
| C(4B)-Fe(1B)-C(12B)-C(11B) | 29.4(14) |
| C(3B)-Fe(1B)-C(12B)-C(13B) | -55.2(8) |
| C(9B)-Fe(1B)-C(12B)-C(13B) | 36.4(5) |
| C(10B)-Fe(1B)-C(12B)-C(13B) | 78.1(6) |
| C(11B)-Fe(1B)-C(12B)-C(13B) | 116.0(7) |
| C(5B)-Fe(1B)-C(12B)-C(13B) | -174.6(5) |
| C(7B)-Fe(1B)-C(12B)-C(13B) | -90.6(6) |
| C(6B)-Fe(1B)-C(12B)-C(13B) | -133.9(6) |
| C(4B)-Fe(1B)-C(12B)-C(13B) | 145.4(11) |

| | |
|---|---|
| C(10B)-C(9B)-C(13B)-C(12B) | -1.8(8) |
| Fe(1B)-C(9B)-C(13B)-C(12B) | 59.6(5) |
| C(10B)-C(9B)-C(13B)-Fe(1B) | -61.4(5) |
| C(11B)-C(12B)-C(13B)-C(9B) | 1.3(8) |
| Fe(1B)-C(12B)-C(13B)-C(9B) | -60.1(5) |
| C(11B)-C(12B)-C(13B)-Fe(1B) | 61.4(4) |
| C(3B)-Fe(1B)-C(13B)-C(9B) | -87.9(5) |
| C(10B)-Fe(1B)-C(13B)-C(9B) | 36.9(5) |
| C(12B)-Fe(1B)-C(13B)-C(9B) | 119.1(6) |
| C(11B)-Fe(1B)-C(13B)-C(9B) | 80.3(5) |
| C(5B)-Fe(1B)-C(13B)-C(9B) | 144.3(15) |
| C(7B)-Fe(1B)-C(13B)-C(9B) | -132.3(5) |
| C(6B)-Fe(1B)-C(13B)-C(9B) | -173.0(4) |
| C(4B)-Fe(1B)-C(13B)-C(9B) | -47.0(7) |
| C(3B)-Fe(1B)-C(13B)-C(12B) | 152.9(4) |
| C(9B)-Fe(1B)-C(13B)-C(12B) | -119.1(6) |
| C(10B)-Fe(1B)-C(13B)-C(12B) | -82.2(5) |
| C(11B)-Fe(1B)-C(13B)-C(12B) | -38.8(4) |
| C(5B)-Fe(1B)-C(13B)-C(12B) | 25.1(18) |
| C(7B)-Fe(1B)-C(13B)-C(12B) | 108.5(4) |
| C(6B)-Fe(1B)-C(13B)-C(12B) | 67.9(5) |
| C(4B)-Fe(1B)-C(13B)-C(12B) | -166.2(4) |
| C(2B)-N(2B)-C(14B)-C(15B) | -19(15) |
| C(2B)-N(2B)-C(14B)-C(18B) | 161(14) |
| C(2B)-N(2B)-C(14B)-Fe(2B) | 70(15) |
| C(16B)-Fe(2B)-C(14B)-N(2B) | -158.3(5) |
| C(15B)-Fe(2B)-C(14B)-N(2B) | -117.8(5) |
| C(17B)-Fe(2B)-C(14B)-N(2B) | 157.8(5) |
| C(20B)-Fe(2B)-C(14B)-N(2B) | 1.0(4) |
| C(18B)-Fe(2B)-C(14B)-N(2B) | 119.4(5) |
| C(22B)-Fe(2B)-C(14B)-N(2B) | -80.4(6) |
| C(23B)-Fe(2B)-C(14B)-N(2B) | 81.4(8) |
| C(21B)-Fe(2B)-C(14B)-N(2B) | -42.6(5) |
| C(24B)-Fe(2B)-C(14B)-N(2B) | 43.0(5) |
| C(16B)-Fe(2B)-C(14B)-C(15B) | -40.6(4) |
| C(17B)-Fe(2B)-C(14B)-C(15B) | -84.5(4) |
| C(20B)-Fe(2B)-C(14B)-C(15B) | 118.8(3) |
| C(18B)-Fe(2B)-C(14B)-C(15B) | -122.9(4) |
| C(22B)-Fe(2B)-C(14B)-C(15B) | 37.4(6) |
| C(23B)-Fe(2B)-C(14B)-C(15B) | -160.9(6) |
| C(21B)-Fe(2B)-C(14B)-C(15B) | 75.2(3) |
| C(24B)-Fe(2B)-C(14B)-C(15B) | 160.8(3) |
| C(16B)-Fe(2B)-C(14B)-C(18B) | 82.3(4) |
| C(15B)-Fe(2B)-C(14B)-C(18B) | 122.9(4) |
| C(17B)-Fe(2B)-C(14B)-C(18B) | 38.4(4) |
| C(20B)-Fe(2B)-C(14B)-C(18B) | -118.3(3) |
| C(22B)-Fe(2B)-C(14B)-C(18B) | 160.3(5) |
| C(23B)-Fe(2B)-C(14B)-C(18B) | -38.0(8) |
| C(21B)-Fe(2B)-C(14B)-C(18B) | -161.9(3) |

| | |
|---|---|
| C(24B)-Fe(2B)-C(14B)-C(18B) | -76.3(4) |
| N(2B)-C(14B)-C(15B)-C(16B) | -177.6(4) |
| C(18B)-C(14B)-C(15B)-C(16B) | 2.2(5) |
| Fe(2B)-C(14B)-C(15B)-C(16B) | 60.6(3) |
| N(2B)-C(14B)-C(15B)-C(19B) | 1.9(7) |
| C(18B)-C(14B)-C(15B)-C(19B) | -178.3(5) |
| Fe(2B)-C(14B)-C(15B)-C(19B) | -119.9(5) |
| N(2B)-C(14B)-C(15B)-Fe(2B) | 121.8(4) |
| C(18B)-C(14B)-C(15B)-Fe(2B) | -58.4(4) |
| C(16B)-Fe(2B)-C(15B)-C(14B) | 115.2(5) |
| C(17B)-Fe(2B)-C(15B)-C(14B) | 78.8(3) |
| C(20B)-Fe(2B)-C(15B)-C(14B) | -81.8(3) |
| C(18B)-Fe(2B)-C(15B)-C(14B) | 35.9(3) |
| C(22B)-Fe(2B)-C(15B)-C(14B) | -163.8(3) |
| C(23B)-Fe(2B)-C(15B)-C(14B) | 166.9(4) |
| C(21B)-Fe(2B)-C(15B)-C(14B) | -122.0(3) |
| C(24B)-Fe(2B)-C(15B)-C(14B) | -56.4(8) |
| C(14B)-Fe(2B)-C(15B)-C(16B) | -115.2(5) |
| C(17B)-Fe(2B)-C(15B)-C(16B) | -36.4(4) |
| C(20B)-Fe(2B)-C(15B)-C(16B) | 163.0(4) |
| C(18B)-Fe(2B)-C(15B)-C(16B) | -79.3(4) |
| C(22B)-Fe(2B)-C(15B)-C(16B) | 81.0(4) |
| C(23B)-Fe(2B)-C(15B)-C(16B) | 51.7(7) |
| C(21B)-Fe(2B)-C(15B)-C(16B) | 122.8(4) |
| C(24B)-Fe(2B)-C(15B)-C(16B) | -171.6(6) |
| C(14B)-Fe(2B)-C(15B)-C(19B) | 120.0(6) |
| C(16B)-Fe(2B)-C(15B)-C(19B) | -124.8(6) |
| C(17B)-Fe(2B)-C(15B)-C(19B) | -161.2(5) |
| C(20B)-Fe(2B)-C(15B)-C(19B) | 38.2(5) |
| C(18B)-Fe(2B)-C(15B)-C(19B) | 155.9(5) |
| C(22B)-Fe(2B)-C(15B)-C(19B) | -43.8(5) |
| C(23B)-Fe(2B)-C(15B)-C(19B) | -73.1(7) |
| C(21B)-Fe(2B)-C(15B)-C(19B) | -2.0(5) |
| C(24B)-Fe(2B)-C(15B)-C(19B) | 63.6(9) |
| C(14B)-C(15B)-C(16B)-C(17B) | -1.8(6) |
| C(19B)-C(15B)-C(16B)-C(17B) | 178.7(5) |
| Fe(2B)-C(15B)-C(16B)-C(17B) | 58.7(4) |
| C(14B)-C(15B)-C(16B)-Fe(2B) | -60.5(3) |
| C(19B)-C(15B)-C(16B)-Fe(2B) | 120.1(5) |
| C(14B)-Fe(2B)-C(16B)-C(17B) | -81.2(3) |
| C(15B)-Fe(2B)-C(16B)-C(17B) | -121.0(5) |
| C(20B)-Fe(2B)-C(16B)-C(17B) | -168.2(5) |
| C(18B)-Fe(2B)-C(16B)-C(17B) | -36.9(3) |
| C(22B)-Fe(2B)-C(16B)-C(17B) | 122.9(3) |
| C(23B)-Fe(2B)-C(16B)-C(17B) | 81.7(4) |
| C(21B)-Fe(2B)-C(16B)-C(17B) | 163.9(3) |
| C(24B)-Fe(2B)-C(16B)-C(17B) | 52.4(7) |
| C(14B)-Fe(2B)-C(16B)-C(15B) | 39.7(3) |
| C(17B)-Fe(2B)-C(16B)-C(15B) | 121.0(5) |

| | |
|---|---|
| C(20B)-Fe(2B)-C(16B)-C(15B) | -47.2(7) |
| C(18B)-Fe(2B)-C(16B)-C(15B) | 84.1(3) |
| C(22B)-Fe(2B)-C(16B)-C(15B) | -116.1(3) |
| C(23B)-Fe(2B)-C(16B)-C(15B) | -157.3(3) |
| C(21B)-Fe(2B)-C(16B)-C(15B) | -75.1(4) |
| C(24B)-Fe(2B)-C(16B)-C(15B) | 173.4(5) |
| C(15B)-C(16B)-C(17B)-C(18B) | 0.8(6) |
| Fe(2B)-C(16B)-C(17B)-C(18B) | 59.0(4) |
| C(15B)-C(16B)-C(17B)-Fe(2B) | -58.2(4) |
| C(14B)-Fe(2B)-C(17B)-C(18B) | -39.1(3) |
| C(16B)-Fe(2B)-C(17B)-C(18B) | -120.4(5) |
| C(15B)-Fe(2B)-C(17B)-C(18B) | -83.0(4) |
| C(20B)-Fe(2B)-C(17B)-C(18B) | 49.1(8) |
| C(22B)-Fe(2B)-C(17B)-C(18B) | 165.0(3) |
| C(23B)-Fe(2B)-C(17B)-C(18B) | 123.4(4) |
| C(21B)-Fe(2B)-C(17B)-C(18B) | -162.1(5) |
| C(24B)-Fe(2B)-C(17B)-C(18B) | 81.8(4) |
| C(14B)-Fe(2B)-C(17B)-C(16B) | 81.3(3) |
| C(15B)-Fe(2B)-C(17B)-C(16B) | 37.4(3) |
| C(20B)-Fe(2B)-C(17B)-C(16B) | 169.5(5) |
| C(18B)-Fe(2B)-C(17B)-C(16B) | 120.4(5) |
| C(22B)-Fe(2B)-C(17B)-C(16B) | -74.7(4) |
| C(23B)-Fe(2B)-C(17B)-C(16B) | -116.2(3) |
| C(21B)-Fe(2B)-C(17B)-C(16B) | -41.7(8) |
| C(24B)-Fe(2B)-C(17B)-C(16B) | -157.9(3) |
| C(16B)-C(17B)-C(18B)-C(14B) | 0.5(6) |
| Fe(2B)-C(17B)-C(18B)-C(14B) | 59.3(3) |
| C(16B)-C(17B)-C(18B)-Fe(2B) | -58.7(4) |
| N(2B)-C(14B)-C(18B)-C(17B) | 178.0(4) |
| C(15B)-C(14B)-C(18B)-C(17B) | -1.8(6) |
| Fe(2B)-C(14B)-C(18B)-C(17B) | -60.1(4) |
| N(2B)-C(14B)-C(18B)-Fe(2B) | -121.9(4) |
| C(15B)-C(14B)-C(18B)-Fe(2B) | 58.3(3) |
| C(14B)-Fe(2B)-C(18B)-C(17B) | 117.3(5) |
| C(16B)-Fe(2B)-C(18B)-C(17B) | 37.0(4) |
| C(15B)-Fe(2B)-C(18B)-C(17B) | 81.6(4) |
| C(20B)-Fe(2B)-C(18B)-C(17B) | -160.3(4) |
| C(22B)-Fe(2B)-C(18B)-C(17B) | -39.3(8) |
| C(23B)-Fe(2B)-C(18B)-C(17B) | -75.4(5) |
| C(21B)-Fe(2B)-C(18B)-C(17B) | 163.0(6) |
| C(24B)-Fe(2B)-C(18B)-C(17B) | -117.8(4) |
| C(16B)-Fe(2B)-C(18B)-C(14B) | -80.3(3) |
| C(15B)-Fe(2B)-C(18B)-C(14B) | -35.7(3) |
| C(17B)-Fe(2B)-C(18B)-C(14B) | -117.3(5) |
| C(20B)-Fe(2B)-C(18B)-C(14B) | 82.4(4) |
| C(22B)-Fe(2B)-C(18B)-C(14B) | -156.6(6) |
| C(23B)-Fe(2B)-C(18B)-C(14B) | 167.3(3) |
| C(21B)-Fe(2B)-C(18B)-C(14B) | 45.6(7) |
| C(24B)-Fe(2B)-C(18B)-C(14B) | 124.9(3) |

| | |
|---|---|
| C(14B)-Fe(2B)-C(20B)-C(24B) | 124.4(3) |
| C(16B)-Fe(2B)-C(20B)-C(24B) | -156.2(6) |
| C(15B)-Fe(2B)-C(20B)-C(24B) | 167.9(3) |
| C(17B)-Fe(2B)-C(20B)-C(24B) | 44.7(7) |
| C(18B)-Fe(2B)-C(20B)-C(24B) | 80.6(3) |
| C(22B)-Fe(2B)-C(20B)-C(24B) | -81.0(3) |
| C(23B)-Fe(2B)-C(20B)-C(24B) | -37.3(3) |
| C(21B)-Fe(2B)-C(20B)-C(24B) | -119.1(4) |
| C(14B)-Fe(2B)-C(20B)-C(21B) | -116.5(3) |
| C(16B)-Fe(2B)-C(20B)-C(21B) | -37.1(7) |
| C(15B)-Fe(2B)-C(20B)-C(21B) | -73.0(4) |
| C(17B)-Fe(2B)-C(20B)-C(21B) | 163.8(5) |
| C(18B)-Fe(2B)-C(20B)-C(21B) | -160.3(3) |
| C(22B)-Fe(2B)-C(20B)-C(21B) | 38.1(3) |
| C(23B)-Fe(2B)-C(20B)-C(21B) | 81.8(3) |
| C(24B)-Fe(2B)-C(20B)-C(21B) | 119.1(4) |
| C(24B)-C(20B)-C(21B)-C(22B) | 0.8(5) |
| Fe(2B)-C(20B)-C(21B)-C(22B) | -59.5(3) |
| C(24B)-C(20B)-C(21B)-Fe(2B) | 60.3(3) |
| C(14B)-Fe(2B)-C(21B)-C(20B) | 83.6(3) |
| C(16B)-Fe(2B)-C(21B)-C(20B) | 166.2(3) |
| C(15B)-Fe(2B)-C(21B)-C(20B) | 124.5(3) |
| C(17B)-Fe(2B)-C(21B)-C(20B) | -162.8(6) |
| C(18B)-Fe(2B)-C(21B)-C(20B) | 49.9(7) |
| C(22B)-Fe(2B)-C(21B)-C(20B) | -118.6(4) |
| C(23B)-Fe(2B)-C(21B)-C(20B) | -81.1(3) |
| C(24B)-Fe(2B)-C(21B)-C(20B) | -37.5(3) |
| C(14B)-Fe(2B)-C(21B)-C(22B) | -157.8(3) |
| C(16B)-Fe(2B)-C(21B)-C(22B) | -75.2(4) |
| C(15B)-Fe(2B)-C(21B)-C(22B) | -116.9(3) |
| C(17B)-Fe(2B)-C(21B)-C(22B) | -44.3(8) |
| C(20B)-Fe(2B)-C(21B)-C(22B) | 118.6(4) |
| C(18B)-Fe(2B)-C(21B)-C(22B) | 168.5(5) |
| C(23B)-Fe(2B)-C(21B)-C(22B) | 37.5(3) |
| C(24B)-Fe(2B)-C(21B)-C(22B) | 81.1(3) |
| C(20B)-C(21B)-C(22B)-C(23B) | -0.1(5) |
| Fe(2B)-C(21B)-C(22B)-C(23B) | -59.5(3) |
| C(20B)-C(21B)-C(22B)-Fe(2B) | 59.4(3) |
| C(14B)-Fe(2B)-C(22B)-C(23B) | 171.8(4) |
| C(16B)-Fe(2B)-C(22B)-C(23B) | -118.2(4) |
| C(15B)-Fe(2B)-C(22B)-C(23B) | -161.2(3) |
| C(17B)-Fe(2B)-C(22B)-C(23B) | -77.7(4) |
| C(20B)-Fe(2B)-C(22B)-C(23B) | 81.2(3) |
| C(18B)-Fe(2B)-C(22B)-C(23B) | -48.4(8) |
| C(21B)-Fe(2B)-C(22B)-C(23B) | 119.2(4) |
| C(24B)-Fe(2B)-C(22B)-C(23B) | 37.7(3) |
| C(14B)-Fe(2B)-C(22B)-C(21B) | 52.6(6) |
| C(16B)-Fe(2B)-C(22B)-C(21B) | 122.5(3) |
| C(15B)-Fe(2B)-C(22B)-C(21B) | 79.5(3) |

| | |
|---|---|
| C(17B)-Fe(2B)-C(22B)-C(21B) | 163.1(4) |
| C(20B)-Fe(2B)-C(22B)-C(21B) | -38.0(3) |
| C(18B)-Fe(2B)-C(22B)-C(21B) | -167.7(6) |
| C(23B)-Fe(2B)-C(22B)-C(21B) | -119.2(4) |
| C(24B)-Fe(2B)-C(22B)-C(21B) | -81.5(3) |
| C(21B)-C(22B)-C(23B)-C(24B) | -0.7(5) |
| Fe(2B)-C(22B)-C(23B)-C(24B) | -60.1(3) |
| C(21B)-C(22B)-C(23B)-Fe(2B) | 59.4(3) |
| C(14B)-Fe(2B)-C(23B)-C(22B) | -168.8(6) |
| C(16B)-Fe(2B)-C(23B)-C(22B) | 78.6(4) |
| C(15B)-Fe(2B)-C(23B)-C(22B) | 41.5(6) |
| C(17B)-Fe(2B)-C(23B)-C(22B) | 120.9(4) |
| C(20B)-Fe(2B)-C(23B)-C(22B) | -81.8(3) |
| C(18B)-Fe(2B)-C(23B)-C(22B) | 161.8(3) |
| C(21B)-Fe(2B)-C(23B)-C(22B) | -37.9(3) |
| C(24B)-Fe(2B)-C(23B)-C(22B) | -119.0(4) |
| C(14B)-Fe(2B)-C(23B)-C(24B) | -49.7(8) |
| C(16B)-Fe(2B)-C(23B)-C(24B) | -162.4(4) |
| C(15B)-Fe(2B)-C(23B)-C(24B) | 160.6(5) |
| C(17B)-Fe(2B)-C(23B)-C(24B) | -120.1(4) |
| C(20B)-Fe(2B)-C(23B)-C(24B) | 37.2(3) |
| C(18B)-Fe(2B)-C(23B)-C(24B) | -79.1(4) |
| C(22B)-Fe(2B)-C(23B)-C(24B) | 119.0(4) |
| C(21B)-Fe(2B)-C(23B)-C(24B) | 81.2(3) |
| C(21B)-C(20B)-C(24B)-C(23B) | -1.2(5) |
| Fe(2B)-C(20B)-C(24B)-C(23B) | 58.7(3) |
| C(21B)-C(20B)-C(24B)-Fe(2B) | -59.9(3) |
| C(22B)-C(23B)-C(24B)-C(20B) | 1.1(6) |
| Fe(2B)-C(23B)-C(24B)-C(20B) | -58.6(3) |
| C(22B)-C(23B)-C(24B)-Fe(2B) | 59.8(3) |
| C(14B)-Fe(2B)-C(24B)-C(20B) | -76.7(3) |
| C(16B)-Fe(2B)-C(24B)-C(20B) | 160.5(6) |
| C(15B)-Fe(2B)-C(24B)-C(20B) | -33.6(8) |
| C(17B)-Fe(2B)-C(24B)-C(20B) | -161.9(3) |
| C(18B)-Fe(2B)-C(24B)-C(20B) | -119.2(3) |
| C(22B)-Fe(2B)-C(24B)-C(20B) | 82.0(3) |
| C(23B)-Fe(2B)-C(24B)-C(20B) | 119.7(4) |
| C(21B)-Fe(2B)-C(24B)-C(20B) | 37.9(3) |
| C(14B)-Fe(2B)-C(24B)-C(23B) | 163.6(3) |
| C(16B)-Fe(2B)-C(24B)-C(23B) | 40.8(7) |
| C(15B)-Fe(2B)-C(24B)-C(23B) | -153.3(6) |
| C(17B)-Fe(2B)-C(24B)-C(23B) | 78.4(4) |
| C(20B)-Fe(2B)-C(24B)-C(23B) | -119.7(4) |
| C(18B)-Fe(2B)-C(24B)-C(23B) | 121.1(3) |
| C(22B)-Fe(2B)-C(24B)-C(23B) | -37.7(3) |
| C(21B)-Fe(2B)-C(24B)-C(23B) | -81.8(3) |

# Appendix B.

Crystolography Data for $[\{((C_6H_{11})_2P)_2CH_2\}\{Au(CNC_5H_4)\}_2Fe][O_3SCF_3]_2$

**Table B.1.** Crystal Data and Structure Refinement for $[\{((C_6H_{11})_2P)_2CH_2\}\{Au(CNC_5H_4)\}_2Fe][O_3SCF_3]_2$

| | | |
|---|---|---|
| Empirical formula | $C_{19.5}H_{27}AuF_3Fe_{0.5}NO_3PS$ | |
| Formula weight | 668.34 | |
| Temperature | 100(2) K | |
| Wavelength | 0.71073 Å | |
| Crystal system | Monoclinic | |
| Space group | C2/c - $C_{2h}^6$ (No. 15) | |
| Unit cell dimensions | **a** = 15.712 (1) Å | $\alpha$ = 90.000° |
| | **b** = 14.752 (1) Å | $\beta$ = 105.151(1)°. |
| | **c** = 19.890(1) Å | $\gamma$ = 90.000° |
| Volume | 4450.1(5) $Å^3$ | |
| Z | 8 | |
| Density (calculated) | 1.995 $Mg/m^3$ | |
| Absorption coefficient | 7.137 $mm^{-1}$ | |
| F(000) | 2600 | |
| Crystal size | 0.26 x 0.24 x 0.18 $mm^3$ | |
| Theta range for data collection | 2.59° to 30.03°. | |
| Index ranges | $-22 \le h \le 22$, $-20 \le k \le 20$, $-27 \le l \le 28$ | |
| Reflections collected | 25732 | |
| Independent reflections | 6478 [$R_{int}$ = 0.032] | |
| Completeness to theta = 30.03° | 99.6 % | |
| Absorption correction | Empirical | |
| Max. and min. transmission | 0.725 and 0.520 | |
| Refinement method | Full-matrix least-squares on $F^2$ | |
| Data / restraints / parameters | 6478 / 0 / 380 | |
| Goodness-of-fit on $F^2$ | 1.026 | |
| Final R indices [I>2sigma(I)] | $R_1$ = 0.020, $wR_2$ = 0.047 | |
| R indices (all data) | $R_1$ = 0.024, $wR_2$ = 0.048 | |
| Largest diff. peak and hole | 1.792 and -1.301 $e^-/Å^3$ | |

---

$R_1 = \Sigma \, ||F_o| - |F_c|| \, / \, \Sigma \, |F_o|$

$wR_2 = \{ \, \Sigma \, [w(F_o^2 - F_c^2)^2] \, / \, \Sigma \, [w(F_o^2)^2] \, \}^{1/2}$

**Table B.2**. Atomic coordinates ( x $10^4$) and equivalent isotropic displacement parameters ($Å^2$ x $10^3$)for $[\{((C_6H_{11})_2P)_2CH_2\}\{Au(CNC_5H_4)\}_2Fe][O_3SCF_3]_2$. U(eq) is defined as one third of the trace of the orthogonalized $U^{ij}$ tensor.

| | x | y | z | U(eq) |
|---|---|---|---|---|
| Au | 4261(1) | -226(1) | 1829(1) | 14(1) |
| Fe | 5000 | 3618(1) | 2500 | 13(1) |
| P | 4481(1) | -1741(1) | 1705(1) | 12(1) |
| N(1) | 4220(1) | 1908(1) | 1768(1) | 16(1) |
| C(1) | 4196(1) | 1128(2) | 1799(1) | 16(1) |
| C(2) | 5000 | -2376(2) | 2500 | 14(1) |
| C(3) | 4208(1) | 2845(2) | 1759(1) | 15(1) |
| C(4) | 3682(2) | 3395(2) | 2085(1) | 16(1) |
| C(5) | 3892(2) | 4308(2) | 1970(1) | 17(1) |
| C(6) | 4536(2) | 4315(2) | 1585(1) | 17(1) |
| C(7) | 4742(2) | 3407(2) | 1451(1) | 15(1) |
| C(11) | 3474(1) | -2375(2) | 1300(1) | 14(1) |
| C(12) | 2787(2) | -2290(2) | 1725(1) | 16(1) |
| C(13) | 1938(2) | -2779(2) | 1358(1) | 20(1) |
| C(14) | 2107(2) | -3767(2) | 1207(1) | 19(1) |
| C(15) | 2793(2) | -3850(2) | 792(1) | 18(1) |
| C(16) | 3653(2) | -3368(2) | 1160(1) | 16(1) |
| C(21) | 5224(2) | -1858(2) | 1137(1) | 15(1) |
| C(22) | 4738(2) | -1611(2) | 386(1) | 19(1) |
| C(23) | 5349(2) | -1644(2) | -97(1) | 23(1) |
| C(24) | 6150(2) | -1048(2) | 162(1) | 24(1) |
| C(25) | 6644(2) | -1304(2) | 899(1) | 22(1) |
| C(26) | 6049(2) | -1259(2) | 1394(1) | 19(1) |
| S | 3167(1) | 5836(1) | 3324(1) | 19(1) |
| F(1) | 3925(1) | 4608(1) | 4242(1) | 45(1) |
| F(2) | 2800(1) | 5244(2) | 4451(1) | 55(1) |
| F(3) | 4031(2) | 5964(2) | 4638(1) | 62(1) |
| O(1) | 3997(1) | 5983(1) | 3155(1) | 25(1) |
| O(2) | 2696(1) | 6653(1) | 3391(1) | 31(1) |
| O(3) | 2643(1) | 5109(1) | 2943(1) | 28(1) |
| C(8) | 3498(2) | 5397(2) | 4210(2) | 31(1) |

**Table B.3.** Bond lengths [Å] for $[\{((C_6H_{11})_2P)_2CH_2\}\{Au(CNC_5H_4)\}_2Fe][O_3SCF_3]_2$

| | |
|---|---|
| Au-C(1) | 1.999(2) |
| Au-P | 2.2853(6) |
| Au-Au#1 | 3.0469(2) |
| Fe-C(3)#1 | 2.017(2) |
| Fe-C(3) | 2.017(2) |
| Fe-C(7)#1 | 2.043(2) |
| Fe-C(7) | 2.043(2) |
| Fe-C(4) | 2.046(2) |
| Fe-C(4)#1 | 2.046(2) |
| Fe-C(6)#1 | 2.051(2) |
| Fe-C(6) | 2.051(2) |
| Fe-C(5) | 2.055(2) |

| | |
|---|---|
| Fe-C(5)#1 | 2.055(2) |
| P-C(21) | 1.834(2) |
| P-C(11) | 1.834(2) |
| P-C(2) | 1.8345(17) |
| N(1)-C(1) | 1.154(3) |
| N(1)-C(3) | 1.381(3) |
| C(3)-C(7) | 1.428(3) |
| C(3)-C(4) | 1.429(3) |
| C(4)-C(5) | 1.420(3) |
| C(4)-H(4) | 0.92(3) |
| C(5)-C(6) | 1.420(3) |
| C(5)-H(5) | 0.87(3) |
| C(6)-C(7) | 1.420(3) |
| C(6)-H(6) | 0.92(3) |
| C(7)-H(7) | 0.91(3) |
| C(2)-P#1 | 1.8345(17) |
| C(2)-H(2) | 0.84(3) |
| C(11)-C(16) | 1.532(3) |
| C(11)-C(12) | 1.540(3) |
| C(11)-H(11) | 1.01(2) |
| C(12)-C(13) | 1.525(3) |
| C(12)-H(12A) | 0.89(3) |
| C(12)-H(12B) | 0.94(3) |
| C(13)-C(14) | 1.525(4) |
| C(13)-H(13A) | 1.00(3) |
| C(13)-H(13B) | 0.85(3) |
| C(14)-C(15) | 1.526(4) |
| C(14)-H(14A) | 0.92(3) |
| C(14)-H(14B) | 1.02(3) |
| C(15)-C(16) | 1.533(3) |
| C(15)-H(15A) | 0.95(3) |
| C(15)-H(15B) | 1.01(3) |
| C(16)-H(16A) | 0.97(2) |
| C(16)-H(16B) | 0.85(3) |
| C(21)-C(22) | 1.533(3) |
| C(21)-C(26) | 1.541(3) |
| C(21)-H(21) | 0.90(3) |
| C(22)-C(23) | 1.526(4) |
| C(22)-H(22A) | 0.95(3) |
| C(22)-H(22B) | 1.03(3) |
| C(23)-C(24) | 1.511(4) |
| C(23)-H(23A) | 0.90(3) |
| C(23)-H(23B) | 1.00(3) |
| C(24)-C(25) | 1.516(4) |
| C(24)-H(24A) | 0.94(3) |
| C(24)-H(24B) | 0.97(3) |
| C(25)-C(26) | 1.526(4) |
| C(25)-H(25A) | 0.93(3) |
| C(25)-H(25B) | 0.95(3) |
| C(26)-H(26A) | 0.96(3) |
| C(26)-H(26B) | 0.99(3) |
| S-O(2) | 1.4393(19) |
| S-O(3) | 1.441(2) |

| | |
|---|---|
| S-O(1) | 1.4449(18) |
| S-C(8) | 1.822(3) |
| F(1)-C(8) | 1.337(3) |
| F(2)-C(8) | 1.326(3) |
| F(3)-C(8) | 1.325(4) |

Symmetry transformations used to generate equivalent atoms: #1: -x+1, y, -z+1/2

**Table B.4.** Bond angles [°] for $[\{((C_6H_{11})_2P)_2CH_2\}\{Au(CNC_5H_4)\}_2Fe][O_3SCF_3]_2$

| | |
|---|---|
| C(1)-Au-P | 169.05(7) |
| C(1)-Au-Au#1 | 92.70(6) |
| P-Au-Au#1 | 89.535(14) |
| C(3)#1-Fe-C(3) | 111.04(13) |
| C(3)#1-Fe-C(7)#1 | 41.18(9) |
| C(3)-Fe-C(7)#1 | 125.46(9) |
| C(3)#1-Fe-C(7) | 125.46(9) |
| C(3)-Fe-C(7) | 41.18(9) |
| C(7)#1-Fe-C(7) | 162.46(13) |
| C(3)#1-Fe-C(4) | 124.75(9) |
| C(3)-Fe-C(4) | 41.18(9) |
| C(7)#1-Fe-C(4) | 107.28(9) |
| C(7)-Fe-C(4) | 69.74(9) |
| C(3)#1-Fe-C(4)#1 | 41.18(9) |
| C(3)-Fe-C(4)#1 | 124.75(9) |
| C(7)#1-Fe-C(4)#1 | 69.74(9) |
| C(7)-Fe-C(4)#1 | 107.28(9) |
| C(4)-Fe-C(4)#1 | 161.43(13) |
| C(3)#1-Fe-C(6)#1 | 68.09(9) |
| C(3)-Fe-C(6)#1 | 160.16(9) |
| C(7)#1-Fe-C(6)#1 | 40.58(9) |
| C(7)-Fe-C(6)#1 | 155.83(10) |
| C(4)-Fe-C(6)#1 | 121.75(10) |
| C(4)#1-Fe-C(6)#1 | 68.62(9) |
| C(3)#1-Fe-C(6) | 160.16(9) |
| C(3)-Fe-C(6) | 68.09(9) |
| C(7)#1-Fe-C(6) | 155.84(10) |
| C(7)-Fe-C(6) | 40.57(9) |
| C(4)-Fe-C(6) | 68.62(9) |
| C(4)#1-Fe-C(6) | 121.75(10) |
| C(6)#1-Fe-C(6) | 119.84(13) |
| C(3)#1-Fe-C(5) | 159.10(9) |
| C(3)-Fe-C(5) | 68.07(9) |
| C(7)#1-Fe-C(5) | 121.01(9) |
| C(7)-Fe-C(5) | 68.64(10) |
| C(4)-Fe-C(5) | 40.53(9) |
| C(4)#1-Fe-C(5) | 156.91(10) |
| C(6)#1-Fe-C(5) | 105.32(10) |
| C(6)-Fe-C(5) | 40.47(10) |
| C(3)#1-Fe-C(5)#1 | 68.07(9) |
| C(3)-Fe-C(5)#1 | 159.10(9) |
| C(7)#1-Fe-C(5)#1 | 68.64(10) |
| C(7)-Fe-C(5)#1 | 121.01(9) |
| C(4)-Fe-C(5)#1 | 156.91(10) |

| | |
|---|---|
| C(4)#1-Fe-C(5)#1 | 40.53(9) |
| C(6)#1-Fe-C(5)#1 | 40.47(10) |
| C(6)-Fe-C(5)#1 | 105.32(10) |
| C(5)-Fe-C(5)#1 | 120.62(14) |
| C(21)-P-C(11) | 107.22(10) |
| C(21)-P-C(2) | 105.81(8) |
| C(11)-P-C(2) | 104.88(10) |
| C(21)-P-Au | 107.29(8) |
| C(11)-P-Au | 114.10(7) |
| C(2)-P-Au | 116.89(9) |
| C(1)-N(1)-C(3) | 176.0(2) |
| N(1)-C(1)-Au | 174.7(2) |
| N(1)-C(3)-C(7) | 125.4(2) |
| N(1)-C(3)-C(4) | 124.7(2) |
| C(7)-C(3)-C(4) | 109.8(2) |
| N(1)-C(3)-Fe | 123.57(16) |
| C(7)-C(3)-Fe | 70.41(13) |
| C(4)-C(3)-Fe | 70.51(13) |
| C(5)-C(4)-C(3) | 106.2(2) |
| C(5)-C(4)-Fe | 70.06(13) |
| C(3)-C(4)-Fe | 68.31(13) |
| C(5)-C(4)-H(4) | 128.1(18) |
| C(3)-C(4)-H(4) | 125.2(18) |
| Fe-C(4)-H(4) | 132.0(17) |
| C(6)-C(5)-C(4) | 108.8(2) |
| C(6)-C(5)-Fe | 69.63(13) |
| C(4)-C(5)-Fe | 69.41(13) |
| C(6)-C(5)-H(5) | 128(2) |
| C(4)-C(5)-H(5) | 123(2) |
| Fe-C(5)-H(5) | 121(2) |
| C(7)-C(6)-C(5) | 108.9(2) |
| C(7)-C(6)-Fe | 69.42(13) |
| C(5)-C(6)-Fe | 69.90(13) |
| C(7)-C(6)-H(6) | 125.7(18) |
| C(5)-C(6)-H(6) | 124.6(18) |
| Fe-C(6)-H(6) | 119.0(19) |
| C(6)-C(7)-C(3) | 106.2(2) |
| C(6)-C(7)-Fe | 70.01(13) |
| C(3)-C(7)-Fe | 68.41(13) |
| C(6)-C(7)-H(7) | 128.0(17) |
| C(3)-C(7)-H(7) | 125.8(17) |
| Fe-C(7)-H(7) | 124.5(16) |
| P#1-C(2)-P | 118.63(17) |
| P#1-C(2)-H(2) | 107.7(18) |
| P-C(2)-H(2) | 108.1(19) |
| C(16)-C(11)-C(12) | 111.47(19) |
| C(16)-C(11)-P | 112.91(16) |
| C(12)-C(11)-P | 111.39(15) |
| C(16)-C(11)-H(11) | 109.4(14) |
| C(12)-C(11)-H(11) | 107.5(14) |
| P-C(11)-H(11) | 103.8(14) |
| C(13)-C(12)-C(11) | 110.42(19) |
| C(13)-C(12)-H(12A) | 104.7(19) |

| | |
|---|---|
| C(11)-C(12)-H(12A) | 109.3(19) |
| C(13)-C(12)-H(12B) | 102.5(16) |
| C(11)-C(12)-H(12B) | 114.0(17) |
| H(12A)-C(12)-H(12B) | 115(2) |
| C(12)-C(13)-C(14) | 111.8(2) |
| C(12)-C(13)-H(13A) | 105.6(15) |
| C(14)-C(13)-H(13A) | 110.6(15) |
| C(12)-C(13)-H(13B) | 107.6(18) |
| C(14)-C(13)-H(13B) | 111.5(19) |
| H(13A)-C(13)-H(13B) | 110(2) |
| C(13)-C(14)-C(15) | 111.6(2) |
| C(13)-C(14)-H(14A) | 107.6(17) |
| C(15)-C(14)-H(14A) | 110.4(17) |
| C(13)-C(14)-H(14B) | 108.9(14) |
| C(15)-C(14)-H(14B) | 112.0(14) |
| H(14A)-C(14)-H(14B) | 106(2) |
| C(14)-C(15)-C(16) | 111.3(2) |
| C(14)-C(15)-H(15A) | 108.2(17) |
| C(16)-C(15)-H(15A) | 111.0(17) |
| C(14)-C(15)-H(15B) | 110.6(15) |
| C(16)-C(15)-H(15B) | 112.2(15) |
| H(15A)-C(15)-H(15B) | 103(2) |
| C(11)-C(16)-C(15) | 110.48(19) |
| C(11)-C(16)-H(16A) | 111.1(14) |
| C(15)-C(16)-H(16A) | 108.4(14) |
| C(11)-C(16)-H(16B) | 109.8(19) |
| C(15)-C(16)-H(16B) | 108.8(19) |
| H(16A)-C(16)-H(16B) | 108(2) |
| C(22)-C(21)-C(26) | 110.47(19) |
| C(22)-C(21)-P | 110.06(16) |
| C(26)-C(21)-P | 110.86(16) |
| C(22)-C(21)-H(21) | 109.2(19) |
| C(26)-C(21)-H(21) | 110.4(19) |
| P-C(21)-H(21) | 105.7(19) |
| C(23)-C(22)-C(21) | 111.7(2) |
| C(23)-C(22)-H(22A) | 111.2(16) |
| C(21)-C(22)-H(22A) | 107.5(16) |
| C(23)-C(22)-H(22B) | 112.2(16) |
| C(21)-C(22)-H(22B) | 106.5(16) |
| H(22A)-C(22)-H(22B) | 107(2) |
| C(24)-C(23)-C(22) | 111.8(2) |
| C(24)-C(23)-H(23A) | 108.5(17) |
| C(22)-C(23)-H(23A) | 106.0(17) |
| C(24)-C(23)-H(23B) | 112.2(17) |
| C(22)-C(23)-H(23B) | 107.6(17) |
| H(23A)-C(23)-H(23B) | 111(2) |
| C(23)-C(24)-C(25) | 110.8(2) |
| C(23)-C(24)-H(24A) | 107.2(18) |
| C(25)-C(24)-H(24A) | 109.5(18) |
| C(23)-C(24)-H(24B) | 108.9(17) |
| C(25)-C(24)-H(24B) | 107.6(17) |
| H(24A)-C(24)-H(24B) | 113(2) |
| C(24)-C(25)-C(26) | 111.6(2) |

| | |
|---|---|
| C(24)-C(25)-H(25A) | 108.2(17) |
| C(26)-C(25)-H(25A) | 109.3(17) |
| C(24)-C(25)-H(25B) | 107.3(18) |
| C(26)-C(25)-H(25B) | 108.0(18) |
| H(25A)-C(25)-H(25B) | 113(2) |
| C(25)-C(26)-C(21) | 111.3(2) |
| C(25)-C(26)-H(26A) | 112.3(16) |
| C(21)-C(26)-H(26A) | 108.0(16) |
| C(25)-C(26)-H(26B) | 117.9(17) |
| C(21)-C(26)-H(26B) | 107.0(17) |
| H(26A)-C(26)-H(26B) | 99(2) |
| O(2)-S-O(3) | 115.78(12) |
| O(2)-S-O(1) | 114.44(11) |
| O(3)-S-O(1) | 114.56(12) |
| O(2)-S-C(8) | 103.35(13) |
| O(3)-S-C(8) | 102.90(14) |
| O(1)-S-C(8) | 103.43(13) |
| F(3)-C(8)-F(2) | 108.6(3) |
| F(3)-C(8)-F(1) | 107.1(3) |
| F(2)-C(8)-F(1) | 106.7(2) |
| F(3)-C(8)-S | 111.7(2) |
| F(2)-C(8)-S | 110.9(2) |
| F(1)-C(8)-S | 111.6(2) |

Symmetry transformations used to generate equivalent atoms: #1: -x+1, y, -z+1/2

**Table B.5.** Anisotropic displacement parameters ($Å^2 \times 10^3$) for $[\{((C_6H_{11})_2P)_2CH_2\}\{Au(CNC_5H_4)\}_2Fe][O_3SCF_3]_2$. The anisotropic displacement factor exponent takes the form: $-2\pi^2[ h^2 a^{*2} U^{11} + ... + 2 h k a^* b^* U^{12} ]$

| | $U^{11}$ | $U^{22}$ | $U^{33}$ | $U^{23}$ | $U^{13}$ | $U^{12}$ |
|---|---|---|---|---|---|---|
| Au | 18(1) | 8(1) | 16(1) | 0(1) | 1(1) | 0(1) |
| Fe | 14(1) | 9(1) | 16(1) | 0 | 3(1) | 0 |
| P | 15(1) | 8(1) | 13(1) | 0(1) | 1(1) | 0(1) |
| N(1) | 17(1) | 11(1) | 17(1) | -1(1) | 0(1) | 0(1) |
| C(1) | 15(1) | 14(1) | 16(1) | 0(1) | 0(1) | -2(1) |
| C(2) | 17(2) | 8(1) | 15(2) | 0 | 2(1) | 0 |
| C(3) | 17(1) | 9(1) | 18(1) | -1(1) | 1(1) | -1(1) |
| C(4) | 14(1) | 15(1) | 19(1) | 0(1) | 2(1) | 0(1) |
| C(5) | 19(1) | 13(1) | 19(1) | -1(1) | 2(1) | 4(1) |
| C(6) | 19(1) | 11(1) | 19(1) | 4(1) | 3(1) | -1(1) |
| C(7) | 16(1) | 14(1) | 15(1) | 0(1) | 3(1) | -1(1) |
| C(11) | 14(1) | 11(1) | 14(1) | -1(1) | 1(1) | -1(1) |
| C(12) | 16(1) | 14(1) | 17(1) | -2(1) | 3(1) | 2(1) |
| C(13) | 15(1) | 21(1) | 24(1) | -4(1) | 4(1) | 1(1) |
| C(14) | 18(1) | 17(1) | 21(1) | -2(1) | 1(1) | -2(1) |
| C(15) | 19(1) | 15(1) | 20(1) | -4(1) | 3(1) | -1(1) |
| C(16) | 17(1) | 12(1) | 18(1) | -3(1) | 3(1) | -1(1) |
| C(21) | 17(1) | 12(1) | 15(1) | 1(1) | 4(1) | 0(1) |
| C(22) | 19(1) | 21(1) | 16(1) | 1(1) | 3(1) | -1(1) |
| C(23) | 23(1) | 28(1) | 19(1) | 2(1) | 7(1) | -1(1) |

| | | | | | | |
|---|---|---|---|---|---|---|
| C(24) | 23(1) | 28(1) | 22(1) | 6(1) | 7(1) | -4(1) |
| C(25) | 18(1) | 24(1) | 23(1) | 5(1) | 4(1) | -3(1) |
| C(26) | 17(1) | 18(1) | 18(1) | 1(1) | 0(1) | -3(1) |
| S | 20(1) | 14(1) | 24(1) | 1(1) | 8(1) | 1(1) |
| F(1) | 48(1) | 42(1) | 49(1) | 24(1) | 21(1) | 22(1) |
| F(2) | 56(1) | 77(2) | 46(1) | 27(1) | 36(1) | 23(1) |
| F(3) | 80(2) | 64(2) | 29(1) | -5(1) | -8(1) | -1(1) |
| O(1) | 23(1) | 18(1) | 35(1) | 3(1) | 13(1) | 0(1) |
| O(2) | 29(1) | 21(1) | 43(1) | 1(1) | 13(1) | 8(1) |
| O(3) | 30(1) | 23(1) | 33(1) | -4(1) | 11(1) | -8(1) |
| C(8) | 33(2) | 35(2) | 28(1) | 6(1) | 12(1) | 9(1) |

**Table B.6.** Hydrogen coordinates ( x $10^4$) and isotropic displacement parameters (Å$^2$x $10^3$) for $[\{((C_6H_{11})_2P)_2CH_2\}\{Au(CNC_5H_4)\}_2Fe][O_3SCF_3]_2$

| | x | y | z | U(eq) |
|---|---|---|---|---|
| H(4) | 3246(18) | 3183(19) | 2279(14) | 18(7) |
| H(5) | 3690(20) | 4765(19) | 2157(16) | 21(8) |
| H(6) | 4830(20) | 4823(19) | 1504(16) | 21(8) |
| H(7) | 5148(16) | 3209(18) | 1228(13) | 12(6) |
| H(2) | 5387(16) | -2721(19) | 2412(14) | 22(7) |
| H(11) | 3229(15) | -2052(17) | 841(12) | 10(6) |
| H(12A) | 2980(19) | -2580(20) | 2126(15) | 28(8) |
| H(12B) | 2591(18) | -1692(19) | 1760(14) | 21(7) |
| H(13A) | 1696(16) | -2440(18) | 916(13) | 14(7) |
| H(13B) | 1584(18) | -2734(19) | 1615(14) | 19(7) |
| H(14A) | 2295(17) | -4059(18) | 1626(14) | 18(7) |
| H(14B) | 1522(17) | -4062(17) | 957(13) | 13(6) |
| H(15A) | 2549(18) | -3600(20) | 340(14) | 23(7) |
| H(15B) | 2892(17) | -4510(20) | 691(14) | 19(7) |
| H(16A) | 4058(15) | -3417(16) | 871(12) | 7(6) |
| H(16B) | 3880(18) | -3638(19) | 1543(15) | 18(7) |
| H(21) | 5376(19) | -2450(20) | 1155(15) | 35(9) |
| H(22A) | 4493(17) | -1022(19) | 394(13) | 13(7) |
| H(22B) | 4220(20) | -2060(20) | 236(15) | 32(8) |
| H(23A) | 5531(18) | -2220(20) | -94(14) | 19(7) |
| H(23B) | 4990(20) | -1470(20) | -575(16) | 31(8) |
| H(24A) | 5948(19) | -450(20) | 156(15) | 24(7) |
| H(24B) | 6546(19) | -1137(19) | -132(14) | 25(7) |
| H(25A) | 7109(18) | -904(19) | 1048(14) | 20(7) |
| H(25B) | 6834(19) | -1910(20) | 887(15) | 28(8) |
| H(26A) | 5856(17) | -650(20) | 1450(14) | 20(7) |
| H(26B) | 6311(19) | -1410(20) | 1892(15) | 28(8) |

**Table B.7.** Torsion angles [°] for $[\{((C_6H_{11})_2P)_2CH_2\}\{Au(CNC_5H_4)\}_2Fe][O_3SCF_3]_2$

| | |
|---|---|
| C(1)-Au-P-C(21) | 7.0(3) |
| Au#1-Au-P-C(21) | -94.85(8) |
| C(1)-Au-P-C(11) | -111.6(3) |
| Au#1-Au-P-C(11) | 146.54(8) |

| | |
|---|---|
| C(1)-Au-P-C(2) | 125.6(3) |
| Au#1-Au-P-C(2) | 23.69(4) |
| C(3)-N(1)-C(1)-Au | -160(2) |
| P-Au-C(1)-N(1) | -28(2) |
| Au#1-Au-C(1)-N(1) | 73(2) |
| C(1)-N(1)-C(3)-C(7) | 175(3) |
| C(1)-N(1)-C(3)-C(4) | -3(3) |
| C(1)-N(1)-C(3)-Fe | 86(3) |
| C(3)#1-Fe-C(3)-N(1) | -0.19(15) |
| C(7)#1-Fe-C(3)-N(1) | -44.5(2) |
| C(7)-Fe-C(3)-N(1) | 120.1(2) |
| C(4)-Fe-C(3)-N(1) | -119.4(2) |
| C(4)#1-Fe-C(3)-N(1) | 44.2(2) |
| C(6)#1-Fe-C(3)-N(1) | -83.8(3) |
| C(6)-Fe-C(3)-N(1) | 158.5(2) |
| C(5)-Fe-C(3)-N(1) | -157.7(2) |
| C(5)#1-Fe-C(3)-N(1) | 83.3(3) |
| C(3)#1-Fe-C(3)-C(7) | -120.28(14) |
| C(7)#1-Fe-C(3)-C(7) | -164.54(12) |
| C(4)-Fe-C(3)-C(7) | 120.53(19) |
| C(4)#1-Fe-C(3)-C(7) | -75.88(16) |
| C(6)#1-Fe-C(3)-C(7) | 156.1(3) |
| C(6)-Fe-C(3)-C(7) | 38.40(13) |
| C(5)-Fe-C(3)-C(7) | 82.18(14) |
| C(5)#1-Fe-C(3)-C(7) | -36.8(3) |
| C(3)#1-Fe-C(3)-C(4) | 119.19(14) |
| C(7)#1-Fe-C(3)-C(4) | 74.93(16) |
| C(7)-Fe-C(3)-C(4) | -120.53(19) |
| C(4)#1-Fe-C(3)-C(4) | 163.59(12) |
| C(6)#1-Fe-C(3)-C(4) | 35.6(3) |
| C(6)-Fe-C(3)-C(4) | -82.13(14) |
| C(5)-Fe-C(3)-C(4) | -38.35(14) |
| C(5)#1-Fe-C(3)-C(4) | -157.4(2) |
| N(1)-C(3)-C(4)-C(5) | 178.1(2) |
| C(7)-C(3)-C(4)-C(5) | 0.5(3) |
| Fe-C(3)-C(4)-C(5) | 60.13(16) |
| N(1)-C(3)-C(4)-Fe | 117.9(2) |
| C(7)-C(3)-C(4)-Fe | -59.62(16) |
| C(3)#1-Fe-C(4)-C(5) | 159.77(14) |
| C(3)-Fe-C(4)-C(5) | -117.7(2) |
| C(7)#1-Fe-C(4)-C(5) | 117.80(14) |
| C(7)-Fe-C(4)-C(5) | -80.47(15) |
| C(4)#1-Fe-C(4)-C(5) | -164.47(14) |
| C(6)#1-Fe-C(4)-C(5) | 75.78(17) |
| C(6)-Fe-C(4)-C(5) | -36.93(14) |
| C(5)#1-Fe-C(4)-C(5) | 41.8(4) |
| C(3)#1-Fe-C(4)-C(3) | -82.6(2) |

| | |
|---|---|
| C(7)#1-Fe-C(4)-C(3) | -124.54(14) |
| C(7)-Fe-C(4)-C(3) | 37.20(13) |
| C(4)#1-Fe-C(4)-C(3) | -46.81(12) |
| C(6)#1-Fe-C(4)-C(3) | -166.56(13) |
| C(6)-Fe-C(4)-C(3) | 80.73(14) |
| C(5)-Fe-C(4)-C(3) | 117.7(2) |
| C(5)#1-Fe-C(4)-C(3) | 159.5(2) |
| C(3)-C(4)-C(5)-C(6) | -0.4(3) |
| Fe-C(4)-C(5)-C(6) | 58.62(17) |
| C(3)-C(4)-C(5)-Fe | -59.00(15) |
| C(3)#1-Fe-C(5)-C(6) | -173.3(2) |
| C(3)-Fe-C(5)-C(6) | -81.49(15) |
| C(7)#1-Fe-C(5)-C(6) | 159.32(14) |
| C(7)-Fe-C(5)-C(6) | -37.04(14) |
| C(4)-Fe-C(5)-C(6) | -120.4(2) |
| C(4)#1-Fe-C(5)-C(6) | 47.0(3) |
| C(6)#1-Fe-C(5)-C(6) | 118.28(16) |
| C(5)#1-Fe-C(5)-C(6) | 77.25(13) |
| C(3)#1-Fe-C(5)-C(4) | -52.8(3) |
| C(3)-Fe-C(5)-C(4) | 38.95(14) |
| C(7)#1-Fe-C(5)-C(4) | -80.23(16) |
| C(7)-Fe-C(5)-C(4) | 83.41(15) |
| C(4)#1-Fe-C(5)-C(4) | 167.44(15) |
| C(6)#1-Fe-C(5)-C(4) | -121.28(15) |
| C(6)-Fe-C(5)-C(4) | 120.4(2) |
| C(5)#1-Fe-C(5)-C(4) | -162.31(16) |
| C(4)-C(5)-C(6)-C(7) | 0.1(3) |
| Fe-C(5)-C(6)-C(7) | 58.60(17) |
| C(4)-C(5)-C(6)-Fe | -58.49(17) |
| C(3)#1-Fe-C(6)-C(7) | 52.5(3) |
| C(3)-Fe-C(6)-C(7) | -38.96(14) |
| C(7)#1-Fe-C(6)-C(7) | -168.08(14) |
| C(4)-Fe-C(6)-C(7) | -83.42(15) |
| C(4)#1-Fe-C(6)-C(7) | 79.31(16) |
| C(6)#1-Fe-C(6)-C(7) | 161.30(16) |
| C(5)-Fe-C(6)-C(7) | -120.4(2) |
| C(5)#1-Fe-C(6)-C(7) | 120.08(14) |
| C(3)#1-Fe-C(6)-C(5) | 172.9(3) |
| C(3)-Fe-C(6)-C(5) | 81.45(15) |
| C(7)#1-Fe-C(6)-C(5) | -47.7(3) |
| C(7)-Fe-C(6)-C(5) | 120.4(2) |
| C(4)-Fe-C(6)-C(5) | 36.98(14) |
| C(4)#1-Fe-C(6)-C(5) | -160.29(14) |
| C(6)#1-Fe-C(6)-C(5) | -78.29(13) |
| C(5)#1-Fe-C(6)-C(5) | -119.51(17) |
| C(5)-C(6)-C(7)-C(3) | 0.2(3) |
| Fe-C(6)-C(7)-C(3) | 59.10(15) |

| | |
|---|---|
| C(5)-C(6)-C(7)-Fe | -58.89(17) |
| N(1)-C(3)-C(7)-C(6) | -178.0(2) |
| C(4)-C(3)-C(7)-C(6) | -0.5(3) |
| Fe-C(3)-C(7)-C(6) | -60.13(16) |
| N(1)-C(3)-C(7)-Fe | -117.9(2) |
| C(4)-C(3)-C(7)-Fe | 59.68(16) |
| C(3)#1-Fe-C(7)-C(6) | -160.69(14) |
| C(3)-Fe-C(7)-C(6) | 117.62(19) |
| C(7)#1-Fe-C(7)-C(6) | 163.71(14) |
| C(4)-Fe-C(7)-C(6) | 80.42(15) |
| C(4)#1-Fe-C(7)-C(6) | -118.94(14) |
| C(6)#1-Fe-C(7)-C(6) | -42.8(3) |
| C(5)-Fe-C(7)-C(6) | 36.95(14) |
| C(5)#1-Fe-C(7)-C(6) | -76.83(16) |
| C(3)#1-Fe-C(7)-C(3) | 81.7(2) |
| C(7)#1-Fe-C(7)-C(3) | 46.08(12) |
| C(4)-Fe-C(7)-C(3) | -37.20(13) |
| C(4)#1-Fe-C(7)-C(3) | 123.43(14) |
| C(6)#1-Fe-C(7)-C(3) | -160.4(2) |
| C(6)-Fe-C(7)-C(3) | -117.62(19) |
| C(5)-Fe-C(7)-C(3) | -80.68(14) |
| C(5)#1-Fe-C(7)-C(3) | 165.55(13) |
| C(21)-P-C(2)-P#1 | 106.37(8) |
| C(11)-P-C(2)-P#1 | -140.45(8) |
| Au-P-C(2)-P#1 | -12.969(19) |
| C(21)-P-C(11)-C(16) | 55.84(19) |
| C(2)-P-C(11)-C(16) | -56.34(18) |
| Au-P-C(11)-C(16) | 174.49(14) |
| C(21)-P-C(11)-C(12) | -177.84(16) |
| C(2)-P-C(11)-C(12) | 69.99(17) |
| Au-P-C(11)-C(12) | -59.18(17) |
| C(16)-C(11)-C(12)-C(13) | -56.0(3) |
| P-C(11)-C(12)-C(13) | 176.94(17) |
| C(11)-C(12)-C(13)-C(14) | 55.1(3) |
| C(12)-C(13)-C(14)-C(15) | -55.3(3) |
| C(13)-C(14)-C(15)-C(16) | 55.3(3) |
| C(12)-C(11)-C(16)-C(15) | 56.3(3) |
| P-C(11)-C(16)-C(15) | -177.43(16) |
| C(14)-C(15)-C(16)-C(11) | -55.7(3) |
| C(11)-P-C(21)-C(22) | 51.20(19) |
| C(2)-P-C(21)-C(22) | 162.74(17) |
| Au-P-C(21)-C(22) | -71.77(17) |
| C(11)-P-C(21)-C(26) | 173.71(16) |
| C(2)-P-C(21)-C(26) | -74.74(18) |
| Au-P-C(21)-C(26) | 50.74(17) |
| C(26)-C(21)-C(22)-C(23) | 53.8(3) |
| P-C(21)-C(22)-C(23) | 176.51(18) |

| | |
|---|---|
| C(21)-C(22)-C(23)-C(24) | -55.4(3) |
| C(22)-C(23)-C(24)-C(25) | 56.0(3) |
| C(23)-C(24)-C(25)-C(26) | -56.4(3) |
| C(24)-C(25)-C(26)-C(21) | 55.9(3) |
| C(22)-C(21)-C(26)-C(25) | -54.1(3) |
| P-C(21)-C(26)-C(25) | -176.37(17) |
| O(2)-S-C(8)-F(3) | -62.3(2) |
| O(3)-S-C(8)-F(3) | 176.8(2) |
| O(1)-S-C(8)-F(3) | 57.3(2) |
| O(2)-S-C(8)-F(2) | 59.0(2) |
| O(3)-S-C(8)-F(2) | -61.9(2) |
| O(1)-S-C(8)-F(2) | 178.6(2) |
| O(2)-S-C(8)-F(1) | 177.8(2) |
| O(3)-S-C(8)-F(1) | 57.0(2) |
| O(1)-S-C(8)-F(1) | -62.6(2) |

Symmetry transformations used to generate equivalent atoms: #1: -x+1, y, -z+1/2

# Appendix C

Crystallography Data for Au(Cl)($C_{17}H_{15}NO_4$)

**Table C.1.** Crystal data and structure refinement for Au(Cl)($C_{17}H_{15}NO_4$).

| | | |
|---|---|---|
| Empirical formula | $C_{17}H_{15}AuClNO_4$ | |
| Formula weight | 529.72 | |
| Temperature | 100(2) K | |
| Wavelength | 0.71073 Å | |
| Crystal system | Monoclinic | |
| Space group | $P2_1/c - C_{2h}^5$ (No. 14) | |
| Unit cell dimensions | **a** = 14.311(1) Å | $\alpha$ = 90.000° |
| | **b** = 15.779(1) Å | $\beta$ = 93.600(1)°. |
| | **c** = 7.1940(6) Å | $\gamma$ = 90.000° |
| Volume | 1621.3(2) $Å^3$ | |
| Z | 4 | |
| Density (calculated) | 2.170 $Mg/m^3$ | |
| Absorption coefficient | 9.260 $mm^{-1}$ | |
| F(000) | 1008 | |
| Crystal size | 0.18 x 0.16 x 0.06 $mm^3$ | |
| Theta range for data collection | 2.58° to 30.55° | |
| Index ranges | $-20 \le h \le 20$, $-22 \le k \le 22$, $-9 \le l \le 10$ | |
| Reflections collected | 19433 | |
| Independent reflections | 4966 [$R_{int}$ = 0.040] | |
| Completeness to theta = 30.55° | 99.8 % | |
| Absorption correction | Semi-empirical from equivalents | |
| Max. and min. transmission | 1.000 and 0.631 | |
| Refinement method | Full-matrix least-squares on $F^2$ | |
| Data / restraints / parameters | 4966 / 0 / 219 | |
| Goodness-of-fit on $F^2$ | 1.043 | |
| Final R indices [I>2sigma(I)] | $R_1$ = 0.029, $wR_2$ = 0.068 | |
| R indices (all data) | $R_1$ = 0.036, $wR_2$ = 0.071 | |
| Largest diff. peak and hole | 3.55 and -1.75 $e^-/Å^3$ | |

---

$R_1 = \Sigma \, ||F_o| - |F_c|| \, / \, \Sigma \, |F_o|$

$wR_2 = \{ \, \Sigma \, [w(F_o^2 - F_c^2)^2] \, / \, \Sigma \, [w(F_o^2)^2] \, \}^{1/2}$

**Table C.2.** Atomic coordinates ( x $10^4$) and equivalent isotropic displacement parameters (Å$^2$ x $10^3$) for Au(Cl)($C_{17}H_{15}NO_4$). U(eq) is defined as one third of the trace of the orthogonalized $U_{ij}$ tensor.

| | x | y | z | U(eq) |
|---|---|---|---|---|
| Au | 153(1) | -543(1) | -2217(1) | 17(1) |
| Cl | -1281(1) | -540(1) | -3714(1) | 25(1) |
| O(1) | 2380(2) | -2297(1) | -98(3) | 18(1) |
| O(2) | 3728(2) | -2838(2) | 1135(4) | 26(1) |
| O(3) | 2441(2) | 1087(1) | -238(3) | 17(1) |
| O(4) | 3550(2) | 1607(2) | 1799(4) | 22(1) |
| N(1) | 2123(2) | -600(2) | -290(4) | 16(1) |
| C(1) | 1388(3) | -571(2) | -989(5) | 18(1) |
| C(2) | 3017(2) | -605(2) | 562(5) | 14(1) |
| C(3) | 3548(2) | -1345(2) | 973(4) | 14(1) |
| C(4) | 4417(2) | -1072(2) | 1848(4) | 16(1) |
| C(5) | 4396(2) | -141(2) | 1944(4) | 14(1) |
| C(6) | 3513(2) | 129(2) | 1137(4) | 15(1) |
| C(7) | 5134(2) | -1611(2) | 2522(5) | 18(1) |
| C(8) | 5995(2) | -1399(2) | 3422(5) | 18(1) |
| C(9) | 6368(2) | -602(2) | 3811(5) | 17(1) |
| C(10) | 5981(2) | 198(2) | 3446(5) | 17(1) |
| C(11) | 5105(2) | 403(2) | 2639(4) | 15(1) |
| C(12) | 3255(2) | -2230(2) | 689(4) | 15(1) |
| C(13) | 2011(2) | -3153(2) | -239(5) | 18(1) |
| C(14) | 1040(2) | -3095(2) | -1165(5) | 21(1) |
| C(15) | 3186(2) | 1012(2) | 964(4) | 15(1) |
| C(16) | 2049(2) | 1939(2) | -426(5) | 18(1) |
| C(17) | 1116(2) | 1853(2) | -1531(5) | 21(1) |

**Table C.3**. Bond lengths [Å] for Au(Cl)($C_{17}H_{15}NO_4$)

| | | | |
|---|---|---|---|
| Au-C(1) | 1.926(4) | C(3)-C(12) | 1.470(4) |
| Au-Cl | 2.257(1) | C(4)-C(7) | 1.397(5) |
| O(1)-C(12) | 1.346(4) | C(4)-C(5) | 1.470(5) |
| O(1)-C(13) | 1.451(4) | C(5)-C(11) | 1.398(4) |
| O(2)-C(12) | 1.206(4) | C(5)-C(6) | 1.422(4) |
| O(3)-C(15) | 1.335(4) | C(6)-C(15) | 1.472(4) |
| O(3)-C(16) | 1.460(4) | C(7)-C(8) | 1.396(5) |
| O(4)-C(15) | 1.214(4) | C(8)-C(9) | 1.388(5) |
| N(1)-C(1) | 1.138(5) | C(9)-C(10) | 1.396(5) |
| N(1)-C(2) | 1.384(4) | C(10)-C(11) | 1.386(5) |
| C(2)-C(6) | 1.407(4) | C(13)-C(14) | 1.506(5) |
| C(2)-C(3) | 1.413(4) | C(16)-C(17) | 1.517(5) |
| C(3)-C(4) | 1.425(4) | | |

**Table C.4**. Bond angles [°] for Au(Cl)($C_{17}H_{15}NO_4$)

| | | | |
|---|---|---|---|
| C(1)-Au-Cl | 178.3(1) | C(11)-C(10)-C(9) | 128.8(3) |
| C(12)-O(1)-C(13) | 115.3(2) | C(10)-C(11)-C(5) | 128.6(3) |
| C(15)-O(3)-C(16) | 115.3(2) | O(2)-C(12)-O(1) | 122.8(3) |
| C(1)-N(1)-C(2) | 178.0(3) | O(2)-C(12)-C(3) | 124.7(3) |
| N(1)-C(1)-Au | 178.5(3) | O(1)-C(12)-C(3) | 112.5(3) |
| N(1)-C(2)-C(6) | 124.1(3) | O(1)-C(13)-C(14) | 107.3(3) |
| N(1)-C(2)-C(3) | 124.5(3) | O(4)-C(15)-O(3) | 123.5(3) |
| C(6)-C(2)-C(3) | 111.3(3) | O(4)-C(15)-C(6) | 124.4(3) |
| C(2)-C(3)-C(4) | 106.6(3) | O(3)-C(15)-C(6) | 112.0(3) |
| C(2)-C(3)-C(12) | 127.7(3) | O(3)-C(16)-C(17) | 106.6(3) |
| C(4)-C(3)-C(12) | 125.6(3) | | |
| C(7)-C(4)-C(3) | 124.9(3) | | |
| C(7)-C(4)-C(5) | 127.5(3) | | |
| C(3)-C(4)-C(5) | 107.6(3) | | |
| C(11)-C(5)-C(6) | 124.6(3) | | |
| C(11)-C(5)-C(4) | 127.8(3) | | |
| C(6)-C(5)-C(4) | 107.5(3) | | |
| C(2)-C(6)-C(5) | 107.0(3) | | |
| C(2)-C(6)-C(15) | 127.0(3) | | |
| C(5)-C(6)-C(15) | 126.0(3) | | |
| C(8)-C(7)-C(4) | 128.6(3) | | |
| C(9)-C(8)-C(7) | 128.8(3) | | |
| C(8)-C(9)-C(10) | 129.7(3) | | |

**Table C.5.** Anisotropic displacement parameters ($Å^2 \times 10^3$) for Au(Cl)($C_{17}H_{15}NO_4$). The anisotropic displacement factor exponent takes the form: $-2\pi^2[ h^2 a^{*2} U_{11} + ... + 2 h k a^* b^* U_{12} ]$

| | $U_{11}$ | $U_{22}$ | $U_{33}$ | $U_{23}$ | $U_{13}$ | $U_{12}$ |
|---|---|---|---|---|---|---|
| Au | 10(1) | 17(1) | 22(1) | -1(1) | -4(1) | 0(1) |
| Cl | 13(1) | 34(1) | 27(1) | -1(1) | -6(1) | 0(1) |
| O(1) | 14(1) | 12(1) | 26(1) | 1(1) | -5(1) | -2(1) |
| O(2) | 18(1) | 13(1) | 44(2) | -1(1) | -11(1) | 1(1) |
| O(3) | 14(1) | 14(1) | 20(1) | 0(1) | -5(1) | 3(1) |
| O(4) | 21(1) | 13(1) | 32(1) | -2(1) | -8(1) | -1(1) |
| N(1) | 14(1) | 11(1) | 22(1) | -1(1) | -2(1) | 0(1) |
| C(1) | 18(2) | 12(1) | 24(2) | -2(1) | 2(1) | -1(1) |
| C(2) | 10(1) | 16(2) | 18(1) | 1(1) | -1(1) | 2(1) |
| C(3) | 12(1) | 11(1) | 19(1) | 0(1) | -1(1) | 1(1) |
| C(4) | 13(1) | 15(1) | 19(2) | -2(1) | -1(1) | -1(1) |
| C(5) | 12(1) | 14(1) | 18(2) | 0(1) | 0(1) | 0(1) |
| C(6) | 13(1) | 14(1) | 19(2) | 2(1) | -2(1) | 1(1) |
| C(7) | 14(1) | 14(1) | 24(2) | -1(1) | -3(1) | 1(1) |
| C(8) | 13(1) | 17(2) | 24(2) | 1(1) | -4(1) | 4(1) |
| C(9) | 12(1) | 19(2) | 20(2) | -2(1) | -2(1) | -1(1) |
| C(10) | 12(1) | 19(2) | 21(2) | -2(1) | -2(1) | -4(1) |
| C(11) | 14(2) | 13(1) | 18(2) | -1(1) | 0(1) | 0(1) |
| C(12) | 13(1) | 12(1) | 20(2) | -2(1) | 0(1) | -1(1) |
| C(13) | 16(1) | 13(1) | 26(2) | -2(1) | -2(1) | -4(1) |
| C(14) | 17(1) | 20(2) | 27(2) | 1(1) | -4(1) | -5(1) |
| C(15) | 13(1) | 13(1) | 19(2) | 1(1) | -3(1) | 1(1) |
| C(16) | 17(1) | 13(1) | 24(2) | 1(1) | -2(1) | 3(1) |
| C(17) | 15(1) | 20(2) | 28(2) | 4(1) | -3(1) | 3(1) |

**Table C.6.** Hydrogen coordinates ( x $10^4$ ) and isotropic displacement parameters ($Å^2$ x $10^3$) for Au(Cl)($C_{17}H_{15}NO_4$)

| | x | y | z | U(eq) |
|---|---|---|---|---|
| H(7) | 5022 | -2199 | 2343 | 21 |
| H(8) | 6378 | -1865 | 3822 | 22 |
| H(9) | 6977 | -600 | 4417 | 21 |
| H(10) | 6371 | 665 | 3799 | 21 |
| H(11) | 4969 | 991 | 2545 | 18 |
| H(13A) | 1988 | -3407 | 1015 | 22 |
| H(13B) | 2413 | -3510 | -988 | 22 |
| H(14A) | 753 | -3659 | -1212 | 32 |
| H(14B) | 1075 | -2877 | -2434 | 32 |
| H(14C) | 659 | -2711 | -453 | 32 |
| H(16A) | 2474 | 2313 | -1087 | 22 |
| H(16B) | 1959 | 2185 | 817 | 22 |
| H(17A) | 842 | 2417 | -1749 | 32 |
| H(17B) | 691 | 1507 | -830 | 32 |
| H(17C) | 1211 | 1581 | -2729 | 32 |

**Table C.7**. Torsion angles [°] for Au(Cl)($C_{17}H_{15}NO_4$)

| | |
|---|---|
| C(2)-N(1)-C(1)-Au | 137(10) |
| Cl-Au-C(1)-N(1) | 1(16) |
| C(1)-N(1)-C(2)-C(6) | 1(11) |
| C(1)-N(1)-C(2)-C(3) | -179(100) |
| N(1)-C(2)-C(3)-C(4) | -179.7(3) |
| C(6)-C(2)-C(3)-C(4) | 0.1(4) |
| N(1)-C(2)-C(3)-C(12) | -3.6(5) |
| C(6)-C(2)-C(3)-C(12) | 176.2(3) |
| C(2)-C(3)-C(4)-C(7) | 178.2(3) |
| C(12)-C(3)-C(4)-C(7) | 2.0(5) |
| C(2)-C(3)-C(4)-C(5) | -0.3(3) |
| C(12)-C(3)-C(4)-C(5) | -176.5(3) |
| C(7)-C(4)-C(5)-C(11) | 3.7(5) |
| C(3)-C(4)-C(5)-C(11) | -177.9(3) |
| C(7)-C(4)-C(5)-C(6) | -178.1(3) |
| C(3)-C(4)-C(5)-C(6) | 0.4(3) |
| N(1)-C(2)-C(6)-C(5) | 179.9(3) |

| | |
|---|---|
| C(3)-C(2)-C(6)-C(5) | 0.1(4) |
| N(1)-C(2)-C(6)-C(15) | 0.6(5) |
| C(3)-C(2)-C(6)-C(15) | -179.3(3) |
| C(11)-C(5)-C(6)-C(2) | 178.1(3) |
| C(4)-C(5)-C(6)-C(2) | -0.3(3) |
| C(11)-C(5)-C(6)-C(15) | -2.6(5) |
| C(4)-C(5)-C(6)-C(15) | 179.1(3) |
| C(3)-C(4)-C(7)-C(8) | -178.7(3) |
| C(5)-C(4)-C(7)-C(8) | -0.6(6) |
| C(4)-C(7)-C(8)-C(9) | -2.6(6) |
| C(7)-C(8)-C(9)-C(10) | 1.4(7) |
| C(8)-C(9)-C(10)-C(11) | 2.0(7) |
| C(9)-C(10)-C(11)-C(5) | -1.7(6) |
| C(6)-C(5)-C(11)-C(10) | 179.9(3) |
| C(4)-C(5)-C(11)-C(10) | -2.1(6) |
| C(13)-O(1)-C(12)-O(2) | 4.8(5) |
| C(13)-O(1)-C(12)-C(3) | -173.8(3) |
| C(2)-C(3)-C(12)-O(2) | -176.9(3) |
| C(4)-C(3)-C(12)-O(2) | -1.5(5) |
| C(2)-C(3)-C(12)-O(1) | 1.6(5) |
| C(4)-C(3)-C(12)-O(1) | 177.0(3) |
| C(12)-O(1)-C(13)-C(14) | -179.4(3) |
| C(16)-O(3)-C(15)-O(4) | -3.1(5) |
| C(16)-O(3)-C(15)-C(6) | 177.4(3) |
| C(2)-C(6)-C(15)-O(4) | 164.4(3) |
| C(5)-C(6)-C(15)-O(4) | -14.8(5) |
| C(2)-C(6)-C(15)-O(3) | -16.1(4) |
| C(5)-C(6)-C(15)-O(3) | 164.7(3) |
| C(15)-O(3)-C(16)-C(17) | -169.0(3) |